

Contents

Introduction	8
1. Cofactors	9
1.1 Cofactor Definition & Classification	9
1.2 History of Cofactors.....	10
1.3 Organic Cofactors	11
1.4 Inorganic Cofactors.....	14
1.4.1 Metal ions.....	14
1.4.2 Iron sulfur cluster core	14
1.5 Mixed Cofactor System	15
1.5.1 Molybdenum (Moco)	15
1.5.2 Haem groups (a, b, c, o).....	16
1.6 Thiamine Diphosphate - Vitamin B ₁ Structure	17
1.6.1 Breslow Intermediate	19
1.6.2 Thiamine intermediates.....	20
1.7 Thiamine Synthesis.....	22
1.7.1 Chemical Synthesis of Thiamine	22
1.7.2 Synthesis of Pyrimidine	22
1.7.3 Biochemical Synthesis of Thiamine	23
1.7.4 Biosynthetic Inhibition (Bacimethrin)	25
1.7.5 RNA Regulation and ThDP Riboswitch Inhibition	25
1.7.6 Vitamin B ₁ Deficiency	27
1.8 Non-Enzymatic ThDP Roles.....	28
1.8.1 Cyclodextrins	28
1.8.2 Stetter & Benzoin Pathways	30
1.8.3 Asymmetric Benzoin & Stetter	31
1.9 Thiamine Diphosphate Enzymes	33
1.9.1 Pyruvate Decarboxylase (PDC)	34
1.9.2 Pyruvate Dehydrogenase.....	34
1.9.3 General Enzyme Structure	35
1.9.4 ThDP Active Site of Pyruvate Decarboxylase	35
1.10 Thiamine Analogues for Studies of ThDP Active Sites.....	39
1.10.1 Pyrithiamine & Oxythiamine	40
1.10.2 Synthesis of Pyrithiamine	41
1.10.3 Synthesis of Oxythiamine	42
1.11 Synthesis and Testing of Leeper Analogues	43

1.11.1 3-Deazathiamine	44
1.11.2 Synthesis of 3-Deazathiamine.....	45
1.11.3 Synthesis of 1,3-Disubstituted Phenyl ThDP.....	47
1.11.4 The 1,4-Disubstituted-[1, 2, 3]-Triazoles & Diphosphate Mimics	49
1.11.5 Synthesis of 1,4-disubstituted [1,2,3] Triazole Mimics	50
1.11.6 The Furan ThDP Analogue	51
1.11.7 Synthesis of Furan ThDP	51
1.12 Enzyme Promiscuity	53
1.12.1 Baeyer-Villiger FMO cofactor system (BVMO's)	53
1.12.2 (Vitamin B ₆) Pyridoxamine modified coenzyme	54
1.12.3 Synthetic Enzymes.....	55
1.12.4 Catalytic Antibodies (Abzymes).....	55
2. The Project	59
Results & Discussion.....	67
Chapter 1 – Chain extensions as a potential scaffold for novel cofactor chemistry.....	67
1.0 Synthesis of Leeper Cofactor.....	67
1.1 Synthesis of azide via sulfite S _N A _R	68
1.2 Synthesis of Leeper clicks	69
1.3 Synthesis of Increased 1,4-disubstituted Triazole Chain Lengths	71
1.4 Synthesis of Alkyne and Tosylate Linkers	72
1.5 Synthesis of 1, 4-Disubstituted [1,2,3]-Triazole Extended Alcohol Linkers	73
1.6 Synthesis of 1,4-Disubstituted Triazole Extended Tosylate Linkers	74
1.7 Synthesis of 1,4-Disubstituted Triazole Extended Diphosphate Linkers.....	76
1.8 Conclusion	76
Chapter 2 - ThDP <i>in silico</i> modelling.....	79
2.0 ThDP Pyruvate Enzyme Comparison	79
2.1 Docking and Construction of Amine Analogues	80
2.2 His 113/His114 amino acids	82
2.3 Conclusion	84
Chapter 3 – Synthesis of Test Analogues from the Methylene Bridge.....	87
3.0 Synthesis of Model ThDP Test Compounds.....	87
3.1 Retrosynthesis.....	87
3.2 Synthesis of the Nitrile.....	89
3.3 Protection of Primary Aromatic Amine	89
3.4 Synthesis of 2-methyl-4-amino pyrimidine carbaldehyde	91
3.5 Synthesis of Methyl – Butyl Alcohols	93
3.6 Synthesis of Methyl – Butyl Azides	95
3.7 Synthesis of Methyl – Butyl Tosylates	97

3.8 Synthesis of Methyl – Butyl Diphosphate	99
Chapter 4-Synthesis of Tertiary amine ThDP 1,4 – disubstituted [1,2,3]-Triazole	106
4.0 The Synthetic Target – Tertiary Amine	106
4.1 The Baylis-Hillman Reaction.....	106
4.2 Enzyme Promiscuity – A Proposed Baylis-Hillman Cofactor System	109
4.2.1 Enzyme Promiscuity – The Tertiary Amine Active Site	110
4.2.2 Initial Baylis-Hillman testing.....	112
4.3 Synthesis of Tertiary Amine Grignard’s.....	113
4.3.1 Synthesis of Azide Tertiary Amine.....	115
4.3.2 Methylation and <i>N</i> -Oxide Protection	117
4.5 The Alkene Synthesis and Ring Opening Approach.....	120
4.6.1 The Wittig Approach	121
4.6.2 The Tebbe Olefination	122
4.6.3 The Corey-Chaykovsky Epoxidation (CCE)	123
4.6.4 Acid Catalysed Dehydration	124
4.6.5 Activation and E2 Elimination.....	125
4.7 Synthesis of Alkene Derivatives for Potential Functionalization	126
4.7.1 Grubbs Cross Metathesis	126
4.7.2 Synthesis of 2-methyl-4-amino-5-(1-hydroxybutene) pyrimidine.....	127
4.7.3 Cross Metathesis of compound 383 with Grubbs 2 nd Generation.....	130
4.7.4 Hydroboration and Ozonolysis of Alkene Derivatives	131
4.7.5 Proposed Ozonolysis.....	131
4.7.6 Proposed Hydroboration	132
4.7.7 Synthesis of 2-methyl-4-amino-5-(5-pentene-1-ol)pyrimidine.....	133
4.7.8 Synthesis of 2-methyl-4-amino-5-(1-azidopentene) pyrimidine.....	134
4.7.9 Synthesis of 2-methyl-4-amino-5-(1-azidohexene)pyrimidine.....	135
4.8 Synthesis 1,3-dioxolane-2-methyl-4-aminopyrimidine derivatives	136
4.8.1 The Reductive Amination	136
4.9 Synthesis of Rigid Alkyne “Spacer”	143
4.9.1 Protection of Secondary Alcohol in Alkyne Linker.....	144
4.10 Cross Coupling Approach.....	146
4.10.1 Synthesis of Iodo-Alkyne.....	147
4.11 The “Umpolung”	147
4.11.1 The Dithiane Protection	147
4.11.2 The Stetter Approach	148
4.12 The Reformatsky/Blaise Approach.....	150
4.12.1 Synthesis of 2-methyl-4-amino-5-(1,3-diketone) pyrimidine	151
4.13 Conclusion to Chapter.....	154

Chapter 5 – Coupled Bioassay	156
5.0 Biological Testing	156
5.1 The NADH coupled Assay	156
5.2 General Introduction to Enzyme Kinetics.....	157
5.3 Types of Inhibition.....	158
5.4 Assay Conditions	161
5.5 Calculation of K_M	161
5.7 Holoenzyme - Order of Reagents.....	164
5.8 Holoenzyme - Testing with Inhibitor.....	165
5.9 Apo Enzyme - Preparation of coupled assay	166
5.10 Apo Enzyme - Pre Incubation Controls	167
5.11 Inhibitor Concentration - Range Finder	167
5.12 Testing of Methyl – Butyl ThDP analogues	168
Chapter 6 – Enantioselective Synthesis of Secondary Alcohols	177
6.1 Enzyme Three Point Rule	177
6.2 Synthesis of Chiral Secondary Alcohols.....	178
6.3 Synthesis of 2-methyl-4-amino-5-ethanol pyrimidine	179
6.4 Synthesis of Prochiral Ketone.....	181
6.5 The Schlenk Equilibrium and Conjugate Addition Product	184
6.6 Synthesis of Dihydropyrimidine	185
6.7 XRD structure and Analysis	185
6.8 Asymmetric Reactions	187
6.9 Conclusion to chapter	190
Chapter 7-Synthesis of Diisopropyldifluoromonophosphate alkyne's	192
7.0 Aim & Previous Difluoromonophosphates.....	192
7.1 Previous Synthesis of Difluorophosphonylated chains.....	193
7.2 Synthesis of Alkyne Synthon.....	193
7.3 Synthesis of 2-methyl-4-amino-5-methyl iodide pyrimidine.....	194
7.4 Synthesis of 2-methyl-4-amino-5-methyl iodide pyrimidine via S_NAr with NaI.....	195
7.5 Synthesis of Alkyne Diisopropyldifluoromonophosphate	196
7.6 Synthesis of Diisopropyldifluoro derivatives	197
7.7 Synthesis of diisopropyldifluorobutanol phosphate.....	197
7.8 Synthesis of Diisopropyldifluorobutanal phosphate	198
7.9 Synthesis of diisopropyldifluoropentyne phosphate	200
7.10 The 1,4-CuAAC Synthesis of Diisopropyldifluorophenylpentyne	201
7.11 Conclusion to Chapter.....	203
Conclusion to Thesis	204
Future Work	206

References - Results & Discussion	208
Experimental	213
General Conditions and Reagents	214
Synthesis of 5-azidomethyl-2-methylpyrimidin-4-ylamine	215
Synthesis of but-3-ynyl toluene-4-sulfonate	215
Synthesis of 5-hexyn-1-tosylate	216
Synthesis of 6-octyn-1-tosylate	218
Synthesis of hept-6-yn-1-ol	218
Synthesis of oct-7-yn-1-ol	219
Synthesis of 2-[1-(4-amino-2-methylpyrimidin-5-ylmethyl)-1 <i>H</i> -[1,2,3]triazol-4-yl]- ethanol	219
Synthesis of 2-[1-(4-amino-2-methylpyrimidin-5-ylmethyl)-1 <i>H</i> -[1,2,3]triazol-4-yl]- propanol	220
Synthesis of 2-[1-(4-amino-2-methylpyrimidin-5-ylmethyl)-1 <i>H</i> -[1,2,3]triazol-4-yl]- butanol	221
Synthesis of 2-[1-(4-amino-2-methylpyrimidin-5-ylmethyl)-1 <i>H</i> -[1,2,3]triazol-4-yl]- pentanol	221
Synthesis of 2-[1-(4-amino-2-methylpyrimidin-5-ylmethyl)-1 <i>H</i> -[1,2,3]triazol-4-yl]- hexanol	222
Synthesis of 2-bromo[1-(4-amino-2-methylpyrimidin-5-ylmethyl)-1 <i>H</i> -[1,2,3] triazol-4-yl]ethane	223
Synthesis of 2-[1-(4-amino-2-methylpyrimidin-5-ylmethyl)-1 <i>H</i> -[1,2,3]triazol-4-yl] ethyl toluene-4-sulfonate	224
Synthesis of 3-(1-(4-amino-2-methylpyrimidin-5-ylmethyl)-1 <i>H</i> -[1,2,3]-triazol-4-yl)- butyl 4- methylbenzenesulfonate	225
Synthesis of 2-methyl-4-aminopyrimidine carbonitrile	227
Synthesis of 2-methyl-4-aminopyrimidine carbaldehyde	227
Method A – Raney Nickel	227
Method B – Lithium aluminium hydride reduction	228
Method C – Hydrogenation	228
Synthesis of (+/-)-1-(4-amino-2-methylpyrimidin-5-yl)ethanol	229
Synthesis of (+/-)-1-(4-amino-2-methylpyrimidin-5-yl)propanol	230
Synthesis of (+/-)-1-(2-methyl-4-aminopyrimidin-5-yl)butanol	230
Synthesis of (+/-)-1-(2-methyl-4-aminopyrimidin-5-yl)pentanol	231
Synthesis of (+/-)-1-(2-methyl-4-aminopyrimidine-3-en-5-yl)butanol	232
Synthesis of 2-methyl-4-amino-5-dipropene pyrimidine	233
Synthesis of (+/-)-1-(2-methyl-4-aminopyrimidin-5-ylethyl) azide	233
Synthesis of (+/-)-1-(2-methyl-4-aminopyrimidin-5-yl)propyl azide	234
Synthesis of (+/-)-1-(2-methyl-4-aminopyrimidin-5-yl)pentyl azide	235
Synthesis of 1- <i>N</i> -(methyl)-2-methyl-4-amino pyrimidin-5-ylmethyl azide	236

Synthesis of 2-[1-(4-amino-2-methylpyrimidin-5-ethyl)-1 <i>H</i> -[1,2,3]triazol-4-yl] ethoxy-tosylate	237
Synthesis of 2-[1-(4-amino-2-methylpyrimidin-5-propyl)-1 <i>H</i> -[1,2,3]triazol-4-yl]- ethoxy-tosylate	238
Synthesis of 2-[1-(4-amino-2-methylpyrimidin-5-butyl)-1 <i>H</i> -[1,2,3]triazol-4-yl] ethoxy-tosylate	239
Synthesis of 2-[1-(4-amino-2-methylpyrimidin-5-propyl)-1 <i>H</i> -[1,2,3]triazol-4-yl] ethoxy-tosylate	239
Synthesis of 2-(1-(4-amino-2-methylpyrimidin-5-ethyl)-1 <i>H</i> -1,2,3-triazol-4-yl)ethyl trihydrogen diphosphate	240
Synthesis of 2-(1-(4-amino-2-methylpyrimidin-5-propyl)-1 <i>H</i> -1,2,3-triazol-4-yl)ethyl trihydrogen diphosphate	241
Synthesis of 2-(1-(4-amino-2-methylpyrimidin-5-butyl)-1 <i>H</i> -1,2,3-triazol-4-yl)ethyl trihydrogen diphosphate	241
Synthesis of 2-(1-(4-amino-2-methylpyrimidin-5-pentyl)-1 <i>H</i> -1,2,3-triazol-4-yl)ethyl trihydrogen diphosphate.....	242
Synthesis of (<i>N,N</i> -dimethyl)-1-chlorobutanol hydrochloride	243
Synthesis of (<i>N,N</i> -dimethyl)-6-chlorohexanamide	243
Synthesis of 4-(4-amino-2-methylpyrimidin-5-yl)-4-hydroxy- <i>N,N</i> dimethylaminobutylamine	244
Synthesis of 2-methyl-4-(NH-BOC)pyrimidinecarbonitrile	244
Synthesis of β -Hydroxy- α -methylene-4-nitrobenzenepropanoic acid methyl ester.....	245
Synthesis of β -Hydroxy- α -methylene-4-nitrobenzenepropanoic acid ethyl ester.....	246
Synthesis of 5-(4-amino-2-methylpyrimidin-5-yl)-5-hydroxypent-1-ene	246
Synthesis of 6-(4-amino-2-methylpyrimidin-5-yl)-6-hydroxyhex-1-ene.....	247
Synthesis of 6-azido-6-(methyl-4-aminopyrimidin-5-yl)hex-1-ene.....	248
Synthesis of 3-(2-methyl-4-aminopyrimidin-5-yl)-2-(1,3-dioxolanyl)propan-1-ol	248
Synthesis of 1-azido-1-(2-methyl-4-aminopyrimidin-5-yl)-2-(1,3-dioxolanyl)propane.....	249
Synthesis of 2-methyl-4-aminobenzoazaazapine pyrimidine	250
Synthesis of 3-(2-methyl-4-aminopyrimidine-5-yl)-3-hydroxyprop-1-yne	250
Synthesis of 3-(2-methyl-4-amino-pyrimidin-5-yl)-3-methoxyprop-1-yne.....	251
Synthesis of 3-(2-methyl-4-aminopyrimidine-5-yl)-3-hydroxy-2,2 - dimethylpropane	252
Synthesis of ethyl 3-(2-methyl-4-aminopyrimidin-5-yl)-3-imino-propanoate	252
Synthesis of 1-(2-methyl-4-aminopyrimidin-5-yl)ethanone	253
Synthesis of 1-(2-methyl-4-aminopyrimidin-5-yl)propanone	253
Synthesis of 1-(2-methyl-4-aminopyrimidin-5-yl)-cyano-6-ethyl.....	254
Synthesis of 1-(2-methyl-4-aminopyrimidine-5-yl)-butan-1-one	254
Synthesis of 1-(2-methyl-4-aminopyrimidine-5-yl)-cyano-6-propyl.....	255
Synthesis of 1-(2-methyl-4-aminopyrimidine-5-yl)-5-cyano-6-butyl.....	255
Synthesis 2-methyl-4-amino-5-cyano-6-methyl-dihydropyrimidine	256
Synthesis 2-methyl-4-amino-5-cyano-6-ethyl-dihydropyrimidine	256

Synthesis of 2-methyl-4-amino-5-cyano-6-vinyl dihydropyrimidine	257
Synthesis of 5-diethylphosphonate-1-pentyne	
Synthesis of 2-[1-(4-Amino-2-methylpyrimidin-5-ylmethyl)-1 <i>H</i> -[1,2,3]triazol-4-yl]-1-choloropropane	258
Synthesis of Diisopropylmercaptomethylphospha.....	258
Synthesis of Diisopropyldifluorobutanol	259
Synthesis of Diisopropyldifluorobutaldehyde	260
Synthesis of Diisopropyldifluoro-4-pentyne.....	260
Synthesis of Ohira-Bestmann reagent.....	261
Preparation of Tosyl azide	261
Preparation of Ohira-Bestmann reagent.....	261
Preparation of 3-dimethylamino-1-propylmagnesium chloride.....	262
Preparation of allylmagnesium bromide	262
Preparation of 4-but-1-enylmagnesium bromide	263
Preparation of 5-pent-1-enyl magnesium bromide	263
Preparation of 2-(1,3-dioxolanyl) ethyl magnesium bromide.....	263
Preparation of <i>t</i> -butylmagnesium bromide	264
Preparation of MOM-chloride	264
Synthesis of <i>N</i> -iodomorpholine	265
HPLC Conditions.....	265
Assay Conditions	266
Preparation of MES.KOH Buffer.....	266
Preparation of the apo enzyme.....	266
Preparation and filling of a dialysis membrane	266
Removing the apo enzyme from membrane	267
Centrifuge Vials	267
General Enzyme Assay	267
Timed pre-incubation assay	267
Experimental references.....	268

Introduction

1. Cofactors

Enzymes have varied and complex structures which are capable of catalysing thousands of different chemical transformations, however this versatility sometimes requires additional functionality to be introduced by what are referred to as cofactors. Cofactors are small non-protein molecules located within an enzyme's active site which may participate in numerous biochemical transformations that are not catalysed by the functional groups present in the active site. This avoids a situation whereby the enzyme is restricted to one catalytic path, and as such can be involved in numerous catalytic mechanisms with different enzymatic species⁽¹⁾ (figure 1). Thus, even though enzymes have excellent specificity and catalytic properties, they sometimes require cofactors to improve their “chemical repertoire” such as reduction/oxidation, bond cleavage/formation and rearrangements⁽²⁾. Some of these roles include electron transport by FAD and NADH, acyl transfers by acetyl Co-A/biotin and the transport of oxygen using Haem groups.

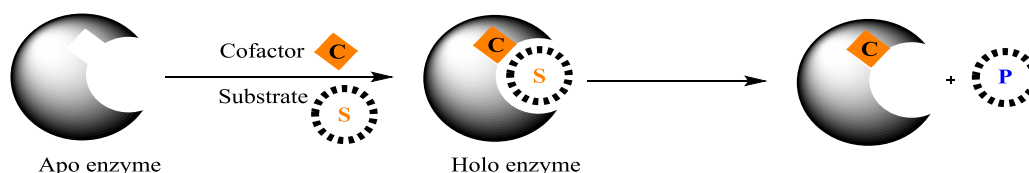


Figure 1: Graphical representation of cofactor role

Enzymes are able to select a substrate molecule and maintain it in the desired conformation for the “helper” cofactor to undertake the synthetic transformation and therefore many crucial biochemical reactions in the cell require not only the enzymes for catalysis but also organic cofactors or metal ions too⁽²⁾.

1.1 Cofactor Definition & Classification

Cofactors are broadly classed into two main categories and comprise of small organic molecules, inorganic metal ions and/or a mixture of protein metal-organic frameworks (figure 2)⁽¹⁾. The organic cofactors are sometimes further subdivided into coenzyme and prosthetic groups to define their types of binding. A coenzyme is thought to be dissociable entity, whereas a prosthetic group can be covalently bound throughout the catalytic process. These terms however, are used interchangeably depending on the scenario⁽²⁾. The term holoenzyme can be used to define the catalytically active enzyme, when both the substrate and cofactor are closely bound within the

active site. An enzyme without cofactor is referred to as the apoenzyme, and no catalysis is possible under these conditions.

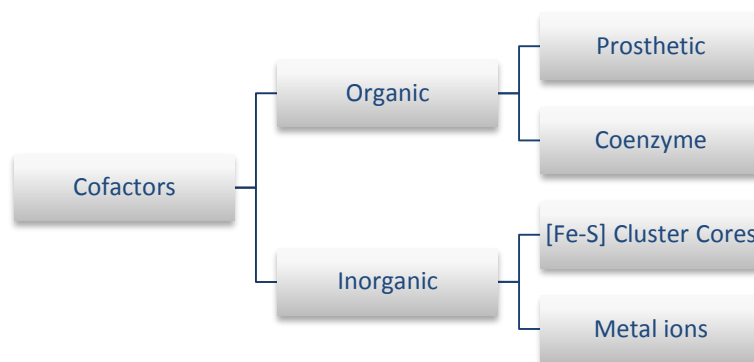


Figure 2: The Cofactor hierarchy

1.2 History of Cofactors

During the 17th century sailors and pirates suffered from the dietary disorder scurvy which is linked to the lack of vitamin C by reduction in collagen synthesis (figure 3, compound 1). The harsh symptoms of this disease include lethargy, gum disease and sharp changes in mood. The scientific links to this were recognised by naval doctor James Lind, who noticed that being away from port prevented the crew from maintaining the supplies of fresh fruit and vegetables. He found that increased portions of citrus fruit within the diet improved the health of the sailors. This link was later proved to be related to a depletion of vitamin C.

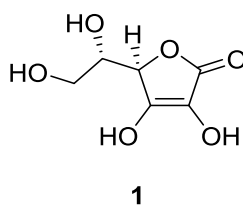


Figure 3: The structure of vitamin C

As more discoveries of this type were made, Casmir Funk⁽³⁾ coined these small molecules “vital amines” because many of the first cofactors to be elucidated contained the amine functionality. The first cofactor to be identified was thiamine, a vitamin required for the decarboxylation of α -keto acids. Once again, the astute observations of naval doctor Takaki Kanehiro of the Japanese navy during the 19th century helped in identifying the role of this vitamin. More privileged sailors were given brown rice containing higher concentrations of thiamine, in contrast to the poorer ones

who were given polished rice which containing less thiamine due to the removal of the husks and bran. Further research by Dr Christiann Eijkman and Sir Fredrick Hopkins began to identify its link to the peripheral nervous disorder beriberi using chickens to test this theory and they surmised that beriberi was somehow linked to the unpolished and polished rice. This work won them the Nobel Prize in medicine and physiology in 1929 and in the coming years this unknown compound was elucidated as thiamine (Vitamin B₁), (figure 4, compound 2).

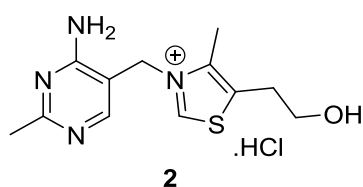


Figure 4: Structure of Vitamin B₁

1.3 Organic Cofactors

As vitamins are ubiquitous throughout nature, organic cofactors are normally acquired from the diet by using vitamins as their biosynthetic precursors or by using the vitamin itself ⁽⁴⁾. As many of the organic cofactors contain the adenosine mononucleotide monophosphate (AMP) structural motif (figure 5, compound 3) it is thought that many examples originate from a ribosomal (RNA) influence, due to its structural resemblance which can be seen in many examples including FAD, NAD⁺ and ATP^{(4), (5)}. It is possible that the AMP functionality could act as a general recognition site for multiple enzymes therefore making their early diversification easier for incorporation into multiple catalysed pathways.

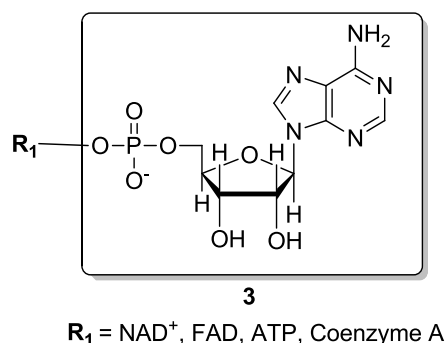


Figure 5: Adenosine mononucleotide monophosphate (AMP) group

There are six enzyme classes (table 1) that use organic cofactors to accomplish their synthetic transformations. Interestingly, oxidoreductases are the primary operators with a staggering 80%

using helper molecules to accomplish the desired chemistry, whereas only 30% are used by other classes of enzyme.

Enzyme Class	Chemical Reaction	Sample Enzyme
Ligase	Group joining with ATP	Acetyl Co-A
Oxoreductase	Redox	Cytochrome P ₄₅₀
Lyase	Group removal	Oxalate decarboxylase
Isomerase	Atom rearrangement	Alanine racemase
Transferase	Group transfer (amino, acetyl)	Acetate kinase
Hydrolase	Hydrolysis	Sucrase

Table 1: Enzymatic classes and reactions

This has been attributed to the structures of the cofactors used in these enzymatic environments which employ many “pteridine based cofactors, quinones and porphyrins (figure 6, (A) Petrin, (B) quinones, (C) porphyrins), which seem to be mainly involved in electron transport and redox chemistry”^{(2),(6)}.

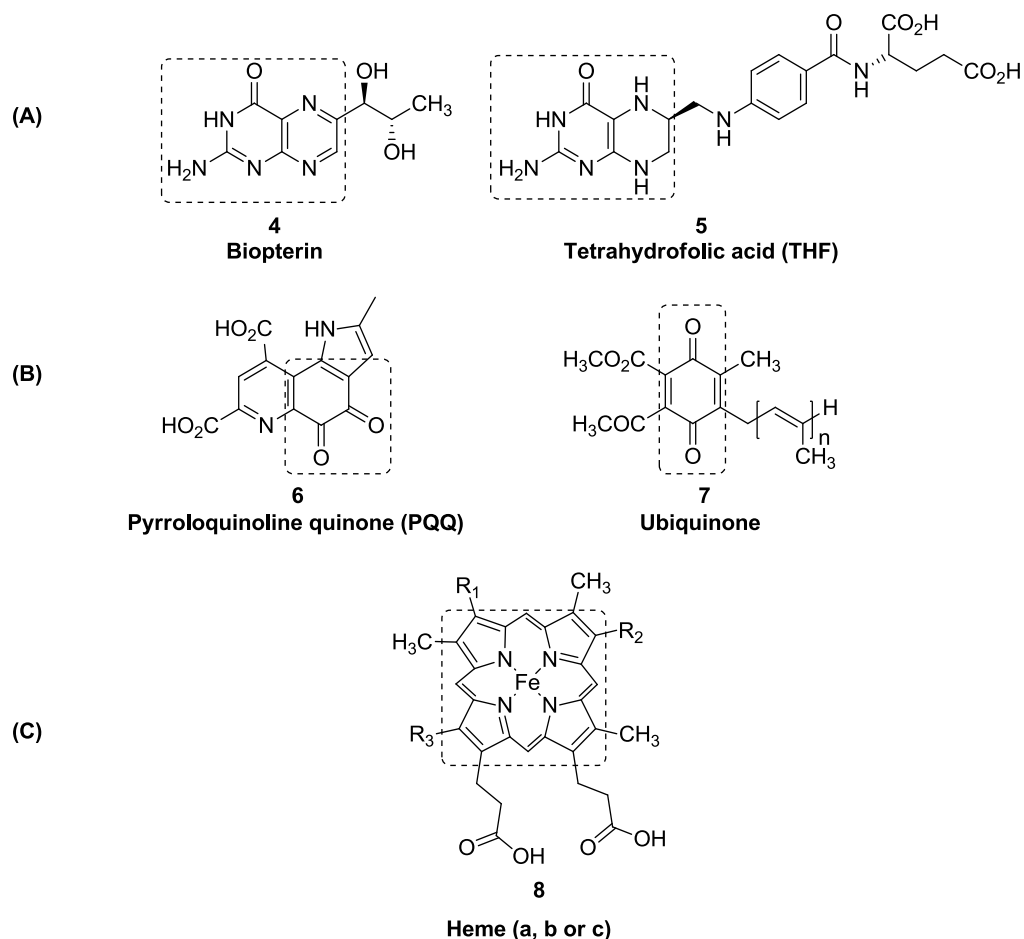


Figure 6: General motifs associated with electron transport

The versatility of these organic frameworks relies heavily on their affinity for their particular enzyme classes and some examples of their other transformations and related deficiencies can be observed below (table 2).

Vitamin	Deficiency	Transformation	Coenzyme
Thiamine (B1)	Beri-Beri	α -carbon cleavage	ThDP (Thiamine diphosphate)
Riboflavin (B2)	Pellegra	electron transfer	FAD (Flavin adenine dinucleotide)
Niacin (B3)	Pellegra	electron transfer	NADH (Nicotinamide-adenine dinucleotide)
Pantothenic acid (B5)	Apathy, Fatigue	Acyl transfer	Coenzyme A
Pyridoxine (B6)	Neuropathy	Transamination	PLP (Pyridoxal phosphate)
Biotin (H)	Alopecia	CO ₂ transfer	Biotin
Cobalamine (B12)	Neurological dysfunction	DNA synthesis	Methylcobalamine
Vitamin C	Scurvy	Electron transfer	Ascorbic acid

*Table taken from reference (106)

Table 2: Example cofactor systems with biotransformation & deficiencies

1.4 Inorganic Cofactors

Characteristically inorganic cofactors play important roles in binding of substrates and organic cofactors to the polypeptide backbone within the active site. As many of the organic cofactors have synthetic recognition sites, it is common to be “combined with the appropriate metal ions”⁽⁴⁾.

1.4.1 Metal ions

Examples of metal ions that are associated with the cofactor-protein interface include zinc, manganese, magnesium, copper and nickel which can assume a (+2) oxidation state to promote strong binding to diphosphate groups and other anionic analogues⁽¹⁾. One example of this is the binding of Mg^{2+} in thiamine dependant enzymes (figure 7) where it forms an octahedral coordination sphere with two oxygens within the active site of PDC⁽⁷⁾.

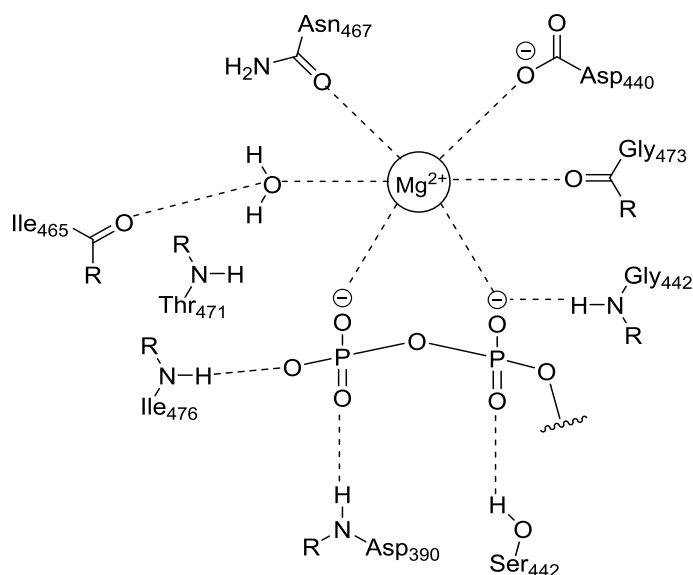


Figure 7: Octahedral binding of Mg^{2+} to diphosphate

1.4.2 Iron sulfur cluster core

In the 1960s the [Fe-S] cluster core of the protein ferredoxin was discovered in the anaerobic bacterium *Clostridium pasteurianum* and is thought to be one of the oldest cofactor systems known due to its involvement in many biological pathways⁽⁸⁾. Iron-sulfur clusters are extremely oxygen-sensitive unless located deep in the active site, and ongoing research is attempting to understand how these motifs are able to survive in an aerobic environment⁽⁹⁾. The familiar structure of iron-sulfur cores can be seen in (figure 8, compounds 9 & 10) as either a two or four

iron-sulphur component system and frequently consists of three or four bonds to surrounding cysteines situated in the active site^{(10), (11)}. A full review of the biosynthesis of these [Fe-S] cores has been published⁽¹²⁾.

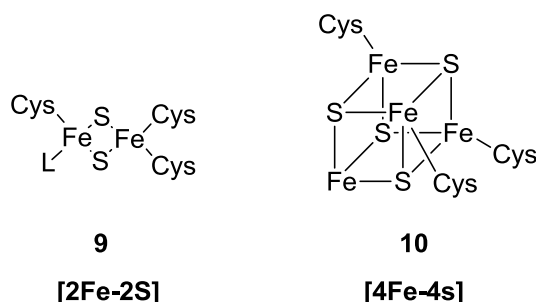


Figure 8: The [2Fe-2S] & [4Fe-4S] iron-sulfur cluster cores

At the time of their discovery, the purpose of chemistry with these inorganic species was believed to only accommodate SET (single electron transfer) as their primary function⁽¹³⁾. However further research has elucidated the other roles undertaken by [Fe-S] cluster cores including the regulation of gene expression,⁽¹⁰⁷⁾ initiation of radical reactions by activation of the C-H bond in SAM mediated enzymes and the storage and insertion of metal cofactors^{(13), (14)}.

1.5 Mixed Cofactor System

After the synthesis of the respective organic cofactor is complete, it may in some cases need to be associated with an inorganic motif to establish the chemistry required in the apoprotein⁽⁴⁾. Two examples of this are the Moco and Haem cofactors which are both ubiquitous throughout nature.

1.5.1 Molybdenum (Moco)

Principally found within bacteria, Moco dependant enzymes are essential in the redox chemistries observed in all biochemical machinery as they carry out roles within the nitrogen, carbon and sulfur cycles^{(8), (15)}. The Moco cofactor (figure 9, compound 11) consists of a tricyclic pterin ring system which can effectively shuttle electrons to and from the molybdenum atom by adopting various oxidation states of (+4) and (+6)⁽¹⁵⁾. This unique ring system means that the cofactor can effectively position the molybdenum atom deep within the active site at its required catalytic centre. The key principle behind this system is that the molybdenum is catalytically inactive under conditions without the organic framework. Hence both cofactor entities need to present for

1.6 Thiamine Diphosphate - Vitamin B₁ Structure

Thiamine (figure 11, compound 2) derives its name from “thio-vitamine” by nature of its sulfur containing thiazole ring and is not restricted to one particular biosynthetic transformation.

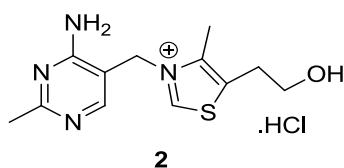
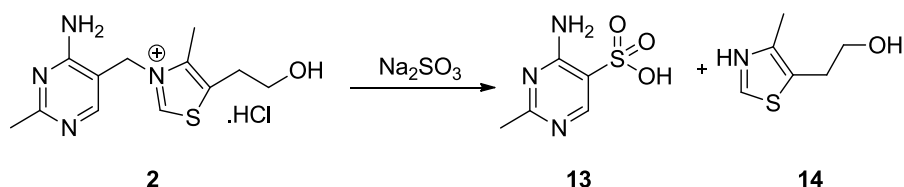


Figure 11: Structure of Thiamine hydrochloride

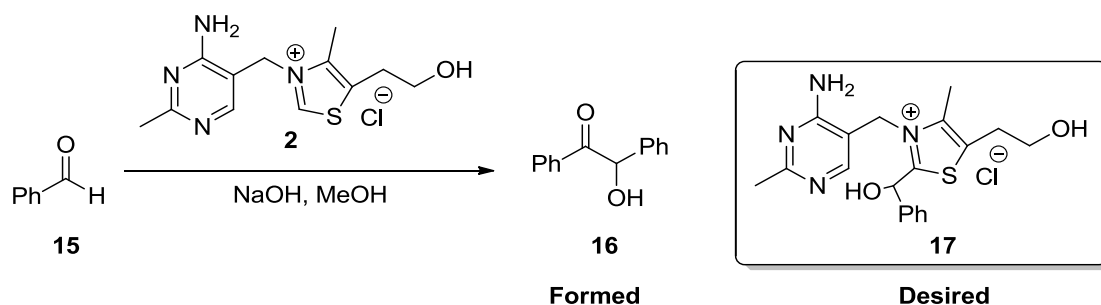
Its structure was deduced by Williams in 1935^{(18), (19)}. Scission of molecule 2 by reaction with a sulfite ion allowed tentative analysis of the constituent parts which were assigned as the aminopyrimidine ring 13 and thiazole core 14 respectively (scheme 1). Work by the same groups to establish a synthetic route for industrial scale-up was then undertaken to reduce malnutrition.



Scheme 1: Sodium sulfite cleavage of thiamine hydrochloride

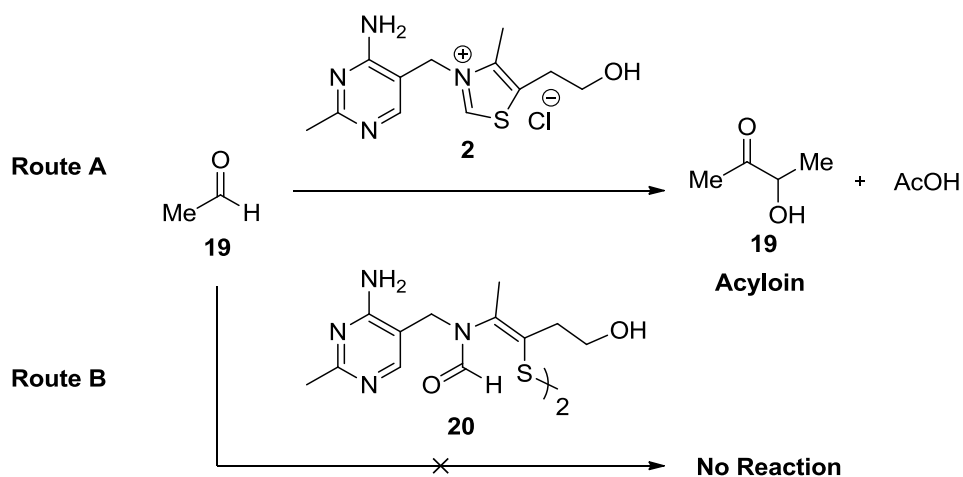
Around the time of this discovery, other research groups were focused on the mechanistic approach that thiamine enzymes adopted. This work was advanced further when Lohmann and Schuster⁽²⁰⁾ identified the active species in *pyruvate decarboxylase* as thiamine diphosphate. Langenbeck had mentioned in 1933⁽²¹⁾ that the amine group was potentially able to undergo a Schiff base reaction with pyruvate and that it was likely to be the point of catalysis. However, this hypothesis was deemed incorrect when Melnick proved that the primary amine group was unreactive and therefore unable to complete this mysterious reaction pathway^{(22), (23)}. As the role of thiamine diphosphate was now becoming more complex, and in the absence of a role for the amine within the mechanism, a study of thiazolium compounds by two Japanese research groups was published^{(24), (25), (26)} (schemes 2 & 3). They noted that α -hydroxyl ketones 16 are formed by the action of the thiazolium and thiazole mimics 2 on aldehyde functionalities 15 and not that of

desired product **17**. This result then suggested that a similar process is achieved within the PDC catalytic cycle as noted by Lohmann and Schuster⁽²⁰⁾.



Scheme 2: The Ugai observation

The work by Mizuhara^{(25), (26)} illustrated that, under normal conditions with thiamine as the catalyst, a classic acyloin system (scheme **3**, route **A**, compound **19**) was constructed, but upon removal of the thiazole moiety no reaction was observed (scheme **3**, route **B**, compound **20**). The following years brought many further interpretations of these new findings and further mechanistic studies, but they never advanced the fundamental understanding of the process. It was clear that the real heart of the reaction actually concerned the central thiazolium ring and its ability to form an acyl anion equivalent like that found in the benzoin reaction⁽²⁷⁾.



Scheme 3: The Mizuhara test

Based on these conclusions, Breslow highlighted the resemblance of the intermediate anion formed during the benzoin condensation to that found within the catalytic cycle of thiamine diphosphate ThDP enzymes, and explained how they both become stabilised by delocalisation

into the positively charged quaternary nitrogen, or corresponding nitrile enolate in the benzoin process (Figure 12).

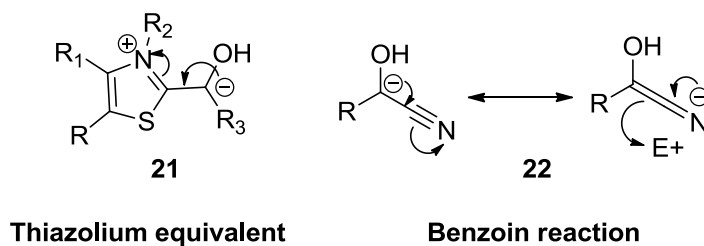
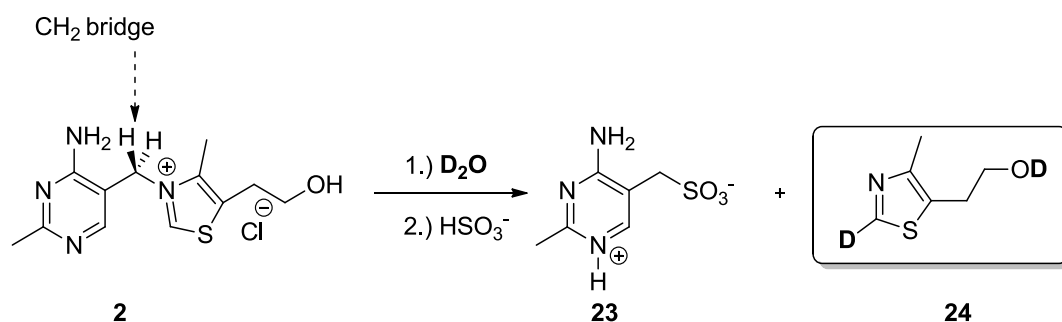


Figure 12: Anionic intermediate of benzoin condensation

1.6.1 Breslow Intermediate

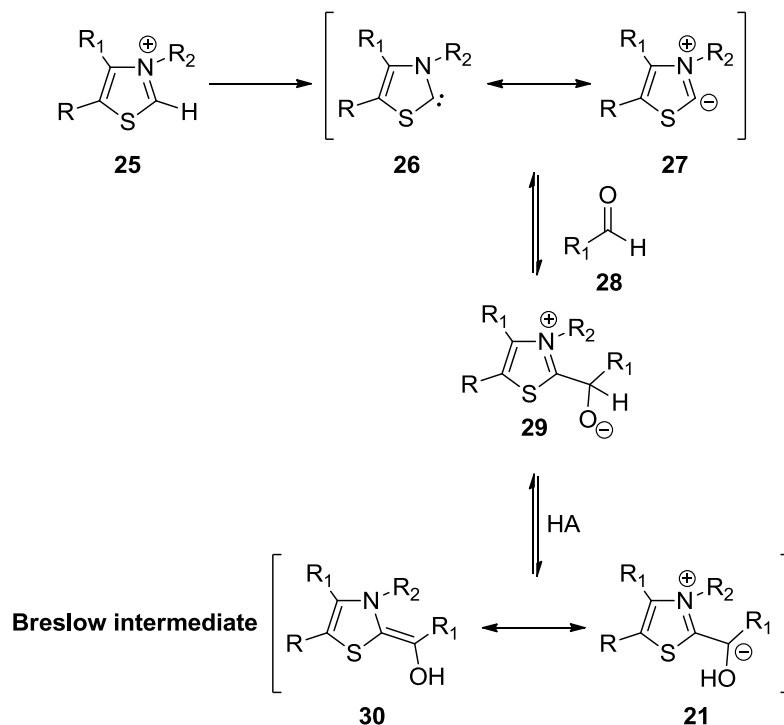
To explain the observed cleavage of (α , β)-carbon-carbon bonds requires that a nucleophilic centre is formed by removal of an existing proton on or near to the central thiazolium ring. In the beginning, Breslow⁽²⁹⁾ established that the protons situated on the CH_2 bridge alpha to the quaternary centre would be acidic enough to permit formation of a stabilised intermediate anion (ylide/carbene). Evidence for this proposal was however refuted when Westheimer “unambiguously confirmed the conclusion that there is no exchange at the methylene group of thiamine”⁽²⁸⁾. This led to ongoing controversy as originally it had been reported that no incorporation of deuterium was observed on the amino pyrimidine ring (scheme 4, compound **23**). In trying to disprove this hypothesis, it was later realised that incorporation had actually taken place upon the thiazole ring at the C2-H position (scheme 4, compound **24**).



Scheme 4: D₂O exchange and sulphite scission of ThDP

Upon realising this mistake, Breslow undertook a deuterium exchange experiment and confirmed the incorporation into the thiazole C2-H bond by ¹H NMR⁽²⁹⁾. As anions on triply bonded carbons are known to be stable⁽³⁰⁾, it is feasible that the acidic “C2-H can ionize and function as a

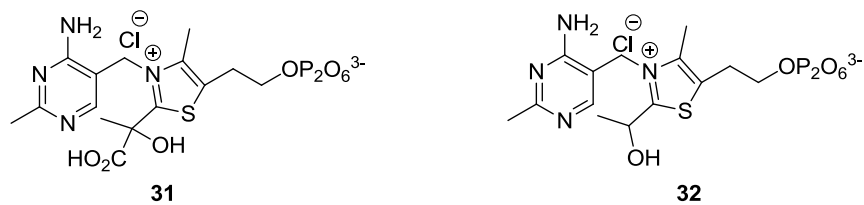
nucleophile or leaving group with respect to carbonyl addition, which is the key part of its function”⁽³¹⁾. The accepted mechanism is shown in scheme 5 and in conjunction with the Lapworth model is used to predict and elucidate mechanisms relating to the benzoin, Stetter and thiamine diphosphate chemistries⁽¹⁰⁵⁾.



Scheme 5: The Breslow intermediate

1.6.2 Thiamine intermediates

Following this supposition by Breslow, other workers began to test this theory by synthesising potential intermediates and analogues. The research groups of Kluger⁽³¹⁾ and Krampitz⁽³²⁾ began isolating the intermediates formed during catalysis and synthesising motifs that exist before the decarboxylation step so that enzyme kinetics and mechanisms could be studied. During the decarboxylation of pyruvate, formation of a covalent adduct was observed as depicted by LTDP in figure 13 (compound 31), to give the intermediate proposed by Breslow⁽³³⁾. Shortly after this, the common decarboxylation step takes place to give HETDP (figure 13, compound 32), but during their testing of these two analogues, it was noted that the apparent affinity of LTDP 31 is much lower in the apo enzyme than that of HETDP 32⁽³⁵⁾.

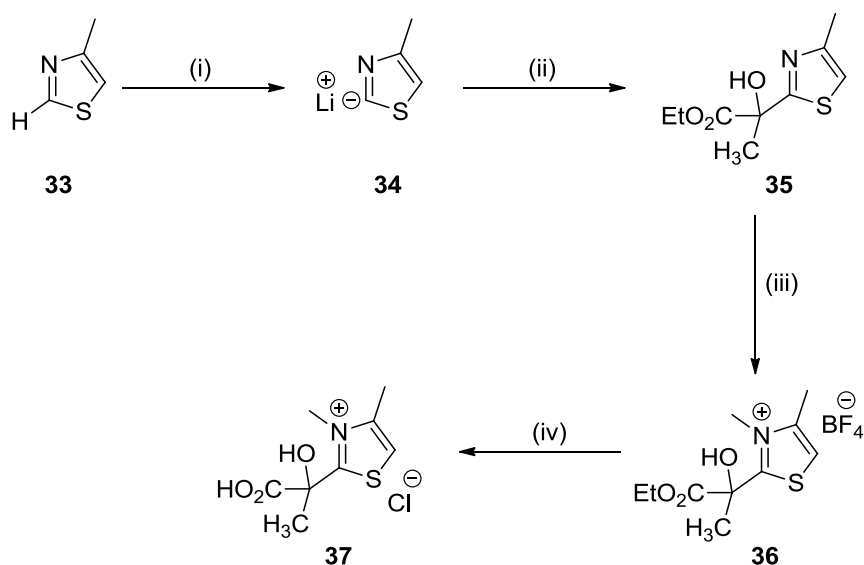


2-(2-Lactyl)thiamin diphosphate (LTDP)

2-(Hydroxyethyl)thiamin diphosphate (HETDP)

Figure 13: Reactive intermediates LTDP and HETDP of thiamine diphosphate

This improved affinity was suggested to originate from the structural resemblance of the transition state between LTDP to HETDP and the stable structure formed after decarboxylation⁽³⁶⁾. At this stage no groups had successfully accomplished the synthesis of a compound that shared a likeness to the intermediate LTDP **31**. As such Lienhard^{(35), (36)} began to synthesise intermediate analogues (scheme **6**), and in subsequent years others began to develop their own derivatives which have permitted additional studies of both non-enzymatic and enzymatic roles^{(31), (38), (39)}.



Reagents & Conditions: (i) *n*-BuLi, (ii) 2,3 pentandione, HCl, (iii) $(\text{CH}_3)_3\text{OBF}_4$, CH_3NO_2 , (iv) anion exchange, HCl.

Scheme 6: Synthesis of the thiazolium LTDP compounds

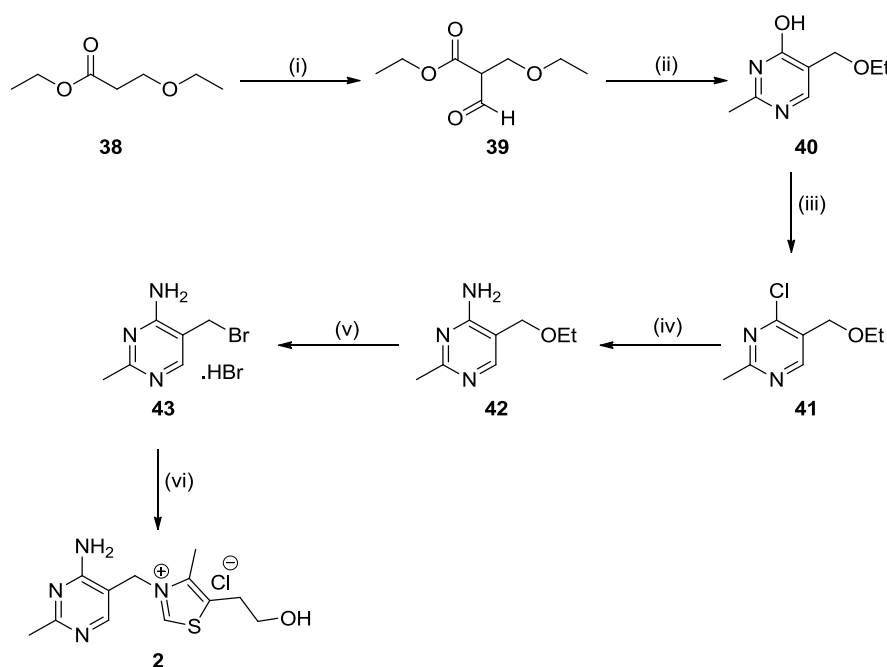
1.7 Thiamine Synthesis

1.7.1 Chemical Synthesis of Thiamine

Shortly after William elucidated the chemical structure in 1935^{(18), (19)}, a synthetic strategy was employed to drive forward additional research on the subject area and to provide an industrial source of thiamine to remedy thiamine deficiencies^{(40), (41)}. Vitamin B₁ is produced by a convergent synthesis which involves the synthesis of the pyrimidine and thiazole rings as shown below in scheme 7, and is now patented by Merck & Co.

1.7.2 Synthesis of Pyrimidine

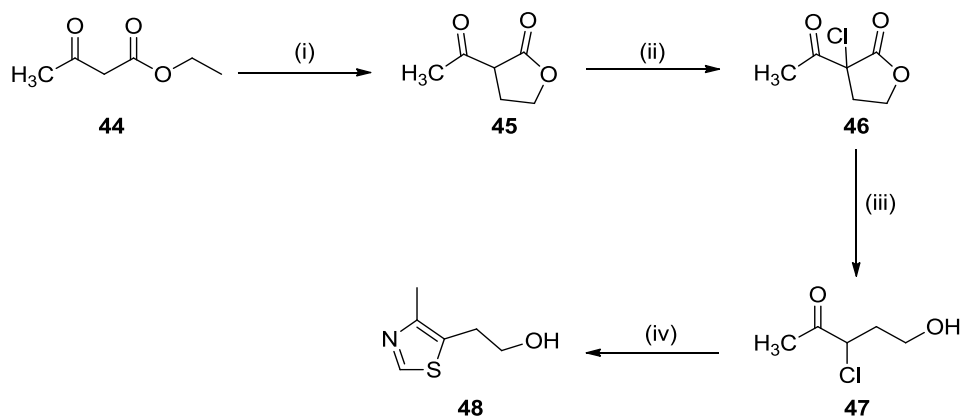
The synthesis⁽⁴⁰⁾ begins with enol-formation of the ethyl-3-ethoxypropionate **38** and subsequent attack onto ethyl formate. Condensation of intermediate **39** with the free base of acetamidine hydrochloride allows creation of the core pyrimidine ring **40**. Treatment with phosphorus oxychloride (POCl₃) then results in the S_NAr displacement of the hydroxyl group to give **41** which on treatment with ammonia solution gives the amine functionality **42**. Addition of hydrobromic acid then completes the synthesis of the pyrimidine scaffold by protonation and S_N2 displacement of the ethyl ether to give **43** as the hydrobromide salt. Treatment of **43** with 4-methyl-5-thiazoleethanol then completes a second S_N2 displacement to give the final structure **2**.



Reagents & Conditions: (i) HCO₂Et, (ii) acetamidine, (iii) POCl₃, (iv) alc. NH₃, (v) HBr, (vi) 4-methyl-5-thiazoleethanol.

Scheme 7: William's pyrimidine synthesis

Although thiazoles could be synthesised via the Hantzsch reaction^{(42), (43)}, an alternative procedure by Buchman follows that outlined in scheme 8⁽⁴¹⁾. This started with α -aceto- γ -butyrolactone compound **44** which undergoes deprotonation and subsequent treatment with ethylene oxide to give the α -ethan-2-ol, which upon cyclisation gives the γ -lactone **45**. Chlorination with sulfuryl chloride then produces compound **46**, and treatment with dilute acid enables ring opening of the γ -lactone to give **47**. Addition of thioformamide then completes the thiazole cyclisation to form compound **48**.



Reagents & Conditions: (i) NaOEt, ethylene oxide, (ii) SO₂Cl₂, (iii) dil. HCl, (iv) HCSNH₂.

Scheme 8: Buchner thiazole synthesis

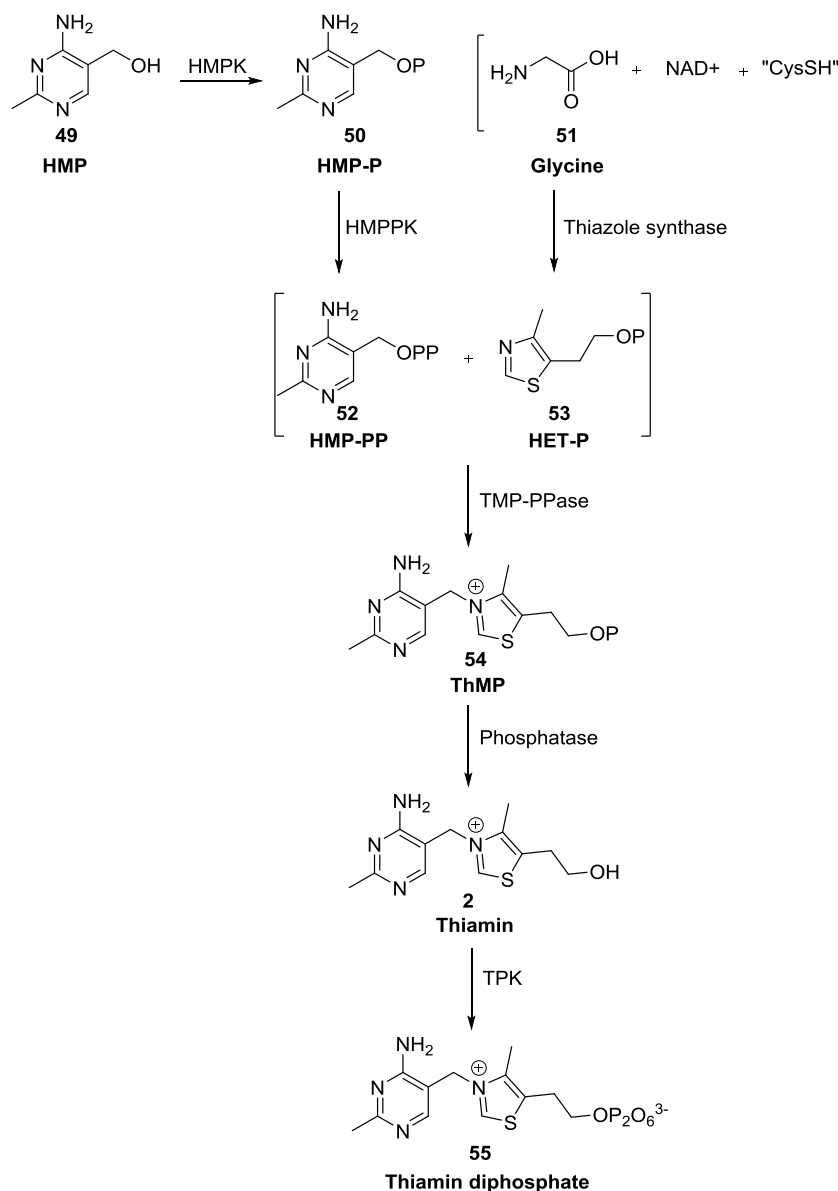
1.7.3 Biochemical Synthesis of Thiamine

Thiamine is utilised by all avenues of life and can be synthesised by fungi, bacteria and plants but cannot be biosynthetically made in humans, which makes it a requirement in our diets⁽⁴⁾. An understanding of these strict mechanistic approaches has allowed the design and development of novel drug targets and pharmaceutical remedies. The biosynthetic pathway for thiamine is intrinsically complex as reported by Webb⁽¹⁷⁾ and each component can be constructed by an assortment of routes depending on the biological species. Just one of the proposed routes to assemble thiamine is by formation of hydroxymethylene methylpyrimidine diphosphate **52** (**HMP-PP**) and hydroxyethylthiazole phosphate **53** (**HET-P**) (scheme 9). Condensation to give the general thiamine monophosphate **54** (**ThMP**) is then achieved under the influence of a thiamine-phosphate synthase enzyme (**TMP-PPase**) and the only difference between the prokaryotic and eukaryotic cells at this stage is the starting materials and genes used to accomplish the initial synthesis of **52** and **53**. In eukaryotes the ThMP can then be hydrolysed to thiamine and

phosphorylated by thiamine phosphokinase (**TPK**) to the catalytically active thiamine diphosphate **55 (ThDP)** (figure 14), or by thiamine monophosphatase.



Figure 14: Thiamine phosphokinase conversion of thiamine



Scheme 9: Biosynthesis of thiamine in yeast

1.7.4 Biosynthetic Inhibition (Bacimethrin)

As novel antibiotics and anti-cancer remedies are required, alternative approaches in synthesis and design are being devised. One such route could utilise the interruption of thiamine biosynthesis⁽⁴⁴⁾ as proposed in the previous section (scheme 9). Structural similarities to the HMP precursor in the HMP-P synthesis have been reported in the isolated compound bacimethrin (figure 15, compound 56) from *Bacillus megaterium* which has shown strong inhibitory effects against both eukaryotic and prokaryotic mediums⁽⁴⁵⁾.

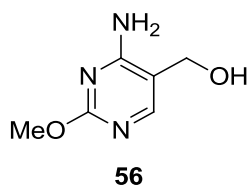
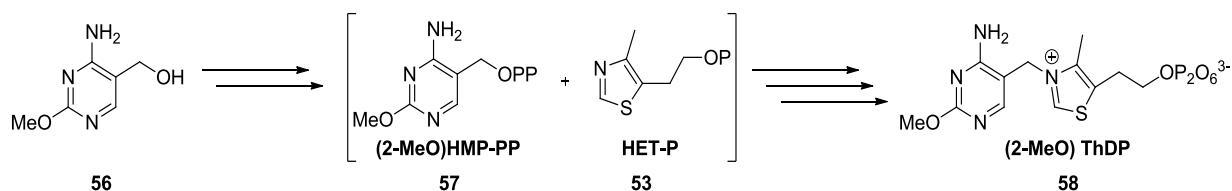


Figure 15: Bacimethrin analogue

The proposed inhibitory effect of bacimethrin is due to the mimicking of compound 49 (HMP) and assimilation of the typical biosynthetic pathway to produce the antimetabolite 2-methoxythiamin (2-MeO-ThDP) (scheme 10, compound 58).



Scheme 10: Bacimethrin inhibition of thiamine biosynthetic pathway

The corresponding synthesis of bacimethrin 56^{(46), (47)} and its analysis have indicated that 57 is converted into the active inhibitor 58 much faster than the normal HMP pathway. So the resultant toxicity is derived from the final 2-MeO ThDP 58. Proof of this was obtained by gene mutation of the kinase enzyme (HMPK) as shown above in scheme 9, whereby HMP 49 or 2-MeO-HMP 56 are converted into their monophosphate derivatives HMP-P/2-MeO HMP-P⁽⁴⁸⁾.

1.7.5 RNA Regulation and ThDP Riboswitch Inhibition

As these biosynthetic pathways are regulated by riboswitches it is important to discuss an exciting trick that thiamine is able to accomplish by self-regulation of its biosynthesis. The riboswitch is a folded region of mRNA that can be accessed by interaction with the specific coenzymes upon

its aptamer region. This aptamer section controls the intrinsic nature of the tRNA by undergoing a conformational change upon binding to a coenzyme. This results in changes to the amino acid sequence and the final protein structure that is assembled. Subsequent research has identified the thiM gene as one such region that can undergo such a change upon binding of TPP in prokaryotes⁽⁴⁹⁾ and “prevents translation of the mRNA and triggers down-regulation of its own biosynthesis if available at sufficient concentrations”⁽⁵⁰⁾. The structure of the RNA is Y-shaped⁽⁵¹⁾ and the aminopyrimidine and diphosphate groups are bound between the tips of the “Y” motif into two regions defined as the pyrimidine (P2-P3) and diphosphate helices (P4-P5) (figure 16).

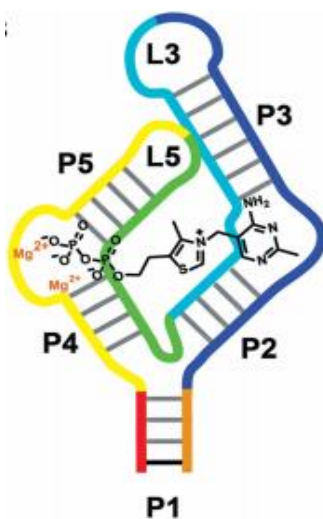


*Image taken from reference (50)

Figure 16: Y-shaped ThDP ribosome

Research has primarily focused on the structure relationships of the ThDP moiety to the TPP riboswitch and the regions concerning binding. Various studies^{(52), (49), (51)} have proved the roles played by the pyrimidine ring in binding and these ThDP analogues have been tested for their affinity. It has been noted that the central 5-membered ring and diphosphate are not as important for the TPP riboswitch when compared to thiamine dependant enzymes and it is only affected by manipulation of the 6-membered aromatic ring as seen in figure 17 which shows the percentage displacement of the natural ThDP ligand^{(7), (31)}. This structural relationship provides the basis for the synthesis of other motifs that prevent mRNA transcription at the aptamer region, therefore preventing translation by tRNA, and thus inhibiting cell proliferation and acting as an anti-tumour agent.

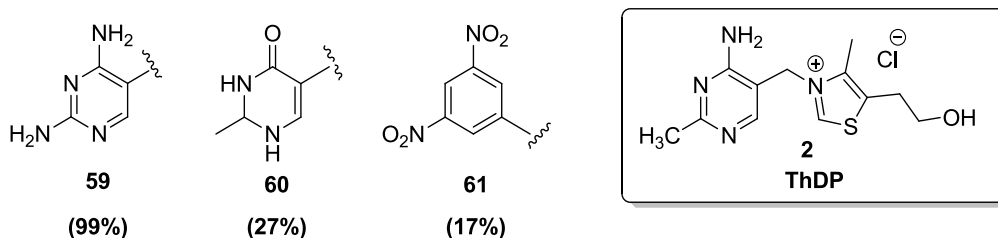


Figure 17: Variants of the A ring in ThDP for aptamer binding in mRNA

1.7.6 Vitamin B₁ Deficiency

The primary reason for all these synthetic and structural elucidations is due to the problems associated with thiamine deficiency in general. A deficiency of any vitamin usually renders one or more biological pathways useless as the vitamins acquired through the diet are frequently converted by their respective biosynthetic routes into the active cofactors. In the absence of thiamine, polyneuritis or cardiovascular failure occurs, which can manifest itself in multiple ways including the conditions of beri-beri and Korsakoff syndrome. In cases where beri-beri exists the patient can exhibit either wet or dry beri-beri which both show devastating effects upon the function of the peripheral nervous system. Dry beri-beri is usually defined as a condition relating to the failure of peripheral nervous system (PNS) whereby motor and sensory dysfunctions are observed, whereas wet beri-beri affects the cardiovascular system. Korsakoff's syndrome is strongly related to the nervous system and can be brought on by increased consumption of alcohol which interferes in the conversion of thiamine to thiamine diphosphate. General symptoms of this include confabulation (memory disturbances), memory loss and severe changes in mood. All of these symptoms are related to poor malnutrition or impaired uptake of thiamine within the diet and some of the drugs designed to combat this are illustrated below (figure 18).

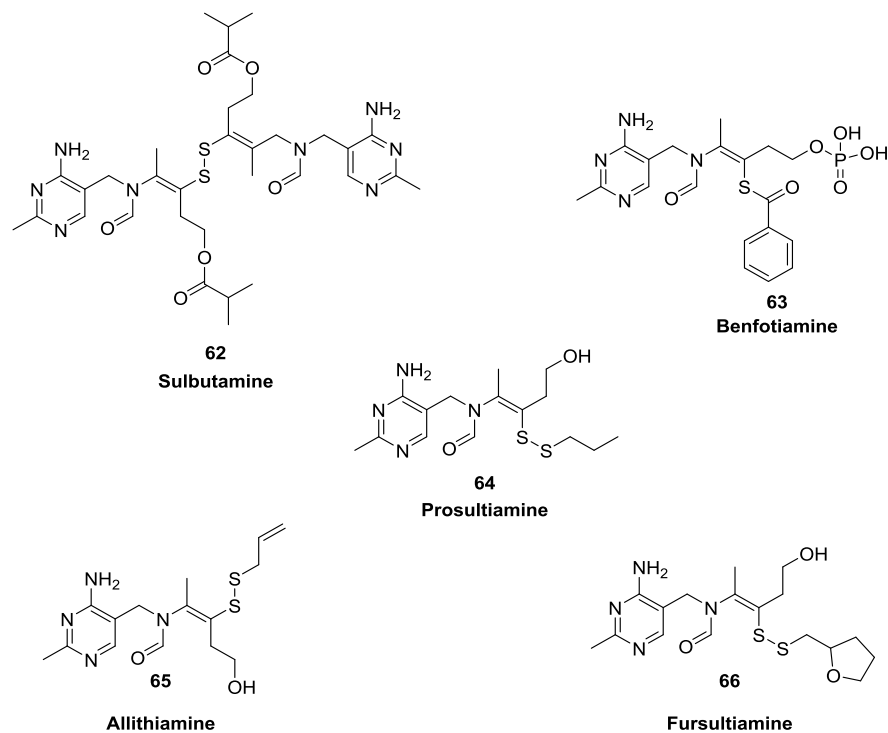


Figure 18: Drug candidates for thiamine deficiency

1.8 Non-Enzymatic ThDP Roles

1.8.1 Cyclodextrins

Artificial enzymes have been exploited as mimics of enzymatic pathways without the use of the protein scaffolds. Many research groups have utilised the architecture of calixarenes and cyclodextrins with their inherent hydrophobic core as a potential site to bind substrates⁽¹⁰⁶⁾. Using this technique allows the enzyme active site to be mimicked whilst modifying the outer rings with functional groups resembling that of the natural biosynthetic pathways. One such example of this was described by Breslow^{(28), (30)} who demonstrated that biomimetic chemistry could be facilitated by using either a β -cyclodextrin or γ -cyclodextrin (figure 19).

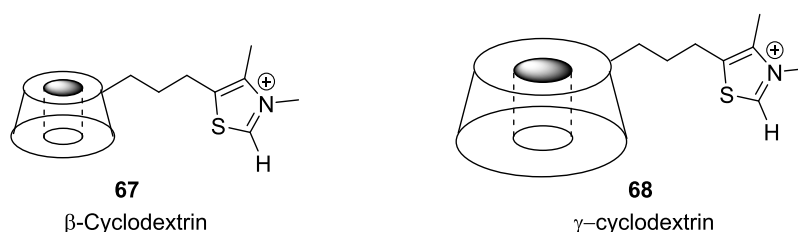
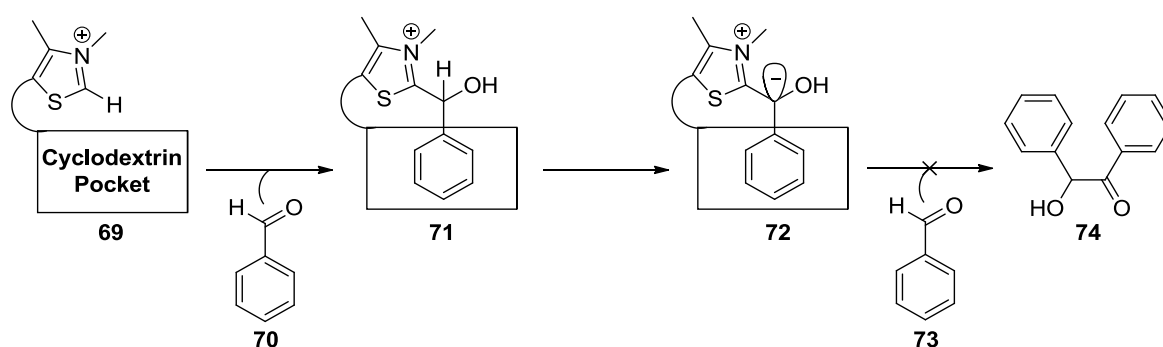


Figure 19: Breslow's ThDP β -cyclodextrin or γ -cyclodextrin mimics

In this example, the use of the thiamine diphosphate pathways *in vivo* shows the potential for the central thiazole ring, and its ability to form the reactive ylide/stabilised nucleophilic carbene

“Breslow intermediate” as a suitable reactive feature. By extending this group from the cyclodextrin ring and utilizing the hydrophobic pocket, an increased rate of acceleration was observed when the respective reactants were in close proximity. As a test reaction, the 7-glucose unit of β -cyclodextrin **69** was reacted with benzaldehyde **70** inside the hydrophobic pocket of the cyclodextrin (scheme **11**)⁽¹⁰⁶⁾. The thiazolium component could then undergo its normal addition to benzaldehyde to form the thiazolium adduct **71** which resembles that of the cyanohydrins observed in the benzoin condensation⁽¹⁰⁵⁾. The benzylic anion **72** was then generated, but unfortunately the test benzoin condensation was not successful as the smaller pocket of the β -cyclodextrin did not allow for a second molecule of benzaldehyde **70** to enter the pocket.

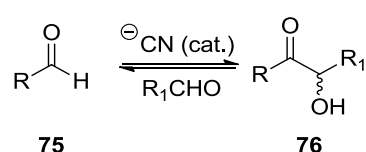


Scheme 11: Mechanism for Breslow β -cyclodextrin or γ -cyclodextrin mimics

Upon using the γ -cyclodextrin with the larger pocket, the reaction proceeded with a 150 fold increase in rate compared to that of the free thiazolium salt. This example is just one of many that display how the functional groups utilised in a biological system can be implemented to carry out a similar function without the normal protein structure. In accomplishing this useful piece of synthetic chemistry, Breslow has highlighted how useful biomimetic chemistry is in the design and synthesis of chemical motifs.

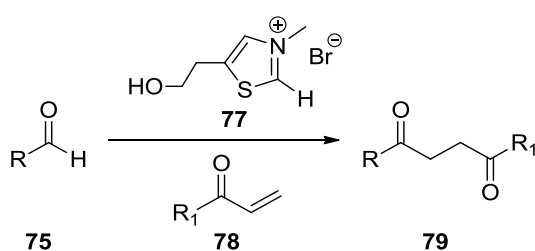
1.8.2 Stetter & Benzoin Pathways

An alternative use of thiamine *in vitro* can include the chemical transformation of aldehydes by employing the central thiazolium ring to act as a nucleophilic carbon with reversed polarity (umpolung synthon) to facilitate the benzoin (scheme 12) and Stetter reactions (scheme 13)⁽⁵³⁾. The synthetic use of thiamine is preferred to the classic cyanide catalyst in the Stetter reaction as aliphatic aldehydes can undergo aldol condensations. Additionally cyanides exhibit high toxicity and remain a significant problem. Generally these reactions are of great synthetic value as the benzoin condensation is able to create important chiral α , β -hydroxyketones, which after further modification can lead to vast chemical libraries.



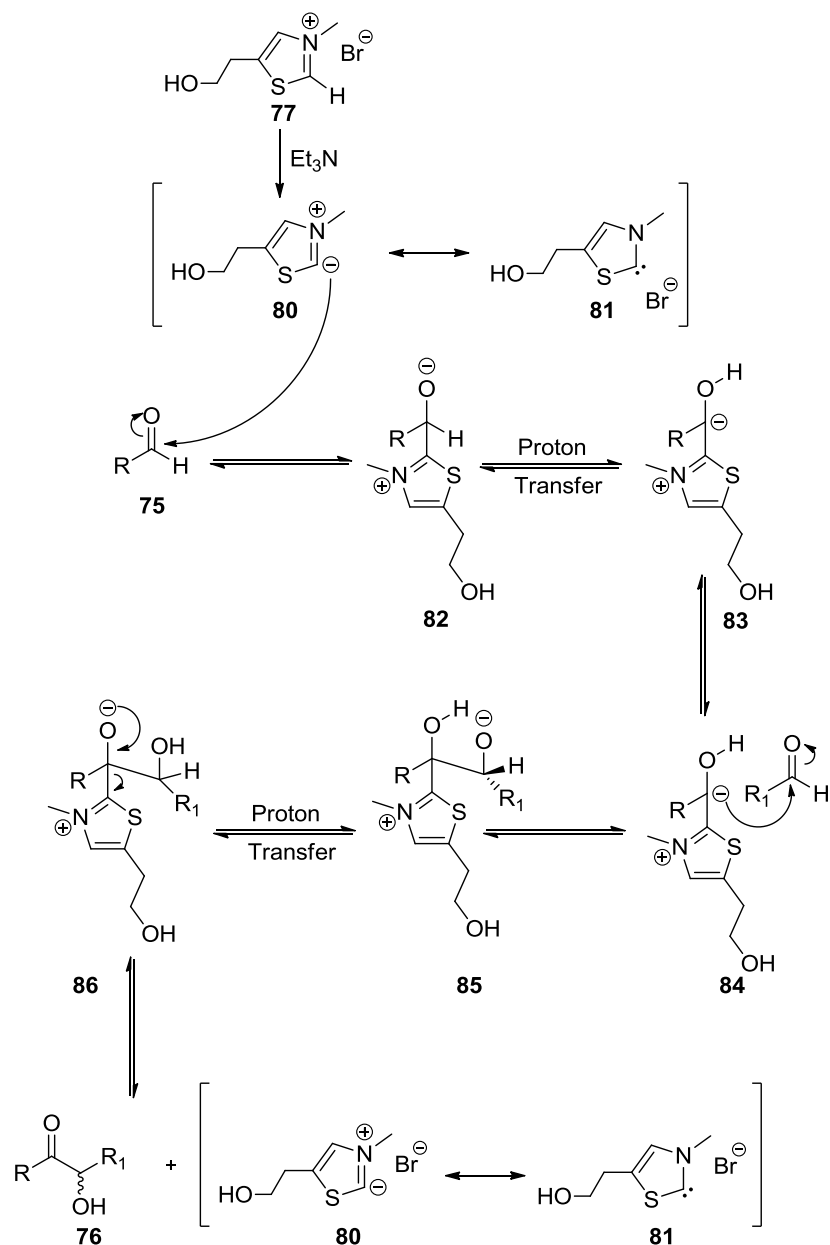
Scheme 12: The benzoin condensation

Furthermore, the Stetter reaction uses the 1,4-Michael addition of the intermediate thiazolium zwitterion onto the alkene to promote construction of a 1,4-dicarbonyl species, which can be difficult to obtain by alternative synthetic strategies. 1,4-dicarbonyl compounds are useful intermediates in the formation of 5-membered heterocycles in the Paal-Knorr process^{(54), (55)}.



Scheme 13: The Stetter reaction

Mechanistic studies for both the benzoin and Stetter reactions follow the same pathway (scheme 14), whereby the “Breslow intermediate” is adopted as described previously in scheme 5. The carbene-ylide tautomer then undergoes umpolung nucleophilic attack upon the desired electrophile to give the respective 1,2- or 1,4-addition products. Benzoin reactions take place faster, tend to be reversible and can revert to their starting aldehyde by kinetic control in an aprotic solvent. In contrast, the Stetter reaction is not reversible after addition to the Michael acceptor as it eliminates the thiazolium catalyst to give the 1,4-diketone⁽⁵³⁾.

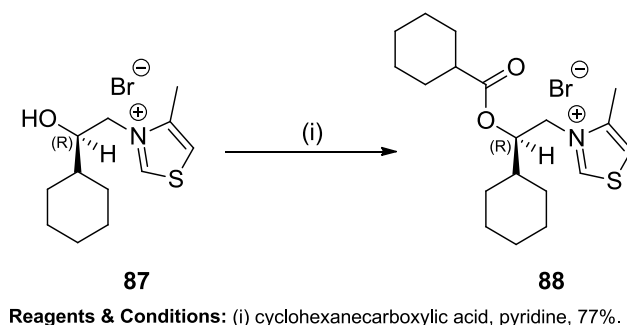


Scheme 14: Mechanism of thiazole catalyzed benzoin reaction

1.8.3 Asymmetric Benzoin & Stetter

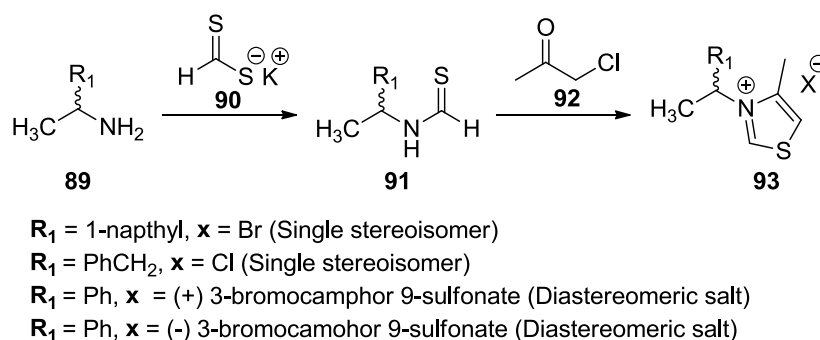
Due to the noticeable power of thiamine's central thiazolium ring in the creation of C-C bonds during the enzymatic pathway, research groups rapidly sought to utilise this chemistry for enantioselective benzoin^{(56), (57)} and Stetter pathways⁽⁵⁵⁾. During the 1960s Sheehan⁽⁵⁶⁾ developed one of the first chiral thiazolium salts that did not require the use of cyanide and could carry out homogeneous enantioselective reactions. *N*-(2-Phenyl-2-hydroxyethyl)-4-methylthiazolium bromide **87** was converted into its camphor sulfonate and then recrystallised to give an optical

rotation of $+76.3^\circ$ (c. 1.29, EtOH). Treatment of (+)-**87** with cyclohexanecarboxylic acid anhydride then gave **88** but in a low enantiomeric excess of 22%.



Scheme 15: First synthesis of chiral thiazolium salt

Further modification of this methodology was made nearly a decade later by Sheehan who utilised the core thiazole motif with two further enhancements including the formation of a chiral centre alpha to the quaternary nitrogen and substitution with a larger group. The synthesis of these salts is shown by scheme **16**. Formation of these chiral thiazolium salts and/or their analogues was then postulated to impart enantiofacial selectivity during addition of the Breslow intermediate to the aldehyde group. This enantioselectivity was implemented by the steric interactions of the substituted groups (R_1) on the α -carbon of the thiazole ring **93** to give either single stereoisomers or diastereoisomeric salts (scheme **16**).



Scheme 16: Synthesis of chiral thiazolium salts

These salts however produced mixed results, as the increase in steric bulk on the α -carbon resulted in a higher enantioselective excess when ($R_1 = \text{naphthyl}$) but with low yields. In contrast to this, high yields were observed when ($R_1 = \text{phenyl}$), but with very low ee%. Sheehan *et al.*⁽⁵⁶⁾ developed a model (figure **20**) to explain this diastereotopic relationship in which addition of the thiazolium

anion to the first mole of aldehyde produces a planar anion that undergoes a second nucleophilic addition onto the *Re* face of the aldehyde, opposite to that of the bulky R_1 group.

Addition to *Re* Face

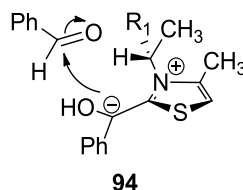


Figure 20: Asymmetric benzoin condensation using chiral thiazolium salts

1.9 Thiamine Diphosphate Enzymes

The thiamine diphosphate enzymes are vastly complex and have been shown over many decades to have established well defined chemistries that carry out specialist roles within nature. Some examples of these include pyruvate dehydrogenase, transketolase and pyruvate decarboxylase⁽⁵⁸⁾,⁽⁵⁹⁾ (figure 21). A brief outline concerning PDC and PDH will be explained although there are many other examples of thiamine dependant enzyme systems that will not be discussed in detail here.

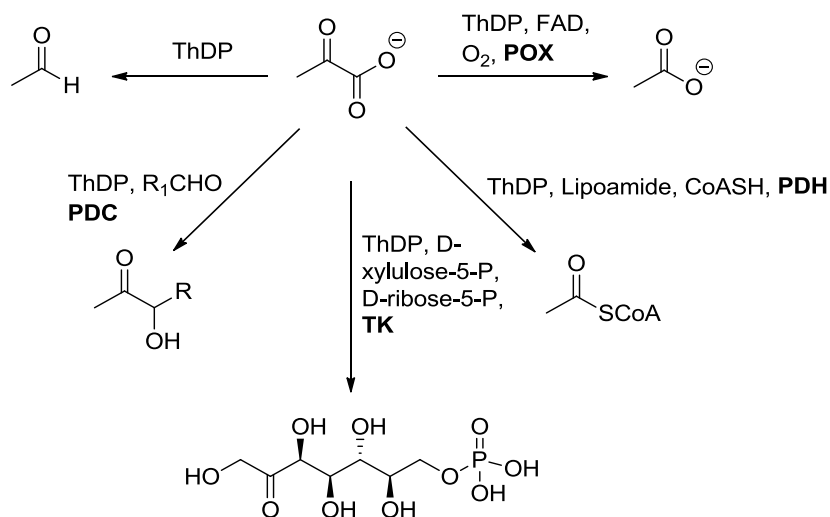
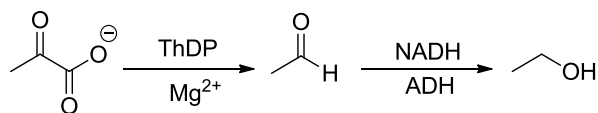


Figure 21: Examples of ThDP catalysed reactions

1.9.1 Pyruvate Decarboxylase (PDC)

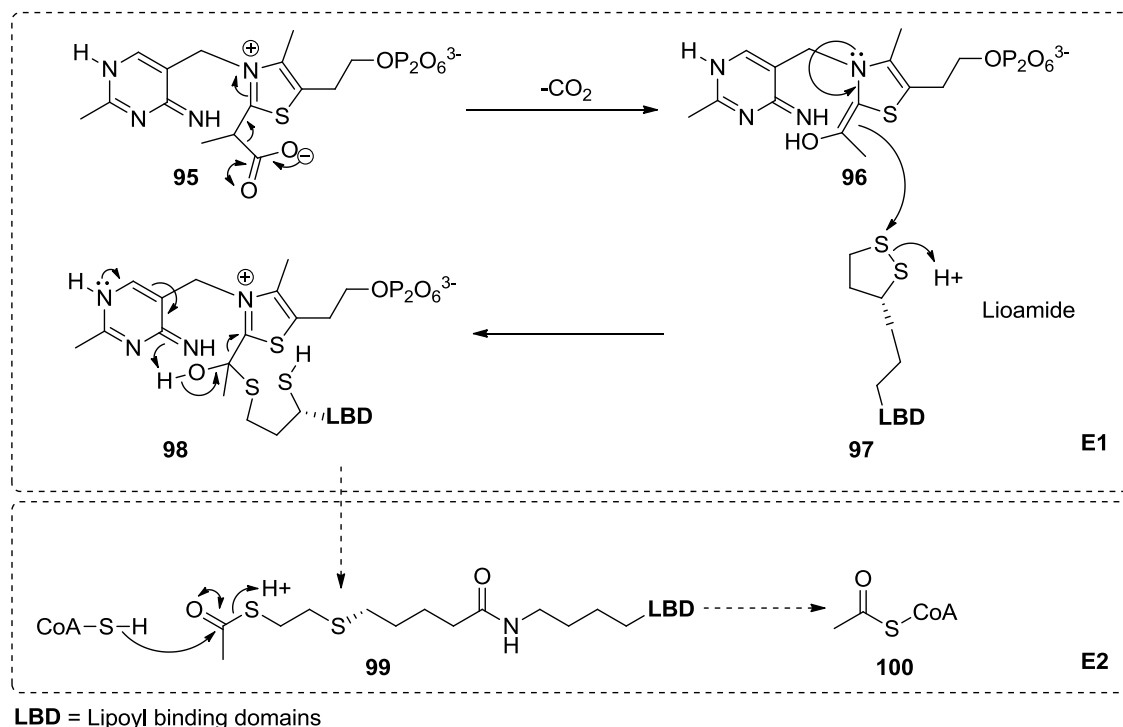
The pyruvate decarboxylase enzyme is primarily concerned with the conversion of pyruvate into acetaldehyde prior to reduction into ethanol during the fermentation process, as proposed earlier by the Breslow intermediate (scheme 17) ^{(58) (60) (30)}.



Scheme 17: PDC enzymatic pathway

1.9.2 Pyruvate Dehydrogenase

The pyruvate dehydrogenase enzyme is part of a larger enzyme complex that carries out the synthesis of acetyl CoA, which is extremely important in the citric acid cycle ^{(60), (59)}. After formation of the intermediate **95** in scheme 18, decarboxylation and reductive acetylation of lipoamide **97** then takes place by attack upon the disulfide linkage. Subsequent collapse of the intermediate **98** ejects acetyl CoA **100** which goes on to react further in the E2 subunit of the pyruvate dehydrogenase complex via the lipoyl binding domain (**LBD**) and eventually the citric acid cycle.



Scheme 18: Initial E1 & E2 stages of the Pyruvate dehydrogenase complex (PDH)

1.9.3 General Enzyme Structure

ThDP dependant enzymes tend to consist of four nearly identical subunits forming a homotetramer as highlighted by the differing colours in figure 22. Further examination of the structure shows that its catalytic form can be described as a “dimer of dimers” and gives the minimal functional unit for catalysis and its asymmetric behaviour ^{(61), (62)}.

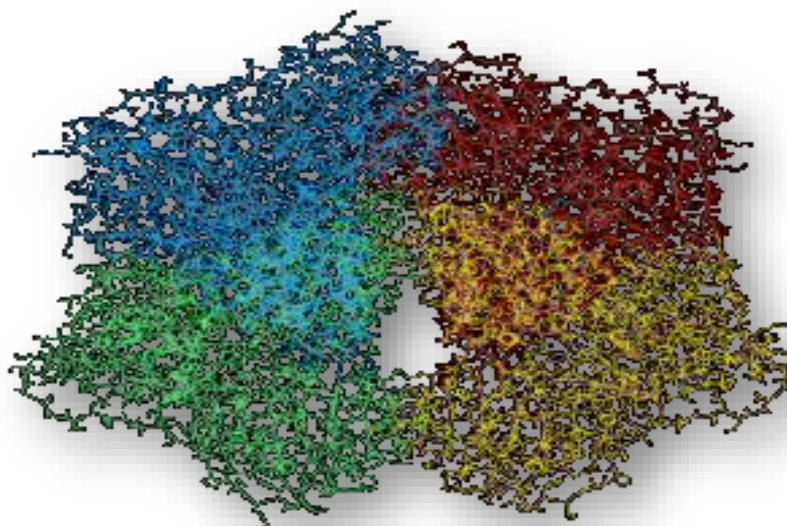


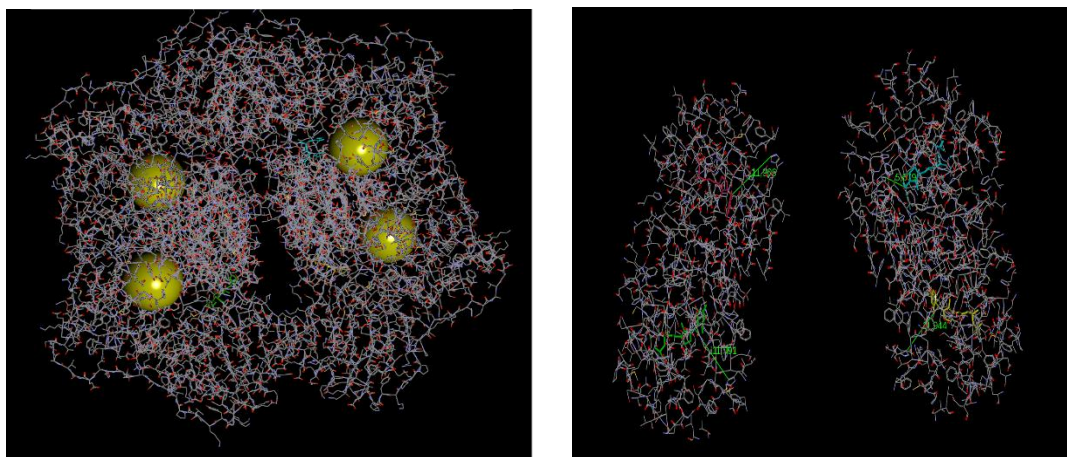
Figure 22: Pyruvate decarboxylase homotetramer assembly

Each dimer can be regarded as an identical entity related by a 2-fold symmetry axis ⁽⁵⁹⁾. Each dimer contains two separate monomer units ($2 \times \alpha$) and ($2 \times \beta$) which can be further subdivided into three domains which are denoted pyr, opp, and R respectively with each having varying degrees of binding within the active site ⁽⁷⁾.

1.9.4 ThDP Active Site of Pyruvate Decarboxylase

In 1993 Lindqvist *et al.* ⁽⁶¹⁾ reported that although enzymes differ in their final biosynthetic goals, they achieve these using a conformation and binding of the ThDP cofactor which is the same and even when the quaternary structures of the enzymes differ vastly ^{(62), (63)}. ThDP enzymes are known to exist in tetrameric forms that contain four ThDP ligands and Mg^{2+} ions. The active dimer therefore contains two ThDP molecules and two magnesium ions per dimer (figure 23) ⁽⁵⁹⁾. It is common to find the ThDP cofactor and its Mg^{2+} ions bound in a enzymatic cleft between each of the asymmetric monomer units of the dimer using the α and γ domains. This causes the ThDP to be located in a deep hydrophobic active site of 10 Å wide and 8 Å deep ⁽⁵⁹⁾. The aminopyrimidine

ring is associated with both the α and γ domains denoted (PYR), whereas the diphosphate is bound almost exclusively in the γ domain denoted as (OPP) ⁽⁶²⁾.



Figure's 23: Graphical presentation of four ThDP active sites (2 ThDP per dimer)

For the ThDP cofactor to be recognised in all classes of pyruvate catalysed pathways, requires that a specific thirty unit amino acid sequence is maintained within the γ domain ⁽⁵⁹⁾. This domain is found to stabilise the diphosphate section of the ThDP cofactor by binding of the anionic oxygens to a divalent Mg^{2+} cofactor in an octahedral geometry, formed by the amino acids Asp444, Asn471, Gly473, the two diphosphate oxygens and a water molecule (figure 24) ^{(59), (7)}. This compares to the amino pyrimidine ring which does not require the same conserved amino acid residues but undergoes activation via a similar pathway. It is generally accepted that the N'1 of the aminopyrimidine ring is H-bonded to the glutamic acid residue (Glu50 PDC-Zm/51 PDC-Sc) whilst N'3 is H-bonded to Ile 415 and Gly473 with N'4 ^{(59), (64)}.

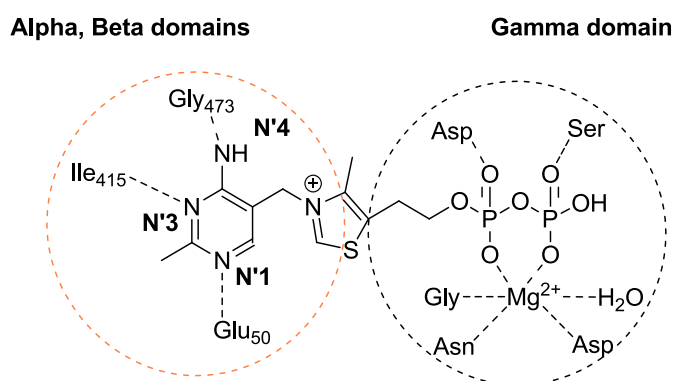
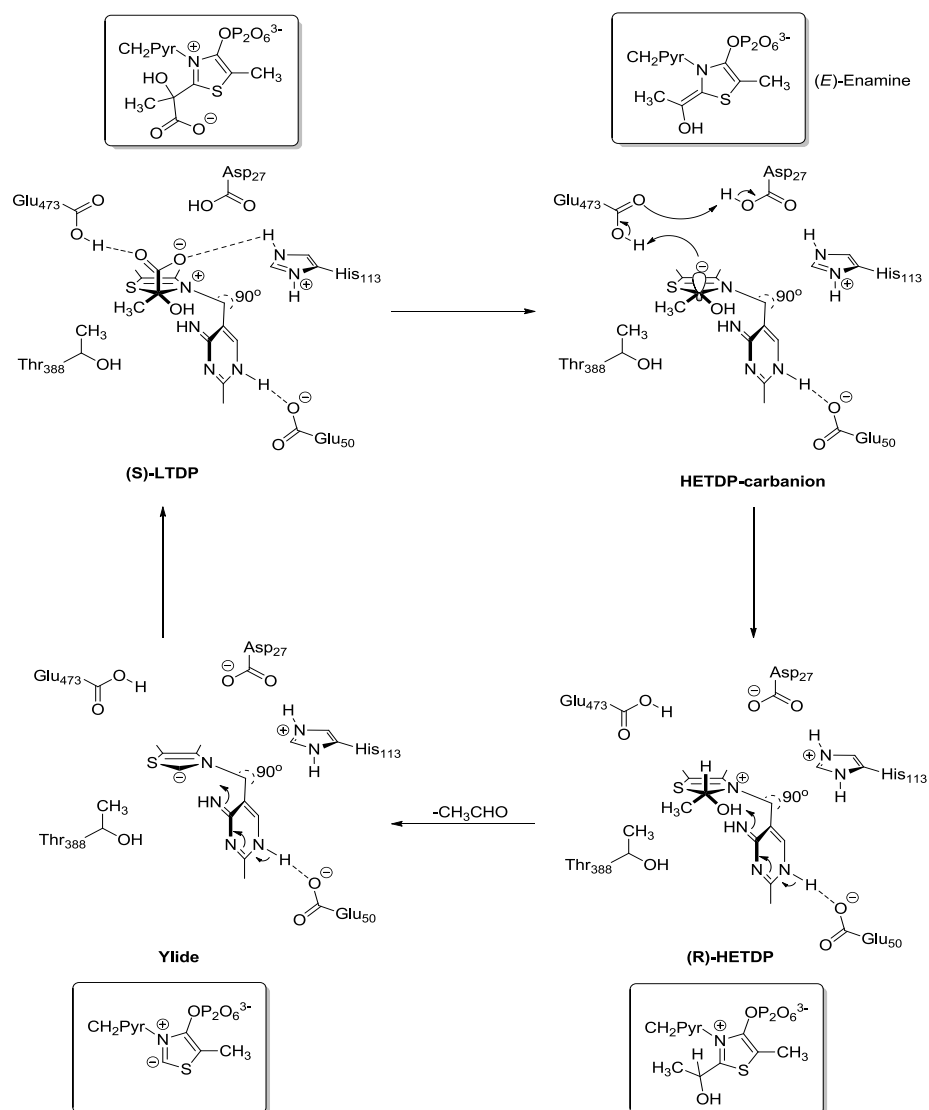


Figure 24: α , β & γ binding domains of PDC ThDP enzyme

The interaction of these glutamic acid residues (Glu50/51) with the N'1 nitrogen is typical of this domain and consequently initiates the imino-amino tautomerisation to promote abstraction of the

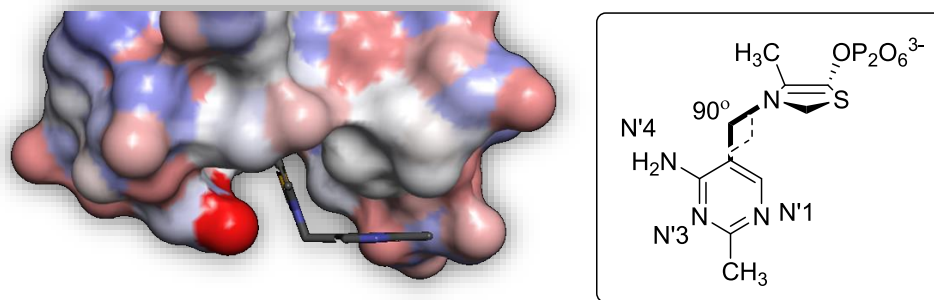
proton (pK_a 17-19) on the C-2 thiazolium ring by the imino-amine N⁷4⁽⁵⁹⁾ (scheme 19). Further evidence for this mechanism was proved by Schellenberger⁽⁶³⁾, who sequentially exchanged the nitrogens located in the pyrimidine ring with those of the carbon framework to observe what happened to catalysis. Site directed mutagenesis of Glu50/Glu51 indicated that this prevents catalysis due to its primary role in activation of the imino-amine tautomeric forms.



Scheme 19: Activation and amino acid triad for ThDP catalysis

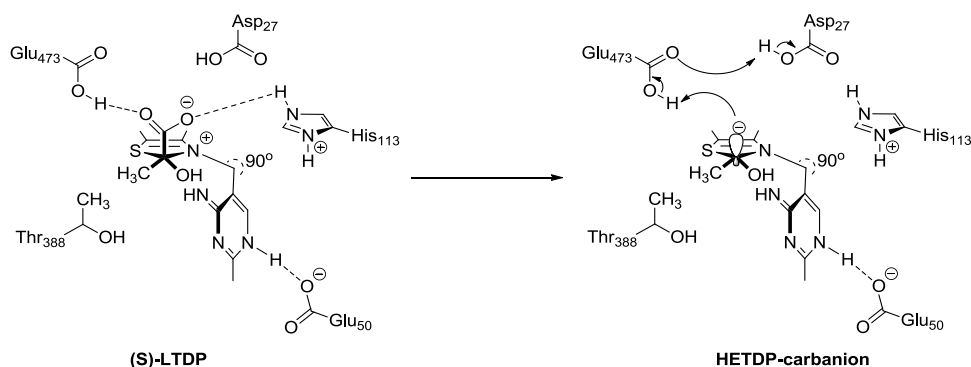
Further assistance to this mechanism is provided by the lower pK_a of the glutamic acid (pK_a 4) compared to the pK_a of the N⁷1 which exists at (pK_a 5-6) therefore favouring the acid-base catalysis and proton transfer from the acid to the imino group⁽⁵⁹⁾. This binding across the dimer-dimer interface causes the reactive thiazolium ring to be situated in the middle of the enzymatic cleft for optimum catalysis conditions. ThDP is stringently conserved in a “V” conformation

throughout all classes of ThDP enzymes by interactions with the hydrophobic Ile415 which holds the central thiazolium ring close enough the pyruvate keto group, and distinguishes the two proposed conformations of C2-substituted (**S**) with a torsion angle of ($\varnothing_T = 100^\circ$, $\varnothing_P = 150^\circ$) and free (**F**) with angles of ($\varnothing_T = 0^\circ$, $\varnothing_P = 90^\circ$) for the thiazolium and aminopyrimidine rings in relation to the methylene bridge ^{(65), (59)} (figure 25).



Figures 25: Free conformation torsion angles of ($\varnothing_T = 0^\circ$, $\varnothing_P = 90^\circ$) for the thiazolium and aminopyrimidine rings in relation to the methylene bridge of PDC

Forcing of the reactive thiazolium C2 anion towards the pyruvate provides an intermediate carboxylate which is tightly bound within the pocket⁽⁷⁾, stabilised by the amino acids Asp27, His113, His114, Thr388 and Glu473 (scheme 20, (S)-LTDP). Decarboxylation then proceeds rapidly as the tetrahedral intermediate collapses to release steric strain, and allows the resultant HEDPT-carbanion to become immediately stabilised by the perpendicular Glu473, which is thought to promote an acid-base proton shuttle between itself and Asp27 ⁽³¹⁾. This incidentally results in inhibiting the reaction with another pyruvate molecule due to the ionisation of Asp27 which now repels any further substrate molecules. At this point the cofactor-bound hydroxyl-ethyl intermediate as shown above in scheme 19 promotes the release of acetaldehyde and re-generates the ylide/carbine for further catalysis.



Scheme 20: (S)-LTDP conversion to HEDPT-carbanion

A final interesting point regarding these active sites is that they are non-equivalent during catalysis with only one active site participating in catalysis at any one time whilst the other three remain dormant ⁽⁶³⁾. This was first identified in transketolase and was then found in all ThDP enzymes and gave rise to the alternating sites theory (AST), which proposes that a reversible proton wire is used to communicate between the ThDP ligands in each active site ⁽⁶⁶⁾, thus dictating the catalysis allowed per catalytic cycle (figure 26).

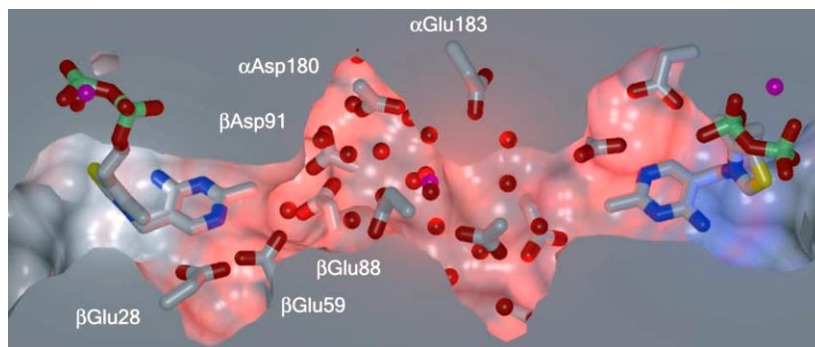


*Image taken from reference (66)

Figure 26: Site communication and proton wire between two ThDP ligands

1.10 Thiamine Analogues for Studies of ThDP Active Sites

As the development and understanding of thiamine diphosphate grew, the scientific community started to probe further how this small molecule was involved in so many biological pathways. To study the modes of action, many research groups made significant modifications to the thiamine framework (figure 27) whereby changing certain functionalities might render thiamine inactive and hence help in elucidating the biochemical mode of action by binding long enough to acquire x-ray data. Alternatively additional groups were added in the hope that this may allow the transition state of the pathways to be investigated or its interactions with amino acids in the active site to be elucidated/confirmed.

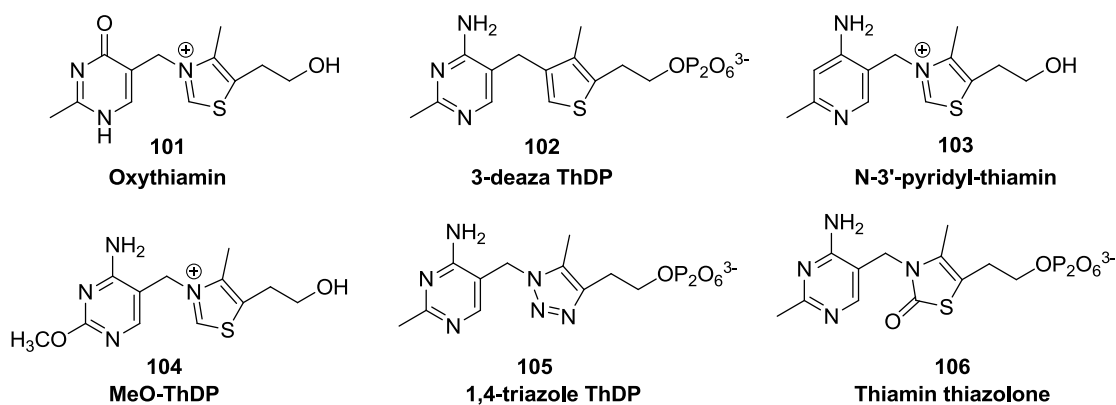
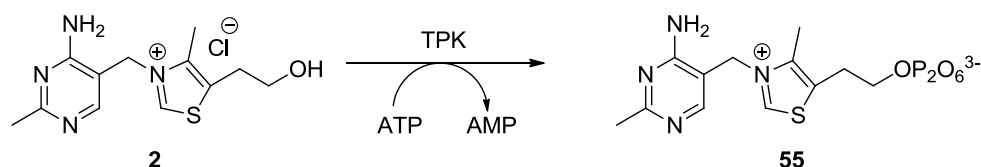


Figure 27: Structural analogues of vitamin B₁

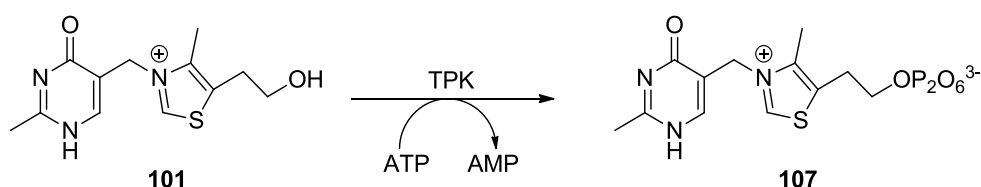
1.10.1 Pyrithiamine & Oxythiamine

The lack of thiamine within the diet has already been shown to cause the Wernicke-Korsakoff syndrome as noted above and the start of these deficiencies can arise from disruption to thiamine diphosphate (ThDP) production. This is normally catalysed by the enzyme thiamine pyrophosphokinase whereby ATP is utilized to transfer phosphates onto the hydroxyl of thiamine to generate the active thiamine diphosphate (ThDP) (scheme 21).



Scheme 21: Biosynthesis of ThDP

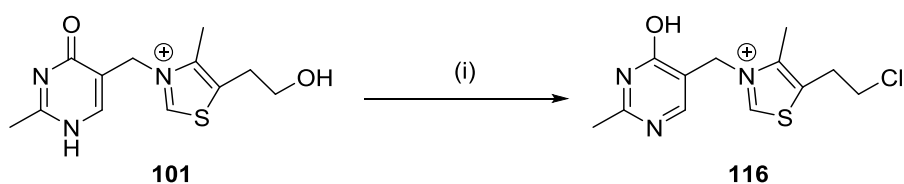
Oxythiamine and pyrithiamine are two classes of inhibitors that have been synthesised to investigate the mechanism of thiamine deficiency by promoting effects similar to those observed in patients suffering from these types of disorders and/or from long term alcoholism ^{(67), (68)}. Inhibiting the thiamine phosphokinase enzyme (TPK) with pyrithiamine or oxythiamine ⁽⁶⁹⁾ allowed the widespread testing of catalytic routes within many types of biological systems. One intriguing fact is that the behaviours of oxythiamine and pyrithiamine upon the test substrates are very distinct and generate different symptoms. Generally the administration of oxythiamine produces feelings of lethargy and induces anorexia whilst showing no observed behaviours relating to the Wernicke-Korsakoff syndrome ⁽⁶⁹⁾. It is thought that oxythiamine **101** is a potential competitive inhibitor for the TPK enzyme by undergoing conversion to the active oxythiamine diphosphate **107** (scheme 22) and therefore interferes with the catalysis via exchange of the hydroxyl moiety for the more frequently seen amino (4-NH₂) functionality as depicted in scheme 21.



Scheme 22: Enzymatic TPK conversion of oxythiamine to oxythiamine ThDP

1.10.3 Synthesis of Oxythiamine

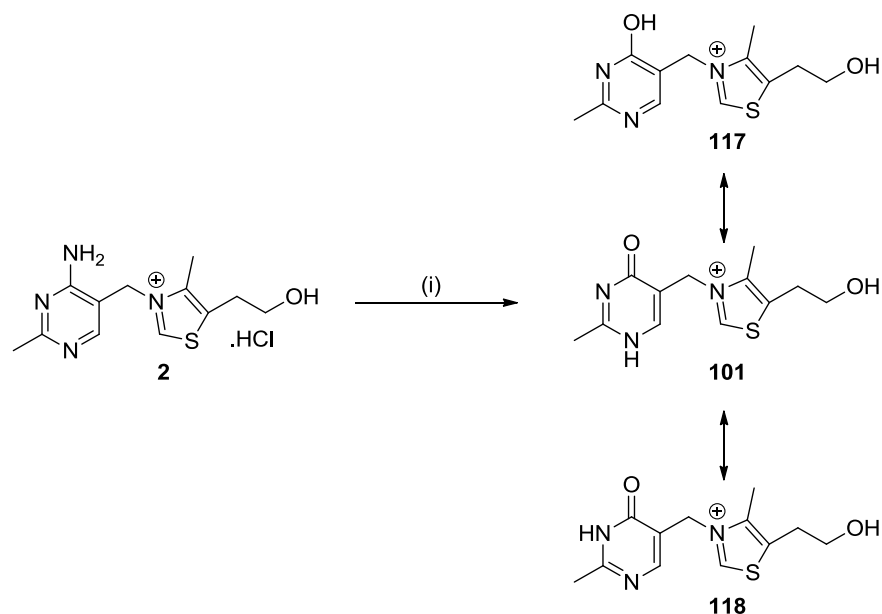
In 1950, efforts were made by Rydon *et al.* ⁽⁶⁷⁾ to improve on the already reported synthesis of oxythiamine, as previous synthetic routes by Bergel & Todd ⁽⁷²⁾ were long-winded and arduous. Meanwhile, other groups including Cerecedo, Soodak ⁽¹¹¹⁾ and Eusebi ⁽⁷³⁾ reported making the inhibitor in yields of 50-70%. Previous studies of the structure of thiamine had revealed that using strong acids and excessive heating of 150 °C gave the formation of an alternative product to thiamine ⁽⁷⁵⁾. Some of these observations included a report that the addition of 2N HCl releases one mole of ammonia whilst not removing the sulfur atom ⁽⁷⁶⁾. The addition of strong acid also seemed to inactivate the vitamin towards its normal synthetic tasks ⁽⁷⁷⁾. From the general chemical properties of crystallisation and with the empirical formulae both containing twelve carbons ⁽⁷⁵⁾ it was concluded that a structure resembling thiamine is present, but that the amine had been hydrolysed and the terminal OH of **101** had undergone conversion into its alkyl chloride **116** (scheme 24).



Reagents & Conditions: (i) 5N HCl, 150°C

Scheme 24: Previous attempted synthesis of oxythiamine

Based on this knowledge, Rydon *et al.* ⁽⁶⁷⁾ used milder conditions to achieve the same chemical transformation but with a shorter reaction time. This provided the product in higher yields of 80% with no un-reacted thiamine material as the side product, and in three tautomeric forms (scheme 25, compounds **101**, **117** & **118**).

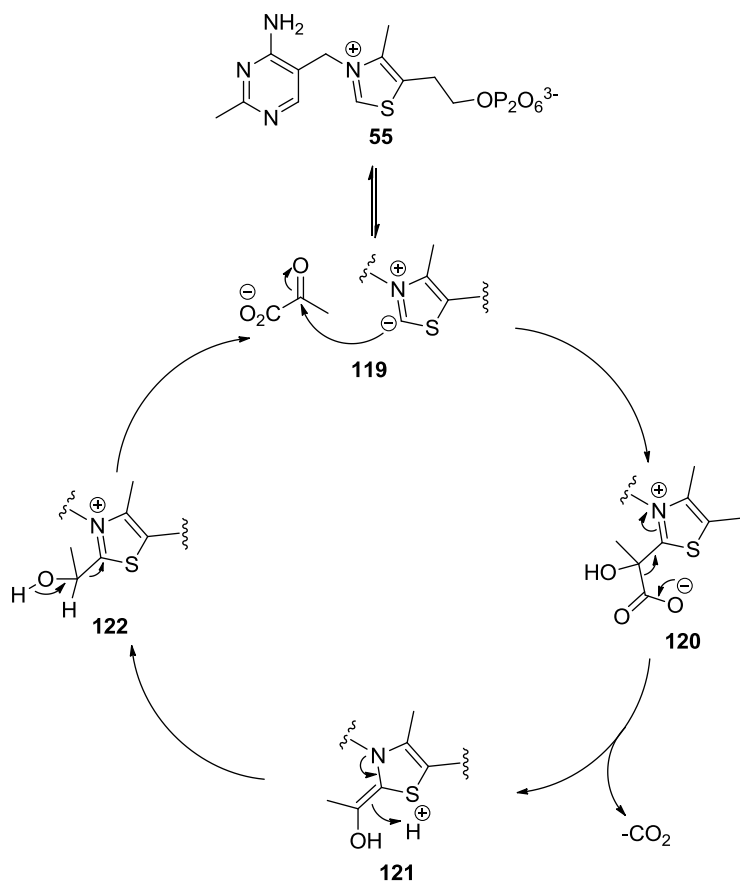


Reagents & conditions: (i) 5N HCl, 6 hrs

Scheme 25: Current synthesis of oxythiamine and tautomer's

1.11 Synthesis and Testing of Leeper Analogues

In the literature it is widely reported that the general mechanism of thiamine diphosphate enzymes⁽⁷⁸⁾ proceeds as depicted in scheme 26 as elucidated by Breslow⁽²⁹⁾. Interestingly, even though the mechanism for the catalysis of pyruvate is well documented there are very few examples of how the catalysis actually takes place within the active site. The reason for this is due to the speed at which the substrate is converted into the required product, which is too fast to acquire a set of crystallographic data⁽⁷⁸⁾. To understand this, isoelectronic compounds were sought that could mimic that of the natural ThDP coenzyme but not undergo any biochemical transformation, hence allowing enough time to capture a snapshot of the active site chemistry. In 2001 Leeper's group began synthesising these types of compounds.



Scheme 26: Breslow mechanism for ThDP in pyruvate decarboxylase enzymes (PDC).

1.11.1 3-Deazathiamine

Leeper *et al.* ⁽³⁷⁾ then undertook the synthesis of deaza-ThDP (figure 28), containing a neutral thiophene ring which binds 25, 000 times more strongly than ThDP ($K_i = 14 \text{ pM}$) ⁽³⁸⁾. This was to gain further insight into the reaction pathways and active site chemistries of ThDP enzymes as reported by Lienhard ⁽³⁵⁾.

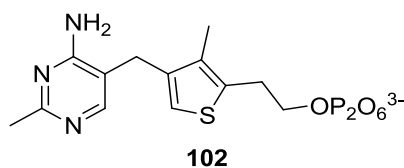
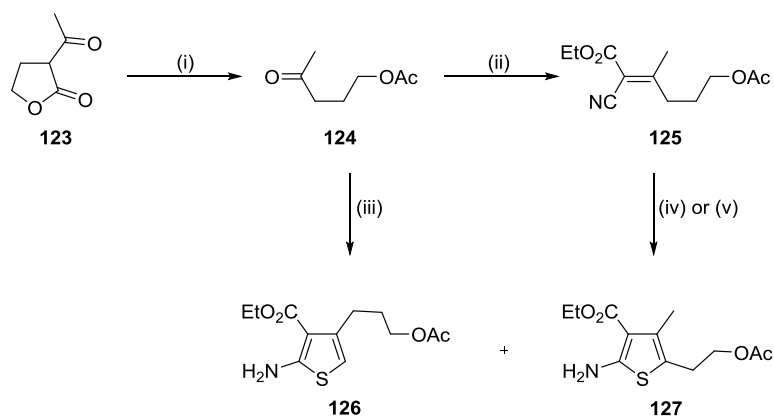


Figure 28: Structure of 3-deazathiamine

Synthesis of this structure was desired as previous studies had indicated that neutral analogues of ThDP might have increased binding affinity” ^{(35), (79)}. Furthermore any functionalization of the C2-H position on the thiophene ring would produce a structure resembling that of the “Breslow intermediate” formed during the typical catalytic pathways ⁽³⁹⁾.

1.11.2 Synthesis of 3-Deazathiamine

The initial synthesis of the deaza-TDP followed that outlined in (scheme 27) employing the procedure previously described by Gewald^{(79), (80)}. Acetolysis of α -acetyl- γ -butyrolactone **123** gave 5-acetoxy-pentan-2-one **124** which after condensation under Dean-Stark conditions gave the product **125** in a 73% yield as a 1:1 mixture of *E* and *Z* isomers⁽³⁹⁾. Addition of sulfur in the presence of diethylamine at 60 °C following the literature method of Shvedov⁽⁸²⁾ then gave the target compound **126** in a 34% yield. However, difficulties then arose with the work up procedures which led to an isomeric mixture of compounds **126** and **127**. An alternative one pot reaction (scheme 27, compound **124-126/127**) was then attempted by adding **124** to ethyl cyanoacetate with flowers of sulfur in an alcohol solvent system. Once again the isomeric mixture was formed, and conditions were changed to bulkier bases to increase steric demands upon the reaction, although the product yields still remained low and could not be purified.

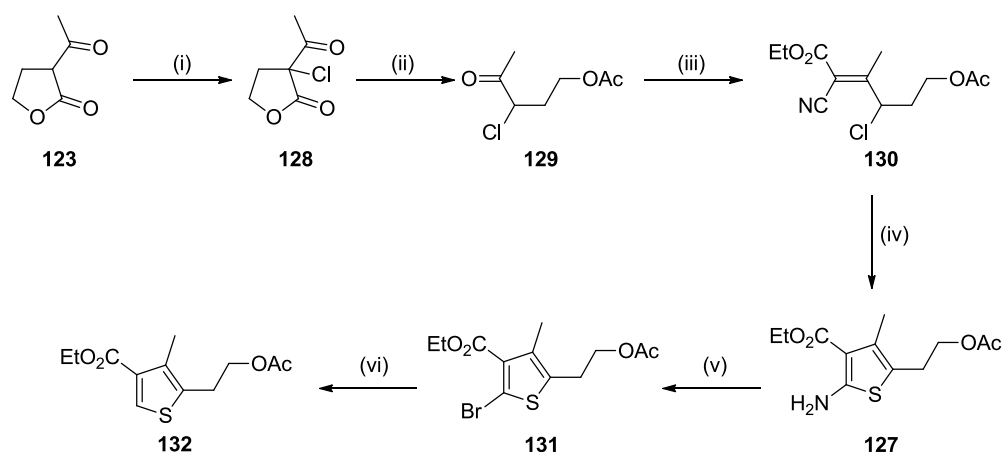


Reagents & Conditions: (i) AcOH, HCl, 85%; (ii) NCCH₂CO₂Et, AcONH₄, AcOH, C₆H₆, 73%; (iii) NCCH₂CO₂Et, S₈, EtOH, morpholine 35%; (iv) S₈, Et₂NH, EtOH, 34%; (v) S, morpholine, *t*-BuOH, 38%.

Scheme 27: Original synthesis of 3-deazathiamine

Leeper *et al.* then attempted to circumvent this by removing any possibility of forming an isomeric mixture. This alternative synthetic route began by reacting **123** with sulfur chloride to insert the chloride leaving group into the necessary position to give a single isomeric compound (scheme 298 compound **128**). Meanwhile decarboxylation of the lactone **128** by prolonged heating in HCl resulted in ring opening followed by subsequent trapping with acetic anhydride to give the acetoxy protected compound **129** in good yields of 85%. Ethyl cyanoacetate condensation with **129** then generated the product **130** as a 1:1 mixture of *E* to *Z* isomers in a 43% yield. Treatment

of **130** with sodium hydrogen sulphide then resulted in precipitation of the aminothiophene compound **127** from the solution.

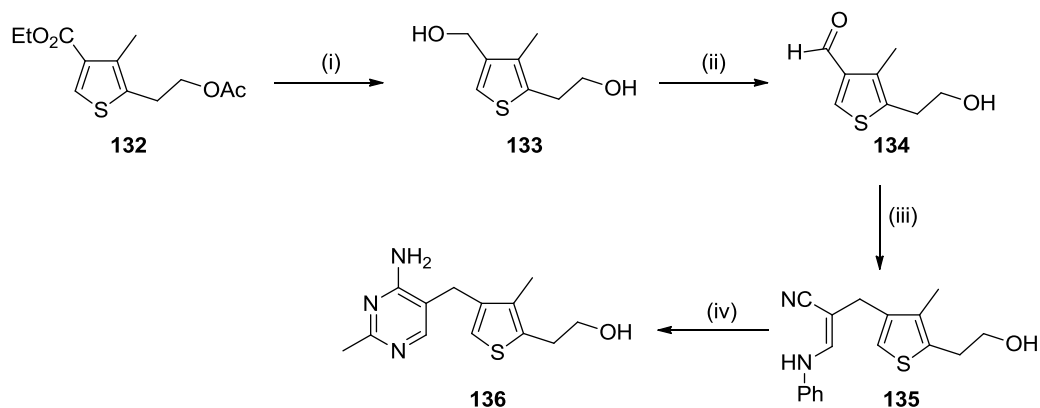


Reagents & conditions: (i) SO_2Cl_2 , 89%; (ii) a) AcOH , HCl , b) Ac_2O , 85%; (iii) $\text{NCCH}_2\text{CO}_2\text{Et}$, AcONH_4 , AcOH , PhMe , 43%; (iv) NaSH , EtOH , 82%; (v) CuBr_2 , $t\text{-BuONO}$, CH_3CN ; (vi) Zn , AcOH , 87% (over 2 steps).

Scheme 28: Modified thiophene synthesis for single regioisomer

Deamination at the alpha position was then attempted with several reagents and conditions, but yields remained low and purification of the final product was difficult⁽³⁹⁾. A Sandmeyer reaction⁽⁸³⁾ of **127** using anhydrous CuBr and *tert*-butyl nitrite was then employed to convert the α -amine into a halogen, which after treatment with Zn in acid gave the desired single isomer **132** in an 87% yield.

Assembly of the central 5-membered core now required further modifications to install the aminopyrimidine ring as a recognition feature for the active site. This was achieved by a two step procedure (scheme **29**), involving a LiAlH_4 reduction of **132** and subsequent MnO_2 oxidation of the benzylic alcohol to give **133**. This clever tactic also achieved deprotection of the acetoxy group and chemoselective oxidation of only the benzylic alcohol. As above, addition of β -anilinopropionitrile then produced the intermediate **135** as a 1:1 mixture of *E* to *Z* isomers which were easily separated by altering workup conditions⁽³⁹⁾. Compound **135** was then a prerequisite for reaction with acetamide to form the amino pyrimidine ring by refluxing in hot ethanol overnight to furnish the product **136** in 81% yield⁽⁸⁴⁾,⁽⁸⁵⁾. Unfortunately, due to the difficulties found in the synthesis of deazaTPP, it was decided that a shorter structural motif could be synthesised to allow quicker biological testing.

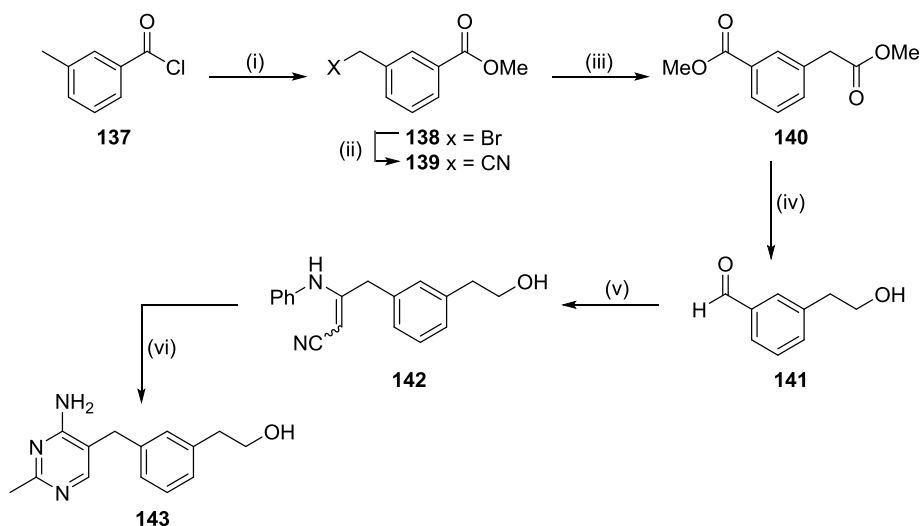


Reagents & conditions: (i) LiAlH_4 , Et_2O , 81%; (ii) MnO_2 , CHCl_3 , 74%; (iii) $\text{PhNHCH}_2\text{CH}_2\text{CN}$, NaOMe , DMSO , MeOH , 94%; (iv) $\text{CH}_3\text{C(=NH)NH}_2\cdot\text{HCl}$, NaOEt , EtOH , 81%.

Scheme 29: Synthesis of 3-deazaThDP

1.11.3 Synthesis of 1,3-Disubstituted Phenyl ThDP

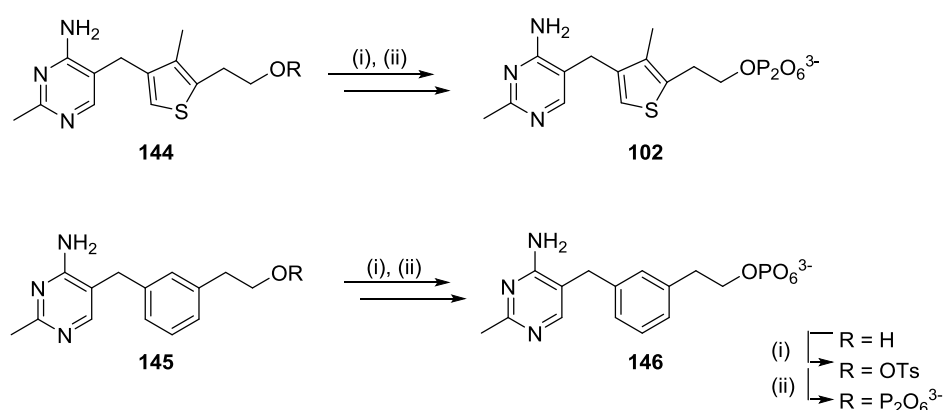
In 2004, *Leeper et al.*⁽⁷⁸⁾ replaced the central thiazolium or thiophene rings with a benzene derivative. The synthesis (scheme 30) began with a radical bromination of the methyl group situated on *m*-toluoyl chloride **137**, which was followed by quenching in MeOH to install the ester functionality **138**. $\text{S}_{\text{N}}2$ reaction of the bromine with potassium cyanide and subsequent methanolysis of the nitrile intermediate **139** gave the diester **140** which was reduced directly to the benzylic alcohol using LiAlH_4 . MnO_2 then completed the oxidation of only the benzylic position to give the aldehyde **141** which underwent a base catalysed condensation with 3-anilinopropionitrile as previously reported to give compound **142** as a mixture of *cis* and *trans* isomers⁽³⁹⁾. Deprotonation of acetamidine using NaOMe and *in situ* refluxing with compound **142** once again produced the pyrimidine product **143**⁽⁸⁵⁾.



Reagents & conditions: (i) Br₂ then MeOH, 65%; (ii) KCN, 18-crown-6, CH₃CN, 91%; (iii) MeOH, HCl, 87%; (iv) LiAlH₄, Et₂O, 60% then MnO₂, CHCl₃, 91%; (v) PhNHCH₂CH₂CN, NaOMe, DMSO-MeOH, 48%; (vi) CH₃(=NH)NH₂, NaOMe, EtOH, 81%

Scheme 30: Synthesis of 1,3-phenyl pyrimidine ThDP

Installation of the diphosphate group was then needed for binding to the “active dimer”. This can be formed by heating in concentrated phosphoric acid and then adding the desired thiamine analogues, although this process reportedly gave a mixture of mono, di and tri anionic phosphates which were difficult to purify by anion exchange chromatography⁽⁸⁶⁾. Rectification of this problem was sought by making the terminal hydroxyl groups into better leaving groups by tosylation, and S_N2 displacement with *tris*(tetra-*n*-butylammonium)pyrophosphate (TBAPP) (scheme 31, compounds **102** & **146**). This method was adopted because it had been described previously when synthesising allylic diphosphates⁽⁷⁸⁾.



Reagents & conditions: (i) Compound **144** & **145**, 3-but-3-ynyl toluene-4-sulfonate (1.0 eqv.) *t*-BuOH/H₂O (1:1 v/v), r.t. 16hr (ii) *tris*(tetra-*n*-butylammonium) hydrogen pyrophosphate (2.0 eqv.), MeCN, -10°C, 24hr, (**102**, 33%), (**146**, 24%).

Scheme 31: Tosylation and S_N2 displacement with TBAPP

This new approach was successful and gave increased yields of 33% for deazaThDP and 24% for the phenyl analogues which were now much easier to purify. One major side product of this reaction was the alkene **147** which formed by elimination of the diphosphate group (figure **29**).

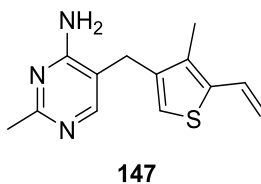


Figure 29: 3-deaza ThDP diphosphate elimination product

Further experimentation found that elevated temperatures increased the degree of elimination, whilst decreasing the temperature and raising the concentration of pyrophosphate salt increased the substituted product. Consequently these conditions were primarily used from here forth ⁽⁷⁸⁾.

1.11.4 The 1,4-Disubstituted-[1,2,3]-Triazoles & Diphosphate Mimics

Previous syntheses and studies by the Leeper group had now produced viable isoelectronic motifs capable of imitating the ThDP pathways. In conjunction with this was the acquisition of the optimum conditions needed to build these small structures. One such area that had not received much attention was the study of diphosphate isostere mimics that could probe the amino acid interactions within the γ -domain, and allow observations of any interesting effects produced by changing the diphosphate group (figure **30**, compounds **148-152**).

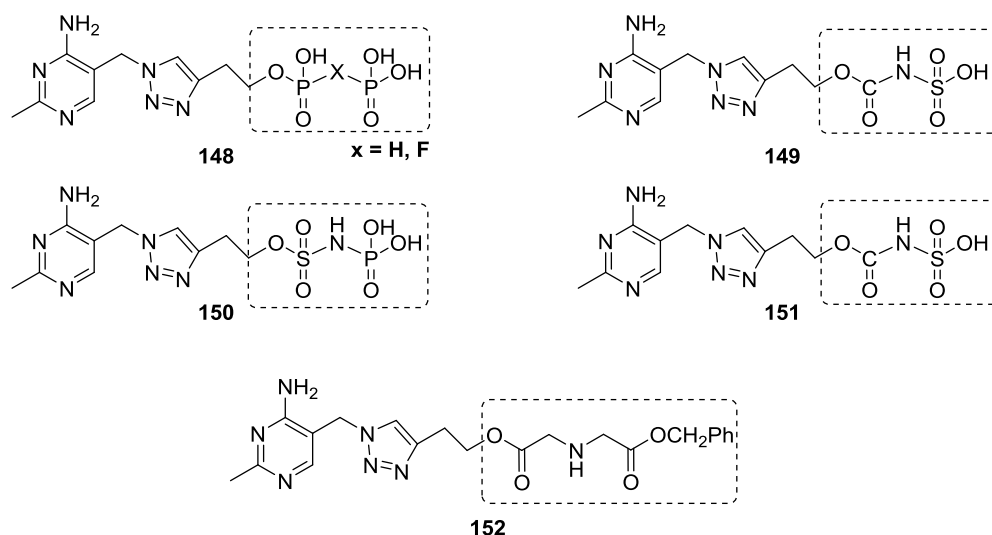
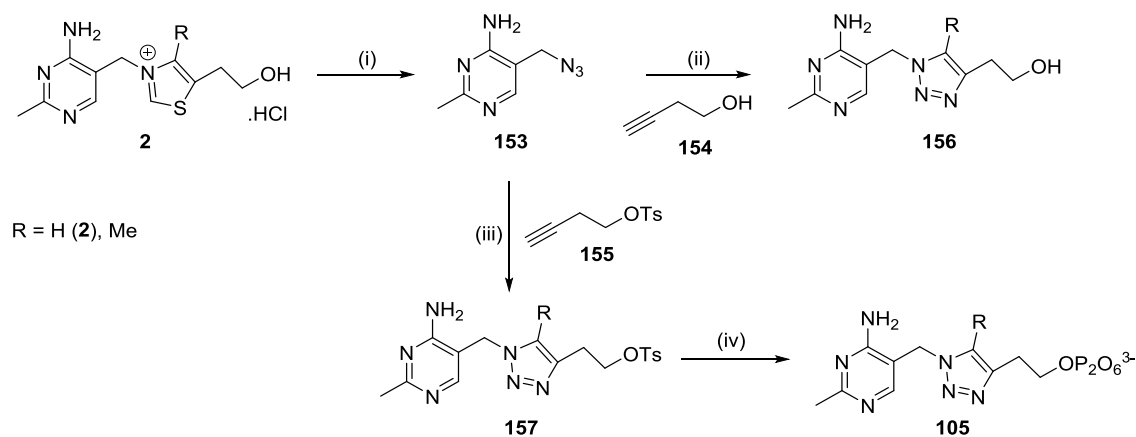


Figure 30: Various 1, 4-disubstituted [1,2,3]-triazole ThDP isosteres

As the synthesis of deaza-ThDP required 12 steps it was decided that a quicker synthetic route should be sought. A 1,4-copper azide-alkyne cycloaddition (CuAAC) is known to rapidly construct triazole rings which uses much simpler starting materials and allows fewer synthetic modifications⁽⁸⁸⁾. Furthermore, Leeper *et al.* had reported that the neutral rings are bound more tightly within the active site of pyruvate enzymes compared to those with charged groups and that a click reaction could allow easier synthesis of these new diphosphate mimics. These were desired because diphosphates are known to be highly charged and suffer from poor bioavailability and cellular uptake, therefore making them unsuitable for whole cell studies and pharmaceutical development⁽⁸⁷⁾.

1.11.5 Synthesis of 1,4-disubstituted [1,2,3] Triazole Mimics

The synthesis (scheme 32) ironically began with a sodium bisulfite-catalysed (S_NAr) displacement of the central thiazolium ring in **2** by reaction with sodium azide to give **153** in 83% yield. The CuAAC reaction then allowed construction of the central [1,2,3]-triazole ring with 1,4-regiochemistry by reaction with either the 3-butyn-1-ol **154** or its tosylate analogue **155** to give products **156** and **157** in 56% and 81% yields respectively. The 5-methyl triazole products were also synthesised by refluxing in 3-pentynol over 72 hours, although it was isolated as a (1:1) mixture of regioisomers which were difficult to separate after purification.



Reagents & conditions: (i) NaN_3 (2.5 eqv.), NaSO_3 (0.1 eqv.), H_2O , 60-65°C, 6h, 83%; (ii) 3-butynol (1.0 eqv.), sodium ascorbate (0.1 eqv.), $\text{CuSO}_4 \cdot 5\text{H}_2\text{O}$ (0.01 eqv.), $t\text{-BuOH-H}_2\text{O}$ (2:1 v/v), 25°C, 16 h, 81%; (iii) 3-butynyl tosylate (1.0 eqv.), sodium ascorbate (0.1 eqv.), $\text{CuSO}_4 \cdot 5\text{H}_2\text{O}$ (0.01 eqv.), $t\text{-BuOH-H}_2\text{O}$ (2:1 v/v), 25°C, 24h, 56%; (iv). $(\text{Bu}_4\text{N})_3\text{HP}_2\text{O}_7$ (2.0 eqv.), MeCN, -5°C to 25°C. 50 - 60%

Scheme 32: 1,4-CuAAC Click chemistry

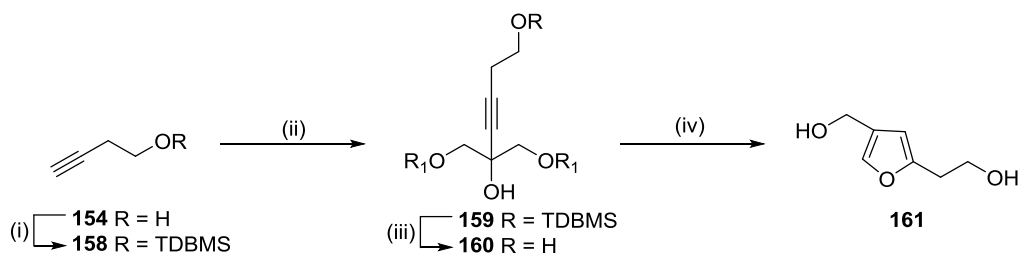
Tosylate **157** could then undergo S_N2 displacement with *tris*(tetrabutylammonium) pyrophosphate followed by purification using anion and cation exchange resins. During these purification stages it was noted that the tosyl anion co-eluted with the desired anionic product and thus an acidic resin was used to remove this impurity as the tosylic acid⁽⁸⁷⁾. Unfortunately this gave rise to a new problem as the acidic resin caused some cleavage of the diphosphate to the monophosphate in approximately (<10%) yield. Despite this it was possible to acquire the lyophilised salt product **105** in yields of 50 - 60%.

1.11.6 The Furan ThDP Analogue

Most recently, the synthesis of a furan derivative has been reported because some mechanistic questions remain unanswered, including “how the substrate binds, roles of the catalytic groups and how each individual step is accelerated”⁽³⁸⁾. This furan ThDP was envisaged to remove all the problems associated with past derivatives including lengthy routes, lack of functionalisation at the C2-H position and problematic purification procedures. Furthermore, a short synthesis allowed easy functionalisation by Freidel Crafts acylation.

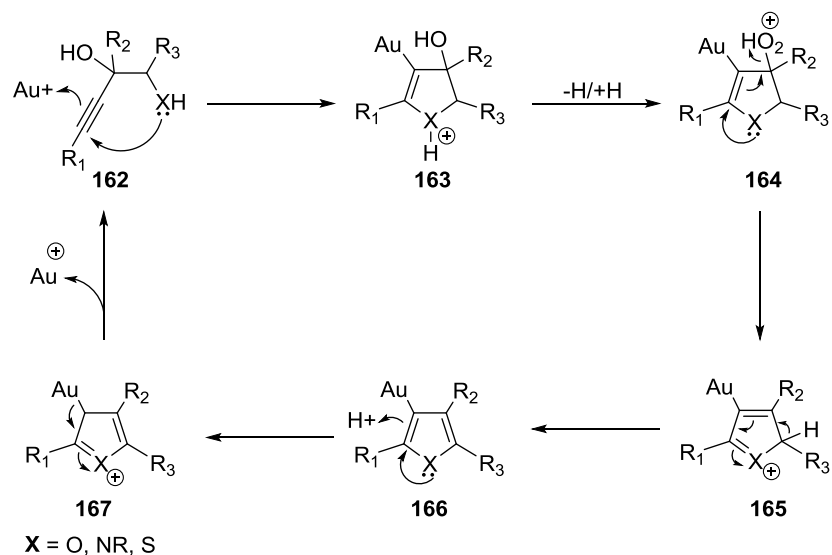
1.11.7 Synthesis of Furan ThDP

The synthesis (scheme 33) again used cheap and commercial 3-butyn-1-ol **154** and its protection with TBDMS-Cl to give **158**. Deprotonation of the terminal alkyne proton (pK_a 25) with *n*-BuLi then revealed the anion and facilitated nucleophilic attack upon the TBDMS protected 1,3-dihydroxyacetone to give compound **159**. Deprotection of the silyl ether **159** was then achieved using TBAF reagent, and furan formation was completed by a dehydrative AuCl cyclisation of **160** as proposed by the authors to give compound **161** (scheme 34)⁽³⁸⁾.



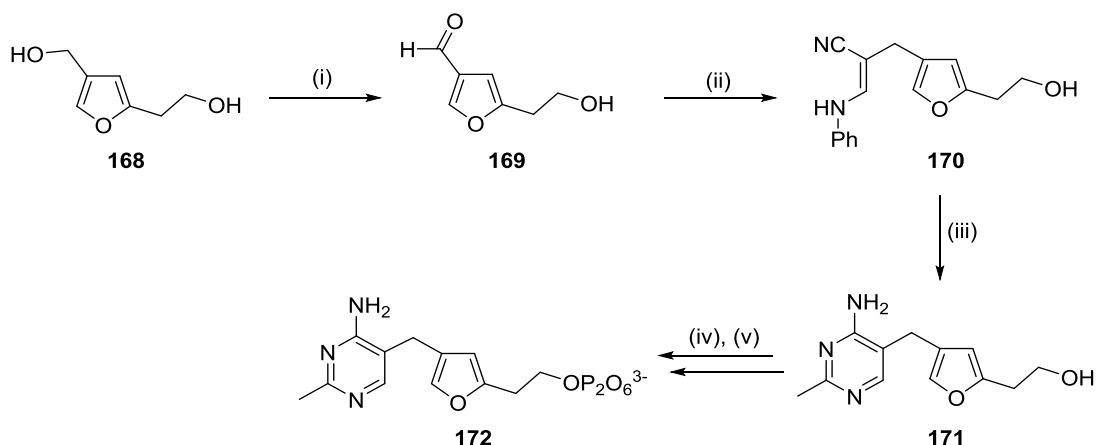
Reagents & Conditions: (i) TBDMS-Cl, N-methylimidazole (ii) dihydroxyacetone, *n*-BuLi, -78°C-r.t., 55% (iii) TBAF, THF, 79% (iv) AuCl, THF, 85%.

Scheme 33: Synthesis of furan intermediate for ThDP synthesis



Scheme 34: Au (I) catalysed cyclisation of pyrrole's, furan's and thiophenes

Chemistry then followed that that shown below in scheme 35, based on previous work within the Leeper group including the synthesis of 3-deaza ThDP **102** and the phenyl ThDP **143** analogues (39), (85), (78).



Reagents & Conditions: (i) MnO_2 , CHCl_3 , 74%; (ii) $\text{PhNHCH}_2\text{CH}_2\text{CN}$, NaOMe , DMSO , MeOH , 76%; (iii) $\text{CH}_3\text{C(=NH)NH}_2\cdot\text{HCl}$, NaOEt , EtOH , 65%; (iv), (v) TsCl , pyridine -5°C , TBAPP , MeCN , 4°C , 30%.

Scheme 35: Leeper synthesis of 1,4-disubstituted furan ThDP

These past few sections have highlighted some of the more recent synthetic approaches for constructing the thiamine framework as a secure scaffold for use in the elucidation and interpretation of ThDP enzyme mechanisms, but what if the scaffold could be used as a disguise to introduce new chemistry into an existing protein active site.

This area belongs in the realms of enzyme promiscuity and the promotion of new and exciting bio catalytic processes.

1.12 Enzyme Promiscuity

Biocatalysts are becoming ever more popular in academic and industrial settings due to their preferred “green” approach avoiding toxic metal catalysts and costly organic solvents ⁽⁸⁹⁾. As enzyme promiscuity is a way of introducing new and intriguing reactions, it has opened the door to directed alterations on either the protein or cofactor frameworks. This change can force the enzyme to undergo a novel synthetic route that is not completed by the native enzymatic pathway. Figure 31 shows the typical enzymatic pathway by the native cofactor (yellow) and how it reacts with its substrate to produce the normal product. Exchanging this native cofactor for an unnatural one as shown in orange, may then permit a reaction with a substrate to produce an alternative novel enzymatic outcome.

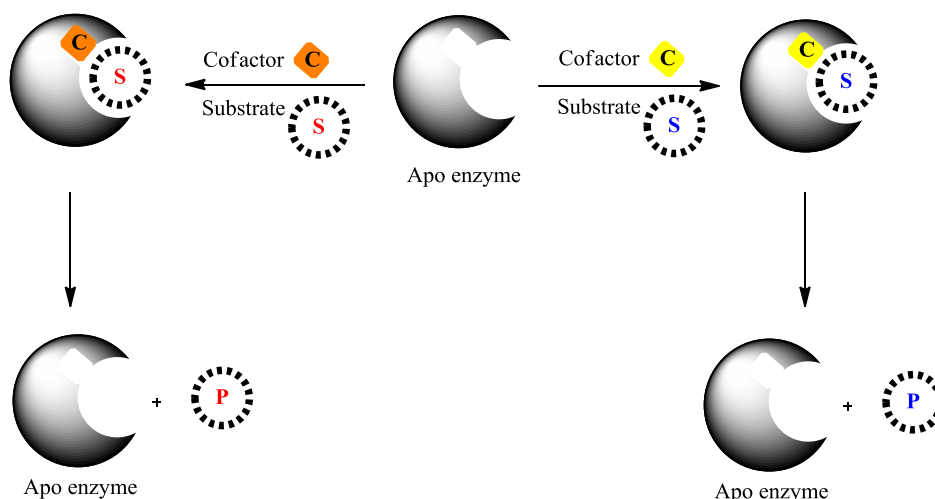
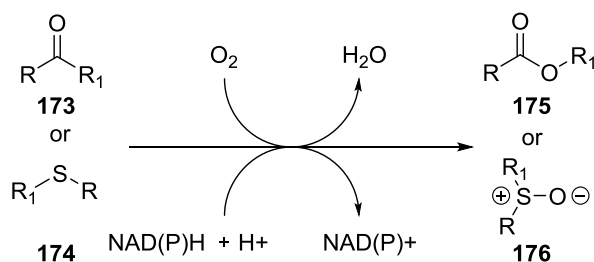


Figure 31: Alternate enzymatic pathways-Enzyme promiscuity

1.12.1 Baeyer-Villiger FMO cofactor system (BVMO's)

One example of enzyme promiscuity is the use of flavin-monooxygenases (FMO's) to complete the installation of oxygen adjacent to carbonyls and/or for sulfoxidation reactions as found in the Baeyer-Villiger process (scheme 36) ⁽⁹⁰⁾. For industrial applications the author reports that gene manipulation has permitted the construction of a single enzymatic module capable of positioning both the reduced FMNH₂ and substrate in close proximity. This is much better when compared to

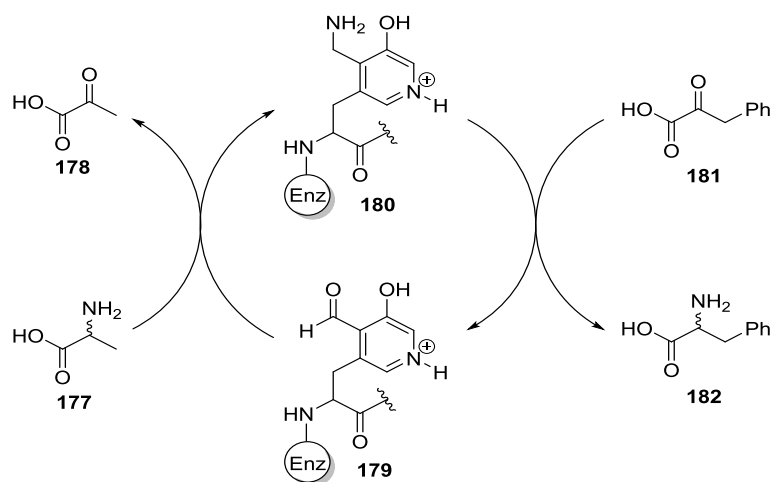
other reported Baeyer-Villiger monooxygenases (BVMO's) that inconveniently undergo their respective reactions in differing domains, and therefore do not allow easy industrial applications, whereby the reactions can run independently^{(91), (92)}.



Scheme 36: BVMO-Flavin modification

1.12.2 (Vitamin B₆) Pyridoxamine modified coenzyme

Another example is pyridoxamine (Vitamin B₆), which is well known to catalyse the formation of α -amino acids from α -keto acids via the transamination reaction. In 1994 Imperiali *et al.* began implementing site-directed mutagenesis as a tool to incorporate the primary synthetic machinery of the pyridoxal coenzyme into the surrounding amino acids located in and around the active site (scheme 37)⁽⁹²⁾. This produced various pyridoxyl-amino acid polypeptides which could then be hosted in a semi-synthetic ribonuclease. This allowed incorporation of the classic transaminase chemistry found with pyridoxal systems to be fixed in the hydrophobic pocket of the enzyme, therefore promoting an artificial aminotransferase reaction under conditions which favour its formation⁽⁹⁴⁾.



Scheme 37: Cofactor manipulation of pyridoxamine catalysed transamination reaction

1.12.3 Synthetic Enzymes

Recently a series of exciting synthetic enzymes have been reported by Ward *et al.* ^{(112), (113), (114)}. This methodology incorporates organometallic molecules into a host protein, thereby forming a complementary metallo-enzyme system for applications in enantioselective catalysis, nanotechnology and chemical biology. One example of this is the Streptavidin - biotin metalloenzyme that catalyses a range of enantioselective reactions in high yield and ee% ^{(114), (115)}. This is accomplished with the biotin as the active site recognition and a diphosphine ligand situated at the terminus of a linker chain for catalysis (figure 32).

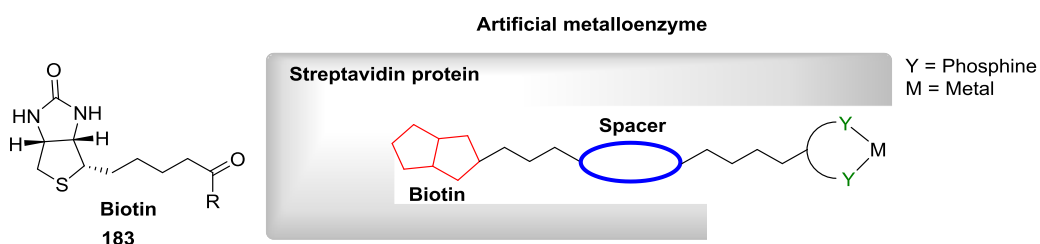


Figure 32: Streptavidin – biotin metalloenzyme

1.12.4 Catalytic Antibodies (Abzymes)

In 1969, W. P. Jencks discovered that antibodies could undergo catalysis by stabilising a reaction's transition state ⁽¹⁰⁸⁾. These catalytic antibodies or abzymes, functioned in a similar way to enzymes by lowering the activation energy within the transition state, to overcome the energy barrier required to react. Antibodies have a Y-shape structure, and frequently bind biological antigens or haptens (unnatural ligands). Two identical recognition sites for these antigens have been identified within the Y-frame, and these are called complementary determining regions (CDRs) (figure 33).

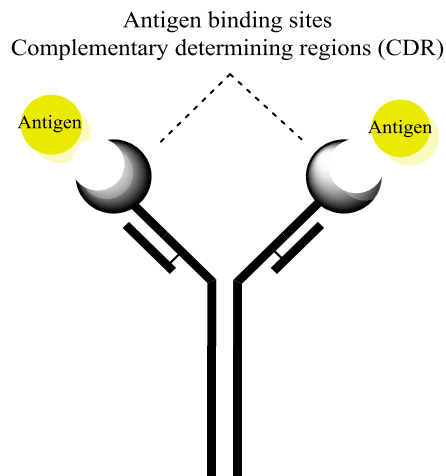
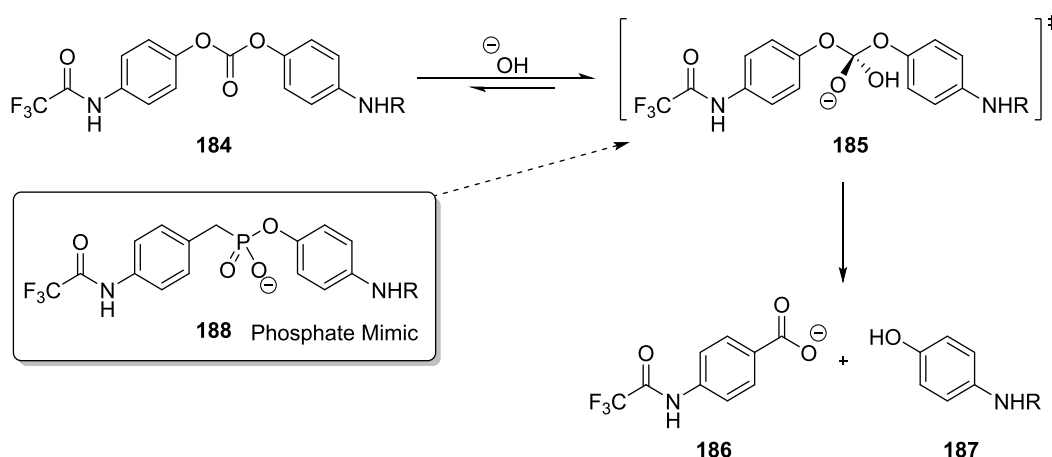


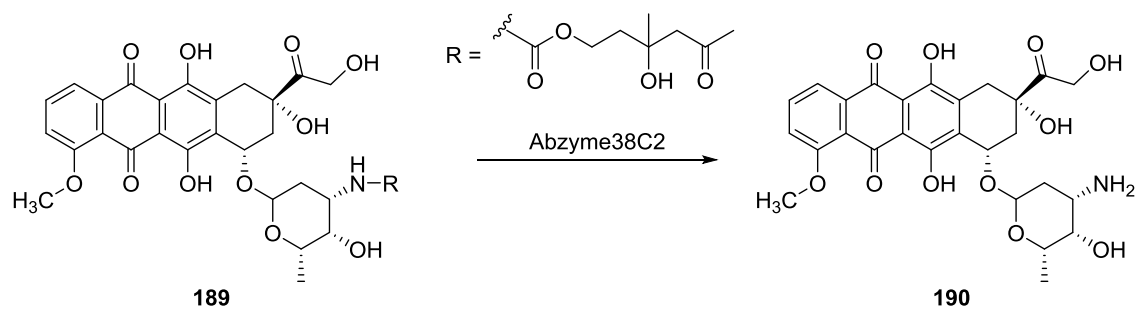
Figure 33: Y-shaped antibody

Later research by Schultz and Lerner ^{(109), (110)} developed custom enzymes that could catalyse hydrolysis of the phosphate ester **188** based on the recognition at the CDRs for an established transition state intermediate in hydrolysis of ester **184** (scheme **38**). After formation of the unstable tetrahedral intermediate **185**, collapse then occurs to give products **186** and **187**.



Scheme 38: Phosphonic acid mimic 188 of the ester transition state 185 by hydrolysis

Focus is therefore placed upon the synthesis of analogues that mimic transition states like **185**, and can then bind to the CDR regions to produce a multitude of chemical products ⁽⁹⁹⁾. This results in new ways for inhibiting antibodies and as biocatalysts for chemical transformations. Intriguingly Rader and List have applied this technique to the treatment of cancer by developing new prodrug candidates such as doxorubicin **190** (scheme **39**) ⁽¹⁰⁰⁾. These prodrug haptens can then be recognised by the antibody CDRs on the tumour surface, and undergo conversion of the prodrug **189** into the active form **190** at the site of a tumour.

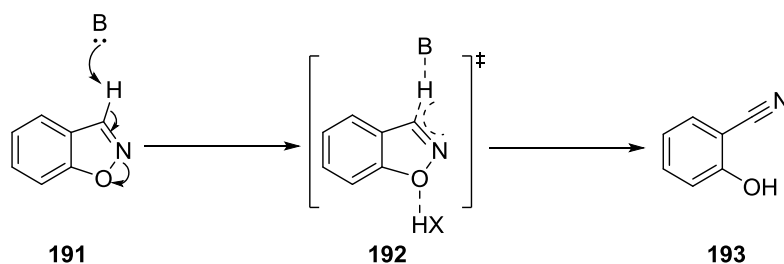


Scheme 39: Abzyme conversion of prodrug 189 to active doxorubicin 190

To date abzymes are one of the best types of enzyme mimics, and are now catalysing a breadth of chemical reactions.

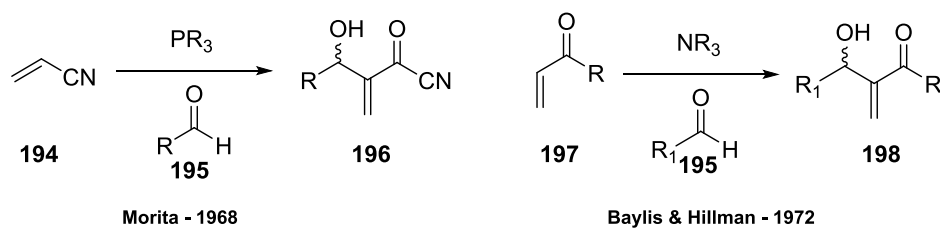
1.12.5 The First Morita-Baylis-Hillman Reaction

Finally a concluding remark regarding enzyme promiscuity is based on the premise that “many important synthetic reactions lack a naturally occurring enzymatic counterpart”⁽⁹⁵⁾. It has been reported that bovine serum albumins (BSAs) which typically carry a multitude of compounds within blood plasma are viable candidates to catalyse the Kemp elimination of benziisooxazoles⁽⁹⁶⁾ (scheme 40). *In silico* studies have revealed that the Kemp elimination mechanism could be promoted by the amino acids situated in the active site of BSAs and effect the base catalysed E2 elimination process^{(96), (95)}.



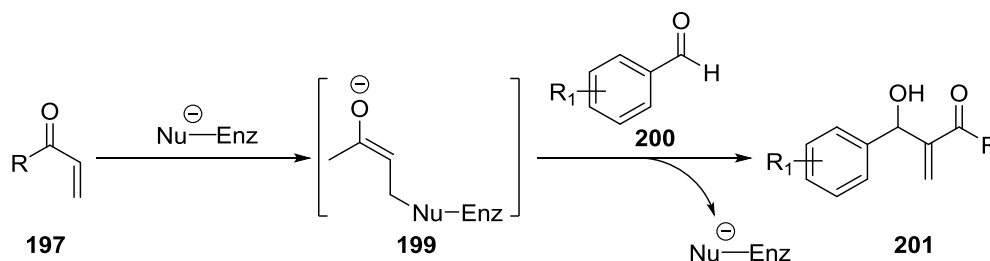
Scheme 40: The Kemp elimination of benziisooxazole

This generalisation allowed Reetz *et al.* in 2007 to propose that serine, histidine and alternative amino acids could behave as catalysts for the Morita-Baylis-Hillman (MBH) reaction⁽⁹⁷⁾ (scheme 41 & 42). Morita initially discovered this reaction in 1968 using a phosphine catalyst and its nucleophilic addition to an electron deficient alkene to produce allylic chiral alcohols.⁽¹¹²⁾



Scheme 41: Phosphine catalysed Morita reaction

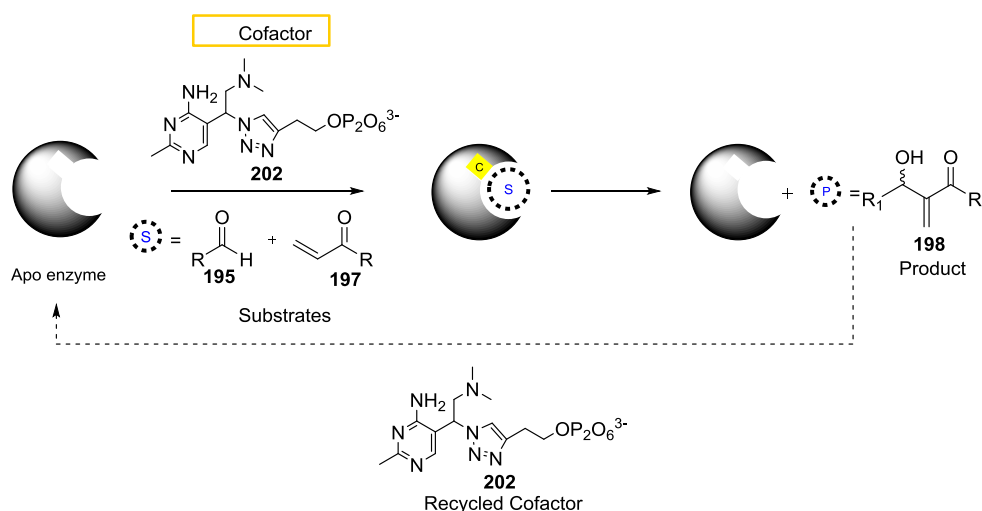
In 1972, Baylis and Hillman devised a new synthetic methodology based on this work which used a tertiary amine catalyst. Even though this showed higher yields and broader substrate ranges, it showed very slow reaction rates and can take many days to reach completion. Due to its absence in nature, an asymmetric MBH would benefit the synthetic toolkit available to the chemist and would be a good candidate for development of novel enzyme promiscuity to hopefully improve on the low yields and slow rate⁽⁹⁸⁾.



Scheme 42: Morita-Baylis-Hillman catalysed pathway via amino acids in active site of BSA

2. The Project

This project aims to introduce unnatural chemistry into an enzyme active site by the synthesis and installation of unnatural analogues of the enzymes cofactor. Modified cofactors are a new approach in the creation of unnatural enzymatic reactions. As enzyme promiscuity grows and biocatalysts are being used more throughout industry and academia, the discovery of new enzyme catalysed routes would add to the existing synthetic toolkit adopted by the chemist⁽⁹⁸⁾. On the basis that Leeper *et al.* have erected a strong foundation in the preparation and testing of their ThDP derivatives it was proposed that one such analogue containing minimal synthetic steps may be a useful anchor from which to assemble a novel chemical platform. Furthermore, these compounds have already undergone biological testing and are known to enter the protein architecture successfully. Utilising CuAAC chemistry, access to the 1,4-disubstituted-[1,2,3]-triazole motif designed by Leeper could permit incorporation of novel chemistries into the active site of a ThDP dependant protein. Once optimised in the active site, it could facilitate a novel asymmetric biocatalysis that is not currently undertaken by these classes of enzymes. One such functional group that may be combined easily with the protein scaffold and remain un-affected by aqueous conditions is that of a tertiary amine which has seen extensive applications in organocatalysis. The Morita-Baylis-Hillman reaction has been extensively researched but does not occur naturally, and so lacks examples of enzymatically mediated reactions that could potentially catalyse asymmetric MBH reactions that are of particular importance for chemical synthesis (scheme 43).



Scheme 43: Proposed synthetic target and desired MBH bio catalytic process

Only recently have Reetz *et al.* demonstrated chemistry of this type in BSA⁽⁹⁸⁾ showing that it is compatible with a biological environment and is consequently a safe choice for a first attempt to introduce it as an unnatural cofactor. Based on this premise we envisaged the creation of a tertiary amine tether by building out from the 1,4-disubstituted triazole ThDP developed by **105** Leeper *et al.* to give **202**. This could then act as a model cofactor system to catalyse the first enzymatic cofactor-mediated Morita-Baylis-Hillman reaction. Reaction of various aldehydes **195** with **197** and **201** could then produce the allylic alcohol **198**, and allow for recycling of the cofactor to ensure it can be suitably transferred into an industrial process.

References - Introduction

1. M. Richter, *Nat. Prod. Reports*, **2013**, *30*, 1324-1345.
2. J. D. Fisher, G. L. Holliday, S. A. Rahman, J. M. Thornton, *J. Mol. Biol.*, **2010**, *403*, 803-824.
3. F. A. Robinson, *The Vitamin Cofactors of Enzyme Systems*, **1966**, Elsevier, Toronto.
4. A. Smith, F.J. Leeper, *Nat. Prod. Reports*, **2007**, *24*, 923-926.
5. V. R. Yadhav, M. Yarus, *Biochemie*, **2002**, *84*, 877-888.
6. G. L. Holliday, J. D. Fisher, J. B. Mitchell, J. M. Thornton, *FEBS*, **2011**, *278*, 3835-3845.
7. D. Dobritzsch, S. Konig, G. Lu, *J. Biol. Chem.*, **1998**, *273*, 20196-20204.
8. G. L. Holliday, J. M. Thornton, A. Marquet, A. G. Smith, F. Rebeille, R. Mendel, H. L. Schubert, A. D. Lawrence, M. J. Warren, *Nat. Prod. Reports*, **2007**, *24*, 972-987.
9. J. A. Imlay, *J. Mol. Microbiol.*, **2006**, *59*, 1073-1082.
10. P. C. Dos santos, D. R. Dean, *Nat. Chem. Biol.*, **2010**, *6*, 700-701.
11. M. K. Johnson, *Curr. Opin. Chem. Biol.*, **1998**, *2*, 173-181.
12. R. Lill, *Nature*, **2009**, *460*, 831-837.
13. A. Marquet, B. T. S. Bui, A. G. Smith, M. J. Warren, *Nat. Prod. Reports*, **2007**, *24*, 1027-1040.
14. R. R. Mendel, A. G. Smith, A. Marquet, M. J. Warren, *Nat. Prod. Reports*, **2007**, *24*, 963-971.
15. F. Rebeille, S. Ravanel, A. Marquet, R. R. Mendel, M. E. Webb, A. G. Smith, M. J. Warren, *Nat. Prod. Reports*, **2007**, *24*, 949-962.
16. J. M. Stevens, T. Uchida, O. Daltrop, S. J. Ferguson, *Biochem. Soc. Trans.*, **2005**, *33*, (pt 4) 792-795.
17. M. E. Webb, A. Marquet, R. R. Mendel, F. Rebeille, A. G. Smith, *Nat. Prod. Reports*, **2007**, *24*, 988-1008.
18. R. R. Williams, *J. Am. Chem. Soc.*, **1935**, *57*, 229-230.
19. R. R. Williams, *J. Am. Chem. Soc.*, **1936**, *58*, 1063-1064.
20. K. Lohmann, P. Schuster, *Biochem. Z.*, **1937**, *294*, 188-214.
21. W. Lagenbeck, F. F. Nord, R. Weidenhagen, *Ergebnisse der Enzymforschung*, **1933**, *5*, 314.
22. K. G. Stern, J. L. Melnick, *J. Biol. Chem.*, **1939**, *131*, 597-613.
23. K. G. Stern, J. L. Melnick, *J. Biol. Chem.*, **1940**, *135*, 365-369.
24. T. Ugai, S. Tanaka, S. J. Dowaka, *J. Pharm. Soc. Jpn.*, **1943**, *63*, 269.
25. S. Mizuhara, *J. Jpn. Biochem. Soc.*, **1950**, *22*, 120.

26. S. Mizuhara, P. Handler, *J. Am. Chem. Soc.*, **1974**, *76*, 571-573.
27. R. Breslow, *Chemistry & Industry*, **1956**, p. 28-29.
28. R. Breslow, *J. Am. Chem. Soc.*, **1958**, *80*, 3719-3725.
29. K. Fry, L. L. Ingram, F. H. Westheimer, *J. Am. Chem. Soc.*, **1957**, *79*, 5226-5227.
30. R. Kluger, K. Tittman, *Chem. Rev.*, **2008**, *108*, 1797-1833.
31. R. Kluger, J. Chin, T. Smyth, *J. Am. Chem. Soc.*, **1981**, *103*, 884-888.
32. L. O. Krampitz, I. Suzuki, G. Greull, *Ann. N. Y. Acad. Sci.*, **1962**, *98*, 466-478.
33. R. Breslow, *Ann. N. Y. Acad. Sci.*, **1962**, *98*, 445-452.
34. R. Kluger, G. Gish, G. Kauffman, *J. Biomol. Chem.*, **1984**, *259*, 8960-8965.
35. J. A. Gutowski, G. E. Lienhard, *J. Biol. Chem.*, **1976**, *251*, 2863-2866.
36. J. Crosby, R. Stone, G. E. Lienhard, *J. Am. Chem. Soc.*, **1970**, *92*, 2891-2899.
37. A. Iqbal, El-Habib Sahraoui, F. J. Leeper, *J. Org. Chem.*, **2014**, *10*, 2580-2585.
38. D. Hawksley, D. A. Griffin, F. J. Leeper, *J. Chem. Soc., Perkin Trans I*, **2001**, 144-148.
39. R. R. Williams, J. K. Cline, *J. Am. Chem. Soc.*, **1936**, *58*, 1504-1505.
40. E. R. Buchman, *J. Am. Chem. Soc.*, **1936**, *58*, 1803-1805.
41. S. E. Bramley, V. Dupplin, D. G. C. Goberdhan, G. D. Meakins, *J. Chem. Soc., Perkin Trans I*, **1987**, 639-642.
42. F. Ni, Y. Yang, W. M. Shu, J. R. Ma, A. X. Wu, *Org. Biomol. Chem.*, **2014**, *12*, 9466-9469.
43. T. L. V. Ulbricht, C. C. Price, *J. Org. Chem.*, **1956**, *21*, 567-571.
44. J. J. Reddick, S. Saha, J. Lee, J. S. Melnick, J. Perkins, T. P. Begley, *Bioorg. Med. Chem. Lett.*, **2001**, *11*, 2245-2248.
45. F. Perandones, J. L. Soto, *J. Heterocyclic Chem.*, **1998**, *35*, 413-419.
46. H. C. Koppel, R. H. Springer, R. K. Robins, C. C. Cheng, *J. Org. Chem.*, **1962**, *27*, 3614-3617.
47. J. L. Zilles, L. R. Croal, D. M. Downs, *J. Bacteriology*, **2000**, *182*, 5606-5610.
48. W. Winkler, A. Nahvi, R. R. Breaker, *Nature*, **2002**, *419*, 952-957.
49. L. Chen, E. Cressina, N. Dixon, K. Erixon, K. Agyei-Owusu, A. G. Smith, J. Micklefield, C. Abell, F. J. Leeper, *Org. Biomol. Chem.*, **2012**, *10*, 5924-5931.
50. T. E. Edwards, F. D. Amare, *Structure*, **2006**, *14*, 1459-1468.
51. E. Cressina, L. Chen, C. Abell, F. J. Leeper, A. G. Smith, *Chem. Sci.*, **2011**, *2*, 157-165.
52. H. Stetter, *Angew. Chem.* **1976**, *15*, 639-712.53. R. U. Braun, T. J. J. Muller, *Synthesis*, **2004**, *14*, 2391-2406.

54. M. Christmann, *Angew. Chem. Int. Ed.*, **2005**, *44*, 2632-2634.
55. G. Bredig, K. Fajans, *Chem. Ber.*, **1908**, *41*, 752-763.
56. J. C. Sheehan, D. H. Hunnerman, *J. Am. Chem. Soc.*, **1966**, *88*, 3666-3667.
57. R. Kluger, *Chem. Rev.*, **1987**, *87*, 863-876.
58. P. Arjunan, T. Umlan, F. Dyda, S. Swaminathan, W. Furey, M. Sax, B. Farrenkopf, Y. Gao, D. Zhang, F. Jordan, *J. Mol. Biol.*, **1996**, *256*, 590-600.
59. L. J. Reed, *Acc. Chem. Res.*, **1974**, *7*, 40-46.
60. L. Guogang, D. Dobritzsch, S. Baumann, G. Schneider, S. Konig, *Eur. J. Biochem.*, **2000**, *267*, 861-868.
61. Y. A. Muller, Y. Lindqvist, W. Furey, G. E. Schultz, F. Jordan, G. Schneider, *Structure*, **1993**, *1*, 95-103.
62. K. S. Tittmann, D. Meyer, J. Arens, C. Wechsler, M. Tietzel, R. Golbik, K. Tittman. *J. Biochem*, **2013**, *52*, 2505-2507.
63. A. Schellenberger, *Ann. New York Acad. Sci.*, **1982**, *378*, 51-62.
64. W. Shin, J. Pletcher, G. Blank, M. Sax, *J. Am. Chem. Soc.*, **1977**, *99*, 3491-3499.
65. R. A. Frank, C.M. Titman, J. V. Pratrap, B. F. Luisi, R. N, Perham. *Science*, **2004**, *306*, 872-876.
66. Sh .Kadyrov, *Khimya Geterosiklicheskikh Soedinenii*, **1966**, *4*, 840-841.
67. N. H. Rydon, *J. Biochem.*, **1951**, *48*, 383-384.
68. Liu-Yuan, J.Timm, E.D. Hurley, D. Thomas, *J. Biol. Chem.*, **2006**, *281*, 6601-6607.
69. A. J. Meyers, G. Garcia-Munoz, *J. Org. Chem.*, **1964**, *26*, 1435-1438.
70. D. P. Wyman, P. R. Kaufman, *J. Org. Chem.*, **1964**, *29*, 1956-1960.
71. L. Yakhontov, M. V. Rubtsovb, *ZhOKh.*, **1962**, *432*, 32.
72. F. Bergel, A. R Todd, *J. Chem. Soc.*, **1937**, 1504-1509.
73. L. R. Cerecedo, A. L. Eusebi, *J. Am. Chem. Soc.*, **1950**, *72*, , 5749-5749.
74. E. R. Buchman, R. R. Williams, *J. Am. Chem. Soc.*, **1935**, *57*, 1751-1752.
75. A. Windaus, R. Tschesche, H. Ruhkopf, *Nachr. Ges. Wiss. Gottingen Math-Phys. Klasse*, **1932**, *111*, 346.
76. A. Veen, G. Van, *Rec. Trav. Chim.*, **1932**, *51*, 281-283.
77. S. Mann, C. P. Melero, D. Hawksley, F. J. Leeper, *Org. Biomol. Chem.*, **2004**, *2*, 1732-1741.
78. P. N. Lowe, F. J. Leeper, R. N. Perham, *Biochemistry*, **1983**, *22*, 150-157.
79. K. Gewald, *Chem. Ber.*, **1965**, *98*, 3571.

80. K. Gewald, E. Schinke, H. Bottcher, *Chem. Ber.*, **1966**, 99, 94.
81. V. I. Shvedov, V. K. Ryzhkova, A. N. Grinev, *Khim. Geterotsikl soedin.*, **1967**, 3, 239.
82. J. K. Kochi, *J. Am. Chem. Soc.*, **1957**, 79, 2942-2948.
83. B. S. Rauckmann, B. Roth, *J. Med. Chem.*, **1981**, 24, 933-941.
84. P. Stenbuck, R. Baltzly, H. M. Hood, *J. Org. Chem.*, **1963**, 28, 1983-1988.
85. K. M. Erixon, C. L. Dabalos, F. J. Leeper, *Org. Biomol. Chem.*, **2008**, 6, 3561-3572.
87. F. Himo, T. Lovell, R. Hilgraf, V. V. Rostovtsev, L. Noodleman, K. B. Shapless, V. V. Fokin, *J. Am. Chem. Soc.*, **2005**, 127, 210-216.
88. D. J. Pollard, J. M. Woodley, *Trends in Biotechnology*, **2006**, 25, 68-73.
89. C. N. Jensen, J. Cartwright, J. Ward, S. Hart, J. P. Turkenburg, S. T. Ali, M. J. Allen, G. Grogan, *Chem. Bio. Chem.*, **2012**, 13, 872-878.
90. K. H. Jones, R. T. Smith, P. W. Turd Gill, *J. Gen. Microbiology*, **1993**, 139, 797-805.
91. R. Villa, A. Willetts, *J. Mol. Catal.*, **1997**, 2, 193-197.
92. R. S. Roy, B. Imperiali, *Protein engineering*, **1997**, 10, 691-698.
93. Y. Murakami, J.-I. Kikuchi, K. Akiyoshi, T. Imori, *J. Chem. Soc. Perkin. Trans. 2*, **1985**, 1919-1924.
94. D. Rothlisberger, O. Khersonsky, A. M. Wollacott, L. Jiang, J. DeChancie, J. Betker, J. L. Gallaher, E. A. Althoff, A. Zanghellini, O. Dym, S. Albeck, K. N. Houk, D. S. Tawfik, D. Baker, *Nature*, **2008**, 453, 190-195.
95. M. L. Casey, D. S. Kemp, K. G. Paul, D. D. Cox, *J. Org. Chem.*, **1973**, 2294-2300.
96. S. E. Drewes, G. H. P. Roos, *Tetrahedron*, **1988**, 44, 4653-4670.
97. M. T. Reetz, R. Mondiere, J. D. Carballeira, *Tetrahedron Lett.*, **2007**, 48, 1679-1681.
98. G. M. Blackburn, A. S. Kang, G. A. Kingsbury, D. R. Burton, *J. Biochem.*, **1989**, 262, 381-390.
99. B. List, C. Rader, *Chem. Eur. J.*, **2006**, 12, 2091-2095.
100. J. C. Sheehan, T. Hara, *J. Org. Chem.*, **1974**, 39, 1196-1197.
101. H. Kuang, M. D. Distefano, *J. Am. Chem. Soc.*, **1998**, 120, 1072-1073.
102. U. Nilsson, L. Mashalkina, Y. Lindqvist, G. Schneider, *J. Biol. Chem.*, **1997**, 272, 1864-1869.
103. F. Dyda, W. Furey, S. Swaminathan, M. Sax, B. Farrenkopf, F. Jordan, *Biochemistry*, **1993**, 32, 6165-6170.
104. X.-Y. Pei, K. M. Erixon, B. F. Luisi, F. J. Leeper, *Biochemistry*, **2010**, 49, 1727-1736.
105. A. Lapworth, *J. Chem. Soc. Trans.*, **1903**, 83, 995-1005.

106. T. D. H. Bugg. *Introduction to enzyme and coenzyme chemistry*, **2012**, John Wileys & Sons, Chichester.
107. D. C. Johnson, D. R. Dean, A. D. Smith, M. K. Johnson. *Annu. Rev. Biochem.*, **2005**, *74*, 247-281.
108. W. P. Jencks, *Catalysis in Chemistry and Enzymology*, **1969**, 288-290.
109. R. A. Lerner, A. Tramontano, *Trends. Biochem. Sci.*, **1987**, 423-430.
110. P. G. Schultz, *Science*, **1988**, *240*, 426-433.
111. M. Soodak, L. R. Cerecedo, *J. Am. Chem. Soc.*, **1944**, *66*, 1988-1989.
112. Morita, K., Suzuki, Z., and H. Hirose. **1968**. *Bull. Chem. Soc. Jpn.* *41*, 2815-2816.
113. T. R. Ward. *Angew. Chem. Int. Ed.*, **2008**, *47*, 7802-7803.
114. D. R. Hamels, T. R. Ward., *Compr. Inorg. Chem. II.*, **2013**, *6*, 737-761.
115. J. Collot, J. Gradinaru, N. Humbert, M. Skander, A. Zocchi, T. R. Ward, *J. Am. Chem. Soc.*, **2003**, *125*, 9030-9031.

Results & Discussion

Chapter 1

Synthesis of Elongated Chain Motifs for Construction of Reactive Group

Results & Discussion

Chapter 1 – Chain extensions as a potential scaffold for novel cofactor

chemistry

1.0 Synthesis of Leeper Cofactor

Upon beginning this research it was apparent that there have been considerable efforts into the design and syntheses of analogues to not only inhibit biological pathways, but also for the evolution of enzyme promiscuity. This has been more evident in the past decades with work by groups such as Reetz⁽¹⁾, Imperiali⁽²⁾, and Jensen⁽³⁾ who showed that manipulation of the enzyme and cofactor relationships could allow for novel synthetic routes to be undertaken, that are both valuable to the synthetic chemist and industrial processes. On this basis, our investigation began by considering the potential extension and modification of the vitamin B₁ scaffold which has been reported extensively throughout the literature in the past two decades, but largely by the groups of Leeper, Kluger and Mann⁽⁴⁾,⁽⁵⁾,⁽⁶⁾. Any further functionalization of the cofactor framework would need to be at a relatively early stage to maintain a simple synthetic strategy. Almost immediately it became apparent that the thiamine analogues synthesised by Leeper *et al.* were good starting candidates (figure 35).

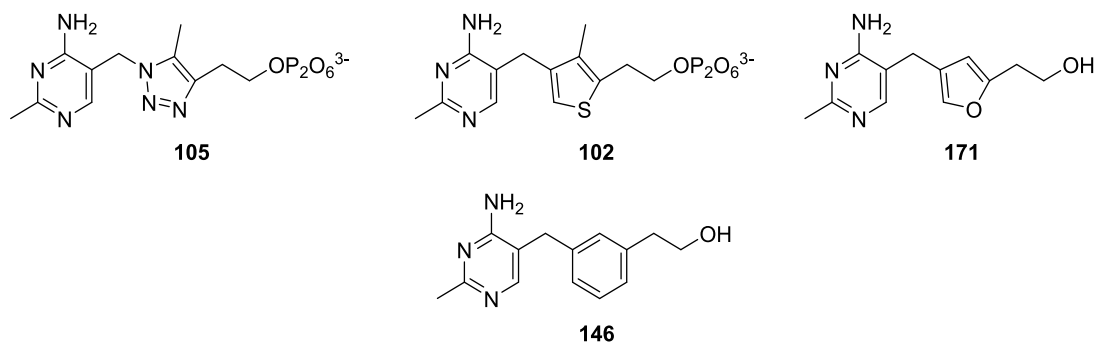
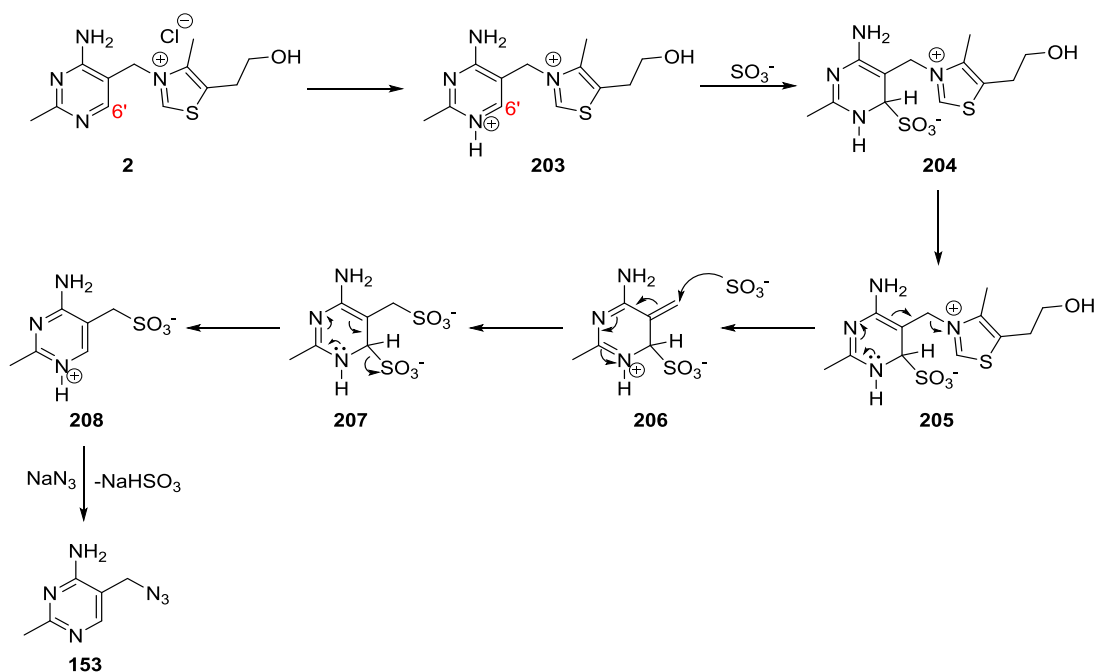


Figure 35: Current Leeper analogues

This was therefore chosen as our primary synthetic target to anchor a reactive entity too. As this topic was new within the group and the chemistry had not been performed previously, the synthesis was repeated to gain experience and to highlight any potential problems that may be encountered.

1.1 Synthesis of azide via sulfite S_NAr

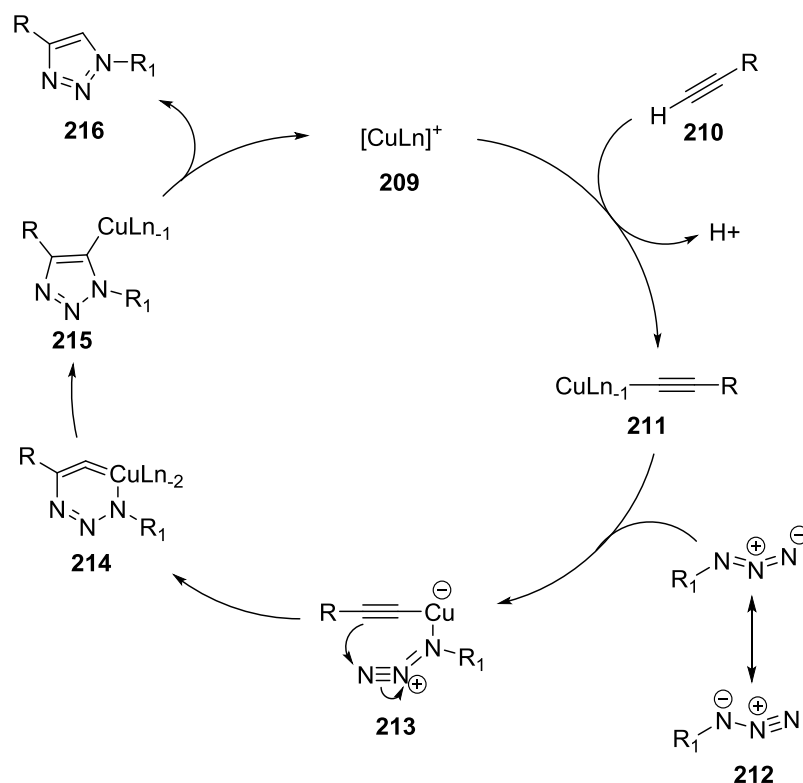
Synthesis of the target molecule began with the azide moiety **153** (scheme **44**) which was relatively straightforward following the reported procedure of Zoltewicz ^{(7), (8), (9)}. An advantage of this procedure was its use of cheap and commercially available thiamine hydrochloride **2**, which undergoes an interesting bisulfite catalysed reaction under mild conditions to give the azide **153** in 74% yield.



Scheme 44: Synthesis of 2-methyl-4-amino-5-methyl azide

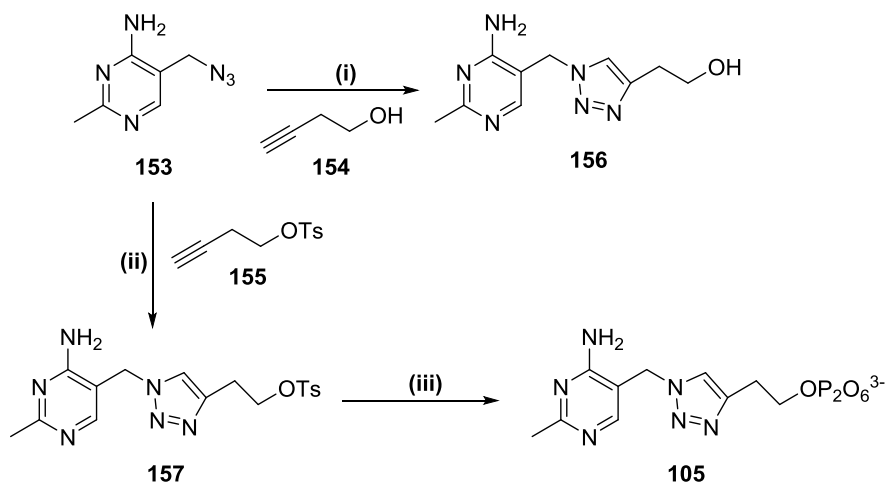
1.2 Synthesis of Leeper clicks

The 1,4-CuAAC developed by Sharpless and Fokin^{(10), (11)} (scheme 45) was then employed using the conditions described by Leeper *et al.*⁽¹⁰⁵⁾ to generate the alcohol **156** or tosylate **157**-triazoles as indicated below (scheme 45/46).



Scheme 45: 1,4-CuAAC Click Reaction

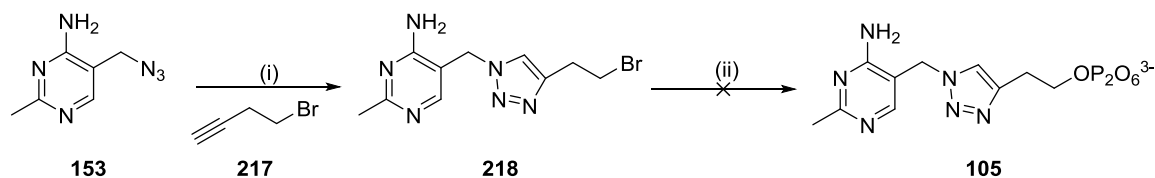
Attempting the click process of **153** with the 3-butyn-1-ol **154** (scheme 46) was straightforward and the product recrystallised nicely to give compound **156** in a good yield. However, click products from the tosylate variant **155** were always impure and further attempts with the recrystallisation solvents reported by Leeper never gave the pure compound **157**. Additional attempts to purify by both column chromatography and preparative TLC also failed.



Reagents & Conditions: (i) 3-butynol (1.eqv.), sodium ascorbate (0.1 eqv.), $\text{CuSO}_4 \cdot 5\text{H}_2\text{O}$ (0.01 eqv.), *t*-BuOH- H_2O (2:1 v/v), 25°C, 16 h, 81%, (ii) 3-butynyl tosylate (1.0 eqv.), sodium ascorbate (0.1 eqv.), $\text{CuSO}_4 \cdot 5\text{H}_2\text{O}$ (0.01 eqv.), *t*-BuOH- H_2O (2:1 v/v), 25°C, 24h, 56% , (iii) $(\text{Bu}_4\text{N})_3\text{HP}_2\text{O}_7$ (2.0 eqv.), MeCN, -5°C to 25°C, 23%

Scheme 46: 1,4-CuAAC of cofactor scaffold

Trituration of the crude material on one attempt did provide a sample with a cleaner spectrum and this was used directly for the subsequent step to introduce the diphosphate group. Treatment of **157** with *tris*(tetrabutylammonium)pyrophosphate (TBAPP) facilitated an $\text{S}_{\text{N}}2$ displacement of the tosylate group to achieve the lyophilised salt **105** in a 23% yield, albeit with a much lower yield that the recorded by Leeper *et al.* (49%). Purification of the diphosphate group was slightly more arduous compared to the literature procedure, as a preparative anion exchange HPLC column was used in their purification protocol. As these columns are costly an adapted glass column was used and packed with DEAE resin. This column although not as efficient, did manage to purify the product albeit in a slower manner and with lower yield. Co-elution of the tosyl salt after $\text{S}_{\text{N}}2$ displacement and purification by anion exchange resin (DEAE) was confirmed. This was removed as reported, by use of a cation exchange resin (DOWEX 50 H^+) to give the tosylic acid⁽¹⁰⁵⁾. Further washes with ammonium bicarbonate (1 M) produced the lyophilised ammonium pyrophosphate salt after two days of freeze drying. An alternative strategy using click chemistry of compound **153** with **217** (scheme 47) was then attempted to give compound **105**. It was thought that another leaving group may remove the problems associated with purification of the two carbon tosylate **157**. The bromo analogue **218** was easy to purify and recovered in good yield, but regrettably did not undergo the formation of diphosphate salt **105**. This could suggest that only a more stabilised leaving group allows the $\text{S}_{\text{N}}2$ displacement pathway with TBAPP to take place.



Reagents & Conditions: (i) 4-bromo-1-butyne (1.0 eqv.), sodium ascorbate (0.1 eqv.), CuSO₄·5H₂O (0.01 eqv.), *t*-BuOH-H₂O (2:1 v/v), 25°C, 16 h, 76%, (ii) (Bu₄N)₃HP₂O₇ (2.0 eqv.), MeCN, -5°C to 25°C, 23%.

Scheme 47: Synthesis of bromo 1,4-disubstituted [1,2,3] triazole ThDP

1.3 Synthesis of 1,4-disubstituted [1,2,3] Triazole with lengthened chains

Now that synthesis of the triazole motif was complete, and the skills required for the difficult and lengthy purification of the diphosphate group had been acquired, attention turned towards further enhancements of the structure (figure 36, compound 219). It was believed that an extension of the alkyl chain connecting the central [1,2,3]-triazole ring and the diphosphate group, could provide a unique place to construct a pendant arm whereby the new chemical reactivity could be attached at locations A-F.

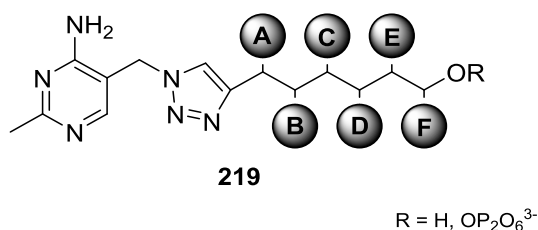


Figure 36: Potential sites to attach chemical reactivity

It was also predicted that elongation of this side arm may increase the distance from what was believed to be a deep active site into a larger cavity (figure 37, **A & B**), thereby facilitating more opportunities for functional group manipulations.

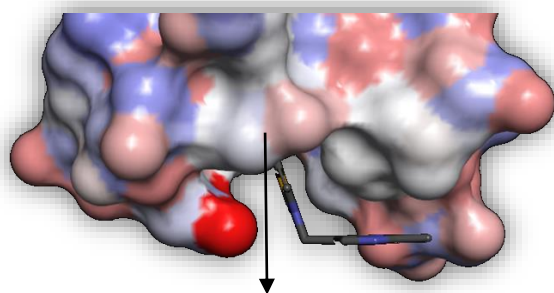


Figure A

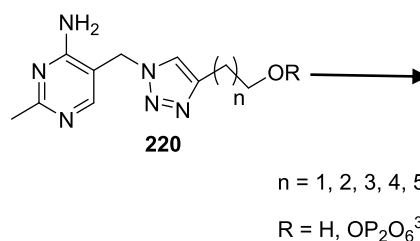
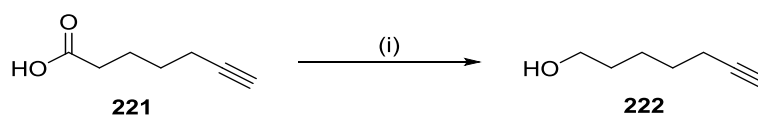


Figure B

Figures 37: A: Graphical representation of enzyme active site and chain elongation, B: Chemical chain elongation of the ThDP triazole

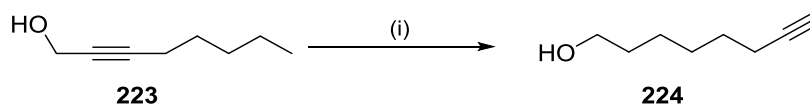
1.4 Synthesis of Alkyne and Tosylate Linkers

The synthesis of these longer chains relied initially on obtaining the corresponding alcohols from commercial sources. Chains longer than four carbon units required additional steps which included LiAlH_4 reduction of 5-heptynoic acid **221** (scheme 48) to give the five carbon unit **222** and an alkyne isomerisation (alkyne zipper reaction) of 3-octyne-1-ol **223** (scheme 49) to give the terminal alkyne **224**.



Reagents & Conditions: (i) LiAlH_4 (3 eqv), -10°C , 3hr, 70%

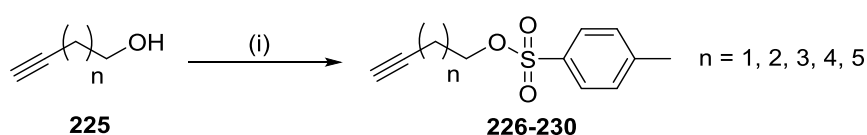
Scheme 48: LiAlH_4 reduction of 5-heptynoic acid



Reagents & Conditions: (i) KH (30%) (3 eq.), 1, 3-Diaminopropane, r.t - 0°C , 3 hr, 85%

Scheme 49: Alkyne zipper reaction of 3-Octyn-1-ol

Tosylation of the alcohols was then attempted in pursuit of forming all five diphosphate analogues for testing in the active site. Using the reported procedure by Fang *et al.* ⁽¹²⁾ and with DMAP as the catalyst (scheme 50), the respective alcohols were tosylated to give the desired products **226-230** in various yields (table 3).



Reagents & Conditions: (i) TsCl , DMAP, Et_3N , 0°C , 16 hr

Scheme 50: Tosylation of alkyne alcohols

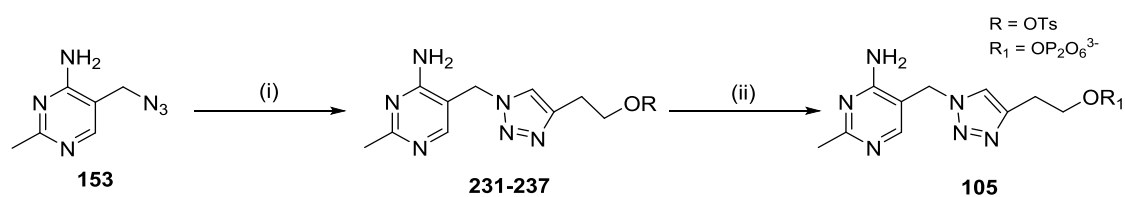
Entry	Chain Length (n)	Compound	Yield
1	1	226	57%
2	2	227	46%
3	3	228	16%
4	4	229	58%
5	5	230	78%

Table 3: Percentage yields of recovered tosylated products

Confirmation of their successful formation was provided by the expected (*dd*) for the symmetrical aromatic ring and the common two protons (*td*) located at 2.13-2.18 ppm split by the terminal alkyne proton as a triplet (*t*) at 2.00 ppm.

1.5 Synthesis of 1,4-Disubstituted [1,2,3]-Triazole Extended Alcohol Linkers

Click chemistry was then utilised as before to produce a series compounds containing chain lengths of $n = 2 - 6$ (scheme 51). As discussed earlier, the synthesis and purification of the two carbon triazole tosylate was difficult and so the alcohol click products were always tested first to assess conditions and purification methods, before attempting the notorious tosylation step. Synthesis of the alcohols normally went without any problems and the products could be purified either by recrystallisation or trituration (table 4).



Reagents & conditions: (i) Butyn-3-ol or butyn-3-tosylate (1.0 eqv.), *t*-BuOH/H₂O (1:1v/v), CuSO₄·5H₂O (0.01 eqv.), (ii) (Bu₄N)₃HP₂O₇ (2.0 eqv.), MeCN, -5°C to 25°C.

Scheme 51: Test synthesis of 1,4-disubstituted triazoles

Entry	Chain Length	R = OH	R = OTs	R = OP ₂ O ₆ ³⁻
1	2	62% (231)	57% (157)	23% (105)
2	3	55% (232)	46% (236)	-
3	4	66% (233)	96% (237)	-
4	5	47% (234)	-	-
5	6	40% (235)	-	-

Table 4: Percentage yields of recovered 1,4-disubstituted [1,2,3]-triazole ThDP linkers

Confirmation of the alcohol click products **231-235** can be seen in figure **38** whereby an additional peak relating to the triazole proton is observed at 7.84 -7.86 as highlighted in red.

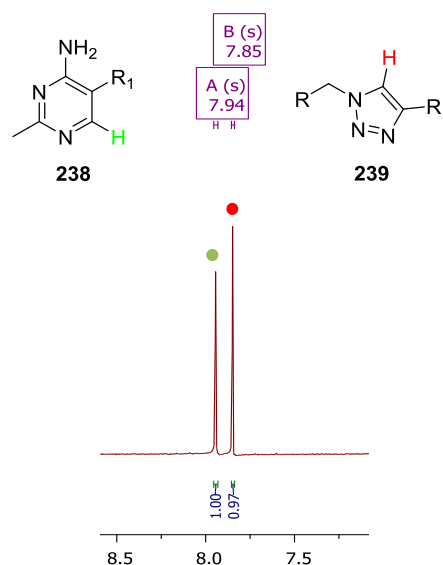
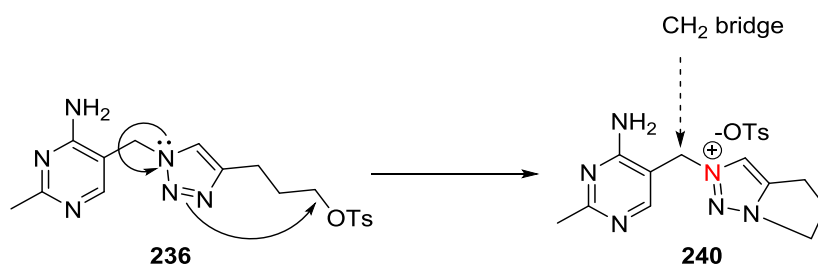


Figure 38: ¹H NMR of triazole and 2-methyl-4-aminopyrimidine protons

1.6 Synthesis of 1,4-Disubstituted [1,2,3]Triazole Extended Tosylate Linkers

Unfortunately synthesis of the three and four carbon linkers for the tosylate variants produced some difficulties in purification. Recrystallisation using the method reported by Leeper *et al.*⁽¹⁰⁵⁾ with an IPA/ hexane systems never gave the desired tosylate products. Many attempts were undertaken to purify these compounds including column chromatography, trituration and preparative TLC but most gave degradation or no pure product. During one attempt a crude product provided a clean ¹H NMR spectrum which showed the characteristic peaks of interest. On analysis of the mass spectrum no M+H peak could be observed for compound **236** (scheme **52**).

The only peak of interest was that found at 231 m/z suggesting the possible rearrangement of the [1,2,3]-triazole framework to give the product **240**.



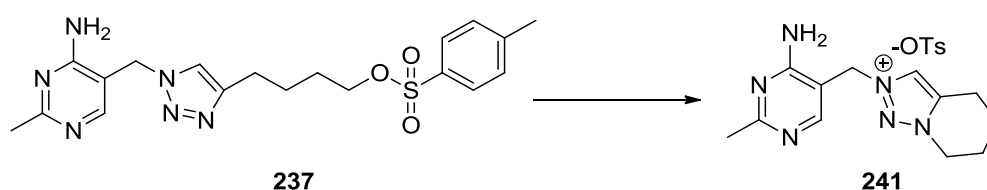
Scheme 52: Proposed 5-*exo-tet* rearrangement of 236

Further analysis of the ^1H and ^{13}C NMR for the two, three and four carbon chains showed that the CH_2 bridge situated adjacent to the quaternary nitrogen did exhibit some additional downfield shifts in the NMR due to its proximity to a charged nitrogen (scheme 52, compound **240**). The three and four carbon linkers both showed increased shifts in ppm relative to the two carbon motif although they did not differ between themselves greatly.

Entry	Chain Length (n =)	^1H (ppm)	^{13}C (ppm)
1	2 (157)	δ 5.40	46.4
2	3 (236)	δ 5.76	52.5
3	4 (237)	δ 5.82	51.5

Table 5: Comparison of ^1H & ^{13}C NMR for 2, 3 and 4 carbon tosylate linkers

This was very interesting as compound **240** (scheme 52) only existed as the rearranged product in mass analysis, whilst the four carbon linker **237** (scheme 53) showed both the expected isotopic peak at $M+H$ 417 m/z and a fragmentation relating to a similar rearrangement producing $M+H$ 245.1505 m/z . It was therefore proposed in combination with the NMR data, that this rearrangement may have only taken place under the conditions applied through mass spectrometry.

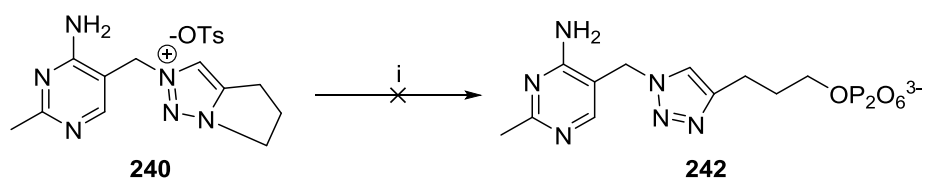


Scheme 53: Proposed 6-*exo-tet* cyclisation of four carbon tosylate

As the five and six carbon chains had already been tosylated for enzyme studies it seemed appropriate to conduct click reactions of these also. This would determine if the trend of cyclisation depreciated as the chain lengths increased. However no click products were formed for both the five and six carbon chain linkers. There was also the potential to exploit these structures as ionic liquids for green chemistry applications if the trend was continued.

1.7 Synthesis of 1,4-Disubstituted Triazole Extended Diphosphate Linkers

Even though the un-predicted formation of the triazolium salts had occurred, it was feasible that the TBAPP could still introduce the diphosphate by ring opening of the cyclised motif **240** to revert to the original [1,2,3]-triazole core with diphosphate functionality **242** (scheme 54). Purification to remove the tosyl anion would then follow the same procedure as before. This however was unsuccessful on both the three and four carbon analogues after repeated attempts and so no further reactions were tried.



Reagents & Conditions: (i) $(\text{Bu}_4\text{N})_3\text{HP}_2\text{O}_7$ (2.0 eq.), MeCN, -5°C to 25°C

Scheme 54: Attempted diphosphate displacement of salt 240

1.8 Conclusion

At this point, an opportunity to visit the laboratory of Professor Ronan Bureau in Caen arose to study the active site by *in silico* modelling. This identified a tight hydrophobic pocket surrounding the alkyl chain (figure 39), with the cofactor occupying a defined space between the active dimer in a deep pocket⁽¹³⁾.

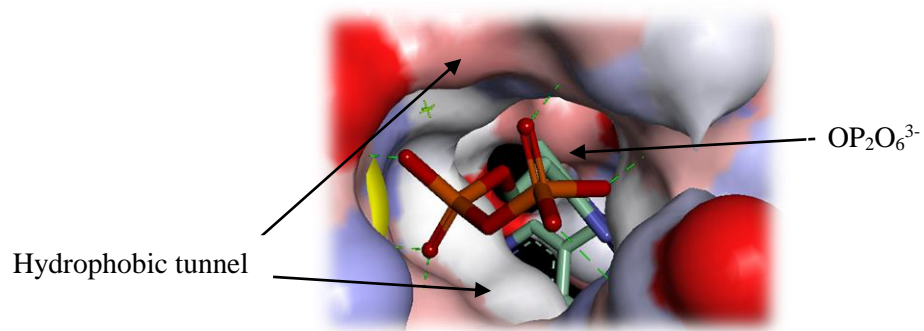


Figure 39: Hydrophobic tunnel to OP₂O₆³⁻

In light of this information no further synthetic work was undertaken on this route, as additional functionalisation of either the alkyl chain or its extension would not be allowed due to steric reasons in and around the γ -domain of the monomer unit. Considering the problematic purification, cyclisation and difficulties in achieving reproducible results, the project focused on further *in silico* studies to identify alternative synthetic targets.

Chapter 2

***In silico* Modelling of ThDP Enzyme and Evaluation of**

Active Site

ThDP *in silico* modelling

2.0 ThDP Pyruvate Enzyme Comparison

Before further synthetic work was attempted on the 1,4-disubstituted triazole ThDP, we began to assess the binding patterns and locations of ThDP in a range of ThDP-dependant enzymes from a variety of species. This information would further our understanding of the enzymes that could be used to preform our novel chemistries. It is reported that “PDC protein sequences from bacteria, fungi and plants are all colinear, so studies on any one PDC are of relevance to all”⁽¹⁴⁾ as illustrated by our comparison of natural and unnatural thiamine analogues below (figure 40).

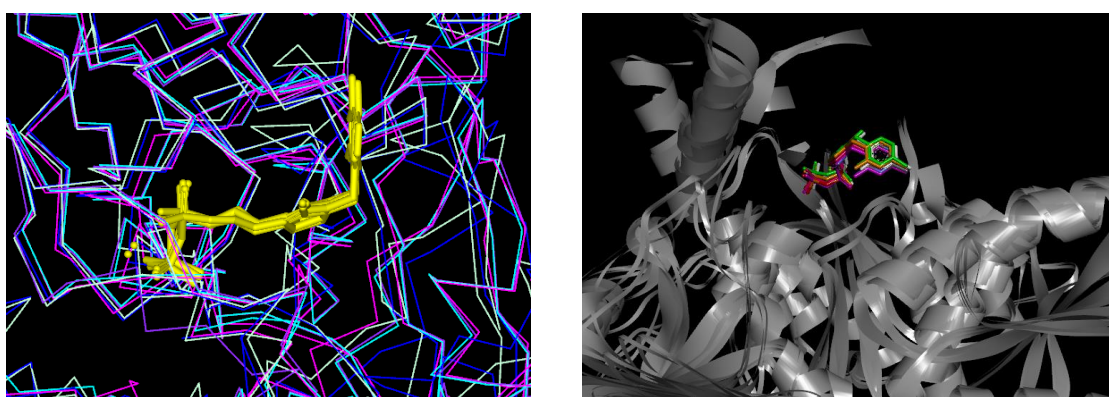


Figure 40: Natural ThDP cofactor and unnatural 1,4-disubstituted [1,2,3]-triazole-ThDP superimposed in ThDP dependant enzymes

Confirmation of the similarities exhibited between the binding amino acids of each species has allowed further comparison of the *Z. mobilis* PDC used by Leeper *et al.*^{(6), (105)} and the protein sequence for PDC from *S. cerevisiae*, which was solved independently by Hohmann *et al.* The active sites of both PDC enzymes of *Z. mobilis* and *S. cerevisiae* contain similarity in their binding amino acids^{(15), (13)}. To confirm this, a sequence alignment was completed of known pyruvate enzymes as shown in figure 41. The highlighted regions show all the binding amino acids involved in the active sites of each species (*S. cerevisiae*, *Z. mobilis*, *K. lactis*, *A. pasteurianus*) to the natural ThDP and unnatural 1,4-[1,2,3]-triazole analogues. From this, it is apparent that the amino acids involved in bonding to both the natural and unnatural cofactors are in accordance with those reported in the literature, and that the enzyme chosen by Leeper and the one tested in our group show high sequence similarity in their binding domains.

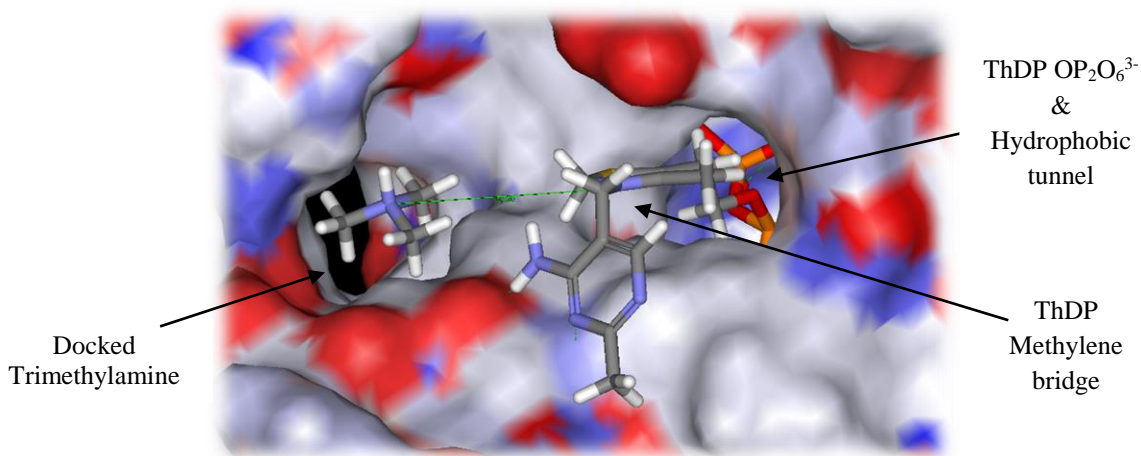


Figure 42: Docked trimethylamine and Leeper compound 105

A distance of 6.13 Å suggested that a chain length of three/four carbon units (~1.2 Å each) should suffice to anchor the tertiary amine to the cofactor scaffold (figure 43, compound 243). To test this hypothesis, the natural ThDP 55 was then removed from the active site of PDC and the novel 1,4-disubstituted triazole 243 was docked into the remaining space.

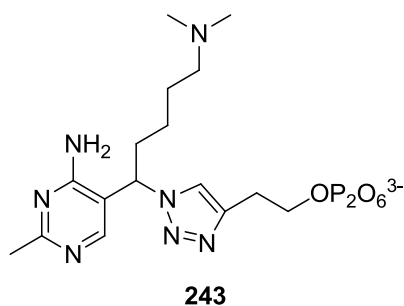


Figure 43: Modified tertiary amine 1,4-disubstituted triazole ThDP

The solvent-assisted model of 243 in PDC (figure 44) indicates that the alkyl chain follows a hydrophobic tunnel up to a defined space capable of locating the tertiary amine. It also shows that the tertiary amine is in close proximity to neighbouring acidic residues (Asp27/28) which could assist in the deprotonation of the tertiary amine at physiological pH and make it catalytically active.

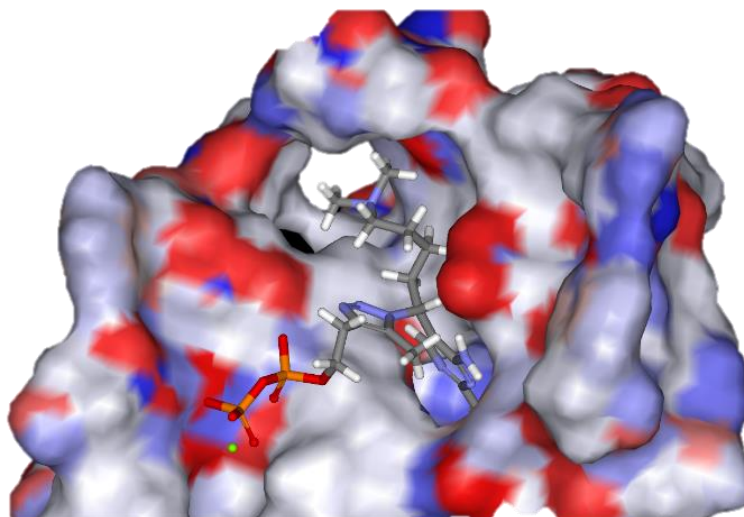


Figure 44: Surface image of docked 1,4-disubstituted [1,2,3] triazole ThDP 243 with α -domain removed

2.2 His 113/His114 amino acids

Measurement of the surrounding amino acids was then attempted to assess any conflicting steric or electronic effects. Two such amino acids that did highlight potential problems were His113 and His114. These are known to be involved in the pre-activation of the active site during catalysis and carry out primary roles within the active site. These include ionisation of ThDP, closure of the active site, provision of the anionic pyruvate with a cationic binding group and as a proton source for anionic substrates ⁽¹⁴⁾. As these two amino acids were conserved in all ThDP enzyme classes and due to the restraints of space surrounding the active site, it was necessary to account for the roles played by these residues and their catalytic effects. Previous studies towards these conserved amino acids by alteration of the pH have indicated an observable alteration in K_{cat} , therefore denoting the presence of an ionisable group within the active site which affects catalysis. Proof of this concept has been achieved by the site directed mutagenesis of His113 and His114 to Gln residues. Mutation of His113 has previously been reported to deactivate the enzyme totally and allowed no calculation of its K_M , whereas His114 was shown to give a 35% decrease in activity ⁽¹⁴⁾.

In the crystallographic snapshot of figure 45, the PDC of *Z. mobilis* remains in a closed state (green structure) where the His113 and His114 are found closer together, which reduces the remaining distance between the methylene bridge and that of the histidine rings to 5.6 Å and 7.3 Å respectively. In contrast to this, the open conformation of the PDC *S. cerevisiae* maintains the His113 at 11.94 Å and His114 at 15.29 Å (yellow structure) which depicts a larger space surrounding the cofactor (table 6).

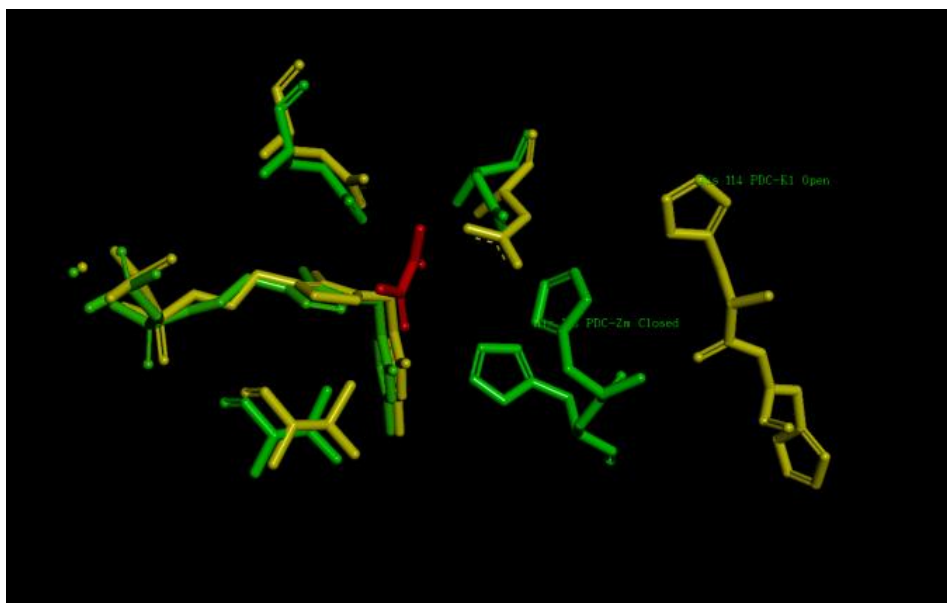


Figure 45: Active site overlap of His113/His114 from (yeast-yellow) *S. cerevisiae* and *Z. mobilis* (bacterium-green)

PDC-species	Distance of methylene bridge to Histidine's 113 & 114
<i>Z. mobilis</i>	5.6 Å & 7.3 Å
<i>S.cerevisiae</i>	11.94 Å & 15.29 Å

Table 6: Distances between methylene bridge of 1,4-disubstituted triazole and Histidine's 113 & 114 in Angstroms

It is possible that this space could be reduced upon allosteric activation whereby a regulatory second site found 18 Å away from the active site is initiated by interaction of the amino acid Cys221 with the substrate. Subsequent site directed mutagenesis studies of Cys221 have proved that this mechanism can be disabled when mutated ⁽¹⁶⁾. Allosteric activation also causes large

changes to the three-dimensional structures at the interface of the PYR and R domains which contain an active site loop ⁽¹⁷⁾. Because of this binding, the active site loop reorganises and causes closure of the active site by forcing the histidine amino acids (His113/His114) into the active site wall and thus reducing the distance within the catalytic site (figure 46). The introduction of our cofactor into this system would thus be interesting, as the initiation of catalysis would now lack the natural pyruvate molecule, and so would not induce the standard catalytic process of allosteric activation. Addition of a novel cofactor into this cavity may therefore produce a change to the enzyme architecture, which could result in an alternative three dimensional conformation being accommodated.

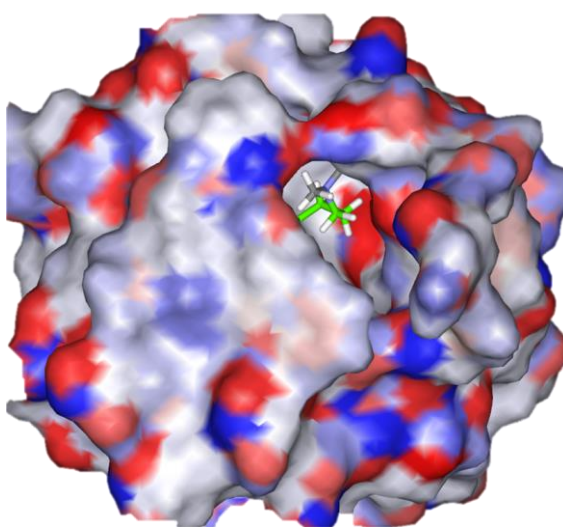


Figure 46: Surface model of compound 243 with α & β domains and open histidine conformation

2.3 Conclusion

In silico modelling of the novel 1,4-disubstituted cofactor **243** showed that the typical catalysis of pyruvate would not occur. This is due to the alkyl chain occupying the original space filled by the pyruvate ligand. The *in silico* modelling has provided further information regarding the chemistries of all PDC enzymes, the related ThDP binding sites and the similarities between active sites of *Z. mobilis* and *S. cerevisiae*. Docking of compound **243** into the active site was successful and indicated that a novel cofactor maybe accommodated within the common space filled by native ThDP **55**. Both His113 and His114 are fundamental parts of the enzymes active site and have been shown to play a large role within this thesis and the reported literature. Further

in silico studies are now required to determine which amino acids if any, could be manipulated to accommodate our model cofactor more efficiently. Barburina *et al.*⁽¹⁶⁾ has discussed the site directed mutagenesis approach, which would permit the design of a new catalytic centre within the active site by modification of these amino acids. Alternatively further studies could be made on other ThDP dependant enzymes which contain larger active sites.

Chapter 3

Synthesis of Model 1,4-Disubstituted ThDP Analogues

Chapter 3 – Synthesis of Test Analogues from the Methylene Bridge

3.0 Synthesis of Model ThDP Test Compounds

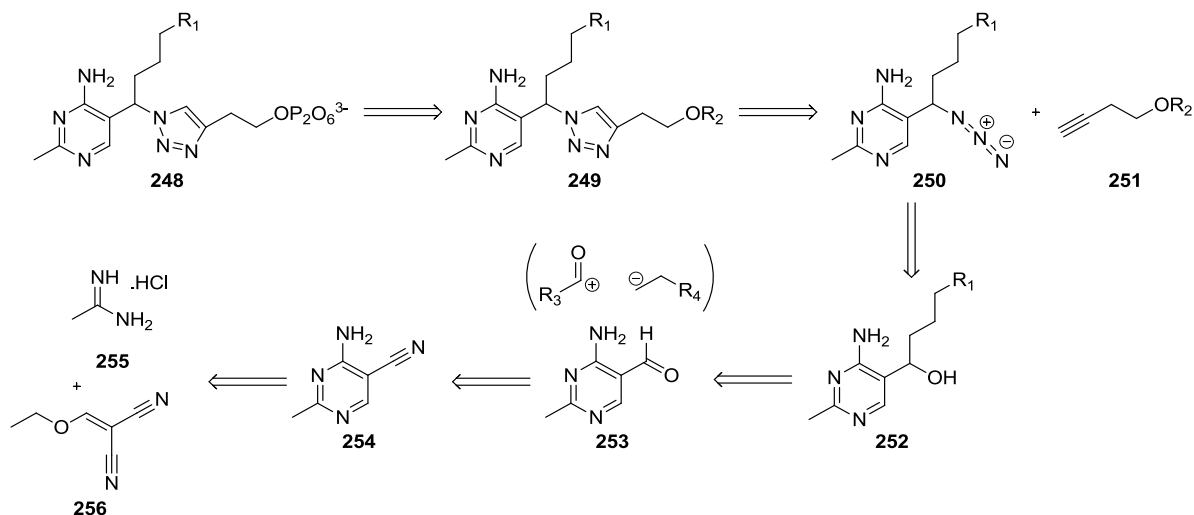
After completion of the *in silico* studies it was decided that a range of model cofactor systems should be synthesised, to test if the PDC enzymes could accommodate the alkyl chain and a reactive functional group. As the chemistry for alkyne **245** had already been established, it was decided that further modifications onto the azide synthon **244** (figure 47) would be our starting point. This also maintained the 1,4-regiochemistry of our motif compared to that of the known 1,4-disubstituted triazole which had undergone biological testing. Any problems associated with this synthesis could then be changed to the reverse synthons **246** and **247** if required.



Figure 47: Relative synthons of 1,4-CuAAC reaction

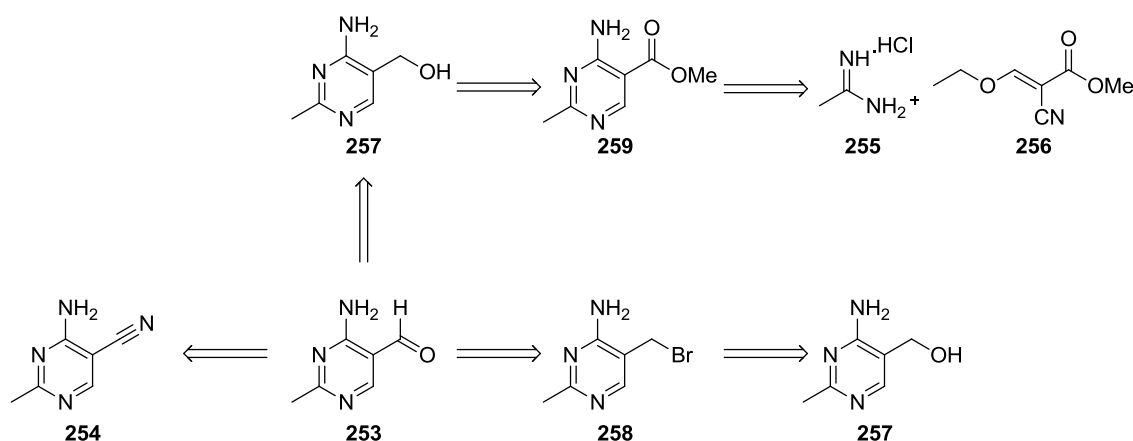
3.1 Retrosynthesis

The start of the retrosynthesis (scheme 55) remains unaltered with an FGI of **248** to the tosylate **249** and follows that of previous work by *Leeper et al.*⁽¹⁰⁵⁾ The azide group **250** could be made via an FGI to the alcohol **252** or a suitably protected alcohol which could undergo subsequent NaN_3 displacement, or by a one-pot procedure using DBU and DPPA. A C-C bond disconnection then produces two fragments of which one contains the synthetic equivalent of an acylium cation (RCO^+), and the other as a negatively charged carbon. Normally a disconnection to a negatively charged carbon would be difficult except for a few reagents including alkyllithium's, Grignard reagents and masked acyl anions which are often employed in umpolung chemistry^{(18), (119)}. Grignard reaction onto the aldehyde **253** would thus establish the secondary alcohol **252** with a variety of R groups possible.



Scheme 55: Retrosynthesis of proposed 1,4-ThDP novel cofactor

FGI of the aldehyde **253** could then be made to a number of functional groups including the benzylic alcohol **257**, benzylic bromide **258** or nitrile **254** (scheme **56**).

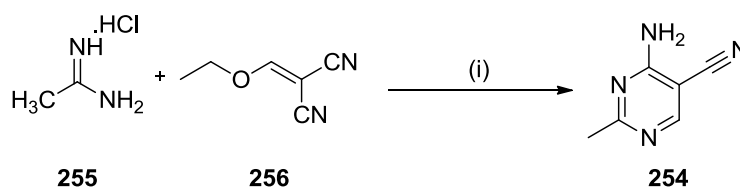


Scheme 56: Potential FGIs of 2-methyl-4-aminopyrimidine carbaldehyde

Syntheses of the benzylic alcohol **257** and bromide **258** have been reported in the past, but usually contain quite a few synthetic modifications^{(20), (121)}. The nitrile could however be introduced by condensation chemistry in a single step by reacting acetamidine **255** and ethoxymethylene malonitrile **256**.

3.2 Synthesis of the Nitrile

The synthetic routes typically proposed by Leeper *et al.* tend to establish the core 5-membered ring first. After condensation and cyclisation the required aminopyrimidine moiety is then generated in the latter stages of the synthesis^{(6), (22)}. In contrast to this, we decided to install the pyrimidine earlier so that we may attach the desired alkyl chain from the methylene bridge after a few steps as depicted in the retrosynthesis (scheme 56). Deprotonation of the hydrochloride salt **255** and *in situ* treatment with **256** produced the nitrile product **254** as fine yellow needles in a 78% yield after recrystallisation from EtOH⁽²³⁾ (scheme 57).

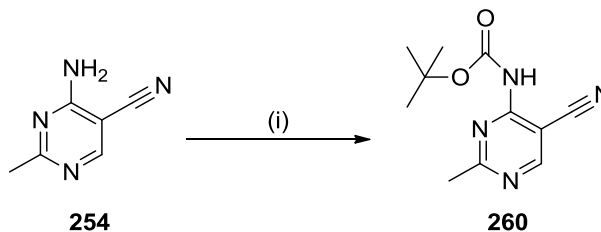


Reagents & Conditions: (i) NaOEt (2 M), EtOH, r.t., 2 hr, 78%

Scheme 57: Synthesis of 2-methyl-4-amino-pyrimidine carbonitrile

3.3 Protection of Primary Aromatic Amine

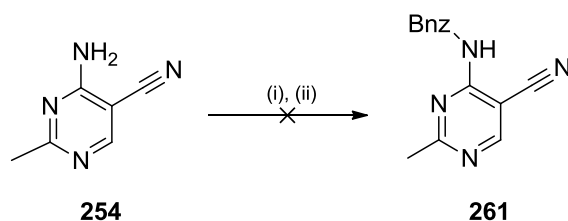
Protection of the primary amine was then sought to prevent any interference with the subsequent synthetic routes and to stop any unwanted side reactions. To begin with, a BOC protection of **254** (scheme 58) was attempted to determine if it was feasible. Surprisingly, in view of the anticipated low reactivity of the nitrogen lone pair because of delocalisation into the nitrile substituent, the protection did take place, but only in a very low yield of 6% and in the presence of a DMAP catalyst.



Reagents & Conditions: (i) BOC₂O (1.2 eqv), DMAP (0.12 eqv), Et₃N (3.0 eqv), THF, 0°C-r.t., 24 hr, 6%

Scheme 58: Boc protection of aromatic primary amine

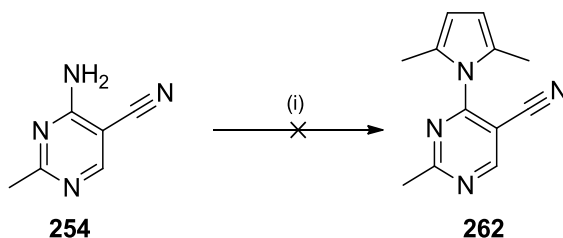
As another test, we choose the benzyl protecting group as shown in scheme 59 by reductive amination with benzaldehyde under reflux conditions and Dean-Stark apparatus. However, the benzyl protected amine 261 was not formed after 72 hours.



Reagents & Conditions: (i) Benzaldehyde (1.1 eqv), AcOH, Toluene, Relux, 30 mins-72 hr, (ii) NaBH(OAc)₃, MeOH, 0°C-r.t.

Scheme 59: Attempted benzylation of primary amine 254

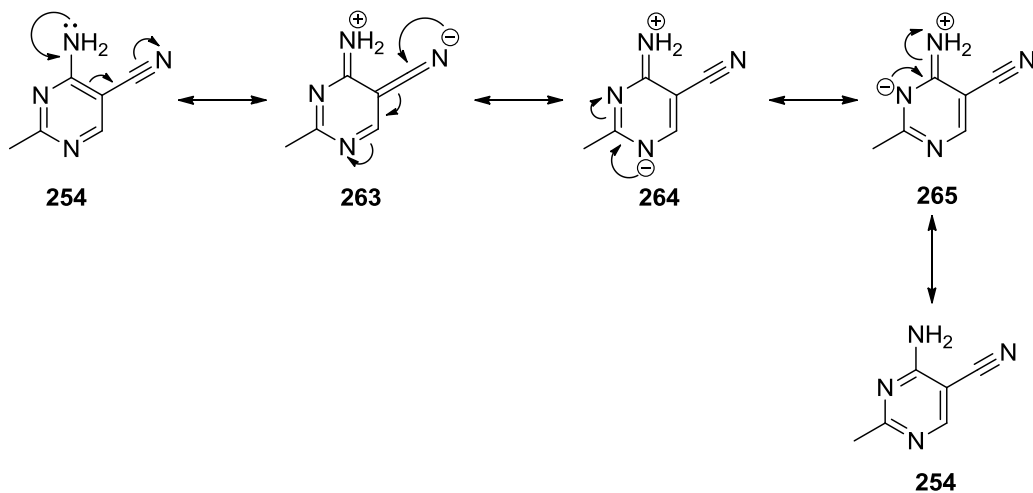
Because some protecting groups could alkylate at the N'1 position on the pyrimidine, we choose a second condensation reaction to protect both amine protons. This was our last attempt and involved formation of a pyrrole group using 2,5-hexandione under Dean-Stark conditions (scheme 60). This was used because of its stability throughout the Grignard addition and the possibility of being removed concomitantly under the acidic work up conditions of the Grignard step.



Reagents & Conditions: (i) 2,5-Hexandione (1.5 eqv), AcOH, (Dean- Stark), Toluene, 24 hr.

Scheme 60: Attempted pyrrole protection

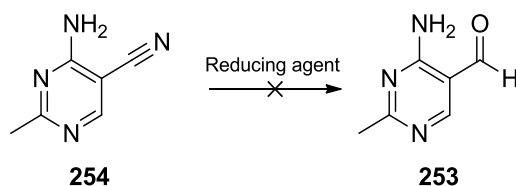
It was decided at this point to stop any further amine protections. It was apparent that protection of this primary amine was extremely difficult presumably because of the mesomeric donation of the nitrogen lone pair into the C-N bond. Additionally the pyrimidine ring is understood to be electron deficient by virtue of the two ring nitrogen's. The *ortho*-nitrile also deactivates the π -system by removing electron density from the aromatic ring as shown by scheme 61⁽²⁴⁾.



Scheme 61: Inductive electron withdrawal and stabilisation by *ortho* nitrile

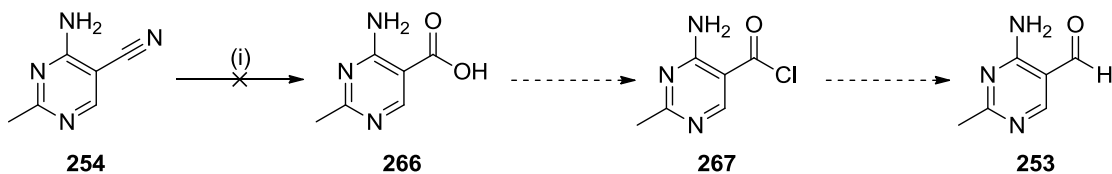
3.4 Synthesis of 2-methyl-4-amino pyrimidine carbaldehyde

Following the work of Begley *et al.* ⁽²⁵⁾ a LiAlH_4 reduction of the nitrile **254** was then attempted which gave the aldehyde **253** (scheme **62**) in a satisfactory yield of 30%, albeit with some starting material present. To reduce the risk of over reduction to the primary amine and for improving on recovered yields, some alternative nitrile reductions were attempted. DIBAL-H is one of the most common reagents for achieving this transformation but gave no product after 16 hours. Reaction with Raney Nickel[®] and formic acid gave the product, but only in yield of 10% and with some remaining starting material in 30% yield ⁽²⁶⁾.



Scheme 62: Nitrile reduction to aldehyde

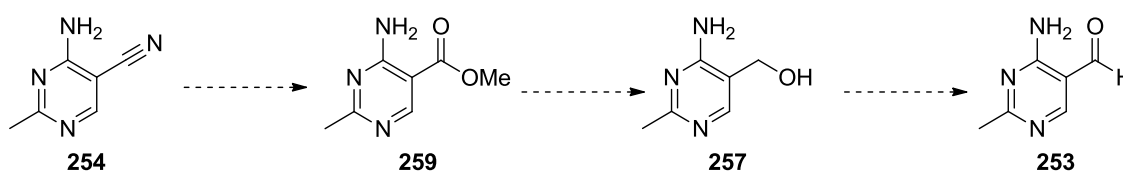
At this point, an alternative synthetic route (scheme **63**) was envisaged that would use a poisoned Rosemund reduction with BaSO_4 to reduce the acyl chloride **267** to its aldehyde counterpart **253**. Unfortunately hydrolysis of the nitrile **254** using the literature procedure of Price *et al.* ⁽²⁷⁾ was not successful after using both acidic and basic approaches, with just nitrile being recovered in quantitative yields.



Reagents & Conditions: (i) KOH (3 M) or HCl (3 M), reflux, 48 hrs

Scheme 63: Aldehyde synthesis via acyl chloride

Other approaches to this synthesis may have included the lengthy procedure (scheme 64) whereby methanolysis of the nitrile **254** to the ester **259** is followed by a LiAlH_4 reduction to give the benzylic alcohol **257** which could be selectively oxidised to the aldehyde **253** by MnO_2 .

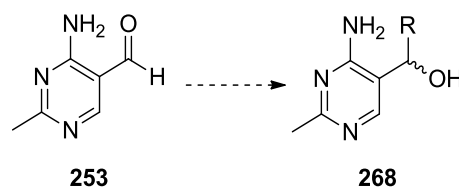


Scheme 64: Proposed three step synthetic route to aldehyde

In 2013, a patent procedure was published using hydrogenation of the nitrile **254** via Pd/C under acidic conditions at an elevated pressure of 45 psi. Upon trying these conditions the aldehyde **253** was recovered in an improved yield of 54% after simple purification by filtration over silica to remove residual Pd/C. Consequently this became the primary method for synthesising the aldehyde product.

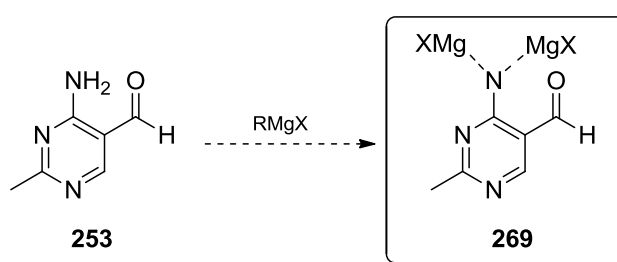
3.5 Synthesis of Methyl – Butyl Alcohols

Attention was now focused on formation of the secondary alcohol **268** (scheme **65**). As protection of the primary amine on **253** was not viable, it was decided to use the Grignard in excess and hope that any side reactions were limited. As Grignard reagents are extremely basic ($pK_a \sim 50$), it was thought that potential problems could arise from the acidity of the amine protons.



Scheme 65: Synthesis of 2-methyl-4-amino pyrimidine secondary alcohols

As there was no reported procedure for this transformation and with two acidic protons, it was decided that an excess of Grignard reagent would be a cheap and efficient way to protect the amine. This was thought to occur by formation of the nitrogen dianion which could then be trapped by the magnesium salts (scheme **66**, compound **269**). This process was apparent whilst running the experiments as the evolution of methane could be seen when methylmagnesium bromide was added. The last remaining equivalents of Grignard reagent would then be free to undergo reaction with the carbonyl group to give the product.



Scheme 66: Trapping of amine anion by magnesium salts

Initial testing then began with addition of the methyl Grignard reagent at lower temperatures due to the inherent high reactivity of Grignard reagents⁽²⁸⁾. Addition to the aldehyde **253** began at lower temperatures with each additional experiment allowing the reaction to warm to higher temperatures. Most of these attempts did not give formation of the product except for entry **3**, which showed a faint spot at an R_f of 0.4 in EtOAc:MeOH (95:5 v/v), but no product could be isolated (entries **1-3**, table **7**). As the reagent was relatively old, a fresh more concentrated methyl

Grignard reagent was purchased, and finally gave the product as shown by entry **4**, (table **7**). At a similar time another literature search uncovered a patent which described this exact procedure and gave the best result yet (entry **5**, table **7**). As the secondary alcohols had begun to be synthesised more readily it was decided that the equivalents would be increased slightly to 3.5 to improve reproducibility. The remaining alkyl chains were then recovered in moderate yields (entries **7-9**, table **7**)

Entry	Grignard	Conc.	Eqv.	Temp (°C)	Time (hrs)	Yield (%)
1	Methyl	1 M	5	-78 - Reflux	16	-
2	Methyl	1 M	5	-78 - RT	16	-
3	Methyl	1 M	5	-78 - (-40)	16	- ^a
4	Methyl	3 M	5	-10	16	48%
5	Methyl	3 M	3	0 - RT	16	61% ^b
6	Methyl	3 M	3.5	0 - RT	16	57%
7	Ethyl	3 M	3.5	0 - RT	16	44%
8	Propyl	3 M	3.5	0 - RT	16	68%
9	Butyl	3 M	3.5	0 - RT	16	55%

a) Reaction worked but not isolated, b) Patent conditions

Table 7: Test conditions for addition of methyllmagnesium bromide (3 M) to aldehyde compound 253

Purification of these compounds was tedious to start with as the workup conditions were not known. Extraction with EtOAc and 1-butanol seemed to provide a satisfactory way of recovering these secondary alcohols although the 1-butanol was hard to remove. This finally resulted in isolation of pure products **270 – 273** in good yields (Figure **48**, table **8**).

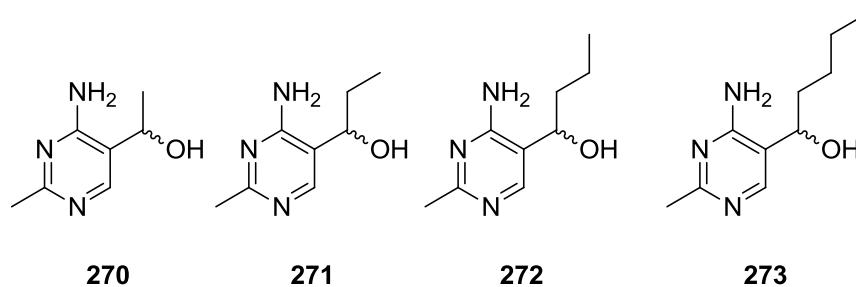
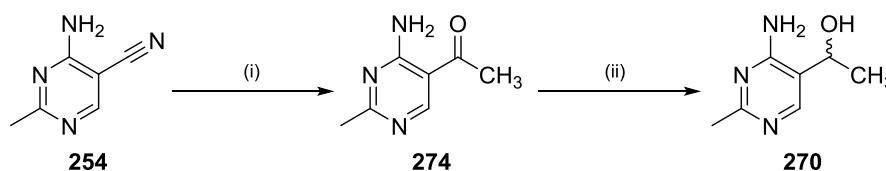


Figure 48: Isolated pyrimidine secondary alcohols

Entry	Compound	Time (hr)	Yield%
1	270	24Hr	61%
2	271	24Hr	44%
3	272	24Hr	68%
4	273	24Hr	55%

Table 8: Yields of isolated secondary alcohols

An attempt to create the ketone **274** (scheme 67) was then completed to compare synthetic yields. This was done by addition of methylmagnesium bromide onto the nitrile **254**, which was successful but only in a lower yield of 41%. LiAlH_4 reduction of the prochiral ketone then gave the racemic alcohol **270** in a 21% yield.



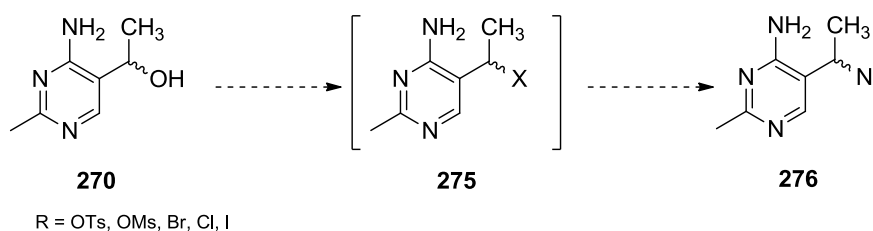
Reagents & conditions: (i) CH_3MgBr (3M) (3.5 eqv.), 0°C-r.t. 24Hr, 41%. (ii) LiAlH_4 , 0°C-r.t. 24Hr, 21%.

Scheme 67: Prochiral ketone formation and LiAlH_4 reduction

On finding the most suitable conditions to effect this transformation and with the workup conditions in hand, a study of the necessary conversion to the azide was now possible.

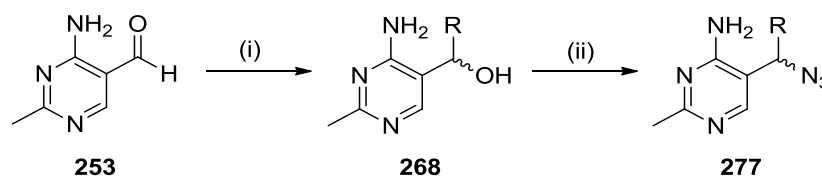
3.6 Synthesis of Methyl – Butyl Azides

The transformation of alcohol to azide can normally be undertaken by *in situ* conversion to a suitable leaving group such as a mesylate, tosylate or halogen and subsequent $\text{S}_{\text{N}}2$ displacement with sodium azide (scheme 68).



Scheme 68: Primary alcohol protection and $\text{S}_{\text{N}}2$ displacement

In the procedure of Nicewonger *et al.* ⁽²⁵⁾ (scheme 69), the alcohol to the azide step was easily achieved by a one pot conversion.



Reagents & Conditions: (i) Grignard (3.5 eq), THF, 0°C-RT, 14 hrs, (ii) DBU (1.3 eq), DPPA (1.2 eq) THF, RT, 16 hrs

Scheme 69: Synthesis of azides

This is facilitated by removal of the alcohol proton by the bulky DBU base. Nucleophilic attack by the alkoxide anion onto the diphenylphosphoryl azide (DPPA) then ensues with collapse of the tetrahedral intermediate releasing the azide anion. The formation of this strong oxygen-phosphorus bond generates the driving force for the reaction as the azide anion displaces the diphenylphosphoryl alcohol via a Walden inversion. A series of azide derivatives were successfully prepared using this methodology in good yields and in a single step (figure 49, table 9).

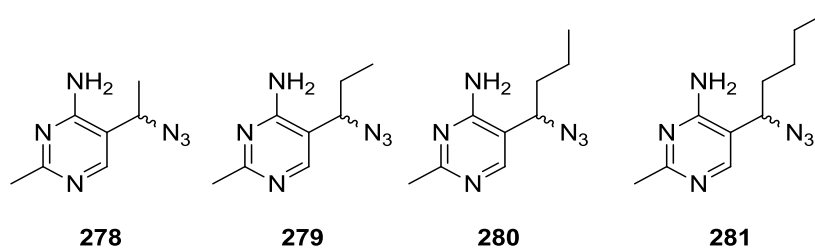


Figure 49: Isolated pyrimidine azides

Entry	Compound	Time (hr)	Yield%
1	278	14Hr	49%
2	279	14Hr	48%
3	280	14Hr	45%
4	281	14Hr	59%

Table 9: Yields of azide compounds 278-281

Purification of these compounds was relatively straightforward with the only problem being their inherent high polarity, which required multiple chromatography to remove the unwanted side product of diphenylphosphoryl alcohol **282** (figure 50).

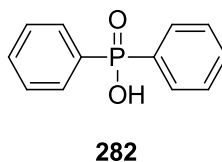
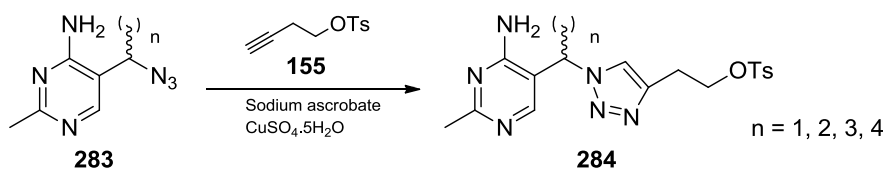


Figure 50: Diphenyl phosphoryl alcohol side product

Otherwise they were stable under bench conditions and never posed any safety problems, even though the carbon to nitrogen ratio is relatively low with the smaller alkyl linkers.

3.7 Synthesis of Methyl – Butyl Tosylates

Conditions to accomplish the tosylate click (scheme 70) were as reported before by Leeper *et al.*⁽¹⁰⁵⁾. After several failed attempts, some more positive results were recorded after stirring overnight at 30° C.



Scheme 70: Synthesis of model tosyl 1,4-disubstituted triazole analogues

Purification of these substituted products was easier compared to that of the original published 1,4-disubstituted [1,2,3]-triazole which was troubled by difficult recrystallisations. Column chromatography of the tosylates (Entries **1-5**, table **10**) went without problems although lengthening of the alkyl chain from the methylene bridge appeared to have a detrimental effect upon the purity of the propyl **288** and butyl **289** products.

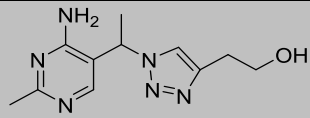
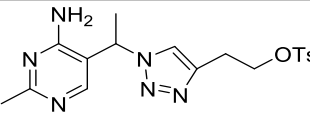
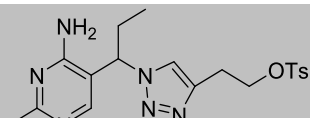
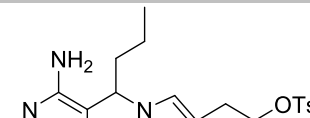
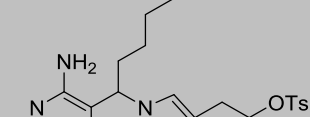
Entry	Compound structure	Compound	Alkyne	Temp	Time	Yield
1		(285)	3-butyn-1-ol	30°C	16Hr	22%
2		(286)	3-butyn-tosylate	30°C	16Hr	14%
3		(287)	3-butyn-tosylate	30°C	16Hr	35%
4		(288)	3-butyn-tosylate	30°C	16Hr	43%
5		(289)	3-butyn-tosylate	30°C	16Hr	23%

Table 10: Percentage yields and reaction conditions for click tosylate formation

The methyl and ethyl analogues are very clean as shown in figure 51 (blue spectrum, methyl derivative **286**), when compared to those of the longer propyl and butyl analogues (red spectrum, propyl derivative **288**). These tended to show the appearance of small residual tosylate peaks at 20% impurity of the primary compound. This was observed by the presence of additional *dds* at 7.7 and 7.1 ppm which is thought to have occurred by some cleavage of the tosylate group upon passing through the silica column.

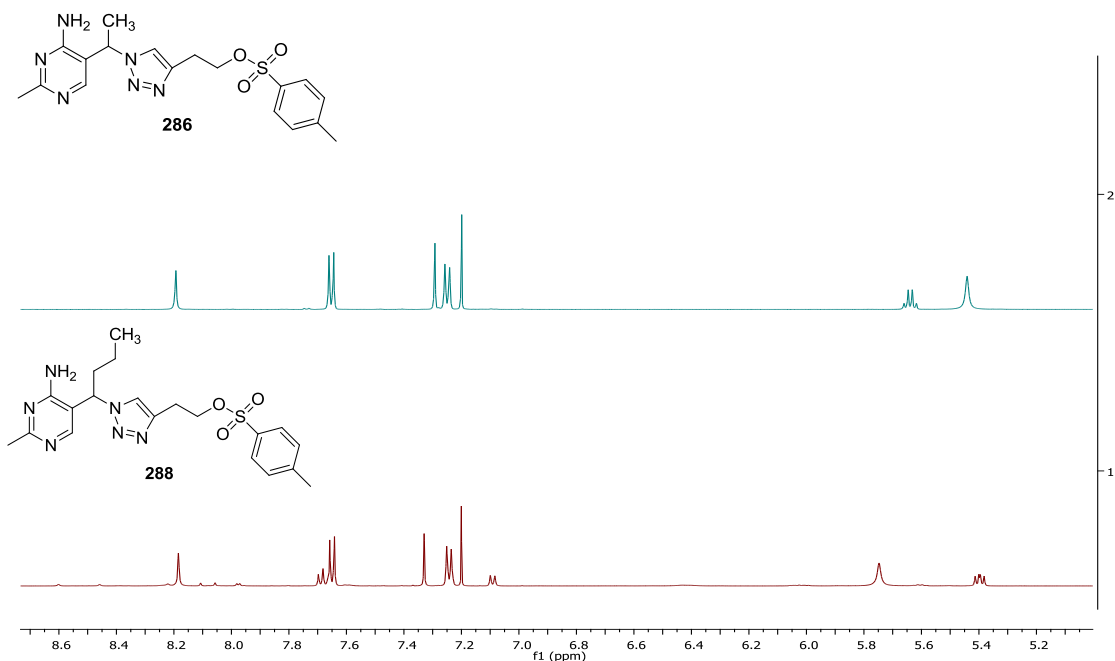
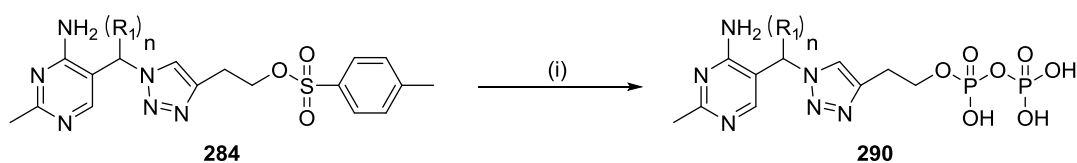


Figure 51: Comparison of methyl tosylate (blue) and propyl tosylate (red)

3.8 Synthesis of Methyl – Butyl Diphosphate

Conversion of the extended triazole tosylates into the diphosphates was carried out as before using the conditions reported by Leeper *et al.* ⁽¹⁰⁵⁾ S_N2 displacement of the tosylate was used to install the diphosphate functionality (scheme 71). This methodology was kept as previous reports by Leeper had mentioned the difficulties noted in purification of the mono, di and tri anionic species formed upon refluxing the alcohols in phosphoric acid.



Reagents & conditions: (i) *tris*(tetra-*n*-butylammonium)pyrophosphate, -10°C, 24 Hr

Scheme 71: S_N2 displacement of tosylate with *tris*(tetra-*n*-butylammonium pyrophosphate) (TBAPP)

Purification of the diphosphates was more difficult than the previously synthesised analogues of Leeper *et al.* This normally involves dilution of the crude mixture with water and purification by a DEAE preparative HPLC column to recover the anionic diphosphate. Due to the high costs of these columns we did not possess this ability, and so a DEAE resin was made up and used in the same way as running a normal silica column, albeit with much longer purification periods. Elution

of the desired diphosphate was then accomplished by increasing the ammonium bicarbonate concentration until competition for the resin caused elution of the product. Interestingly the reported co-elution of tosyl anion occurred, but was removed after acidification with DOWEX 50H⁺ after two or three passes. The lyophilised ammonium salts were then recovered in moderate yields as white powders and used for biological testing with no further steps (table **11**, entries **1-4**).

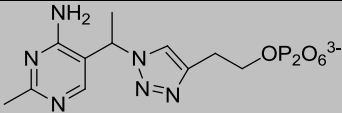
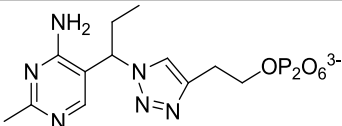
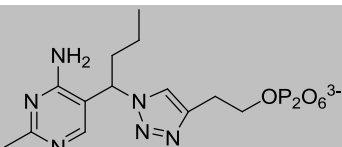
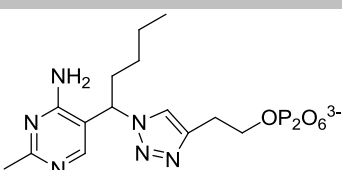
Entry	Compound structure	Compound	Temp(°C)	Time	Yield%
1		291	-10°C	24 Hr	63%
2		292	-10°C	24 Hr	53%
3		293	-10°C	24 Hr	47%
4		294	-10°C	24 Hr	55%

Table 11: Yields of modified 1,4-disubstituted triazole diphosphate motifs

Analysis of the ¹H NMR for the methyl diphosphate compound **291** (figure **52**), shows the CH₃ group split as a doublet (*d*) (red spot) due to its coupling with the adjacent C-H (*q*) (green spot) as shown by the observed coupling in the ¹H COSY spectrum (figure **53**). All other peaks integrated as expected and were found in similar positions to that of the original diphosphate 1,4-disubstituted triazole **105** (page 71).

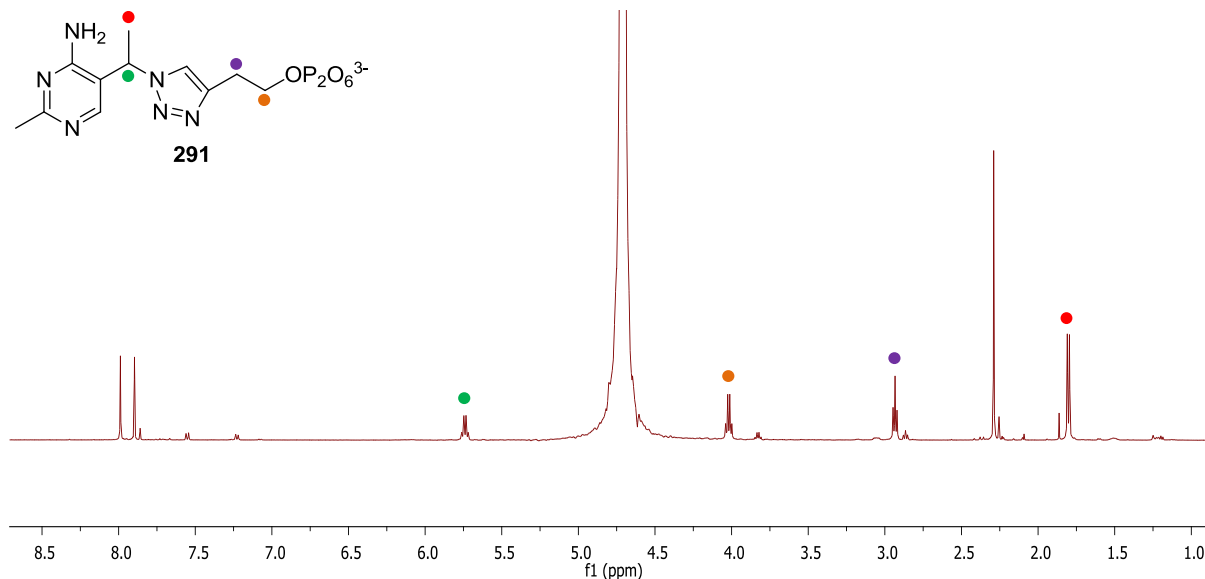


Figure 52: ^1H NMR of methyl diphosphate

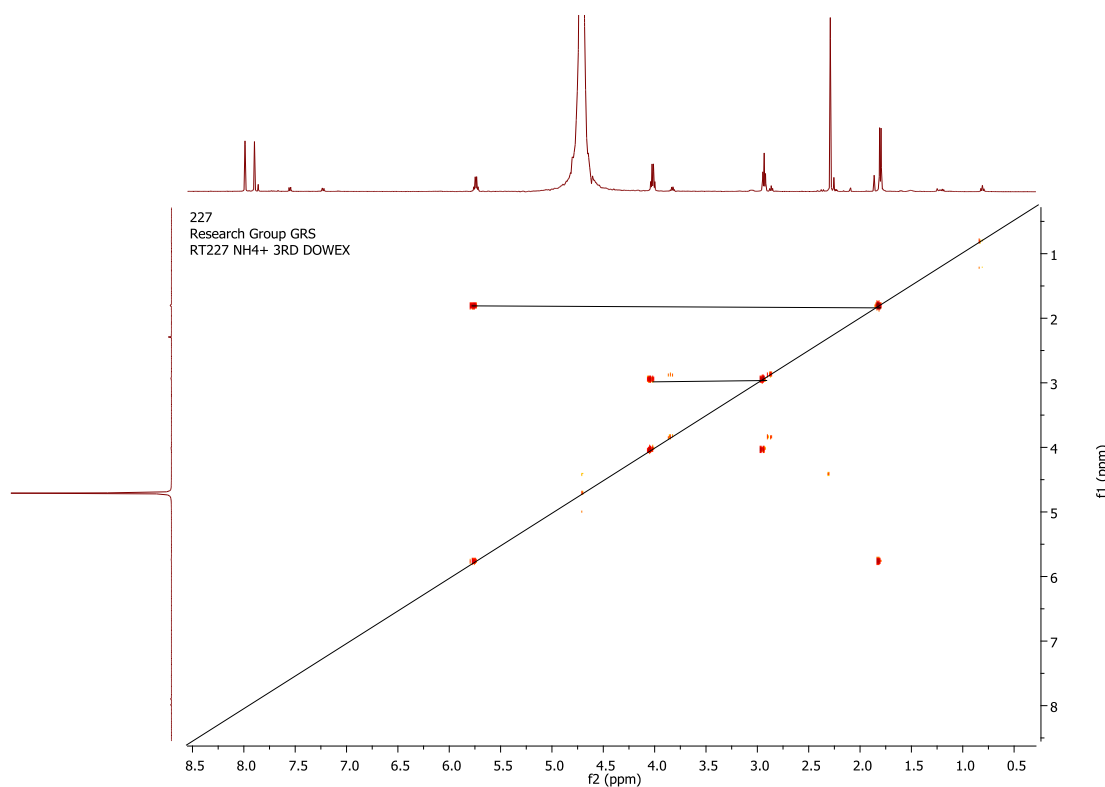


Figure 53: COSY spectrum of diphosphate compound 291

However, an unexpected duplication of the peaks belonging to the core triazole structure was observed when the chain was lengthened from ethyl to butyl. This was not observed in the smaller methyl analogue which integrated normally. It was also more difficult to purify the ethyl, propyl and butyl chains compared to that of the methyl variant and both issues seemed to be linked. As a result of this observation a VT experiment (figure 54) was conducted to see if rotamers were

the cause of this phenomenon. Figure 54 however did not depict the usual coalescence of peaks that is expected upon heating of the reaction mixture and so additional evidence was required.

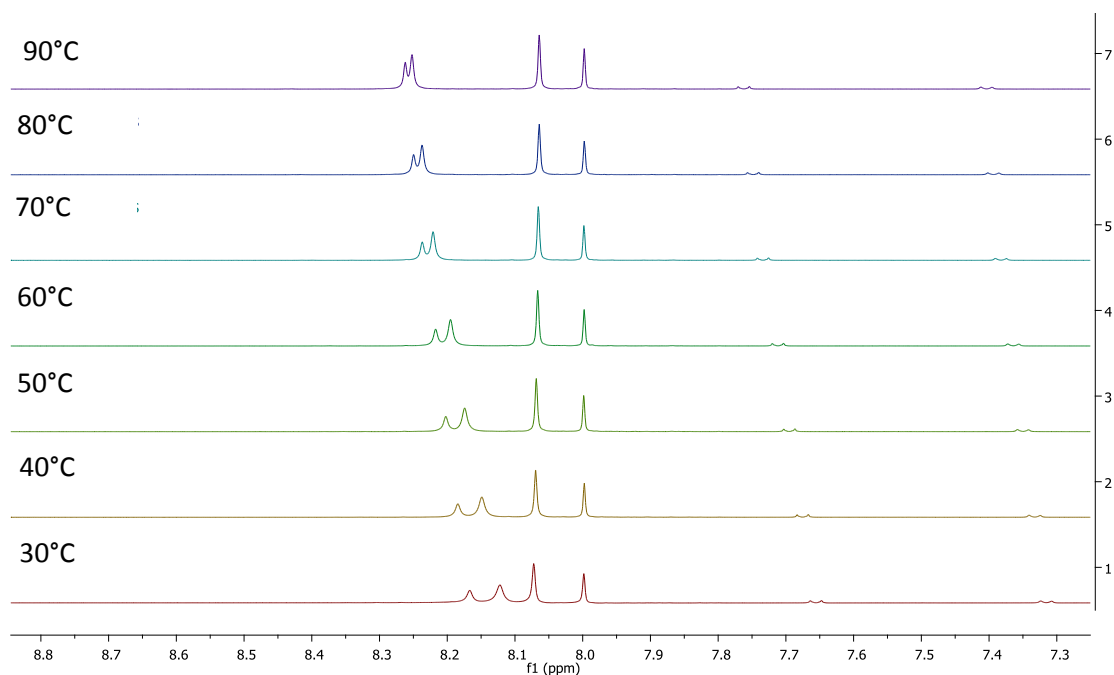


Figure 54: ^1H NMR VT experiment of ethyl diphosphate

Some evidence to support this unusual rotamer effect is given by the integration for each of the two sets of peaks (figure 55), which both integrated as a single proton.

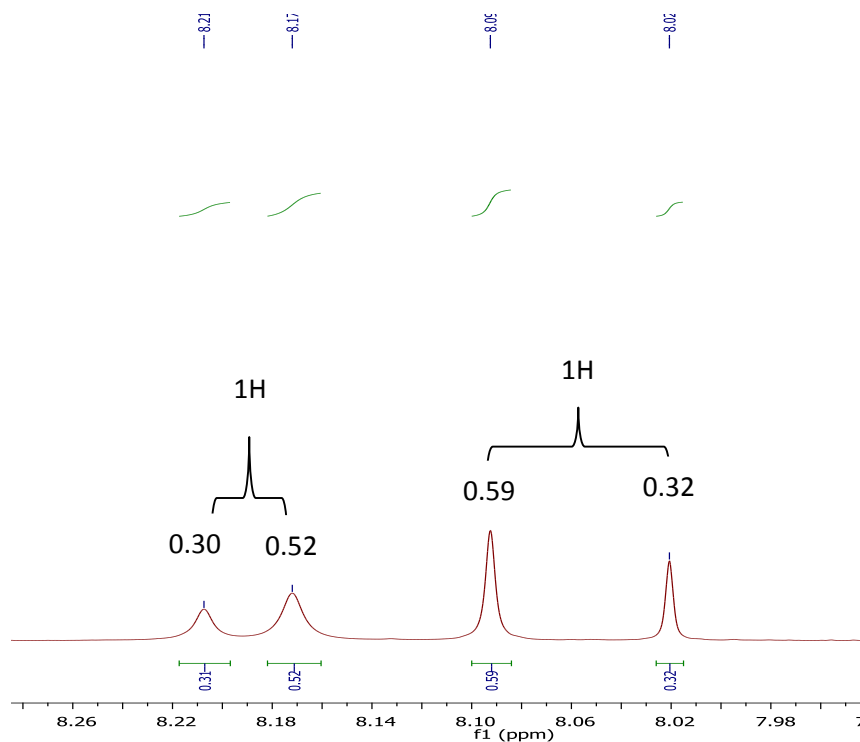


Figure 55: ^1H NMR of rotamer effect of ethyl diphosphate

This could suggest that rotation is observed around the newly constructed alkyl chain from the methylene bridge as it adopts different conformations and causes the remaining ThDP framework to be seen in separate proton environments, possibly by hydrogen bonding of the amine proton to the triazole framework (figure 56).

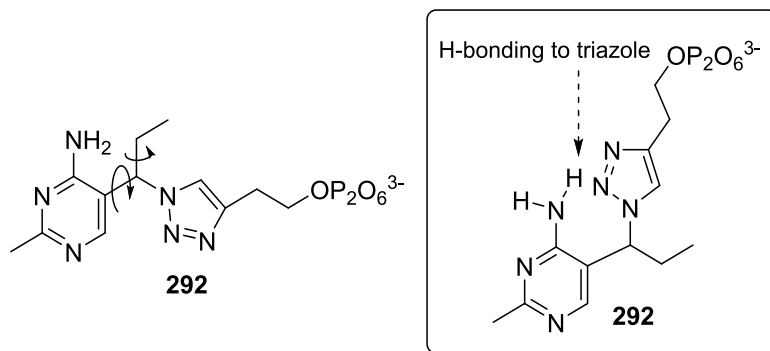


Figure 56: Possible rotamer formation by rotation around alkyl chain

This observation is also made towards the other peaks in the spectrum relating to that of the common ThDP framework (figure 57, grey, orange, and purple spots), but not that of the alkyl chain. This is confirmed by the lack of a second peak relating to the chiral proton (figure 57, green spot) and the remaining protons on the newly formed alkyl chain (red and blue spots).

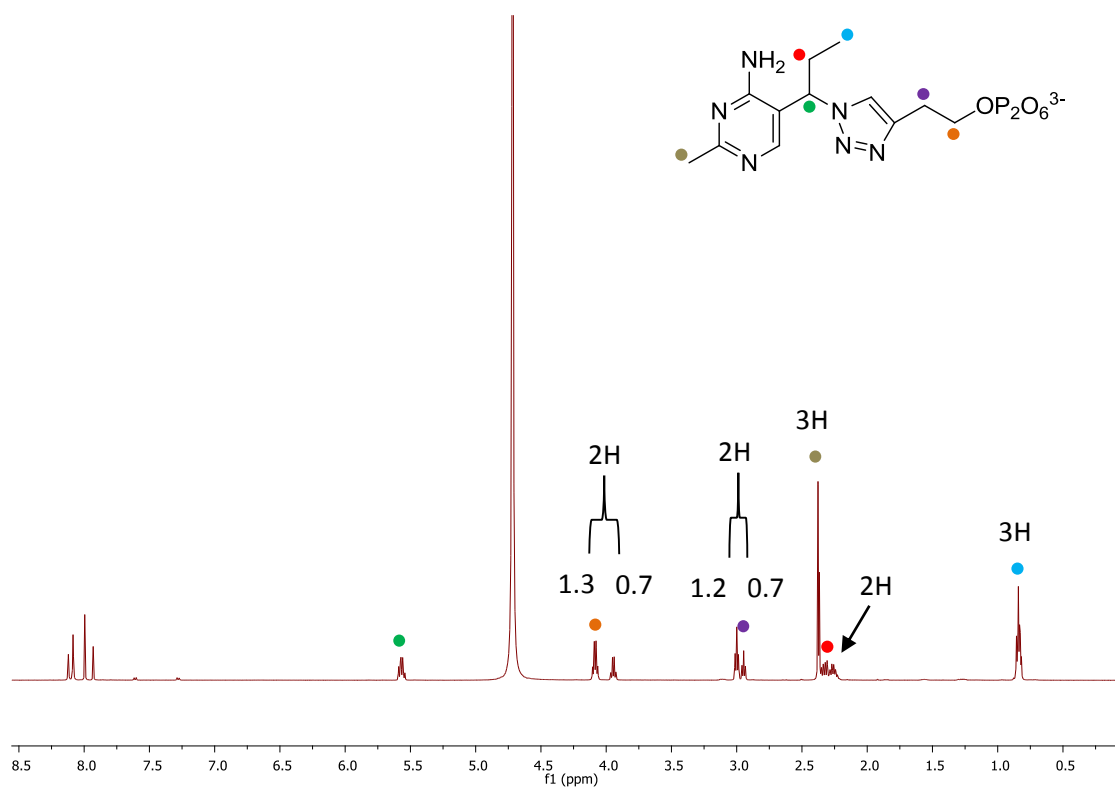


Figure 57: ^1H NMR of compound 292 with rotameric effects

This evidence therefore suggests that a mixture of compounds does not exist due to the lack of other duplicate peaks. Moreover, the ^{13}C shows small duplicate peaks at identical chemical shifts to the primary rotamer, the ^{31}P spectrum only depicts each of the two peaks for the diphosphate and each respective mass spectrum was identified as a single product.

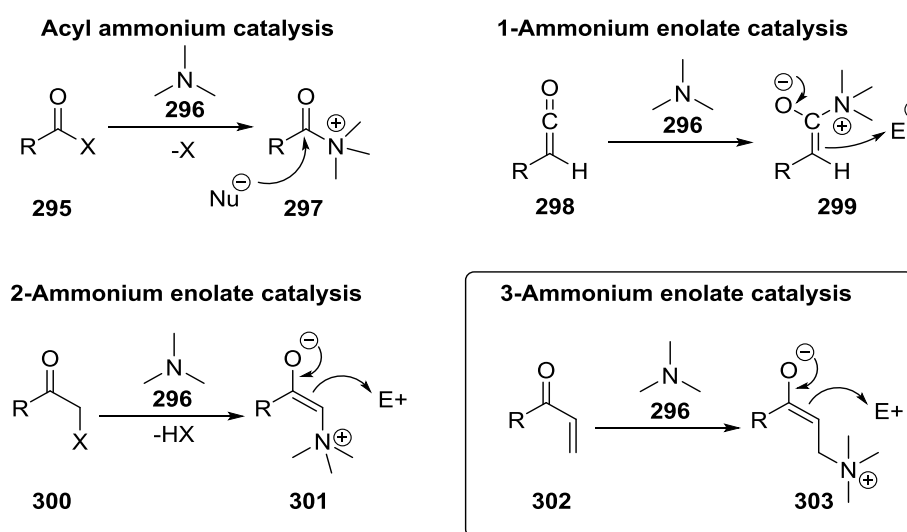
Chapter 4

Synthesis of Tertiary Amine Tether's for a Potential Baylis-Hillman Reaction

4-Synthesis of Tertiary amine ThDP 1,4 – disubstituted [1,2,3]-Triazole

4.0 The Synthetic Target – Tertiary Amine

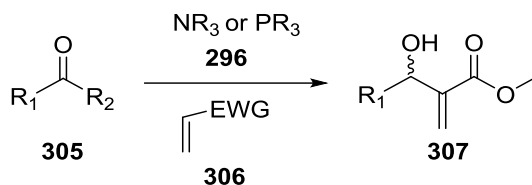
As the synthesis of the four model structures was nearly complete, our attention turned towards different types of chemistries that could be installed at the end of the carbon linker. This chemistry needed to be small enough to fit within the active site and reactive enough that it could facilitate the desired chemistry. It also needed to catalyse the reaction in the presence of aqueous media, whilst working alongside the amino acids found within the active site. One functional group that would fit this criterion is the tertiary amine, which is known to occur in many organocatalytic systems (scheme 72).



Scheme 72: Organocatalytic pathways catalysed by tertiary amines

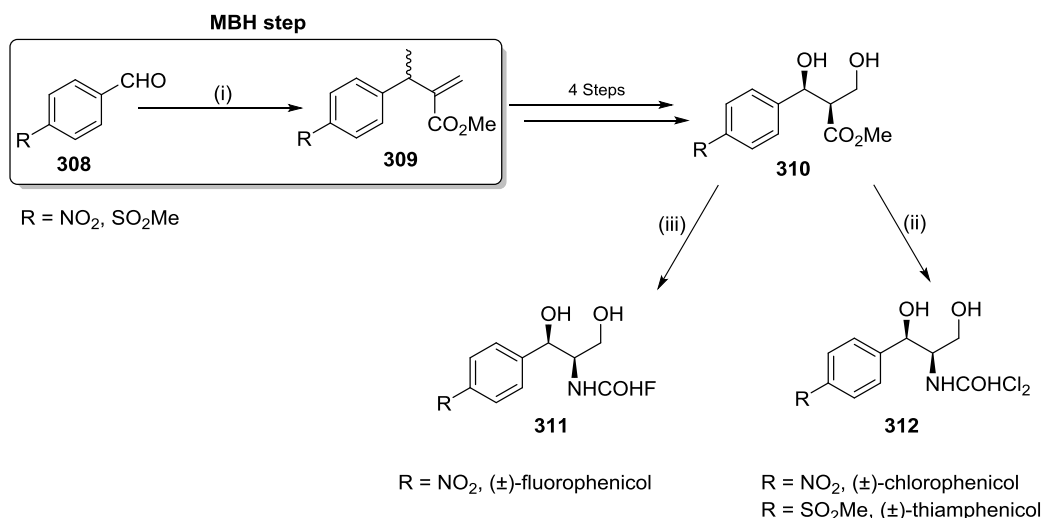
4.1 The Baylis-Hillman Reaction

One particular reaction which has seen widespread research is the Baylis-Hillman reaction (MBH)/ Rauhut-Currier reaction (scheme 73). This was patented in 1972 for its ability to form complex chiral allylic alcohols such as **307** with relative ease. A common MBH reaction normally involves an electron poor alkene **306**, a simple catalyst **296** and a variety of aldehyde or imine electrophiles **305** ⁽²⁹⁾.



Scheme 73: Typical Morita-Baylis-Hillman reaction

Morita-Baylis-Hillman (MBH) reactions typically involve the formation of carbon-carbon bonds between the α -position of an activated alkene and an aldehyde or ketone, in the presence of a tertiary amine catalyst such as DABCO, DMAP or DBU. Sometimes a phosphine catalyst can be used and this is known as the Rauhut-Currier modification. The MBH reaction is highly desirable because it can form chiral centres from prochiral electrophiles, uses easily accessible starting materials and gives highly functionalised products that are powerful reagents for synthetic chemistry⁽³⁰⁾. One such example of its synthetic ability is in the synthesis of fluoro/chlorophenicol derivatives as reported by Coelho and Rossi⁽⁹⁹⁾ (Scheme 74).



Reagents & Conditions: (i) DABCO, Methyl acrylate, ultrasound, 95%, (ii) Methylchloroacetate, reflux, 67%, (iii) Methyldifluoroacetate, reflux, 85%.

Scheme 74: MBH initiated synthesis of Fluoro and chlorophenicol

Chiral allylic alcohols also exist throughout nature (figure 58, Tulipalin B **313** & Furaquinocin **314**) and in a multitude of synthetic chemistry as they provide a useful way to introduce chirality into a chemical motif (figure 58, epoxidation of allylic alcohol **315**)⁽³²⁾.

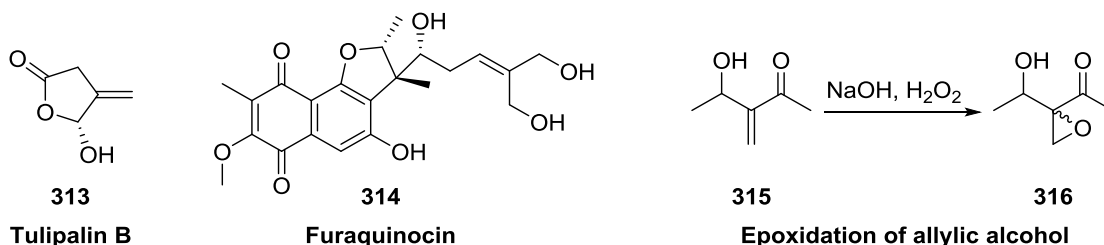
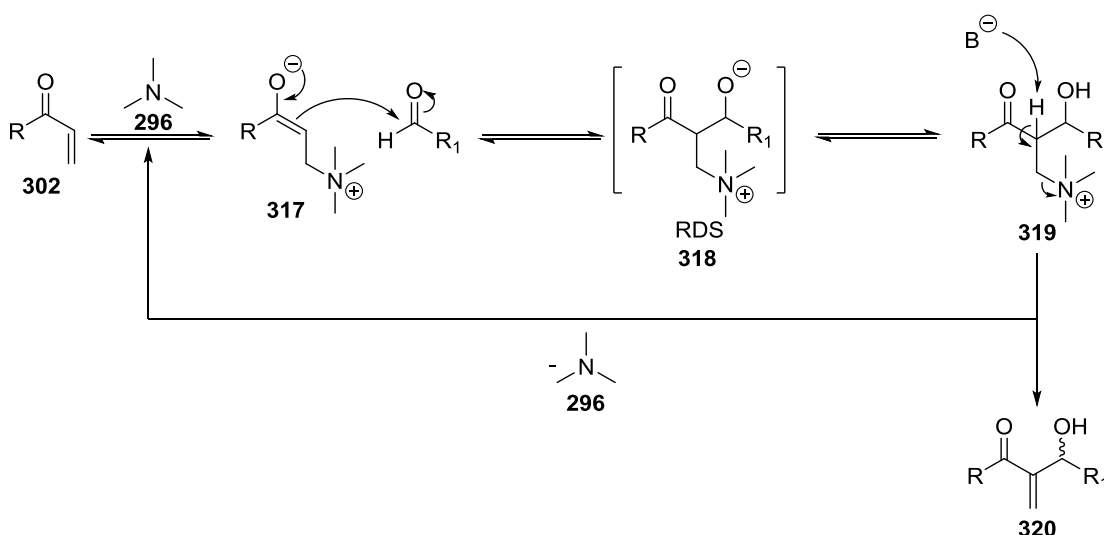


Figure 58: Natural products utilising allylic alcohols

The MBH reaction (scheme 75) begins with nucleophilic attack of the tertiary amine catalyst **296** onto the activated alkene **302** forming an intermediate betaine **317**. Quenching with a range of electrophiles can then produce a library of allylic alcohols **320** as tailored by the synthetic chemist. However the reaction has always suffered from some drawbacks including slow rate, poor control of stereochemistry and side reactions which might be overcome by performing the reaction with a modified cofactor in the enzyme active site⁽³⁰⁾.



Scheme 75: The Morita-Baylis-Hillman (MBH) mechanism

On this basis, it seemed ideal that the tertiary amine catalyst would be small enough to fit within the active site. It is also a reaction mechanism that could benefit from enzyme intervention because of its polar architecture and the surrounding amino acids. In conjunction with this the MBH reaction undergoes a catalytic cycle, and so it is plausible that the cofactor once synthesised could be regenerated for multiple MBH cycles. This would remove the need for stoichiometric quantities of reagent, thus reducing costs for industrial applications and improving the turn over number (TON) of the enzyme. In recent years it has been highly desirable for industry to utilise

this type of enzymatic-cofactor pathway that can regenerate the cofactor *in situ* and do so without wastage. Alternative industrial systems typically employ co-substrates for the reduction of NAD⁺ to NADH or NADP⁺ to NADPH, thereby utilising a second enzyme such as formate dehydrogenase⁽³³⁾. It is also common for some chiral alcohols to undergo dynamic kinetic resolution (DKR) after synthesis by an enzyme to recover the sought after enantiomer (scheme's **76 A & B**)⁽³⁴⁾. This doctoral thesis will hopefully begin to uncover a potential method to form the desired enantiomer in a single step, without the need for additional purification or extra steps.

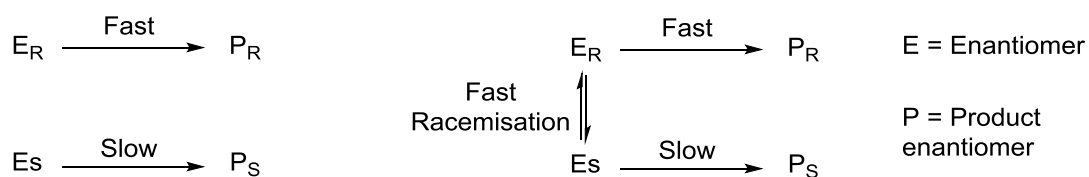


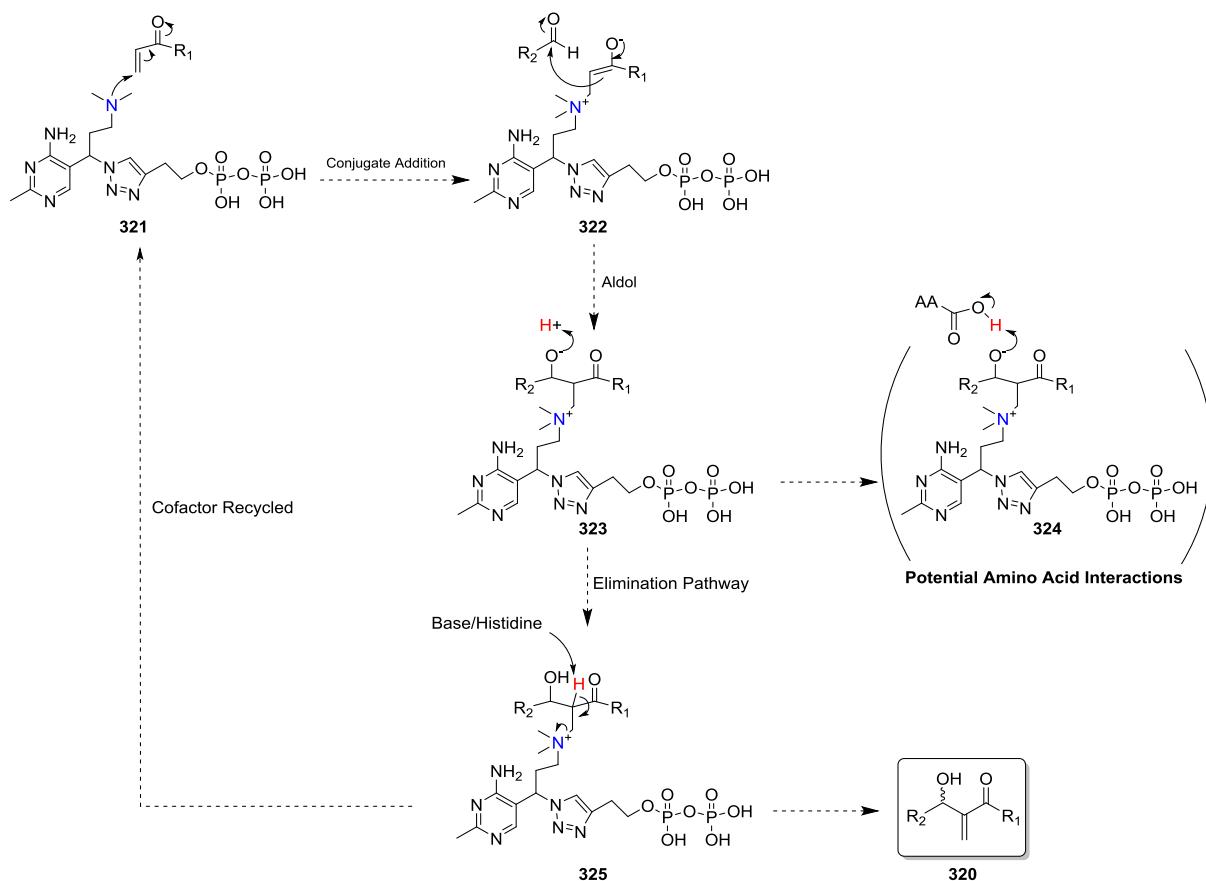
Figure A: Classic Kinetic Resolution

Figure B: Dynamic Kinetic Resolution

Schemes 76 A and B: Kinetic and DKR resolutions

4.2 Enzyme Promiscuity – A Proposed Baylis-Hillman Cofactor System

Based on this speculation, the unnatural cofactor **321** (scheme **77**) could act as an anchor in the active site, thereby allowing the tertiary amine and its tether to infiltrate the space within the enzyme's dimer-dimer interface and undergo nucleophilic addition to a particular Michael acceptor. An intermediate betaine **322** would ideally form and be trapped by an aldehyde/ketone to give compound **323**. Protonolysis of the oxyanion by the aqueous solution or from the surrounding active site **324** could then give **325** as the final catalytic state in which the α -proton on the 1,3-hydroxy ketone is abstracted by a suitably basic entity to release the chiral allylic alcohol **320**. Such a step would then hopefully re-start the catalytic cycle by making the tertiary amine free to undergo another Michael addition.



Scheme 77: Proposed enzymatic-MBH cofactor

4.2.1 Enzyme Promiscuity – The Tertiary Amine Active Site

The proposed empty space surrounding the tertiary amine in pyruvate decarboxylase, is bonded by a collection of four amino acids which include His113, His114, Asp27 and Thr290 which might assist in the proposed MBH process (figure 59). Docking of the tertiary amine shows the nearby amino acids His113 and His114 which are primary parts of the active site. As previously mentioned, these can exist in either closed or open configurations depending on the timeframe of catalysis.

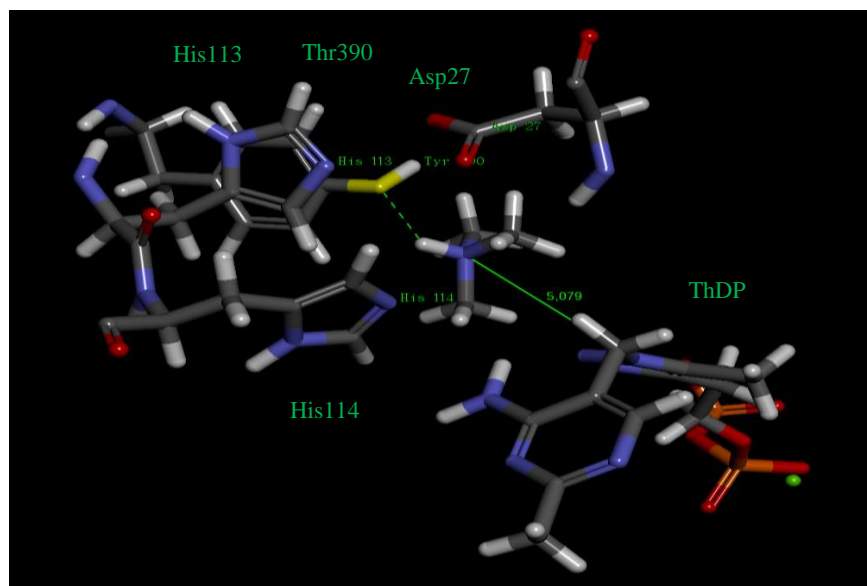


Figure 59: Docked tertiary amine in hydrophilic pocket with distance to methylene bridge of 1,4-disubstituted [1,2,3] triazole ThDP

These histidines could behave as suitable basic groups to remove the α -proton on the allylic alcohol (scheme 77, compound 325) and assist in the potential mechanism of the MBH reaction. Furthermore Asp27 is located 3.8 Å away from the tertiary amine and with a physiological pH of ~7 could exist in a deprotonated state (figure 60). A deprotonated anion could then act as the base, and maintain the nucleophilic free amine for its attack onto the Michael acceptor.

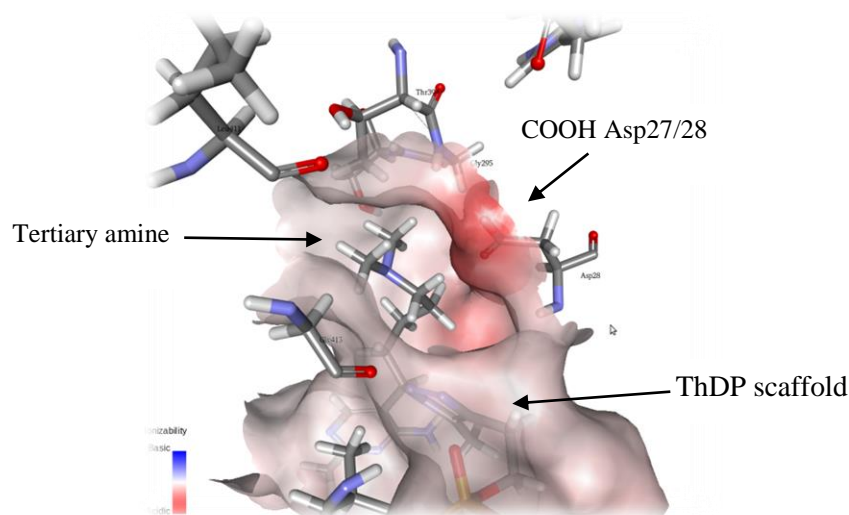


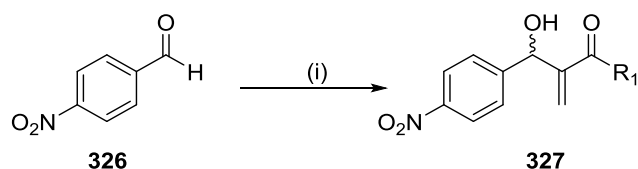
Figure 60: Solvent ionizability of active site surrounding model 1,4-ThDP tertiary amine

Tyr390 is also available to stabilise the tertiary amine by H-bonding to its hydroxyl group at 2.6 Å and could also stabilise the RDS. One potential problem is that the active sites of PDC enzymes

are very small and so incorporating both a Michael acceptor and aldehyde reactant would be difficult in this current model. Future studies may require a combination of protein engineering and *in silico* design to fine tune the active site so it could participate in catalysis, yet not destroy the integrity of the enzymes tertiary structure.

4.2.2 Initial Baylis-Hillman testing

Typically the literature depicts the use of un-hindered tertiary amine catalysts like DMAP, DBU and DABCO due to their higher pK_a 's and linear increase in reaction rate^{(29), (35)}. So before any further synthesis was carried out, a test reaction based on the use of the smaller trimethylamine was envisaged. This was undertaken in the presence of water to mimic the enzymatic reaction medium (scheme 78). Noticeably it is well documented that the use of polar solvents in the MBH reaction can promote increased reaction rates, possibly due to the increased H-bonding to the zwitterions found in the rate-determining step (RDS) (scheme 77, compound 322)⁽³⁶⁾. Using the reported procedure of Tang *et al.*⁽³⁷⁾, dimethylbutylamine was reacted with acrolein (table 12, Entry 1) for 24 hours, but no reaction was observed. In contrast, reaction with methyl acrylate for 24 hours gave the allylic alcohol in its highest yield of 16% (table 12, entry 4).



Reagents & conditions: (i) *N,N*-dimethylbutylamine, Michael acceptor, THF, r.t. 16%.

Scheme 78: Test Baylis-Hillman reaction

As it is well documented that MBH reactions suffer from poor rates, further experimentation with reaction conditions (table 12) was preformed^{(37), (30)}. These showed that increasing the temperature (table 12, entry 5) and reaction times (entry 3) did not promote increased yields of the product. Increasing the equivalents of water also had no extra effect upon the yield of isolated product (entry 4). In comparison of the methyl and ethyl derivatives it was noticeable that the yields were very low even under the same conditions (entry 6), but did increase marginally over a longer time period. Although the rates were extremely poor, it did prove that catalysis could occur with the

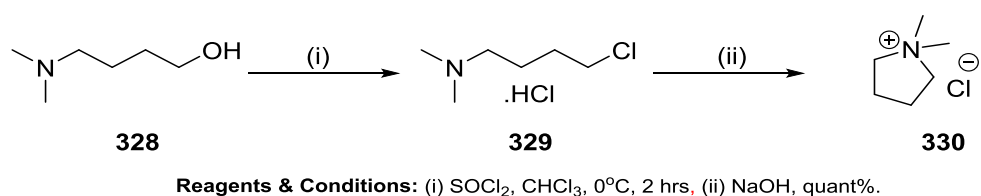
smaller tertiary amine, and importantly left scope to measure improvement with the proposed enzyme-mediated version of the reaction, so synthesis began on the unnatural cofactor.

Entry	Aldehyde (2.0 eqv)	R ₁ (1.0 eqv)	Amine (1.5 eqv)	H ₂ O (μL)	Temp (°C)	Time (Hrs)	Yield (%)
1	Benzaldehyde	H	<i>N,N</i> -dimethylbutaneamine	100	RT	24	-
2	Benzaldehyde	OMe	<i>N,N</i> -dimethylbutaneamine	100	RT	24	15%
3	Benzaldehyde	OMe	<i>N,N</i> -dimethylbutaneamine	100	RT	72	14%
4	Benzaldehyde	OMe	<i>N,N</i> -dimethylbutaneamine	200	RT	24	16%
5	Benzaldehyde	OMe	<i>N,N</i> -dimethylbutaneamine	100	Reflux	24	-
6	Benzaldehyde	OEt	<i>N,N</i> -dimethylbutaneamine	100	RT	24	<5%
7	Benzaldehyde	OEt	<i>N,N</i> -dimethylbutaneamine	100	RT	7d	10%

Table 12: Test conditions for MBH of *N,N*-dimethylbutaneamine

4.3 Synthesis of Tertiary Amine Grignard's

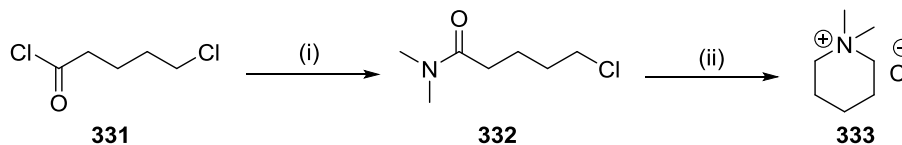
As the test carbon chains had been installed using Grignard reagents, it seemed a logical approach to synthesise a Grignard that contained a tertiary amine or something akin to this which could be manipulated at a later stage. Synthesis then began on developing a tertiary amine alkyl chain which could be easily converted into the corresponding Grignard reagent. Synthesis of the three- four- and five- carbon halogen-substituted linkers followed similar synthetic approaches, although only the three and four carbon linkers were commercially available as the hydrochloride salts. Conversion of the alcohol **328** (scheme 79) using thionyl chloride at 0°C in chloroform gave the four carbon chain as its hydrochloride salt **329**, but upon washing with NaOH it underwent conversion via a *5-exo-tet* cyclisation as predicted by Baldwin's rules into the quaternary amine **330**.



Scheme 79: Formation of four carbon quaternary amine salt

Consequently the conversion of this chain length to the desired Grignard reagent was never completed. Focus on the five carbon chain was then attempted to ascertain if we could make its

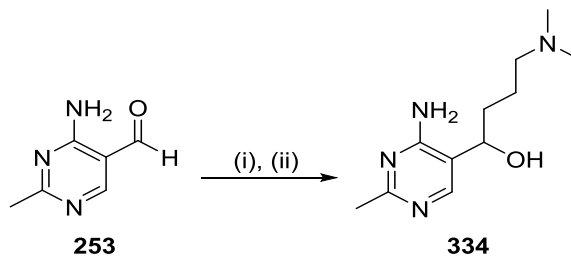
Grignard equivalent without cyclisation (scheme **80**). 5-Chlorovaleroyl chloride **331** was then converted into the amide **332** in a 63% yield following a literature procedure⁽³⁸⁾. The amide **332** was then reduced fully by LiAlH₄ which removed the delocalisation of electrons from the nitrogen into the sigma C-N bond, and resulted in a 6-*exo-tet* cyclisation to give product **333**.



Reagents & Conditions: (i) *N,N*-dimethylamine (1.1 eq), 5-15°C, THF, 75%. (ii) LiAlH₄ (3.5 eqv), 0 °C- r.t., 3hr, 76%.

Scheme 80: Formation of five carbon quaternary tertiary amine salt

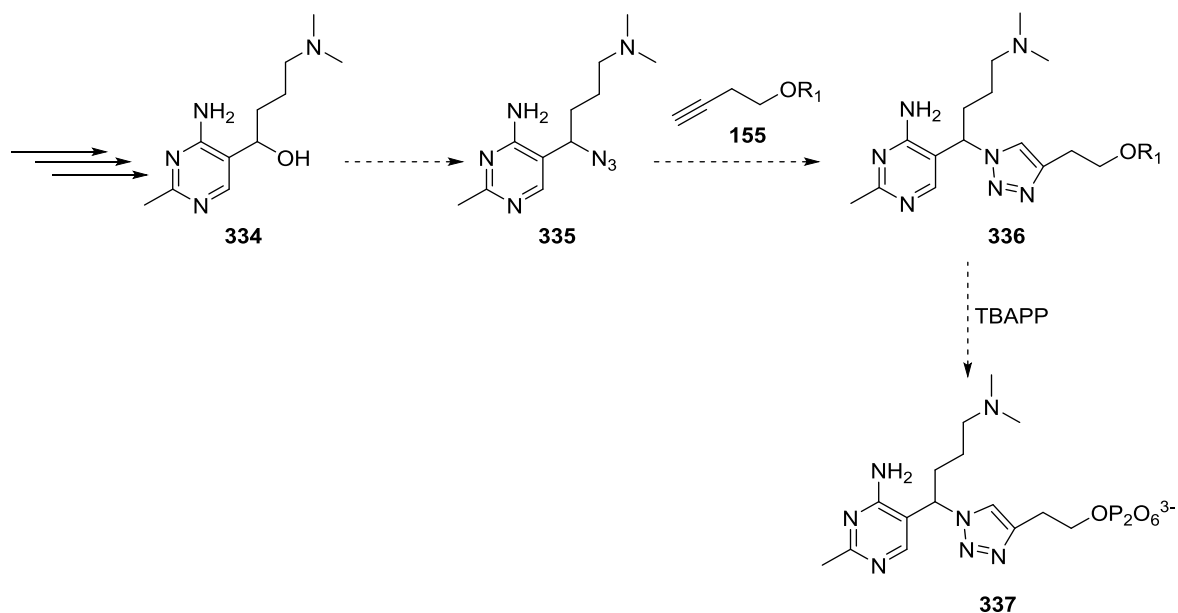
It was then decided that the commercial *N,N*-dimethylpropyl chloride hydrochloride salt could after a simple basic wash undergo conversion into the active Grignard reagent. All synthesis was then stopped on the longer chain Grignard reagents because of the difficulties concerning the cyclisation of their organohalide precursors. Addition to the aldehyde **253** (scheme **81**) was then carried out under similar conditions to earlier with the alkyl test reagents to give product **334** in 46% yield.



Reagents & Conditions: (i) *N,N*-Dimethylpropyl chloride hydrochloride salt, NaOH, (ii) *N,N*-dimethylaminopropyl magnesium chloride (3 M), 0°C -r.t., 24 hrs, 46%

Scheme 81: Installation of tertiary amine tether via Grignard reagent

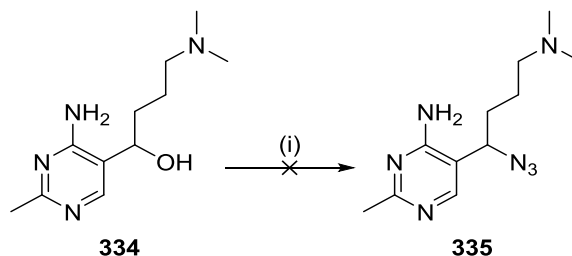
Even though this reaction gave the desired product in moderate yield of 43%, the work up procedure was difficult and required many attempts of trituration with Et₂O to remove some small but persistent impurities. Once this had been achieved, good conditions for conversion of the alcohol **334** into the azide **335** were required (scheme **82**). The same chemistry that assembled the test compounds could then be used to effect this transformation. After click chemistry this would give **336** which after S_N2 displacement of the tosyl group could yield the final compound **337** as the lyophilised salt.



Scheme 82: Synthesis of tertiary amine 1,4-disubstituted ThDP analogue

4.3.1 Synthesis of Azide Tertiary Amine

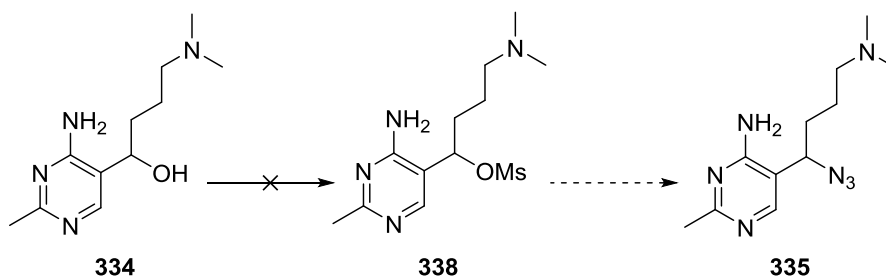
Conversion of the alcohol **334** by DBU and DPPA (scheme **83**) did not prove easy but after several failed attempts it at last seemed to have worked, although with the product located in the aqueous layer. This consequently presented us with a purification problem, because the use of DBU meant that both product and protonated base co-existed in the aqueous layer and made the crude ¹H NMR difficult to interpret. To address this, a base with fewer protons was used to make identification of the product easier and reduce purification problems. Even though tetramethylguanidine (TMG) improved the analysis of the ¹H NMR, it still caused difficulties with purification. It was then decided that potassium *tert*-butoxide could first deprotonate the alcohol **334** and would also generate *t*-BuOH in the process thereby promoting easier removal of side products under reduced pressure. This however, did not give the desired product in the aqueous phase as predicted, and resulted in an even messier ¹H spectrum than before with no recoverable product.



Reagents & Conditions: (i) (DBU), (TMG), (KOtBu), DPPA, THF, r.t., 16 hrs

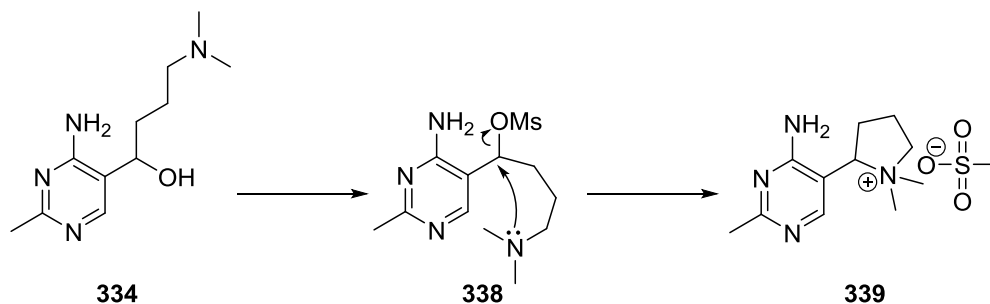
Scheme 83: Conversion of *N,N*-dimethyl tertiary amine alcohol to azide

An alternative synthetic route (scheme **84**) was then attempted due to all the problems associated with this step. A proposed *in situ* activation of the alcohol **334** as its mesylate **338**, and S_N2 displacement with NaN_3 would then hopefully give **335**. It was hoped that this route could potentially circumvent some of the issues found within the previous scheme, whilst testing a hypothesis for the problems associated with the previous step. Purification of compound **335** was now much improved, although the product was still located in the aqueous layer.



Scheme 84: Synthesis of tertiary amine via mesylation & sodium azide displacement

A mass spectrum was then obtained to assist in identification of the intermediate mesylate **338**. This highlighted the possibility that a *5-exo-tet* cyclisation of the tertiary amine (scheme **85**, compound **338**) had occurred by attack onto the carbon bearing the mesylate leaving group to give the mesylate salt **339**. Based on this evidence it was proposed that a similar mechanism took place during the intermediate stages of scheme **84**, with loss of diphenylphosphoryl oxide promoting the formation of the salt product.

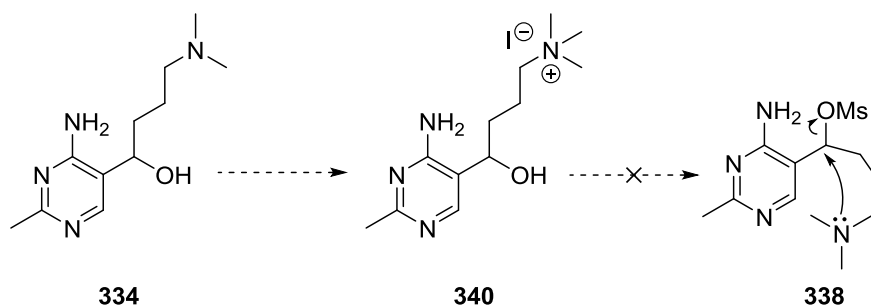


Scheme 85: 5-*exo-tet* rearrangement of tertiary amine azide

Preventing this cyclisation now required that the lone pair of electrons occupying the filled p orbital of the tertiary amine were tied up by interaction with another group.

4.3.2 Methylation and N-Oxide Protection

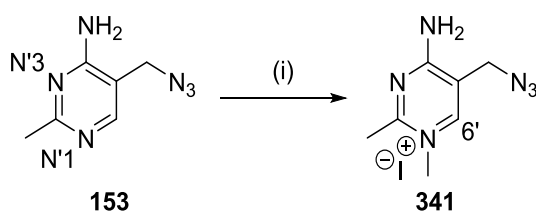
A methylation of the tertiary amine now seemed like a good candidate to prevent further nucleophilic substitution (scheme 86).



Scheme 86: Proposed methylation of tertiary amine

As the tertiary amine product **334** was hard to purify and in small supply we used a test reaction (scheme 86). This was completed on the original compound **153** to assess what effects methylation would have upon the aromatic ring. The reaction was very straightforward and only required little purification after treatment of **153** with MeI. Analysis of the ^1H NMR (figure 60) was now required to indicate the degree of alkylation and position. This is because dialkylation of pyrimidines is known to be difficult using simple alkyl halides⁽³⁹⁾. A NOESY experiment confirmed that methylation had occurred on N¹ (scheme 87). This was achieved by correlation of the protons situated on the new methyl group to those of the single proton located at position 6' on the pyrimidine ring, and with that of the adjacent methyl group situated between the ring nitrogens (scheme 87, compound **341**). On this basis, due to the easy N-methylation at N¹, it was

decided that it may not be feasible to carry out the methylation of the amine as proposed above in scheme **86**.



Reagents & Conditions: (i) MeI, THF, r.t., 16 hr, 5 %

Scheme 87: Test methylation of pyrimidine ring

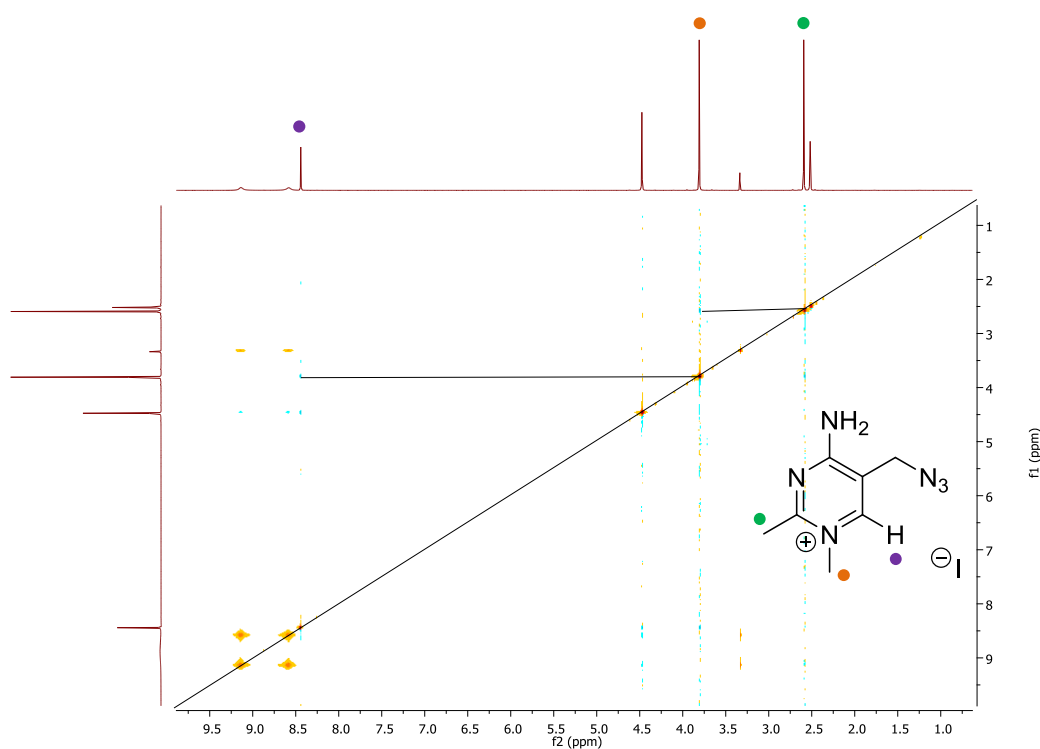
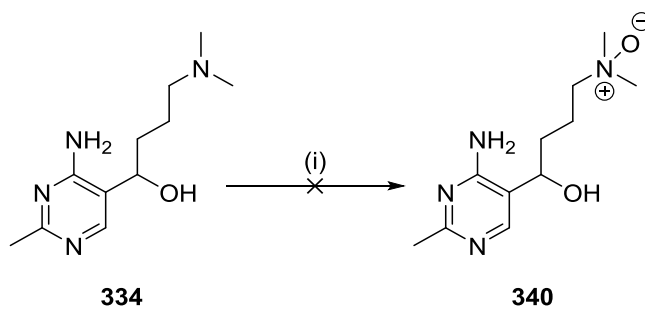


Figure 60: NOESY spectra of methylation on N'1 of pyrimidine

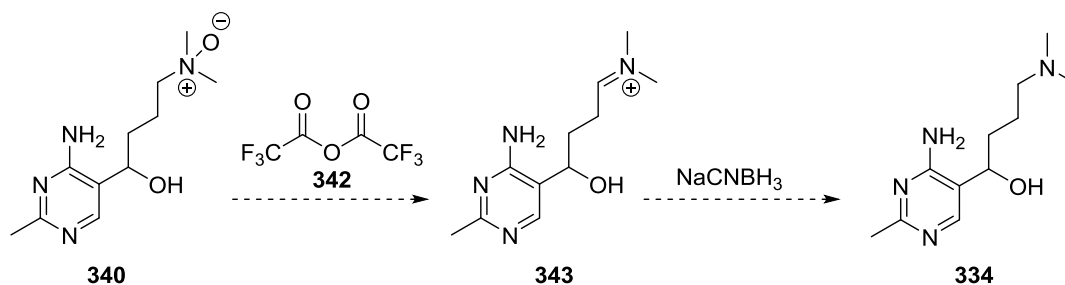
Consequently, an alternative protection (scheme **88**) was now attempted using *m*-CPBA to complete the synthesis of the *N*-oxide compound **340**, whilst avoiding reaction at the pyrimidine ring.



Reagents & Conditions: (i) *m*-CPBA, CHCl₃, rt, 24Hr

Scheme 88: *m*-CPBA protection of tertiary amine

The *N*-oxide protecting group could then potentially been removed by the addition of trifluoroacetic anhydride **342** (scheme **89**) to produce the imine **343** which after reduction may have revealed the desired product **334**.

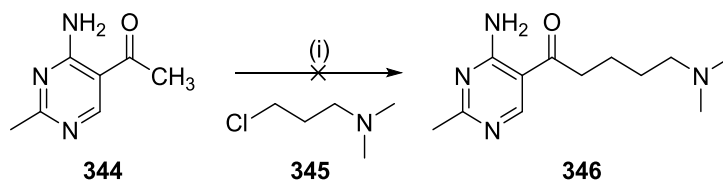


Scheme 89: Proposed deprotection of *N*-Oxide by Polonovski reaction

Regrettably the oxidation of the tertiary amine did not give the desired product **343** and the reaction vessel was deposited with a polymerisation product. Further reading indicated that pyrimidines are extremely sensitive to oxidations when using *m*-CPBA due to instability achieved in formation of the products⁽³⁹⁾, which could be attributed to the reaction's failure.

4.4 The Enolate Synthesis

Meanwhile other synthetic routes were being assessed to construct the extended linkers. A synthetic route was then undertaken to create ketone **344** which could then react with NaH at -78°C to generate the enolate *in situ* (scheme **90**). Quenching with compound **345** formed by a basic wash of the hydrochloride salt may then have resulted in S_N2 displacement of the chloride anion to give **346**. This motif would then have the carbon linker with the tertiary amine in the correct length and position. NaBH₄ reduction could then install the alcohol in the correct location for the azide step, although problems associated with the cyclisation were unknown at this point.



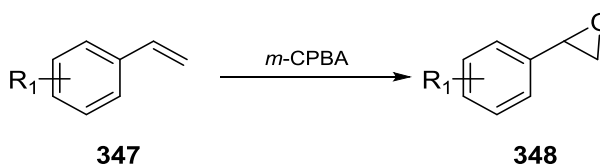
Reagents & Conditions: (i) NaH (1.5 eq.), THF, -78°C, **345** (1.2 eq.), 3 hr

Scheme 90: Enolate synthesis of tertiary amine chain

Even though the reaction did appear to indicate the evolution of H₂ (g) the reaction did not form any new product as monitored by TLC. This could be attributed to the acidity of the primary amine protons and the removal of these being preferential to those of the methyl ketone (pK_a~20). Hence the equivalents of NaH were probably not sufficient for the reaction to take place and an excess would be used in future cases. At this stage in the work, other synthetic routes were begun due to the problems associated with the cyclisation's, which could hopefully remove the problem.

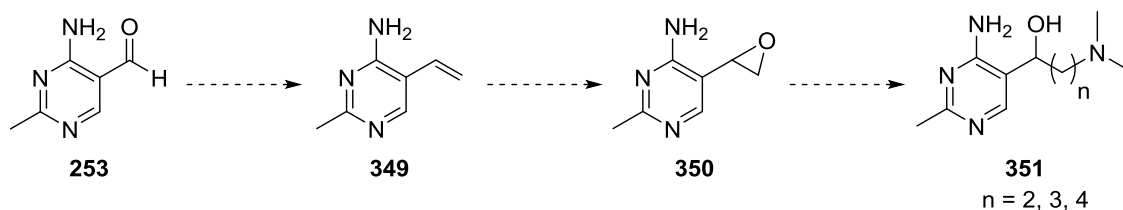
4.5 The Alkene Synthesis and Ring Opening Approach

The ring opening of an epoxide was then debated as a viable way to introduce the chain length (scheme **91**). Reaction of a styrene derivative **347** by epoxidation with *m*-CPBA could then give the desired analogues **348** of our compounds.⁽³²⁾



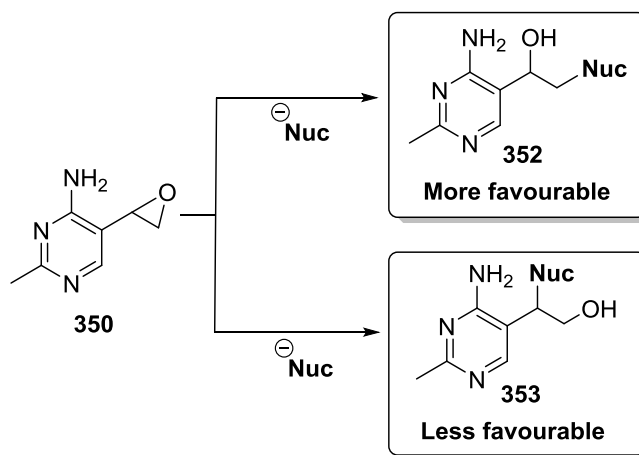
Scheme 91: Prilezhaev Epoxidation

As the aldehyde **253** (scheme **92**) had been generated in sufficient quantities, it was deemed a good idea to explore the formation of a styrene intermediate **349** using alkene synthetic strategies. An epoxidation and ring opening of **350** could possibly generate the desired tertiary amine chain, whilst facilitating formation of the secondary alcohol at the required position.



Scheme 92: Proposed epoxidation synthetic route to tertiary amine chain

This strategy relied heavily on the premise that nucleophilic attack occurs at the least hindered carbon. Hence a potential drawback to this process is the formation of an alternative regioisomer by addition of the Grignard reagent onto the more hindered carbon (scheme 93).



Scheme 93: Nucleophilic attack and ring opening of epoxide

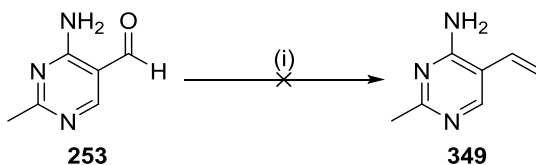
Normally the mechanism is assisted by the presence of a Lewis acid (LA) such as $\text{BF}_3 \cdot \text{OEt}_2$ or by H^+ which promotes opening of the highly strained three membered rings. In our case the close proximity of the amine protons may be able to participate in this mechanism as the epoxide becomes stabilised by the amine proton (scheme 94).



Scheme 94: Proposed assisted LA ring opening

4.6.1 The Wittig Approach

Investigation of the proposed pathway then continued with regards to making the alkene (scheme 95). To start with, a classic Wittig reaction was used due to its ease in preparation of the Wittig salt and cheapness of materials. The ylide was prepared *in situ* by addition of *n*-BuLi to the Wittig salt, which was then slowly added in excess to the aldehyde 253. Unfortunately none of the alkene product 349 was observed even after 24 hours.



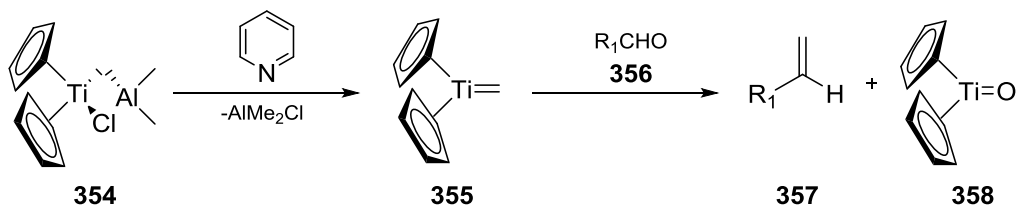
Reagents & conditions: (i) $\text{Ph}_3\text{PCH}_3\text{I}$ (6 eqv.), *n*-BuLi, THF, -78°C -r.t., 24 hr

Scheme 95: Wittig reaction with aldehyde

This could have been attributed to the large steric bulk of the surrounding triphenyl groups attached to the ylide which did not allow the typical 4-membered transition state to be adopted. This prevented triphenylphosphine oxide being released as the driving force for the reaction. Problems associated with addition of Wittig reagents to hindered aldehydes have been reported before along with their non-suitability with acidic groups^{(40), (41), (42)}. In comparison of compound **253** to aniline (pKa 9.1), it is possible that the ylide of Ph_3PCH_3 (pKa 22) became protonated by removal of the amine protons and therefore depleted the reagent required to complete this reaction. An alternative possibility is the lack of strong electrophilicity at the carbonyl carbon due to the mesomeric donation of the electrons from the primary aromatic amine into the π system.

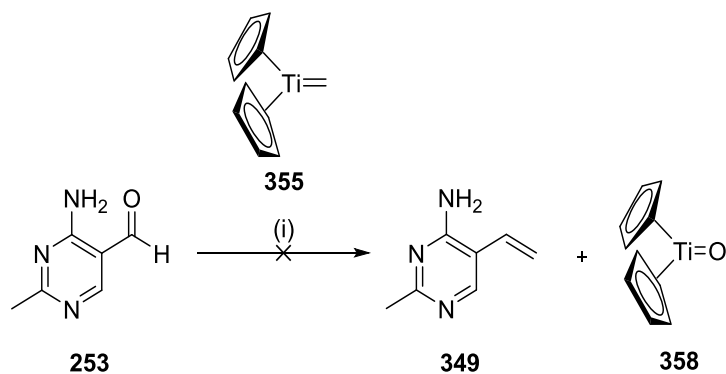
4.6.2 The Tebbe Olefination

The Tebbe olefination was then desired because of its suitable reaction conditions which include; 1.) Easier reactions with hindered aldehydes, 2.) Its non-basicity and 3.) Improved yields compared to the Wittig reagents^{(40), (42)}. Titanium carbenoids are well investigated⁽⁴²⁾ and were one of the first reported compounds that utilised a methylene linker between a transition metal (Ti) and that from the main periodic group metals (Al). For these reasons and because rates of reactions were generally reported to be increased, it seemed a good idea to attempt the Tebbe olefination. The reagent itself **354** (scheme **96**) can be synthesised from reaction of titanocene dichloride with trimethylaluminium, however the pyrophoric nature of this reagent meant that we sought to acquire it commercially. The general procedure involves reaction with a Lewis base to form the active Schrock carbene⁽⁴²⁾ **355** which is nucleophilic and can attack the carbonyl functionality **356**. The alkene **357** is then formed by a Grubbs-like mechanism involving a four membered oxa-titanium transition state which collapses to release a $\text{Ti}(\text{Cp})_2\text{O}$ side product **358**. This acts as the driving force for the reaction like that often described in the Wittig.



Scheme 96: The Tebbe Olefination

Unfortunately the reaction did not work for our compound **253** (scheme **97**) and gave only recovery of starting material. This problem may still be related to that associated within the Wittig reaction and could also suggest that the steric bulk of the surrounding “R” groups is one of the primary reasons for these reactions not working.

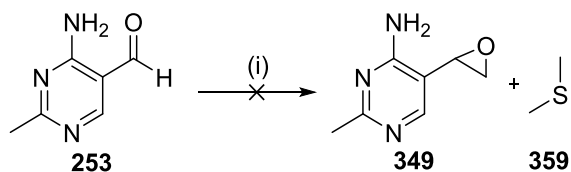


Reagents & conditions: (i) Tebbe reagent **355** (4.0 eqv.), Pyridine (0.8 eqv.), THF -78^oC, 2Hr

Scheme 97: Tebbe olefination of 2-methyl-4-aminopyrimidine carbaldehyde

4.6.3 The Corey-Chaykovsky Epoxidation (CCE)

After further surveys of the literature it was apparent that the Corey-Chaykovsky reaction⁽⁴³⁾ of compound **253** (scheme **98**) could be used to circumvent the difficulty in formation of the alkene, and possibly remove the olefination step altogether. As with the Wittig reaction, (CCE) reactions follow a similar mechanism with formation of the intermediate trimethylsulfonium ylide by deprotonation with sodium hydride. Using the literature procedure of Furstoss *et al.*⁽⁴⁴⁾, attack of the reactive ylide onto the aldehyde **253** should have generated the alkoxide anion, which after collapse of the tetrahedral intermediate would produce the epoxide and expel dimethylsulfide **359**. But once again, the reaction was unsuccessful and so the ylide chemistry was stopped.

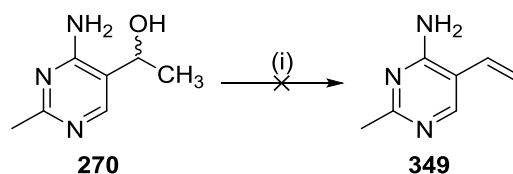


Reagents & Conditions: (i) Trimethylsulfonium iodide (3.2 eq.), NaH (3.2 eq.), DMSO, r.t., 24 hrs

Scheme 98: Attempted Corey-Chaykovsky Epoxidation (CCE)

4.6.4 Acid Catalysed Dehydration

As these routes were clearly causing difficulties an alternative approach was sought that might be more compatible with the presence of the NH_2 group by returning to the previous alkene synthesis. Synthesis of the secondary alcohol made in an earlier Grignard experiment (scheme 67, compound 270) was proposed to serve as a useful intermediate for two new approaches towards the epoxide, but both via the alkene product intermediate. Firstly the acid catalysed dehydration of secondary alcohols has been reported previously⁽⁴⁵⁾ and was attempted by refluxing in H_2SO_4 for 48 hours although this only ever gave unreacted starting material (scheme 99).

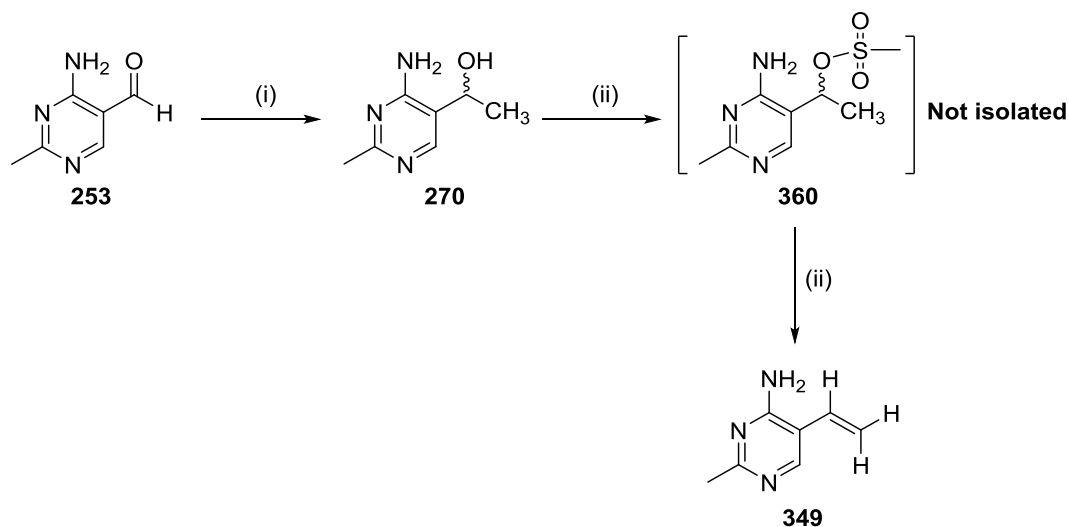


Reagents & Conditions: (i) H_2SO_4 (5 eq.), Reflux, Dean-Stark

Scheme 99: Acid catalysed secondary alcohol dehydration

4.6.5 Activation and E2 Elimination

Finally the *in situ* activation of secondary alcohol **270** (scheme **100**) with a mesylate group and its successive E2 elimination gave compound **349**.



Reagents & conditions: (i) MeMgBr (3 M) (3.5 eqv.) 0°C-r.t., THF, 24 hr, 61%, (ii) MsCl, 0°C-r.t., THF, Et₃N (5.0 eqv.), 24 hr.

Scheme 100: Mesylate formation/E2 elimination to alkene

Interpretation of the ¹H NMR spectrum (figure **61**) shows the *trans*-alkene protons ($J = 17$ Hz) situated around 5.49 & 5.66 ppm which are highlighted with the respective colours. Unfortunately the spectrum still contained some EtOAc solvent peaks and required further removal overnight under vacuum, however this resulted in the product undergoing polymerisation. Further work on this synthetic route was then abandoned on the basis that a procedure which required making the alkene **349** and using it immediately may be difficult to reproduce in combination with unknown conditions for the epoxidation.

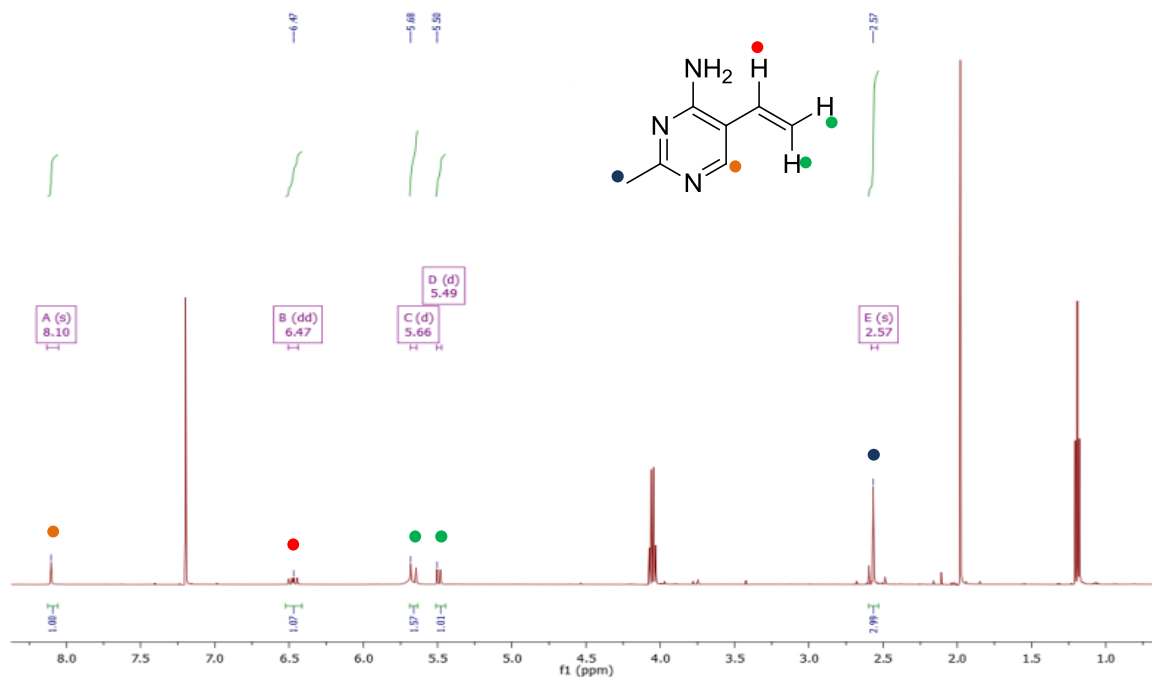


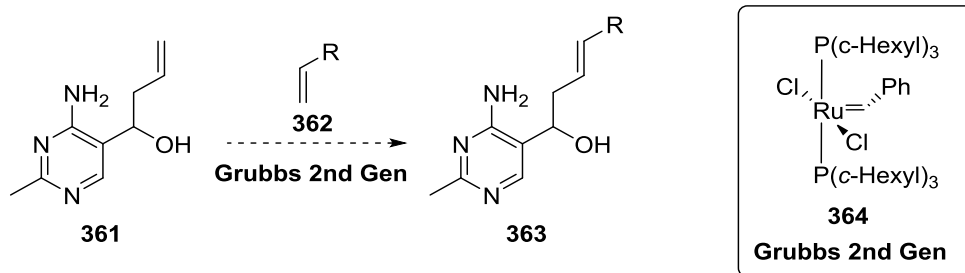
Figure 61: ^1H NMR showing formation of the 2-methyl-4-amino pyrimidine ethene

4.7 Synthesis of Alkene Derivatives for Potential Functionalization

Assembly of the target molecule now took a new route by adapting some of the Grignard chemistry, and attempting manipulations of the different functional groups at later stages within the synthesis.

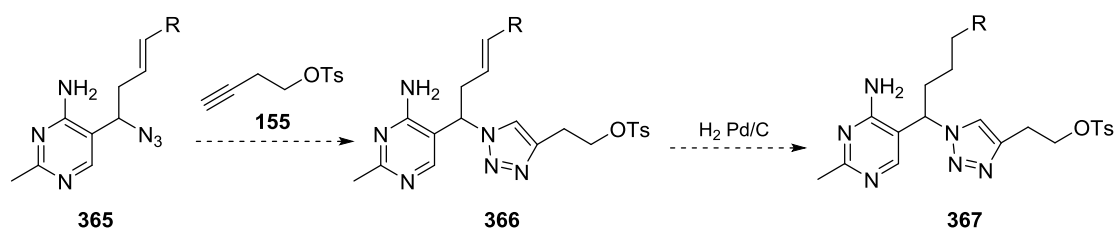
4.7.1 Grubbs Cross Metathesis

It was now decided that Grignard chemistry could allow facile synthesis of the alcohol **361** (scheme 101) which after Grubbs cross metathesis could form the product **363**. Grubbs catalysts are versatile, tolerant to many functional groups and have little sensitivity to air and moisture, thereby making them good candidates for this stage of the synthesis.



Scheme 101: Proposed Grubbs (II) cross metathesis

Transformation of **363** into the azide **365** (scheme **102**) was then proposed to go more smoothly as the *5-exo-tet* and *6-exo-tet* cyclisation's are removed by increased rigidity within the linker. Ideally the *trans*-alkene would decrease the tendency of the problematic cyclisation by the nature of its planar 120° bond angle, which would increase sufficient conformational restraints upon the alkyl chain. Click chemistry with alkyne **155** would then construct a core intermediate that could undergo other synthetic steps before a hydrogenation removes the alkene to give **367** for the final steps.



Scheme 102: Proposed closing synthetic steps of CM pathway

4.7.2 Synthesis of 2-methyl-4-amino-5-(1-hydroxybutene) pyrimidine

The Grignard reagent was made easily from allyl bromide and addition to the aldehyde **253** (scheme **103**) gave the product **361** in a 27% yield after column chromatography. Confirmation of this structure was given by the *ddt* at 5.8 ppm for the alkene (Figure **62**, blue spot) and their coupling in the COSY to the *ddd*'s at ~5.0 ppm, the diastereotopic protons (orange spot) and the *td* at 4.6 ppm for the chiral centre. Furthermore, a lack of aldehyde peak around 9.0 ppm, additional CH₂'s in the DEPT 135 and mass spectrometry corroborated this assignment.

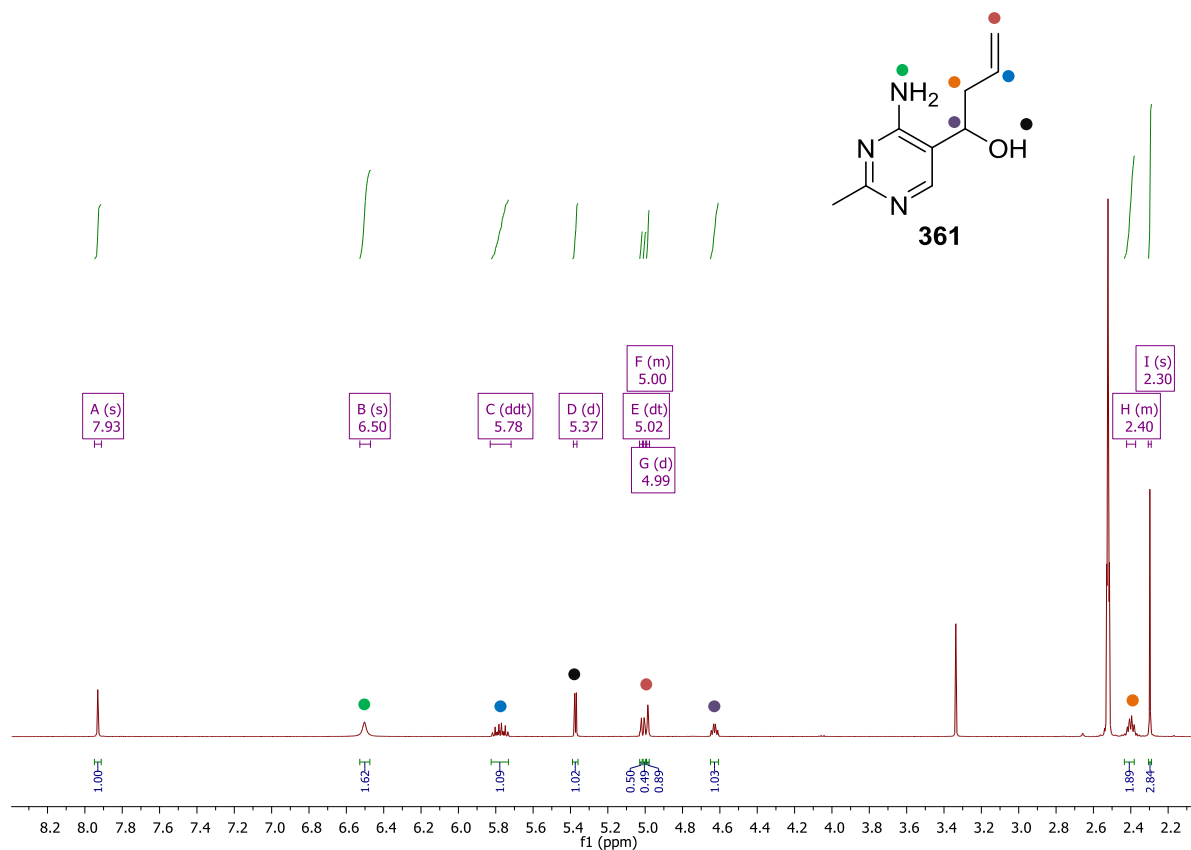
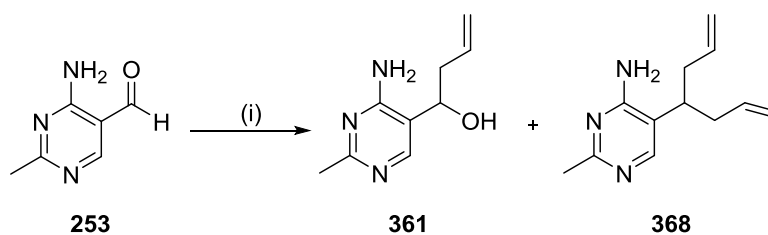


Figure 62: ^1H NMR of compound 361

Surprisingly something happened upon addition of this Grignard that had not occurred with previous Grignard reactions. Upon work up a second spot was observed at an R_f of 0.6 in EtOAc: MeOH 95:5 v/v, whilst the desired product appeared at an R_f of 0.5. After isolation and characterisation this was originally thought to be an isomer of compound **361**. On further analysis of the ^1H and ^{13}C NMR it was clear that the sp^2 alkene protons were double in their respective integration whilst still maintaining the required splitting pattern (Figure 63).



Reagents & Conditions: (i) Allylmagnesium bromide (3 M) (3.5 eqv.), THF, 0°C -r.t., 24 hr, **361** (27%) & **368** (15%).

Scheme 103: Allylmagnesium bromide addition to aldehyde

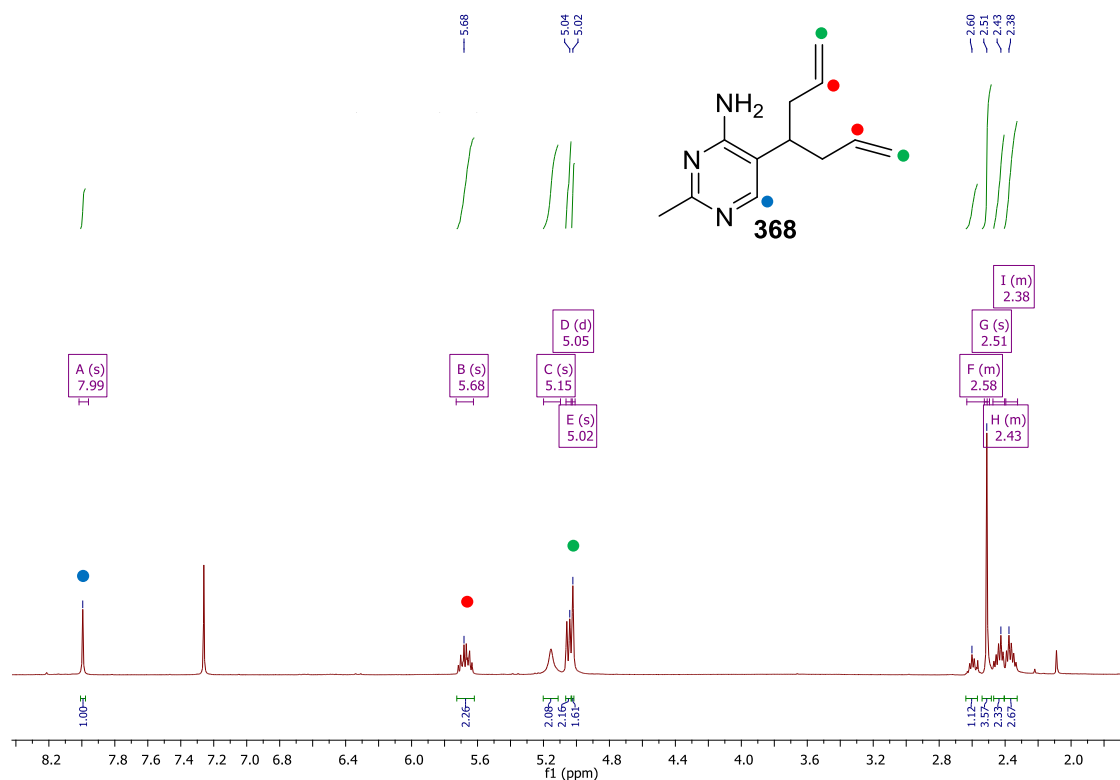
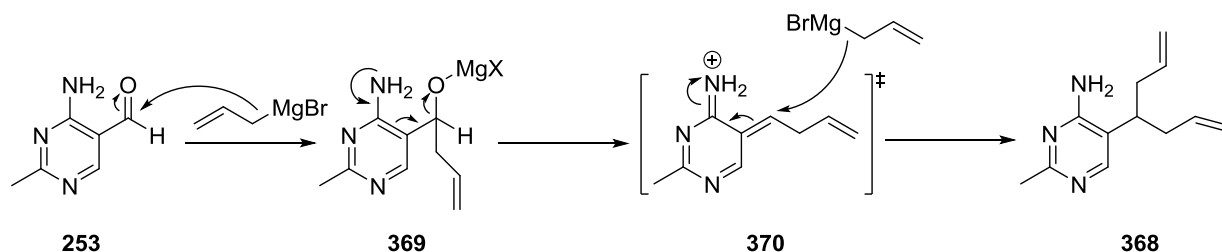


Figure 63: ^1H NMR of *gem*-dialkene product

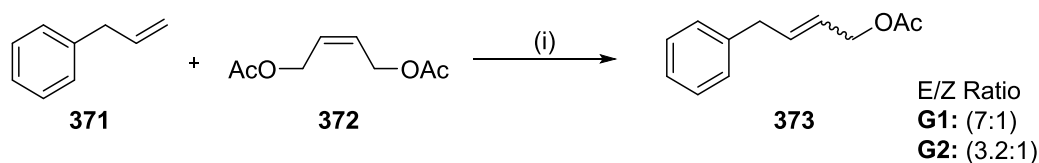
Confirmation of the actual product was only derived after analysis of the DEPT135 which indicated just two CH_2 carbons (the alkyl CH_2 and the alkene CH_2) showing that the two allyl chains were magnetically equivalent. Corroboration with mass spectrometry further confirmed that the *gem*-diallyl structure **368** (scheme **103**) had been isolated. Increasing equivalents of the Grignard reagent was then attempted in hope that formation of the side product could be increased, and open further avenues of research with regards to RCM reactions on these types of structures. Repeating this process did give the side product but it could only be recovered in 5% yield after several attempts and was not reproducible. Further conditions could be examined in later studies to see if this could be improved upon. A possible mechanism for the formation of this *gem*-dialkene has been suggested in scheme **104** and could arise from coordination of the magnesium salt formed during the Grignard reaction. This could be acting as a Lewis acid and coordinating to the intermediate oxygen anion formed in compound **369** after the first mole of reagent has been added. A second equivalent of Grignard reagent could then release the hydroxymagnesium halide and produce the *gem*-diallyl compound **368**.



Scheme 104: Proposed formation of *gem*-dibutene product

4.7.3 Cross Metathesis of compound 383 with Grubbs 2nd Generation

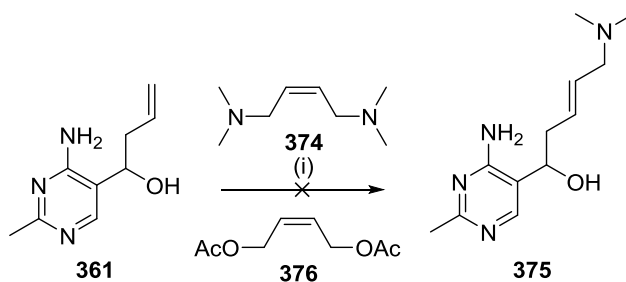
Compound **361** (scheme **105**) and the powerful Grubbs catalyst were then used as a means to construct the required C-C bond ⁽⁴⁶⁾. In 2003 Chatterjee and Grubbs ⁽⁴⁷⁾ reported the best conditions and catalysts for each type of metathesis reaction, and showed that cross metathesis (CM) of type I alkenes can be achieved in fairly good yields, and with some *E/Z* selectivity (scheme **105**). The only drawback is the requirement for one of the CM alkenes (type I) to be in a larger excess to overcome the fast homodimerisation.



Reagents and Conditions: (i) Grubbs 1 or 2 (3 mol %), CH₂Cl₂, 40°C, 12 hrs

Scheme 105: Grubbs (CM) of type I olefins

CM between allylic secondary alcohols (type II) and terminal alkenes (type I) gave moderate yields of cross products, with no protection of the alcohol required and at low stoichiometry's. This prompted us to use the *cis*-1,4-disubstituted tertiary amine **374** in a cross metathesis (CM) like that shown in scheme **106**. Formation of the **375** would hopefully then give the four carbon chain which would already have the desired tertiary amine in place. Conversion of the alcohol into the azide would then follow the same route as before, and should be restricted from cyclisation as outlined above (scheme **102**).



Reagents & Conditions: (i) **374**, Grubbs 2nd Gen, DCM, 40°C

Scheme 106: Cross metathesis of *cis*-1, 4-*N,N* diamino butene

Unfortunately no conditions were established to generate **375** even after 48 hours, and with increasing equivalents of **374** (table 13). Attempts were then made with the diacetate equivalent **376** to ascertain if it was just problematic with the diamine (table 13, entry 4 & 5), but this too gave the same results.

Entry	Grubbs 2 nd Gen	Substrate	Eqv.	Temp (°C)	Result
1	5 mol%	374	1.1 eq.	40	SM
2	5 mol%	374	2.0 eq.	40	SM
3	5 mol%	374	5.0 eq.	40	SM
4	5 mol%	376	2.0 eq.	40	SM
5	5 mol%	376	5.0 eq.	40	SM

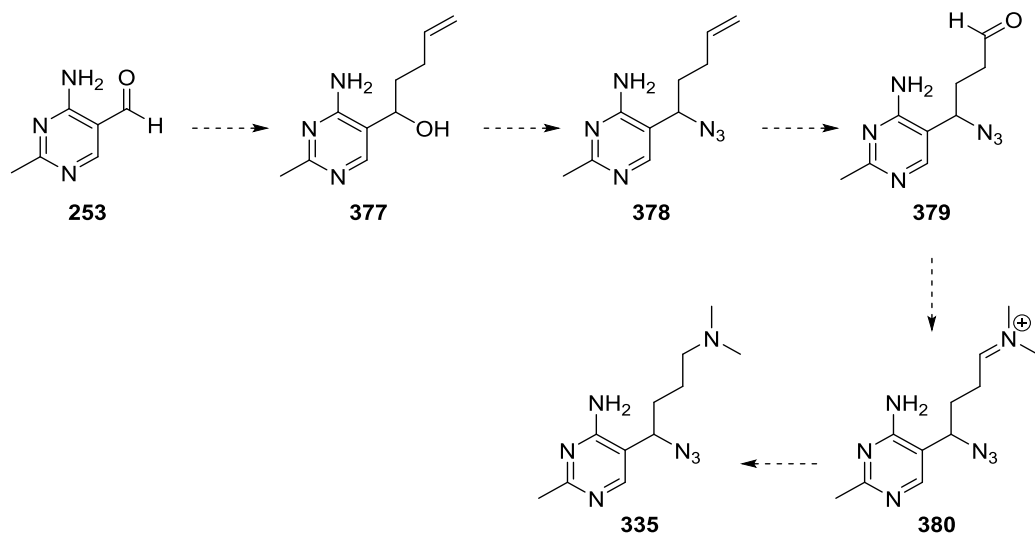
Table 13: Conditions attempted for cross metathesis of allyl alcohol

4.7.4 Hydroboration and Ozonolysis of Alkene Derivatives

The idea of a longer chain containing the sp² functionality was still kept so that other chemistry could be invoked to give the required three and/or four carbon chains. The abundant reactions involving alkene chemistry would then permit many synthetic possibilities to the tertiary amine.

4.7.5 Proposed Ozonolysis

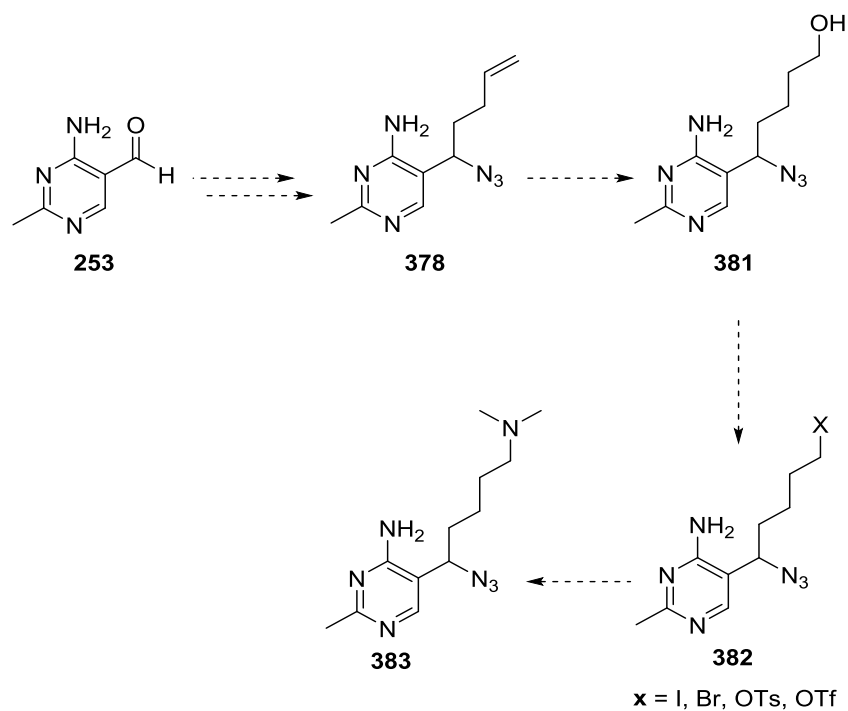
The failure of the Grubbs chemistry lead us to consider yet another alternative. Firstly cleavage of the alkene **377** via ozonolysis, and reductive work up with PPh₃ could give the aldehyde **379**. Reductive amination via the imine **380**, and treatment with NaCN(BH)₃ would ideally restore the nucleophilicity of the tertiary amine **335**. The remaining synthetic steps could then continue as before to the target molecule (scheme 107).



Scheme 107: Proposed ozonolysis and reductive amination route to tertiary amine

4.7.6 Proposed Hydroboration

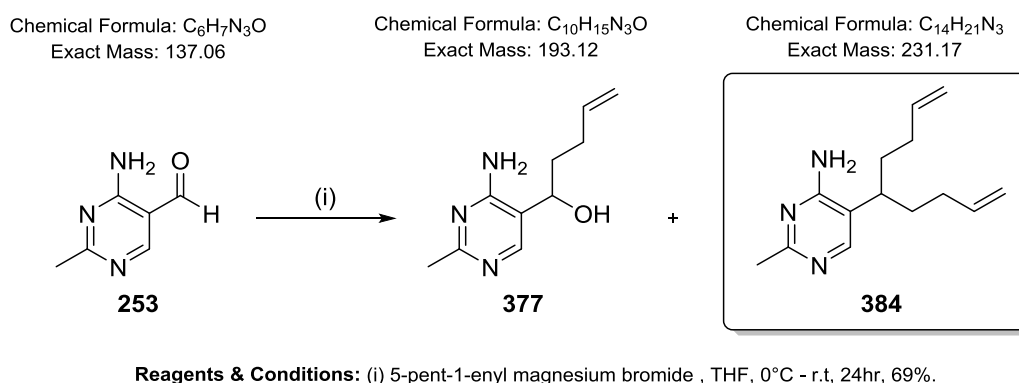
A second possibility is the hydroboration reaction of **378** (scheme **108**) with anti-Markovnikov addition of the hydroxyl across the alkene to create a functionalised four carbon chain. Conversion of alcohol **381** into a suitable leaving group ($X = \text{Br}, \text{I}, \text{OTs}, \text{OTf}$) would have allowed for a $\text{S}_{\text{N}}2$ reaction of **382** with dimethylamine to produce the final structure **383**.



Scheme 108: Proposed hydroboration route to tertiary amine

4.7.7 Synthesis of 2-methyl-4-amino-5-(5-pentene-1-ol)pyrimidine

Synthesis of **377** was straightforward because conditions for this step had already been established during the formation of **361** in scheme **102**. The primary product **377** once again eluted first and was recovered in 69% yield. Closely following this was a second fraction which appeared as a single spot and gave very clean data. A tricky analysis then began as all the relevant data revealed a possible mixture of products. The ^1H NMR was very clean, but the number of protons did not correlate to the mass spectrum which showed an $\text{M}+\text{H}$ at $192.11\ m/z$ and a suggested molecular formula of $\text{C}_{10}\text{H}_{14}\text{N}_3\text{O}$. This did not correlate to any of the compounds **253**, **377** or **384** (scheme **109**), and was not helped by the very messy ^{13}C NMR that contained more than fourteen carbon environments.



Scheme 109: Proposed dibutene side product **406**

Successful crystallisation allowed X-ray diffraction (XRD) which depicted the mysterious compound **385** as shown in figure **64 - A**. This conformed to a planar lattice arrangement of sheets between each individual pyrimidine ring as depicted in figure **64 - B** and was potentially formed by addition of excess Grignard reagent to some remaining nitrile impurity from the starting material.

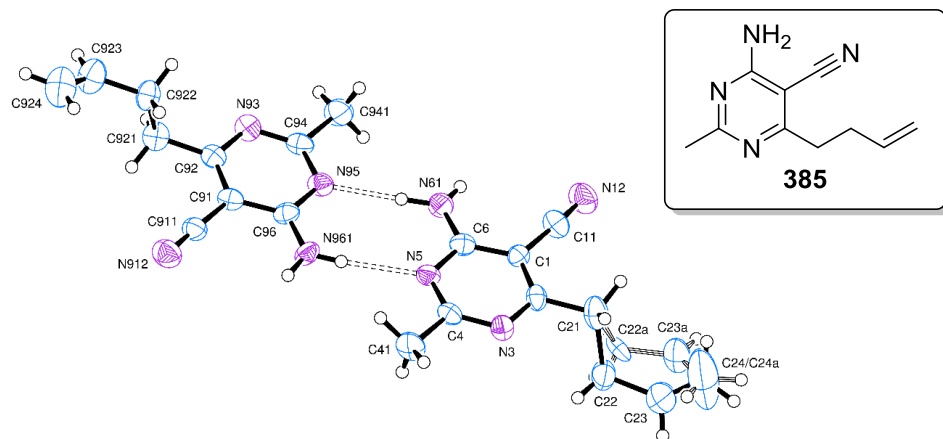


Figure 64 - A: XRD image of dibutene compound 385

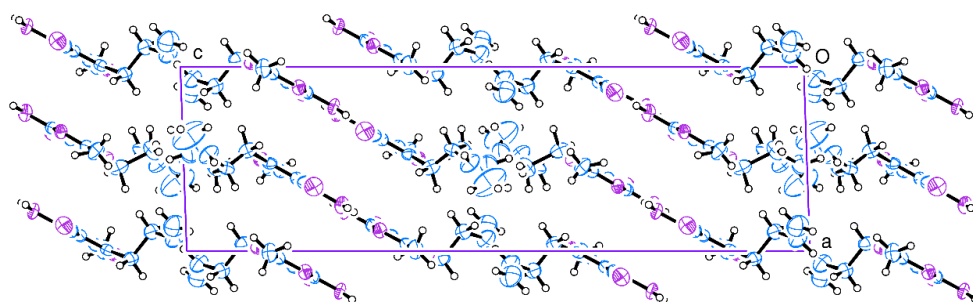
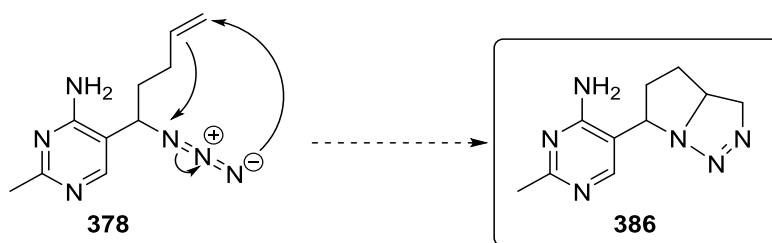


Figure 64 - B: XRD image of dibutene compound 385

4.7.8 Synthesis of 2-methyl-4-amino-5-(1-azidopentene) pyrimidine

Synthesis of the azide **378** (scheme **110**) was unfortunately never possible and the crude ^1H NMR for this reaction was not interpretable and extremely messy. An explanation for this could be the intramolecular 1,3-dipolar cycloaddition ($4\pi e+2\pi e$) of the azide onto the terminal LUMO π^* of the alkene ⁽⁴⁸⁾.



Scheme 110: Potential synthesis of 1,3-dipolar cycloaddition product

This could have generated **386** (scheme **110**) if it is conformationally stable and could maintain the 109° bond angles of the ring system. Generally the allyl anion (azide) contains four electrons

and its molecular orbital (MO) coefficients contain a single node between the three nitrogens. This allows favourable overlap with the LUMO π^* of the alkene to form the stable 5-membered ring (figure 65).

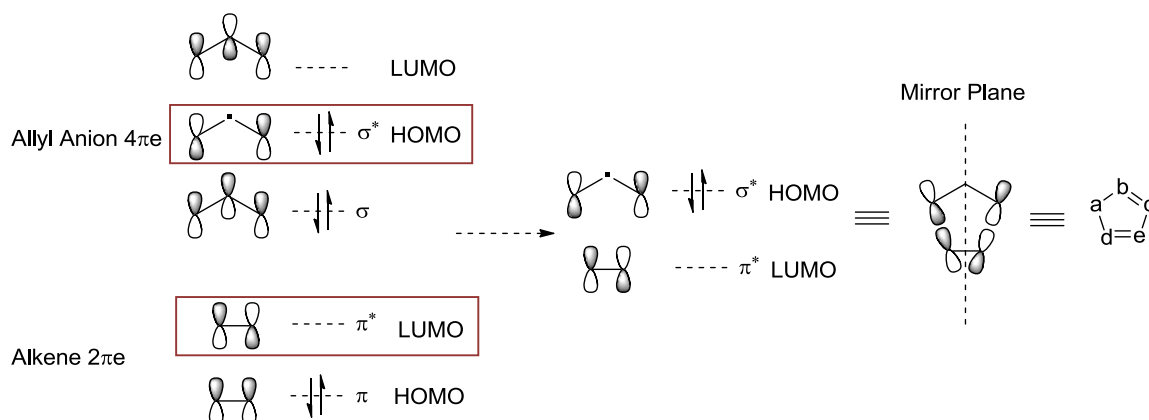
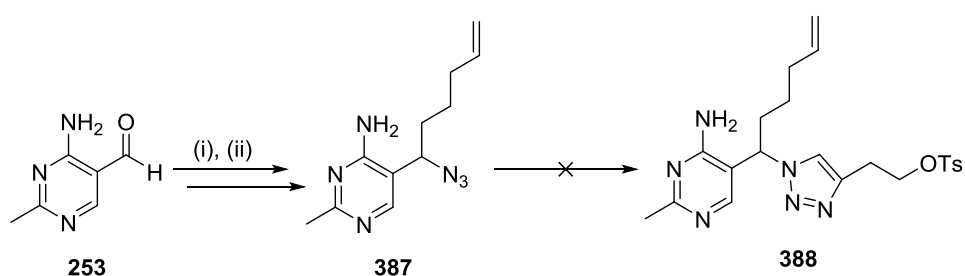


Figure 65: 1,3-Dipolar cycloaddition of azide onto alkene

4.7.9 Synthesis of 2-methyl-4-amino-5-(1-azidohexene)pyrimidine

Compound **387** (scheme 111) was successfully acquired after Grignard chemistry and conversion with DBU and DPPA into the azide. Acquisition of the longer chain now meant that ozonolysis could restore the aldehyde functionality for further chemistry like that depicted in scheme 107. Assembly of the required 1,4-disubstituted triazole ring and its side arm was then attempted to give **388** which could be derivatised further in preparation for the final structure.



Reagents & Conditions: (i) Pentynmagnesium bromide (2 M), THF, 0°C-r.t., 53%, (ii) DBU (1.3 eqv., DPPA (1.2 eqv.), THF, r.t., 50%, (iii) Sodium ascorbate (0.1 eqv.), CuSO₄·5H₂O (0.01 eqv.), r.t.

Scheme 111: Attempted click reaction of 2-methyl-4-amino-5-(1-azidohexene) pyrimidine

Conditions were then modified to give the triazole motif (table 14). These included an increasing stoichiometric equivalents of the copper (Cu), in case donation of the electrons in the alkene HOMO were undergoing some type of addition to the copper in the (Cu²⁺) oxidation state. This

could have prevented sodium ascorbate's ability to reduce Cu(II) to the active Cu(I) species and prevented the CuAAC reaction from taking place. Furthermore the Cu could have become oxidized back to Cu²⁺ and did not have enough equivalents to complete the reaction.

Entry	Alkyne	CuSO ₄ (eqv)	Time (hours)	Temp (°C)	Yield(%)
1	ROH	0.01	48	RT	-
2	ROH	0.02	48	RT	-

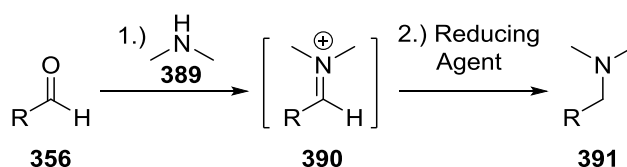
Table 14: Conditions for click reaction of 2-methyl-4-amino-5-(1-azido hexene)pyrimidine

The ozonolysis attempt of compound **387** was then temporarily shelved as the ozonolysis equipment was not accessible at the time. Due to the lack of interesting results and problems with the synthesis, we sought to derive the intermediate aldehyde **379** (scheme **108**) in another way.

4.8 Synthesis 1,3-dioxolane-2-methyl-4-aminopyrimidine derivatives

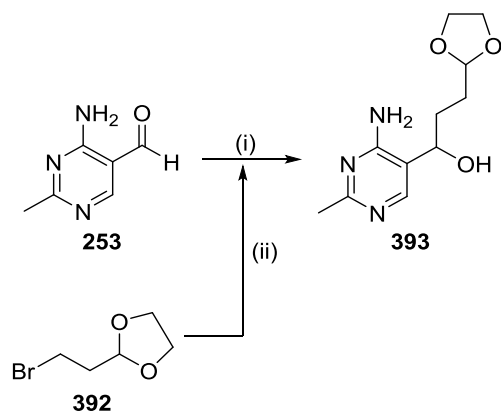
4.8.1 The Reductive Amination

It is well known that the reductive amination of aldehydes⁽⁴⁹⁾ is a useful way to introduce tertiary amine groups (scheme **112**).



Scheme 112: Typical reductive amination

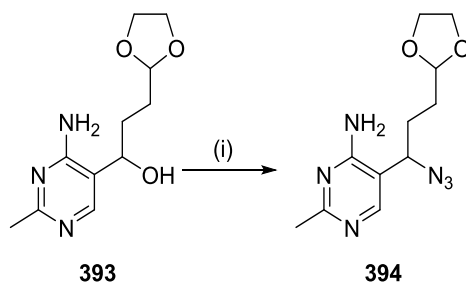
Therefore a new synthetic route began with formation of the 1,3-dioxolane substituted Grignard reagent via conversion of the commercially available starting material **392** (scheme **113**). Addition to the aldehyde at 0°C using 3.5 equivalents as the nucleophile then gave the intermediate **393** in a 37% yield.



Reagents & Conditions: (i) **392** (3.5 eq.), THF, 0°C-r.t., 16 hrs, 37%, (ii) Mg, I₂, THF, r.t, 3 hrs, quant%.

Scheme 113: Synthesis of compound **393**

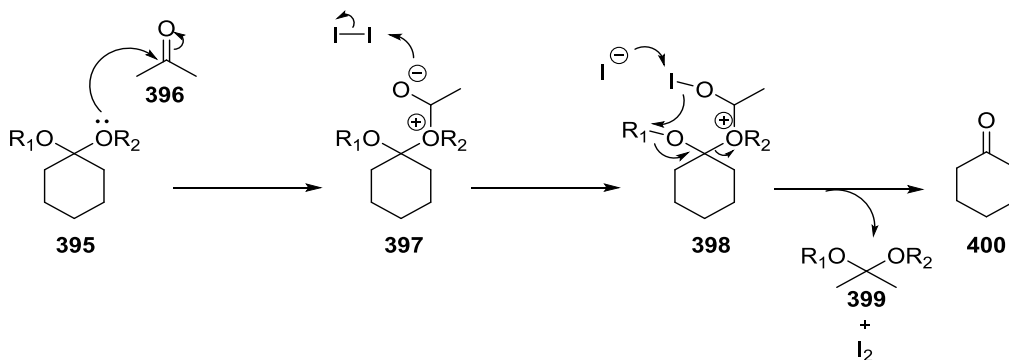
After treatment with DBU and DPPA, the alcohol was converted into the azide **394** in 42% yield (scheme **114**). The synthetic path now took one of two routes; firstly the click reaction could be carried out to construct the 1,4-triazole ring with the necessary alkyl chain containing the tosylate group for the subsequent diphosphate step. Or secondly, a deprotection of the dioxolane could then be followed by either the click chemistry, or conversion into the tertiary amine as described by the alkene motifs earlier.



Reagents & Conditions: (i) DBU (1.3 eq.), DPPA (1.2 eq.) THF, r.t, 16 hrs, 42%

Scheme 114: Synthesis of azide **1,3-dioxolane**

Initially, a deprotection of the 1,3-dioxolane was attempted using a milder approach compared to the commonly reported acid hydrolysis which suffers from incompatibility of many functional groups⁽⁵⁰⁾. The use of milder reaction conditions has been explored before with molecular iodine and acetone (scheme **115**).⁽⁵⁰⁾ This methodology has been described as high yielding, chemoselective and purification free, therefore making it a good selection for our compound.



Scheme 115: Ketal Deprotection with I₂ and acetone

After 48 hours no other spots were observed by TLC, so refluxing in aqueous acid was attempted to deprotect the ketal. To our surprise the co-spot for the crude reaction indicated total consumption of the starting material after 16 hours and it was hoped that the proposed aldehyde product **401** had been formed (figure 66).

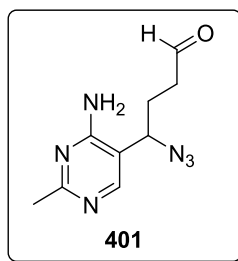
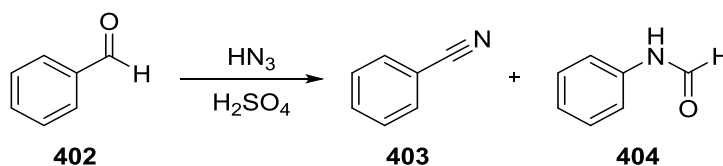


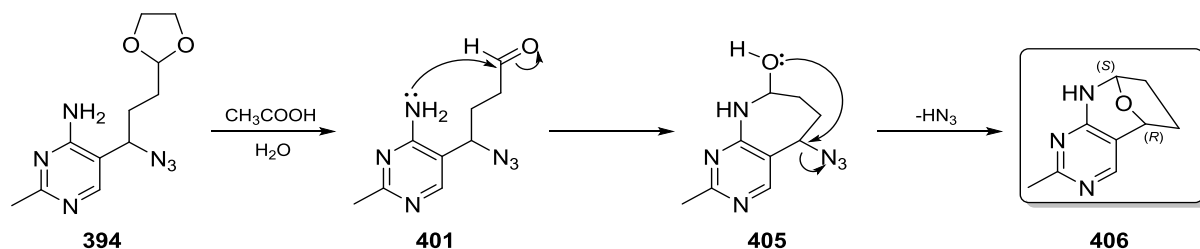
Figure 66: Structure of intermediate aldehyde compound 401

An infra-red spectrum was then obtained to check if the azide was still present as it was thought that a potential intramolecular rearrangement may have taken place via intermediates like that observed in the Schmidt reaction⁽⁵¹⁾ (scheme 116).



Scheme 116: Schmidt reaction of HN₃ onto benzaldehyde

Interestingly the infra-red spectrum did not show the characteristic azide peak⁽⁵²⁾ at 2130 cm⁻¹ which was strong in the starting material. This loss was subsequently confirmed by mass spectrometry, which indicated that no analogues of compounds **403** and **404** were present (scheme 116). This suggested that a Schmidt rearrangement had not occurred. One hypothesis is depicted in scheme 117 and could explain the missing azide group.



Scheme 117: Proposed acid catalysed rearrangement of compound

Analysis of the ^1H NMR (figure 67) indicated that the core structure of the 2-methyl-4-aminopyrimidine still existed but without the aldehyde peak at an expected 9.0 ppm, and instead with just the aromatic proton at 7.81 ppm (pyrimidine proton-blue dot). The remaining two carbon chain connecting the chiral centre to the 1,3-dioxolane was still present as a set of doublets (d) which both integrated as one and were linked separately in the COSY to the CH_2 protons highlighted by the green dots (figure 67). As a single amine proton could be observed at 5.54 ppm it did suggest that some type of nucleophilic addition may have occurred onto the aldehyde. Additional information for this was given by the DEPT135 carbon NMR which changed from 4 \times CH_2 environment's to 2 \times CH_2 and suggested the loss of methylene groups from the acetal protecting group. The only piece of data not in agreement with the suggested structure was now the multiplicity of the protons at the ends of the oxygen bridge (figure 67, red spots) which appear as a set of doublet's and not their expected dd . This is because a single vicinal coupling is observed to only one proton on the adjacent CH_2 protons (figure 67, green spots). The smaller dihedral angle of 0° allows larger orbital overlap between the protons and thereby only depicts a doublet. Due to the lack of azide in the infra-red, mass spectrometry data and deductions made from the ^1H NMR, ^{13}C and DEPT135 carbon, a structure was tentatively proposed as 406.

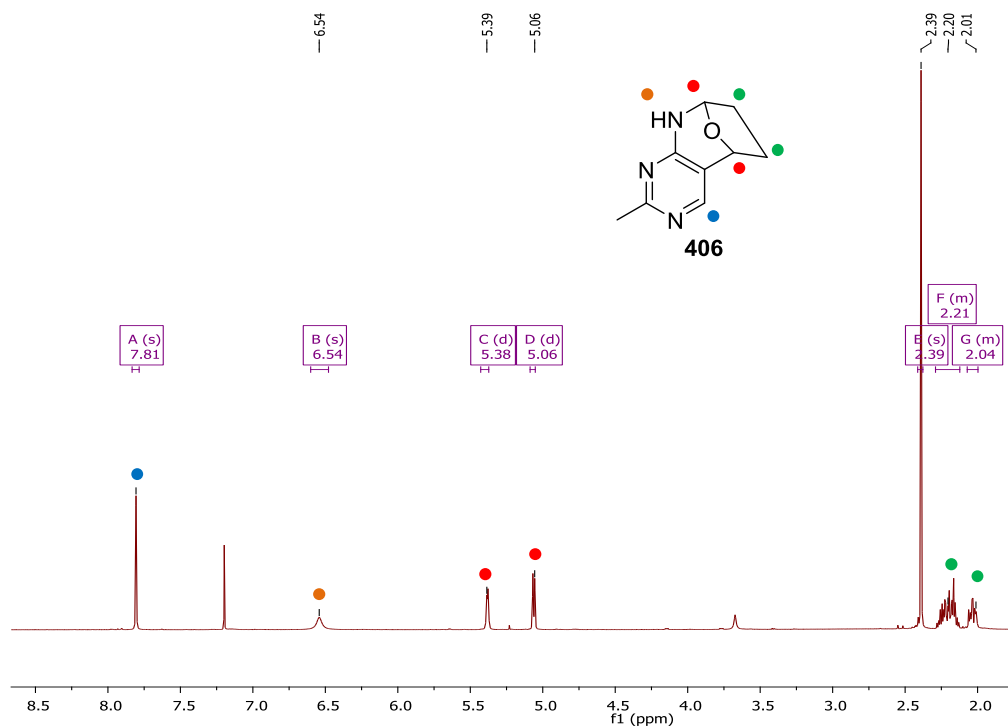


Figure 67: ^1H NMR for proposed product in acidic acetal deprotection

Luckily recrystallisation of **406** in CH_2Cl_2 : pet ether gave cuboid crystals that were examined by X-ray diffraction (XRD) to confirm the postulated structure (figure **68**).

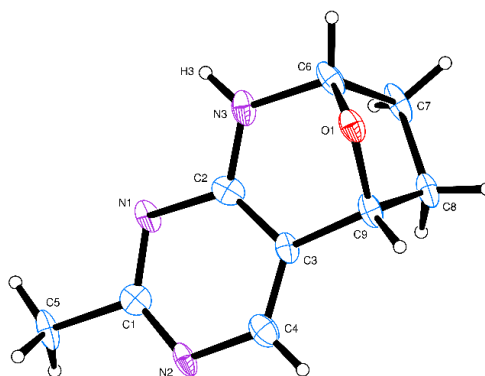


Figure 68: XRD structure of compound 406

The structure is found as a monoclinic crystal with $P2_1/C$ symmetry. By viewing the structure (figure **69**) along the C6-C9 axis it is obvious that the pyrimidine structure lies in a planar conformation and has a torsion angle of (-90.3°) relative to the N₃ of the pyrimidine ring.

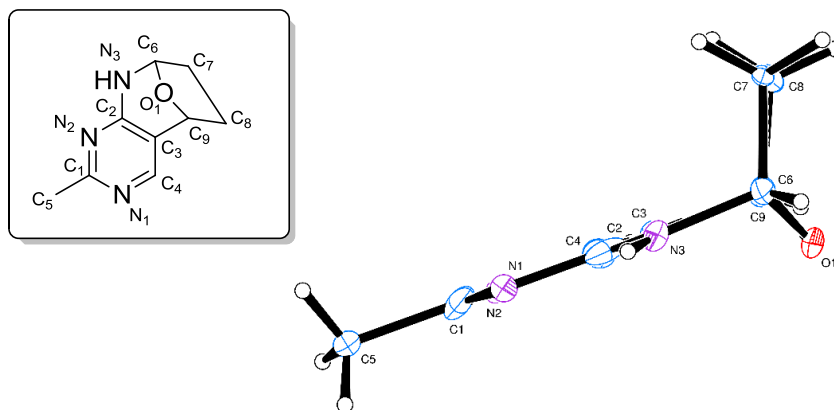


Figure 69: View along C₆-C₉ axis of compound 406

Bond lengths between the positions N3 - C6 and C3-C9 are both 1.5 Å which is interesting when compared to that of the C6 - C7 (1.52 Å) and C9 - C8 (1.49 Å) which differ slightly. Even though this effect is marginal, it is also observed when measuring the C6 - O1 bond which exists at 1.41 Å and is smaller than the C9-O1 bond of 1.48 Å. This increased length could be resulting from the stabilising effect of the nearby sp² (C3)-carbon and its p orbital undergoing some hyperconjugation with the p orbital of the sp³ C-H at position C9 thereby holding it in a more rigid position. Hence, the newly formed bond of C9 – O1 is longer than that of the C6 – O1 which was already established in the previous step, and had assumed its required bond length as the oxy anion. Lastly the molecules are linked by pairs of hydrogen bonds between the N1 and N3 of one molecule and N1' and H3' of the other (figure 70) which produce a centre of symmetry. Consequently water molecules are located between the sets of dimers to form a strong hydrogen bonded network.

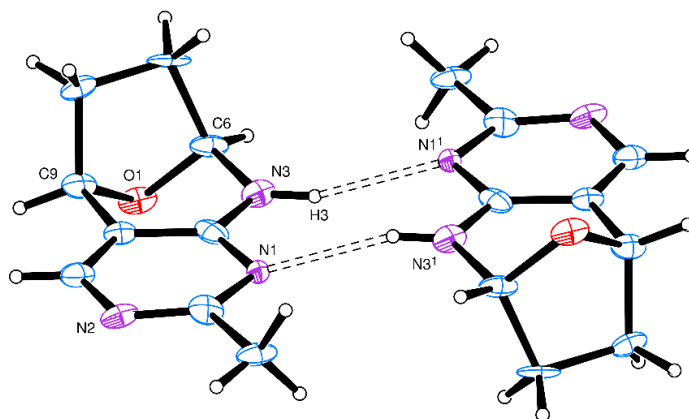
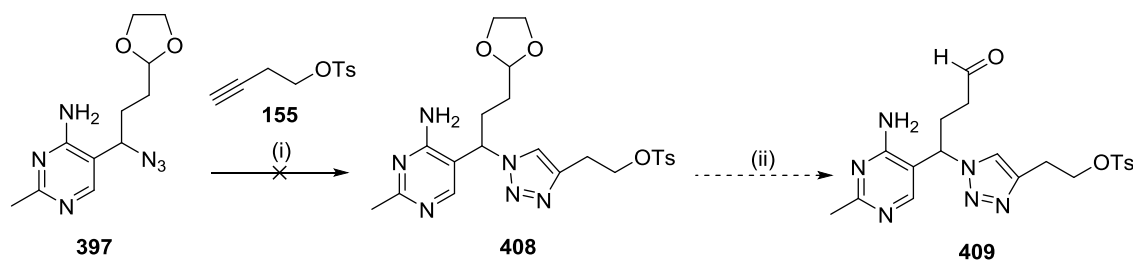


Figure 70: Dimers of compound 406 bridged by hydrogen bonds

This exciting novel compound then caused new problems as the following CuAAC reaction could not be completed without the azide. It was also decided that formation of compound **401** would not be possible by any routes due to this rearrangement, and so the ozonolysis shown in the previous chapter was discarded (scheme **108**). A 1,4-CuAAC of the original azide structure **397** (scheme **118**, table **15**) was then attempted to hopefully establish the main scaffold which could potentially undergo acid hydrolysis of the 1,3-dioxolane at a later stage. This approach did not produce the desired click product and so a new route was sought.



Reagents & Conditions: (i) **155**, Sodium ascorbate (0.1 eq.), CuSO₄·5H₂O (0.01 eq.), r.t. (ii) H⁺/H₂O, r.t.

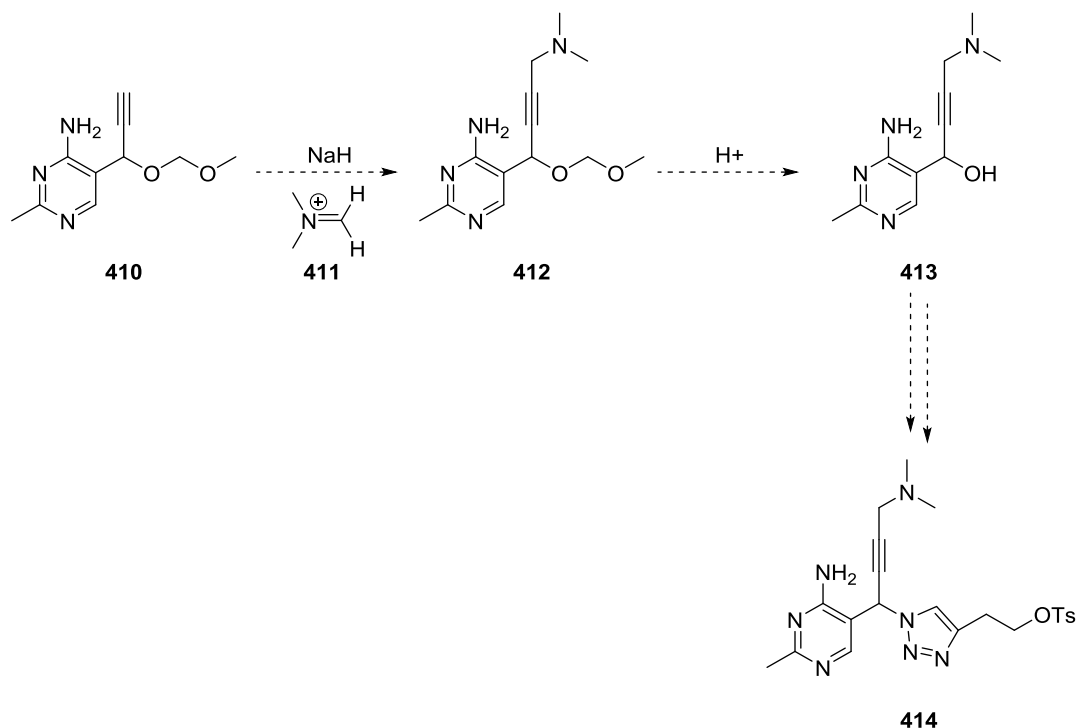
Scheme 118: Attempted CuAAC reaction of 397 as protected 1,3-dioxolane

Entry	Alkyne	Sodium Ascorbate (eqv)	CuSO ₄ (eqv)	Temp (°C)	Time (Hr)	Yield %
1	ROH	0.1	0.02	rt	48	-
2	ROH	0.1	0.02	50	48	-

Table 15: Conditions for click reaction of 397

4.9 Synthesis of Rigid Alkyne “Spacer”

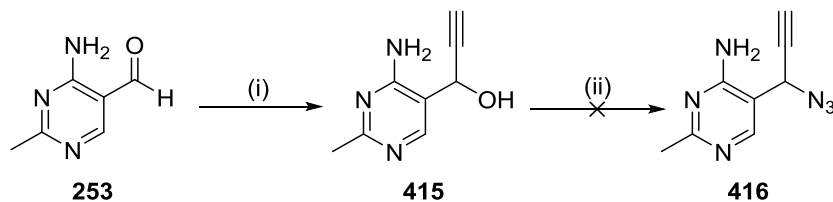
Attention now focused on modifying the alkyl linker with something rigid to prevent the problematic cyclisation step described earlier. The alkyne functionality is a useful way to accomplish this because of its linear 180° bond angle. It was proposed that introduction of the alkyne using Grignard chemistry and protection of the secondary alcohol would give compound **410** (scheme **119**). Deprotonation of the terminal alkyne could then reveal the reactive anion. Quenching with an electrophile such as Eschenmoser’s salt **411** made *in situ* by reacting formaldehyde and dimethylamine could then produce compound **412**. Acidic deprotection of the MOM group, conversion to the azide and click chemistry would then give **414**, which after hydrogenation and conversion to the diphosphate would derive the final target.



Scheme 119: Proposed rigid linker using Eschenmoser’s salt

Synthesis of the alkyne tether was successful after treatment with the respective Grignard reagent to give the product **415** in a 75% yield (scheme **120**). Conversion of **415** into the desired azide **416** was attempted to try and avoid multiple protection and deprotection steps. It was also hoped that the linear bond angles of the alkyne and azide would not be suitable to undergo a suspected 1,3-dipolar cycloaddition when substituted on a *gem*-carbon. However, the crude ¹H NMR showed no promising peaks of either starting material or *gem*-alkyne azide **416**. Extra

confirmation of this outcome was probably highlighted by the lack of literature concerning this type of transformation, although it was found that Banert had reported such analogues⁽⁵³⁾ and their possible isomerisation to [1,2,3]-triazoles. Subsequently this synthesis was stopped and the protection chemistry was followed.

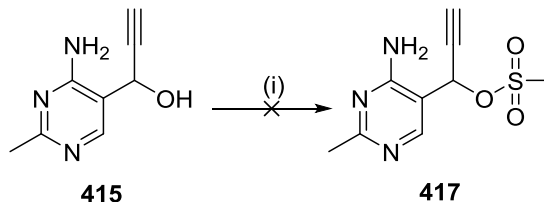


Reagents & conditions: (i) Ethynylmagnesium bromide (0.5 M), 0°C-r.t., 24 hr, 75%, (ii) DBU (1.2 eqv.), DPPA (1.3 eqv.), r.t.

Scheme 120: Synthesis of *gem*-alkyne azide

4.9.1 Protection of Secondary Alcohol in Alkyne Linker

The new direction of synthesis (scheme 121) sought to protect the secondary alcohol **415** as the mesylate compound **417**, and then complete the S_N2 displacement with sodium azide at a later stage after installation of the tertiary amine had been completed.



Reagents & conditions: (i) MsCl (5.0 eqv), Et₃N, 0°C-r.t., 24Hr.

Scheme 121: Mesylate protection and sodium azide S_N2 displacement

It was thought that the mesylated **417** had been successfully constructed due to the additional CH₃ at 3.42 ppm in the ¹H NMR and the extra carbon in the ¹³C spectra. Upon interpretation of the mass spectrum (figure 71) a peak of [M+H]⁺ 178 *m/z* did not correlate to the protected mesylate (*m/z* 241) as first thought.

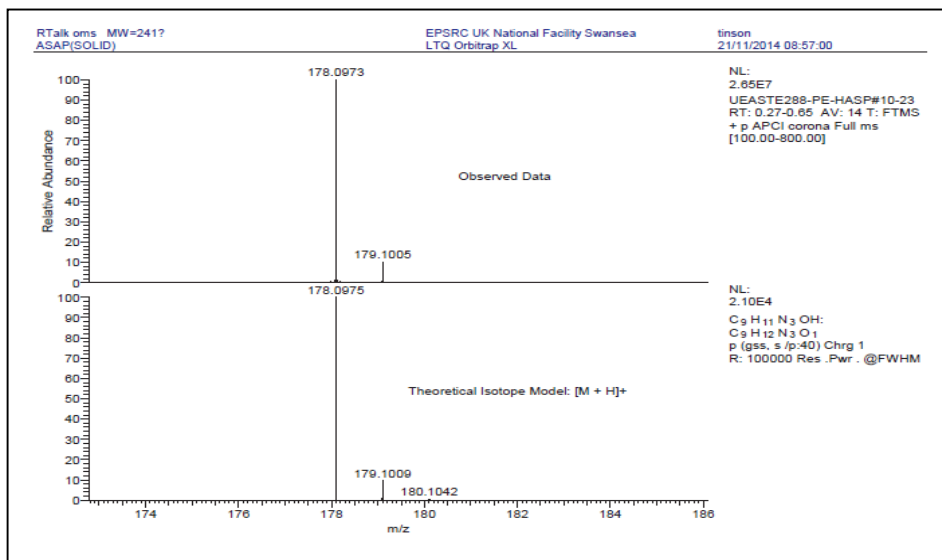
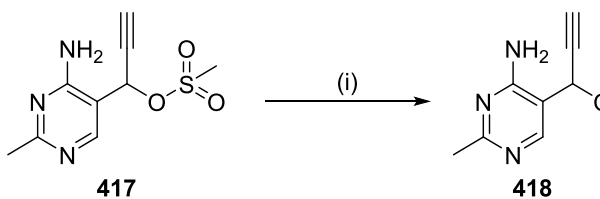


Figure 71: Mass spectrum of suspected mesylate compound

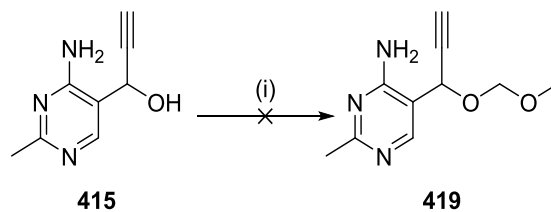
In fact, the observed value of m/z 178 instead suggested that the protected alcohol was actually the methoxy ether **418** (scheme **122**). This is thought to have occurred during the work up process whilst trying to recover the so-called protected alcohol from the aqueous layer by washing with DCM: MeOH (90:10 v/v). Although this problem could be circumvented in further synthetic attempts, the yield of the methoxy ether was very low (<1% yield) and the original protected alcohol was never found. On this basis a new protecting group was attempted that may not favour S_N2 displacement so easily in the highly polar solvents used for purification.



Reagents & conditions: (i) DCM/ MeOH (90:10 v/v), <1%.

Scheme 122: MeOH displacement of mesylate

A protection of the secondary alcohol was then attempted using a less stabilised methoxymethyl (MOM) group (scheme **123**).



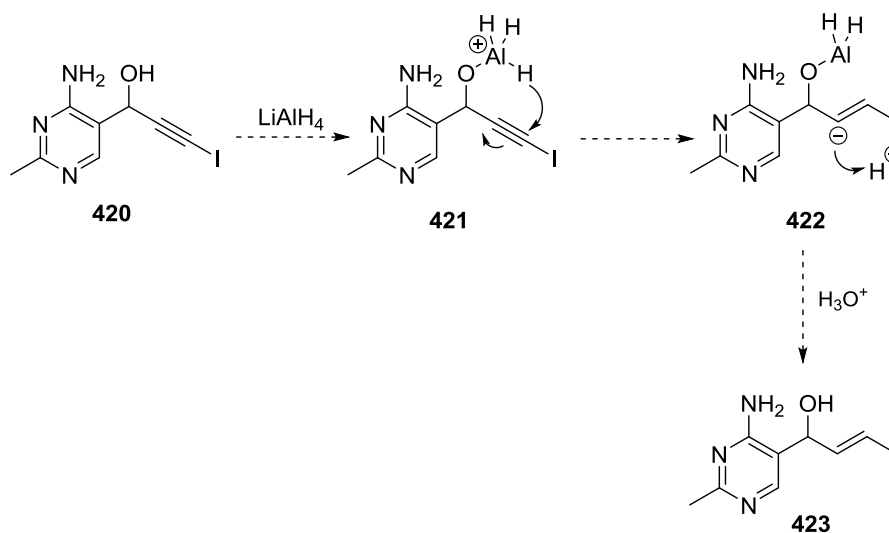
Reagents & Conditions: (i) MOM-Cl, DIPEA, TBAI

Scheme 123: MOM protection of secondary alcohol

Unfortunately no product was formed and attempts to effect this transformation did not seem possible. A slight alteration to the synthesis was then made in hope of forming a vinyl iodide for cross coupling endeavours.

4.10 Cross Coupling Approach

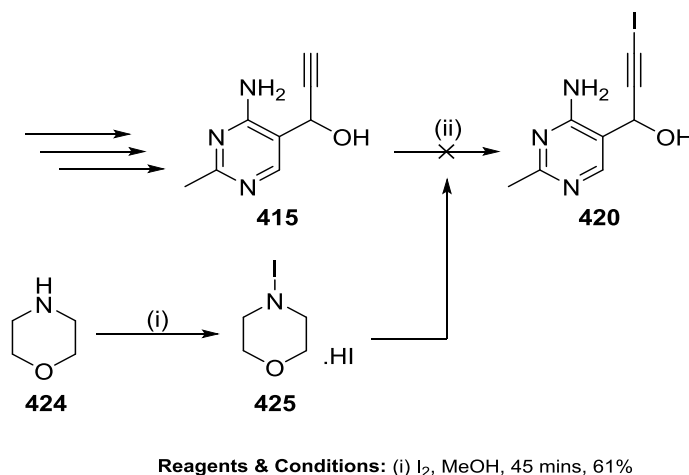
Vinyl iodides are one of the best synthetic precursors in cross coupling chemistry and have been used extensively in the Suzuki⁽⁵⁴⁾ and Sonagashira⁽⁵⁵⁾ reactions. Conversion of the alkyne into a vinyl iodide would facilitate a range of cross coupling chemistries. A proposed synthesis to the vinyl iodide would begin with intermediate **420**, which after treatment with LiAlH_4 should produce the vinyl iodide **423** (scheme **124**).



Scheme 124: Proposed synthesis of vinyl iodide

4.10.1 Synthesis of Iodo-Alkyne

Following the adapted procedure of Tripp *et al.* ^{(11), (56)} a milder synthesis of the β -vinyl iodide was attempted. This involved reaction of the alkyne **415** with a source of I⁺ obtained from *N*-iodomorpholine **425** (scheme **125**). Stirring for 72 hours gave no reaction as confirmed by TLC, and the reaction mixture was very thick and difficult to work with. Further attempts on this route were then discontinued, and a total change in chemistry was employed that did not utilise the initial Grignard reagents.



Scheme 125: Synthesis of terminal alkyne iodination

4.11 The “Umpolung”

4.11.1 The Dithiane Protection

Upon struggling to insert a desirable length chain using the original strategy our focus then turned towards “umpolung” chemistry coined by D. Seebach ^{(57), (18)} in 1965. This involves the reversal in polarity of a traditional covalent bond (figure **72**).

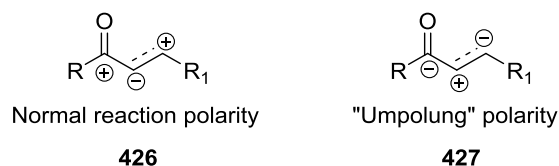
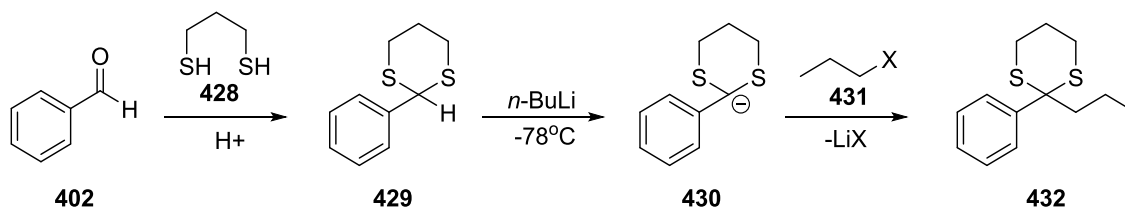


Figure 72: Normal and reversed synthons

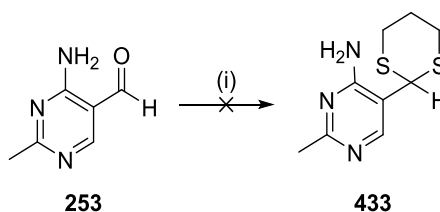
Over the decades this technique has greatly improved the synthetic tools available to the chemist by adding alternative synthetic routes to target molecules. There are quite a few examples of this type throughout the literature but some of the more common include the use of cyanide in the

benzoin condensation ⁽⁵⁸⁾, the Stetter reaction for forming 1,4-dicarbonyl compounds ⁽¹¹⁹⁾ and the dithiane protection of an aldehyde to form a masked “acyl anion” ⁽¹⁸⁾. In all of these cases the carbon centre is rendered temporarily nucleophilic and is able to react with a range of electrophiles (scheme 126)



Scheme 126 Corey-Seebach dithiane protection and umpolung addition

Using a reported procedure ⁽⁵⁹⁾, LiBr was added to the respective aldehyde **253** and the 1,3-dithiopropane was added dropwise (scheme 127). It was thought that the small lithium ion could act as a Lewis acid upon the aldehyde, and improve its electrophilicity for attack by the dithiol. After two days no product was observed by TLC and the reaction was stopped. A potential drawback to this reaction was potentially the large steric bulk of the two sulfur groups in close proximity to the pyrimidine ring.

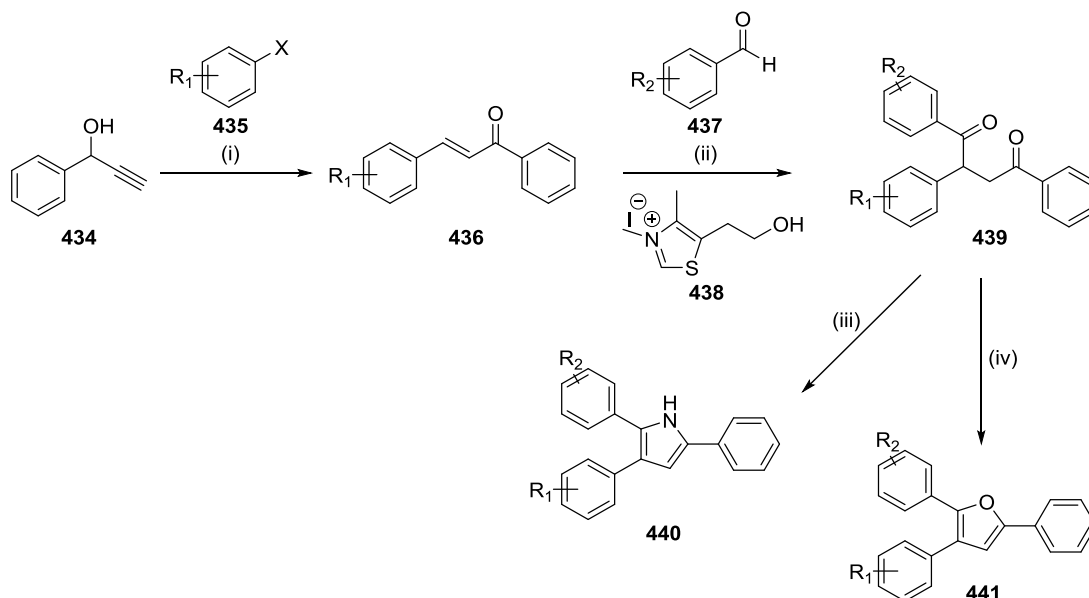


Reagents & Conditions: (i) 1,3-propanedithiol, LiBr, 75°C, 72 hrs

Scheme 127: Attempted dithiane protection of aldehyde with LiBr

4.11.2 The Stetter Approach

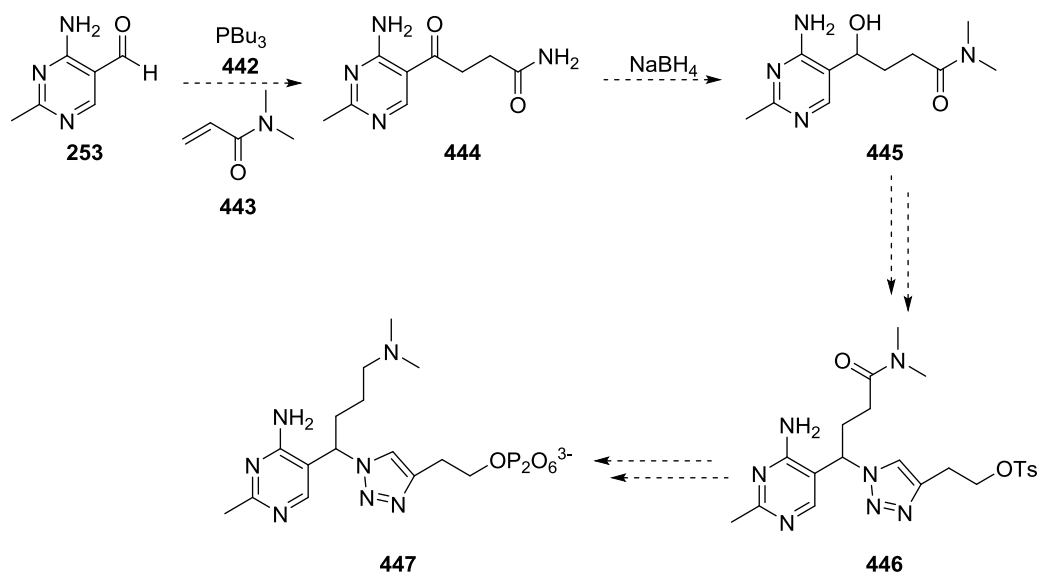
The Stetter reaction has seen clever applications in the construction of 1,4-dicarbonyl systems as these are typically difficult to obtain and are useful intermediates for synthetic manipulation. One of the most popular applications of these intermediates is in the Paal-Knorr reaction which allows construction of the furan, thiophene and pyrrole rings (scheme 128). Due to the problems associated with the dithiane protection, it was decided that umpolung chemistry could still be plausible but using the 1,4-Stetter methodology.



Reagents & Conditions: (i) $\text{PdCl}_2(\text{PPh}_3)_2$ (2 mol%), CuI (1 mol%), Et_3N , 14 hrs, (ii) **437**, **438** (20 mol%), EtOH , 24 hrs, 46-59% (iii) NH_4^+Cl^- , AcOH , 33 hrs, 75-88% (iv) conc HCl , AcOH , 12 hrs, 42-57%.

Scheme 128: Application of Stetter reaction for Paal-Knorr synthesis

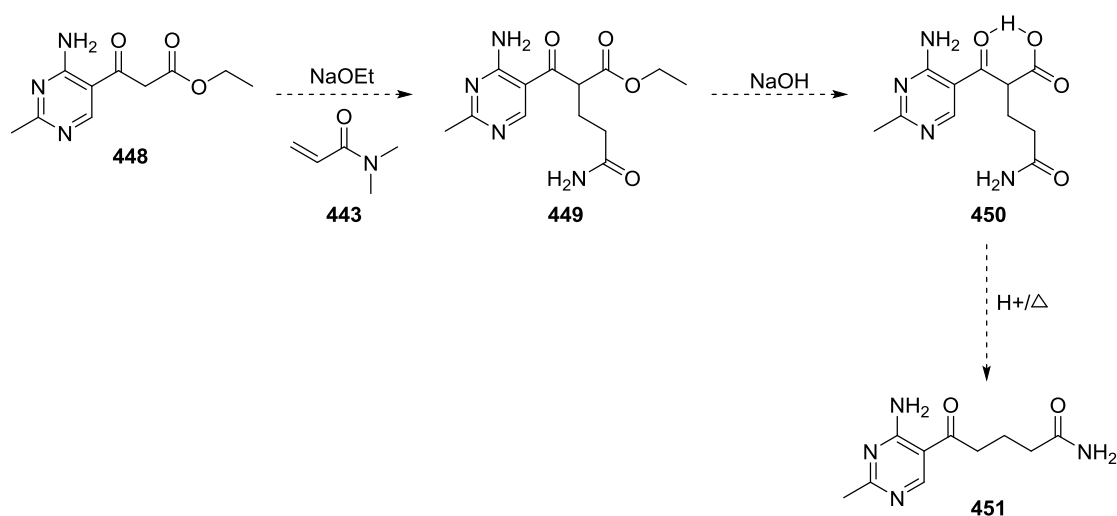
Further reading revealed that Kim *et al.*⁽⁶⁰⁾ had accidentally discovered a process similar to that described above when using tributylphosphine. It was decided that an umpolung reaction onto **443** (scheme 129) would provide a very useful synthetic intermediate. This chain was desired for two reasons: firstly the amide functionality would not undergo cyclisation because the amine electrons are delocalised into the sp^2 amide bond, and secondly because the ketone adjacent to the pyrimidine could be chemoselectively reduced using NaBH_4 to the necessary alcohol. The chemistry could then continue from this point until the penultimate step whereby LiAlH_4 reduction should give the tertiary amine **447**. Two attempts of the Stetter reaction were made on **253**, but unsuccessfully only gave starting material and un-reacted *N,N*-dimethylacrylamide.



Scheme 129: The PBu_3 assisted Stetter reaction

4.12 The Reformatsky/Blaise Approach

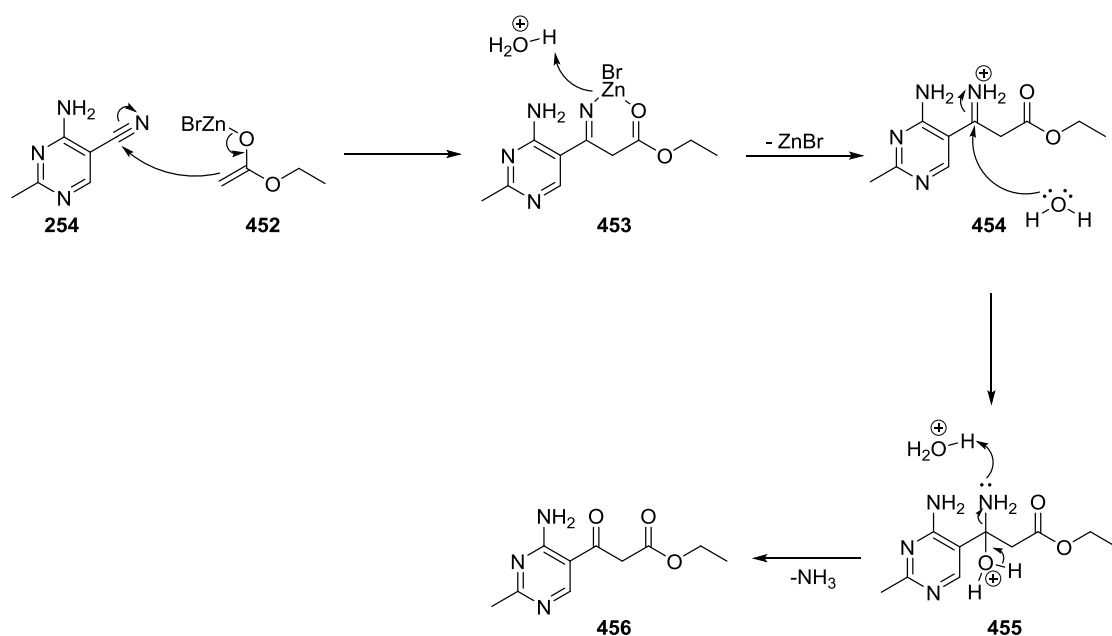
One tactic employed to aid in assembly of the desired chain length was by creating a 1,3-diketone such as **448** (scheme 130). The inherent acidity of the central protons could then be used for further modification. Deprotonation and nucleophilic attack onto **443** would then install the extended functionality to give compound **449**. An ester hydrolysis and decarboxylation would provide the final alkyl chain containing the tertiary amide group with loss of CO_2 to give **451**. Chemistry could then be tailored for the remaining steps and follow something similar to that shown in scheme 129.



Scheme 130: Proposed synthetic route after Blaise reaction

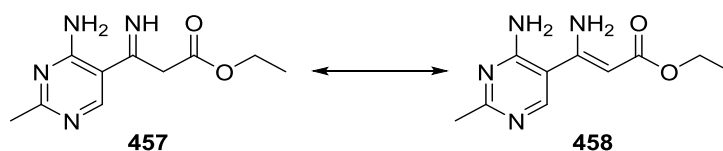
4.12.1 Synthesis of 2-methyl-4-amino-5-(1,3-diketone) pyrimidine

The Blaise reaction is one way of introducing the diketone and is a modified version of the Reformatsky reaction which involves a nucleophilic attack of the zinc enolate onto a nitrile group^{(61), (62)}. Minero's group⁽⁶³⁾ had previously completed this reaction with a variety of compounds including that of benzonitrile. A test reaction on benzaldehyde was then completed to confirm if the Reformatsky reagent was successfully made before it was tested further. The zinc enolate **452** was then added to compound **254** under similar conditions to the literature (scheme **131**).



Scheme 131: The Blaise reaction of 2-methyl-4-aminopyrimidine carbonitrile

The test reaction on benzaldehyde only took five hours whereas reaction with **254** was not complete until after 7 days. Following aqueous workup, a product was recovered in 50% yield, but it was not the desired 1,3-diketone **456** as hoped. Instead the reaction had stopped at compound **457** as an imine-enamine tautomeric mixture⁽⁶³⁾ (Scheme **132**).



Scheme 132: Formation of novel Blaise reaction side product

Confirmation of this product was given by the base peak observed at $[M+H]$ 223.11 m/z in the mass spectrum, which also indicated the loss of 46 a.m.u. from the molecular ion and therefore suggested the loss of ethanol (figure 73).

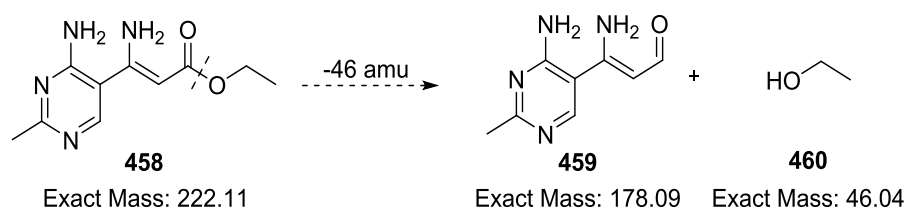


Figure 73: Mass spectrum analysis for compound 458

Analysis of the COSY and NOESY show no other interesting links except between those of the ester group which is corroborated by the peak at 1715 cm^{-1} in the infra-red spectrum. Interestingly the ^{13}C NMR does not show a characteristic peak for ester carbonyl in the 190-220 ppm range, but at the lower value of 169 ppm possibly relating to the increased conjugation within the system (figure 74).

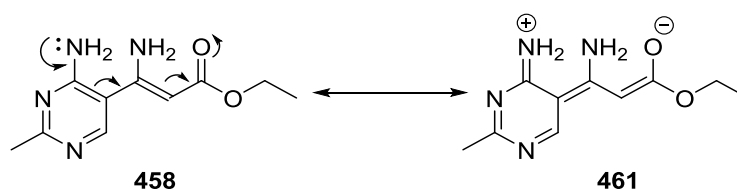


Figure 74: ^1H NMR Up field shift of C=O due to conjugation

Further corroboration was then provided by an overlay of the DEPT135 onto the ^{13}C spectra which denotes the presence of the expected five quaternary carbons as would be found for these structures. The last pieces of proof for the isolated tautomer is the proton situated between the 1,3-dicarbonyl system which integrates as one and does not explain structure 458 which should have a singlet of two protons and one for the imine proton. Lastly, the HMBC shows a 3J coupling between a quaternary carbon at 112 ppm (position 3, figure 75) and that of (position 1, figure 75). Another 2J coupling between position 4 and position 3 can also be seen, whilst a weak coupling can be observed to the nearby carbonyl at 169 ppm.

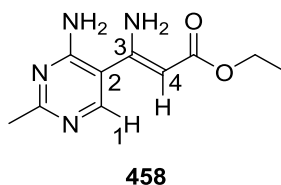
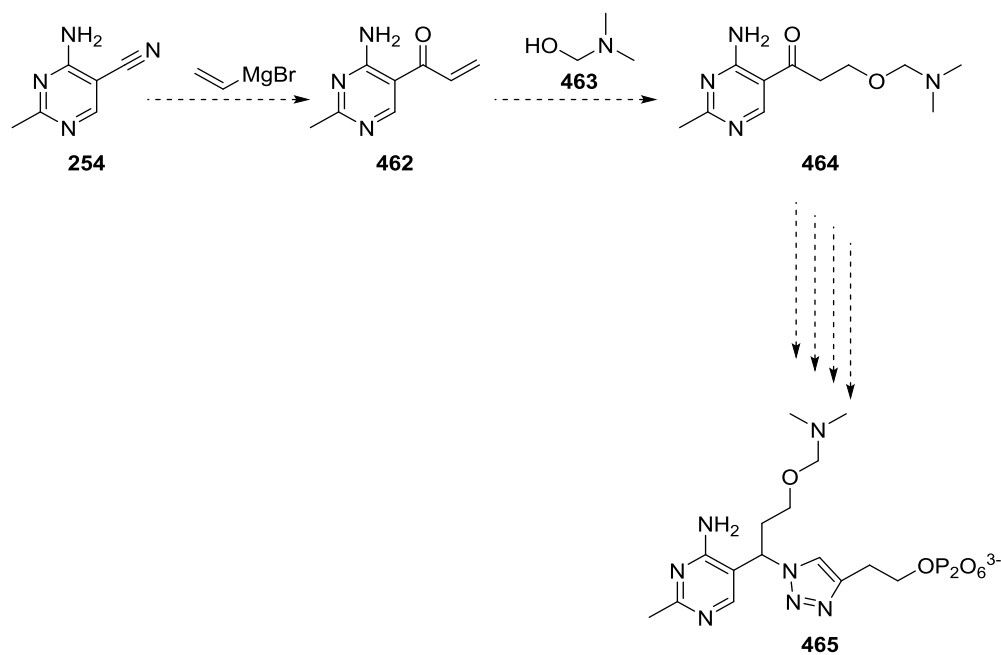


Figure 75: Assignments based on HMBC

Now that the desired product had not been recovered and with the biological results (see chapter 5) indicating problems with the longer alkyl chains, an alternative synthetic target was required. Work then began on a new synthesis (scheme 133) that would incorporate an oxygen linker into the alkyl series. It was thought that positioning an oxygen linker within the tether, could increase the flexibility within the chain and remove one of the bulky carbon units. This would then hopefully allow extra conformational mobility at that position, which is not achievable with the problematic longer three and four carbon chains.



Scheme 133: Proposed synthesis of oxygen linker ThDP

Disappointingly, addition of the vinyl Grignard reagent onto the nitrile **254** did not give the desired vinyl ketone **462** but instead compound **466** (figure 75).

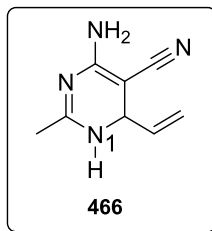


Figure 75: Side product from vinyl addition to nitrile 254

Conformation of this product was given by the extra nitrogen in the mass spectrum, the nitrile stretch at 2171 cm^{-1} in the IR and the additional proton which existed adjacent to N¹ and coupled in the COSY to the proton's located on the nearby alkyl chain.

4.13 Conclusion to Chapter

The past chapter has primarily focused on the attempted synthesis of the tertiary amine tether which has provided new and interesting compounds such as the dihydropyrimidine structure **466** and the geminal dialkene **468** which may act as suitable candidates for the synthesis of chiral ligands and ring closing metathesis reactions. Moreover, a potential route to interesting bicyclic motifs like compound **406** may allow future synthetic approaches to incorporate this structural feature easily. These have arisen though various attempts to construct a carbon linker between the original 1,4-disubstituted triazole and a tertiary amine. This has been extremely frustrating due to the difficult purification of highly polar compounds, intramolecular cyclisation and the lack of reactivity in some cases. These syntheses have also highlighted the problems associated with additions of sterically demanding groups to the aldehyde/ketone and the reduced electrophilicity of these functionalities by resonance donation. Luckily, the side products formed during these reactions may prove useful for future synthetic targets, and the biological testing of the model ThDP has produced results that can dictate future decisions in the development of these ThDP structures for the MBH reaction.

Chapter 5

Biological Investigation into Model ThDP 1,4-[1,2,3] Triazole

Cofactors

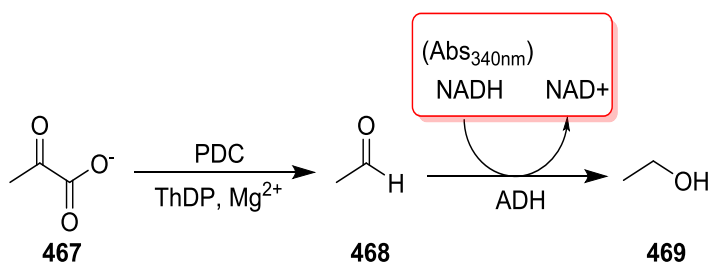
Chapter 5 – Coupled Bioassay

5.0 Biological Testing

Now the synthesis and isolation of these triazole-ThDP's was established, we required a test to assess their viability in binding to the PDC enzyme and to monitor which lengths of carbon chains could be successfully established within the active site. The NADH coupled assay for the enzymatic pathway of ThDP in *pyruvate decarboxylase* has been reported before as a tool to probe these enzymes⁽¹⁰⁵⁾.

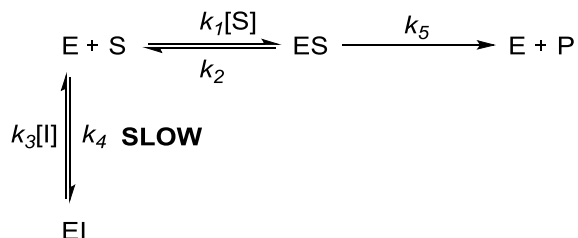
5.1 The NADH coupled Assay

Due to the precedent set by Leeper *et al.*^{(105), (6)}, a coupled assay was used to elucidate the binding of our newly formed ThDP analogues **291-294** (table **11**, page **100**). The assay catalyses the conversion of pyruvate into ethanol using NADH and ADH (scheme **134**).



Scheme 134: The NADH coupled assay of PDC

As the NADH cofactor reduces acetaldehyde, it becomes converted into NAD⁺ and results in a decreasing absorption. The introduction of an inhibitor into the assay would therefore disrupt the equilibrium between the enzyme-substrate complex [ES] and slow product formation. As more enzyme-inhibitor complex [EI] is formed, the equilibrium shifts to the L/H/S to compensate for this effect and results in reducing the rate at which the [ES] complex is formed. This results in reducing product [P] formation and slows the rate of NADH consumption, which in turn produces a measurable response on the Uv/Vis spectrum as a decreasing rate (scheme **135**). Hence, we used this assay to investigate the triazole-ThDP's **291-294** to observe the effects on enzymatic rates.



Scheme 135: Equilibrium of enzyme-substrate complex

5.2 General Introduction to Enzyme Kinetics

As most enzymes follow Michaelis-Menten kinetics, it seemed appropriate to discuss this briefly to help with interpretation of the NADH coupled assay. Kinetics of this type are normally established when the reaction is taking place with one substrate [S] in a pseudo-first order rate, whereby the steady state for the enzyme-substrate complex [E][S] is established (figure 76). Conversion of the substrate [S] into product [P] is then facilitated until all the substrate has been consumed.



Figure 76: The Michaelis-Menten equation

Under normal Michaelis-Menten conditions the substrate [S] is in equilibrium with the enzyme-substrate complex [E][S]. Therefore, any increase of substrate concentration within the reaction will convert more substrate [S] into [E][S], and the dissociation into product will increase until all the enzyme becomes fully saturated. This point is known as V_{Max} and represents the maximum rate for the reaction (figure 76). At this point V_{Max} is the conversion of substrate [S] molecules per unit time and can be denoted as the turnover number (TON). The reaction now runs unimpeded following the typical enzymatic conversion until all the substrate becomes depleted or the [E][S] complex has been shifted by the presence of an inhibitor [I].

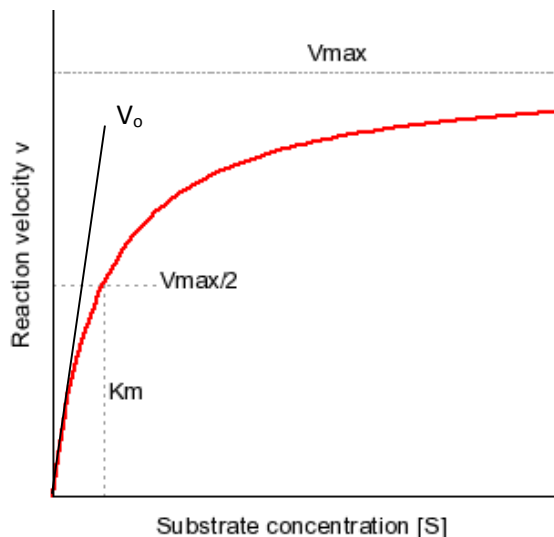


Figure 76: Enzyme catalysed pathway obeying Michaelis-Menten kinetics

From the graphical representation above it is possible to calculate the Michaelis constant (K_M) using equation 1 below. This is the concentration of substrate required to achieve half V_{Max} and is used to compare the efficacy of inhibitor/substrate for the active site (K_i). A smaller (K_M) value would indicate a stronger binding inhibitor which will attain V_{Max} quicker.

$$K_m = \frac{V_{Max}}{2}$$

Equation 1: Calculation of K_M

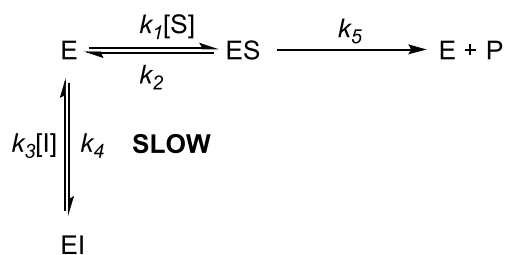
Any calculation of K_M requires a that a series of substrate [S] concentrations are assessed based on the assumption that the enzyme has established steady state kinetics and is converting substrate [S] to product [P] like that shown in figure 76 above.

5.3 Types of Inhibition

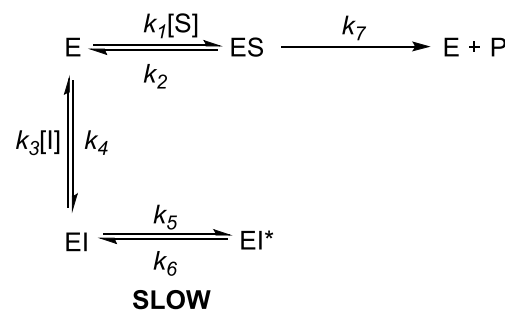
As the NADH coupled assay involves the use of inhibitors to quantify rates, it seemed appropriate to discuss different types of inhibition briefly. Enzymatic catalysis can take multiple paths in the presence of inhibitors and depict different rates bas on how they interact within the active site. Those outlined below in figure 77 show results consistent with an observed decrease in rate when compared to the unimpeded catalysis obeying Michaelis-Menten (figure 77, black line).

the enzyme-substrate complex [E] [S] as predicted by the steady state kinetics in equilibrium with the free enzyme [E]. Upon adding the tight inhibitor, a slow reversible binding takes place which causes a shift in equilibrium towards the enzyme-inhibitor complex [E] [I]. This forces the equilibrium of the [E] [S] back towards the free enzyme [E] and effectively reduces the rate. Over time this slow equilibrium causes the observed rate to decrease and prevents the enzyme from reaching V_{Max} effectively (figure 77, blue line). In **B**, the same initial equilibrium takes place but over time a slow irreversible binding takes place by covalent bond formation of inhibitor to the active site. This effectively renders the active site useless as the new enzyme-inhibitor complex [EI*] cannot undergo a reversible equilibrium with [EI]. The equilibrium then continues to form more [EI*] until the free enzyme has become fully deactivated, which results in reducing the rate and lowering k_{cat} (figure 77 blue line).

Slow binding inhibition (A)



Slow binding inhibition (B)



Scheme 138: Slow binding inhibition pathways

5.4 Assay Conditions

Before any investigation was started on the methyl-butyl model ThDPs **291-294** (page **100**), it was necessary to acquire the skills and conditions that had previously been reported.

5.5 Calculation of K_M

With the quantities of NADH, ADH and ThDP reported in previous kinetic studies we sought to calculate the K_M to gain experience, and to confirm the reported K_M value so that we could complete our own investigations. The K_M was calculated by varying the pyruvate concentrations between 0.5 – 10 mM whilst the other assay conditions were kept constant. These values were then plotted as shown below in figure **78** and the K_M was calculated by fitting the data to the Michaelis-Menton equation. This gave a substrate concentration of 2.4mM to achieve half the observed maximum rate (V_{Max}) which is consistent with the reported K_M value of 1.3mM by Boiteux ⁽¹³⁵⁾.

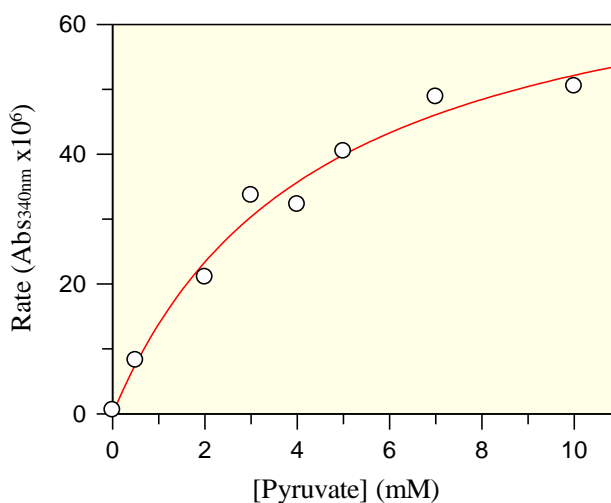
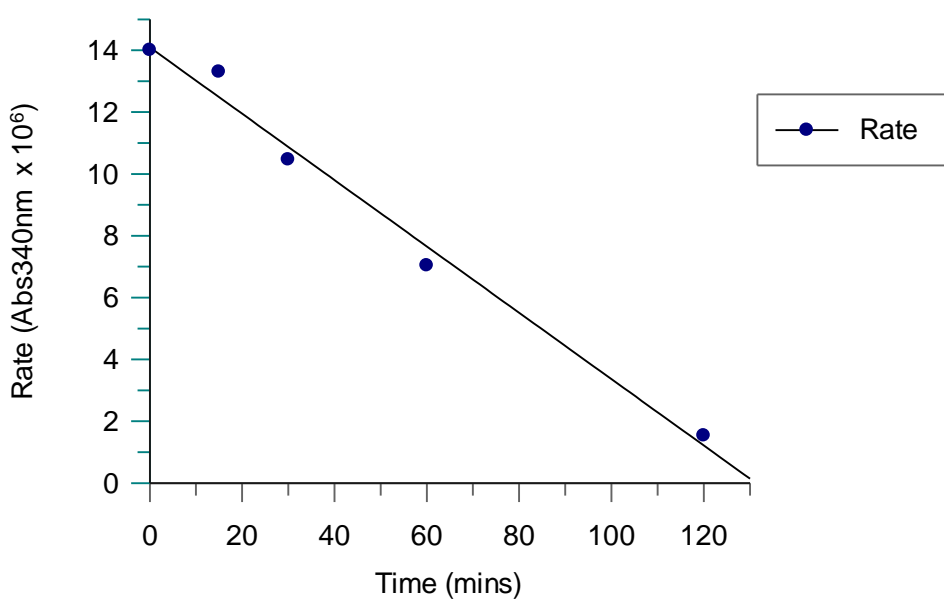


Figure 78: Calculation of K_M using various pyruvate concentrations

5.6 Time Dependent Assay - Holoenzyme

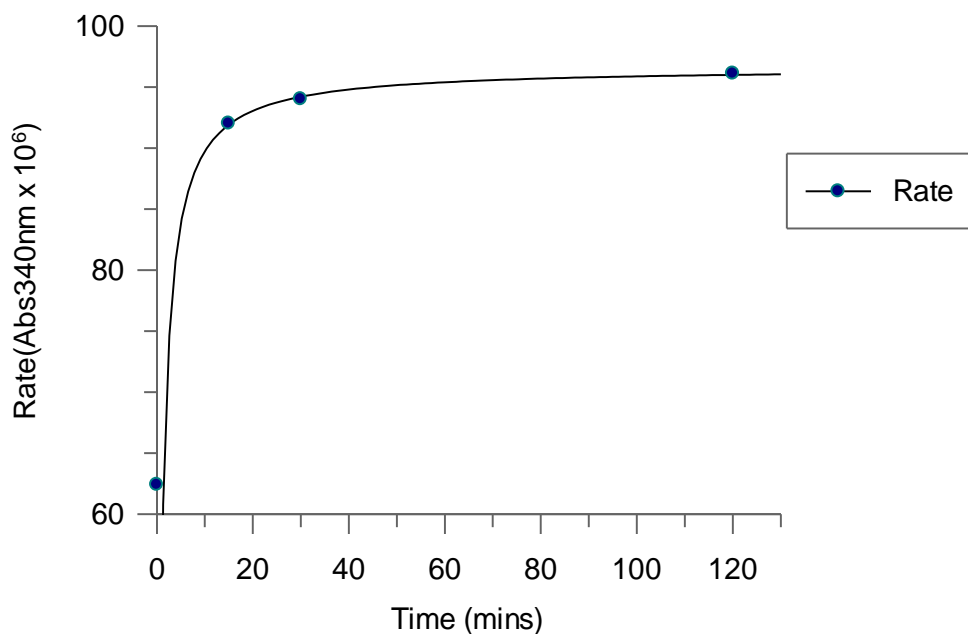
Once calculation of the K_M had been performed, *pyruvate decarboxylase* (PDC) was acquired from Sigma Aldrich, but testing revealed that it already contained some bound ThDP because an increasing rate was observed in the control reaction with only pyruvate. A few investigations were then needed to assess what time scale was required for diluting the bound cofactor from the holoenzyme. This was done by equilibrating in buffer solution and was tested in the absence of ThDP (table 16, graph 1) and in the presence of extra ThDP over a period of 120 minutes (table 17, graph 2).



Graph 1: Holoenzyme with no added ThDP

Pyruvate (mM)	Time (mins)	Results (Abs _{340nm} x 10 ⁻⁶)
2	t = 0	14
2	t = 15	13.3
2	t = 30	10.46
2	t = 60	7.03
2	t = 120	1.53

Table 16: Holoenzyme with no added ThDP



Graph 2: Holoenzyme with added ThDP

ThDP (μM)	Pyruvate (mM)	Time (mins)	Results (Abs _{340nm} x 10 ⁻⁶)
100	2	t = 0	62.4
100	2	t = 15	92.0
100	2	t = 30	94.4
100	2	t = 60	81.6
100	2	t = 120	96.1

Table 17: Holoenzyme with added ThDP

After a one hour period with no added ThDP, the bound cofactor can be reduced to half its activity and after two hours it had reached near inactivation (table 16, graph 1). Upon addition of excess ThDP the activity of the enzyme is maintained at a near constant rate after incubation for 15 minutes. A control for each assay was always undertaken to show that it was definitely undergoing dialysis and not losing activity through other means i.e (dialysis leakage). This was achieved by using a control that included excess ThDP, whilst another sample lacked ThDP. After two hours the relative rates were 95 for (+ThDP) and 4.3 for the control (-ThDP). At this point 0.1 mM of ThDP was added and the rate was monitored over a five minute period. This showed an initial increase to around 16.4 which indicated that the enzyme was not denatured or lost through dialysis leakage. The recovery to full activity was not observed because pyruvate enzymes are known to be slow in their recovery and can take up to a week.⁽¹⁰⁵⁾ This could be attributed to the denaturing or partial inactivation of the protein which requires the amino acid triad seen below in figure 79 to initiate pyruvate catalysis.

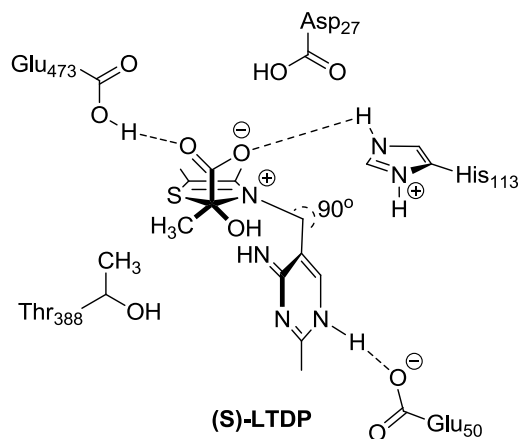


Figure 79: (S)-LTDP pre catalytic state of PDC active site

5.7 Holoenzyme - Order of Reagents

The next experiment was used to ascertain if the rate of reaction would change by alteration of the order in which each reagents is added to the assay. With longer time periods, ThDP is able to establish itself within the active site before adding the pyruvate. From the previous experiments, a pre-incubation period of 120 minutes was introduced to allow for dissociation of the bound cofactor. The native cofactor ThDP **55** was then re-introduced (table **18**) and pyruvate was added to the assay at five minute intervals until a total of 25 minutes had passed.

ThDP (μM)	Pyruvate (mM)	Time (mins)	Results ($\text{Abs}_{340\text{nm}} \times 10^{-6}$)
100	2	t = 0 (125)	27.9
100	2	t = 5 (130)	26.3
100	2	t = 15 (135)	26.3
100	2	t = 20 (140)	27.4
100	2	t = 25 (145)	26.6

Table 18: Pre-incubation for 120 minute followed by addition of pyruvate (2 mM) at set intervals

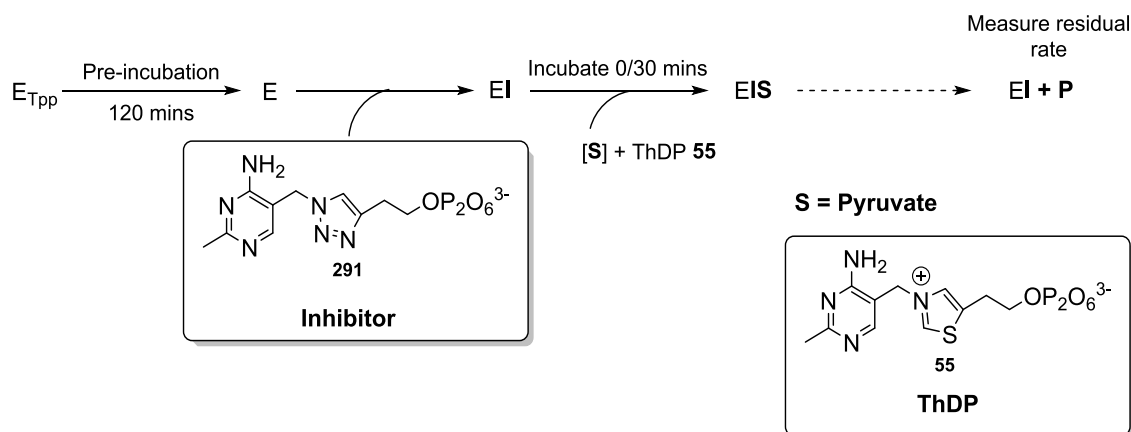
After dilution of the native cofactor **55** from the active site over 120 minutes, it is obvious that addition of the pyruvate gave no further enhancement of the rate. Some controls for this were run in parallel and can be seen below in table **19**. These indicate that at time zero, the rate doubles in the presence of ThDP (table **19**, entries **1** & **2**), but after 120 minutes addition of ThDP only causes a small increase in the rate of recovery (table **19**, entry **4**).

Entry	Preincubation time (mins)	ThDP	Pyruvate	Rate ($\text{Abs}_{340\text{nm}} \times 10^{-6}$)
1	0	-	+	12.4
2	0	+	+	23.9
3	120	-	+	3.93
4	120	+	+	4.43

Table 19: Controls for pre-incubation time in presence of ThDP

5.8 Holoenzyme - Testing with Inhibitor

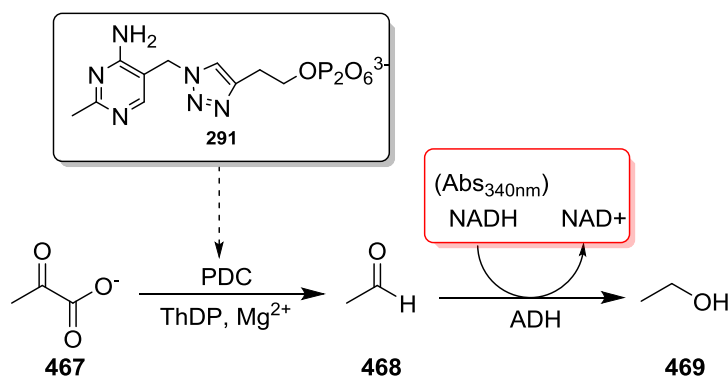
By now the conditions required to give the apoenzyme were established (e.g. dialysis in buffer for 120 minutes), (scheme 139). After 120 minutes, the inhibitor **291** was added at various concentrations of (0 μM , 1 μM and 10 μM) to the apoenzyme [**E**] and left to equilibrate for either 0 or 30 minutes to form the enzyme-inhibitor complex [**EI**] (scheme 139). After these time intervals, the pyruvate and native ThDP **55** were added into the assay solution, with any remaining free apoenzyme [**E**] able to catalyse pyruvate conversion into acetaldehyde. The residual activity of product formation can then be measured against the normal catalytic response.



Scheme 139: Holoenzyme incubation with inhibitor at various concentrations

This experiment generally gave the expected results as shown in table 20. A decreasing rate for both time points is seen when the inhibitor concentration was increased. This can be explained by scheme 139 & 140, in which a slow equilibrium between the free enzyme [**E**] and its bound enzyme-inhibitor complex [**EI**] is established upon addition of inhibitor **291**. This reduces the free apoenzyme [**E**] available to catalyse pyruvate effectively and therefore reduces the rate.

Interestingly there was not a large difference in the observed rate by increasing the amount of time that the inhibitor was allowed to bind within the active site (pre-incubation).



Scheme 140: PDC coupled assay

Entry	[I] (μM)	Time (Mins)	Result ($\text{Abs}_{340\text{nm}} \times 10^{-6}$)
1	0	0	-3.13
2	1	0	-1.57
3	10	0	-0.55
4	0	30	-2.57
5	1	30	-0.50
6	10	30	-0.86

Table 20: Holoenzyme rate after addition of inhibitor at various concentrations and with varying incubation periods

5.9 Apo Enzyme - Preparation of coupled assay

As the holoenzyme required long pre-incubation periods, it was decided to remove the native ThDP **55** totally so that further studies of the active site could be performed and reduce the experimental timeframe. This was achieved by dialysis of the holoenzyme over a two day period which contained a molecular weight cut-off of (10,000 Da). On recovering the apoenzyme it was tested to ensure no leakage of the membrane had occurred by running a control with no ThDP, and then adding the native ThDP (100 mM) back into the assay to prove re-establishment of the normal enzyme activity.

5.10 Apo Enzyme - Pre Incubation Controls

A quick experiment was then completed to monitor the change of rate in respect to both incubation time and inhibitor concentrations in the presence of ThDP at 100 μM (table 21). From interpretation of the data it is clear that a slight decrease in rate is observed for both entries 2 and 4. Interestingly even though no [I] was added, a decrease in rate was observed for entry 2, which possibly results from the dilution of bound cofactor over the two hour period. Entry 4 can be explained by the presence of inhibitor at 100 μM which effects the equilibrium between the free enzyme and substrate, and thus reduces the rate of reaction.

Entry	[I] (μM)	Time (Mins)	Result ($\text{Abs}_{340\text{nm}} \times 10^{-6}$)
1	0	0	-7.6
2	0	60	-6.77
3	100	0	-1.48
4	100	60	-1.02

Table 21: Apo enzyme at 0 μM & 100 μM concentrations for 0 and 60 minutes incubation

5.11 Inhibitor Concentration - Range Finder

Studying the methyl-butyl ThDP analogues 291-294 required an experiment to assess which inhibitor concentrations would give a decent response. These concentrations were found to be between 0-250 μM . Initiation of the reaction was by addition of pyruvate at time zero, which was then monitored over a five minute period. A decreasing reaction rate can be seen in (figure 80, green-line), as the inhibitor concentration is increased. A concentration of inhibitor at 1 μM confirmed the lower limit of range, which had nearly returned to the same activity as the uninhibited control of 4.11×10^5 (figure 80, red line). An inhibitor concentration of 250 μM appeared to give a similar rate to the assay without the ThDP in the control assay (figure 80, blue-line), and was therefore noted as the upper limit to the inhibitor concentrations.

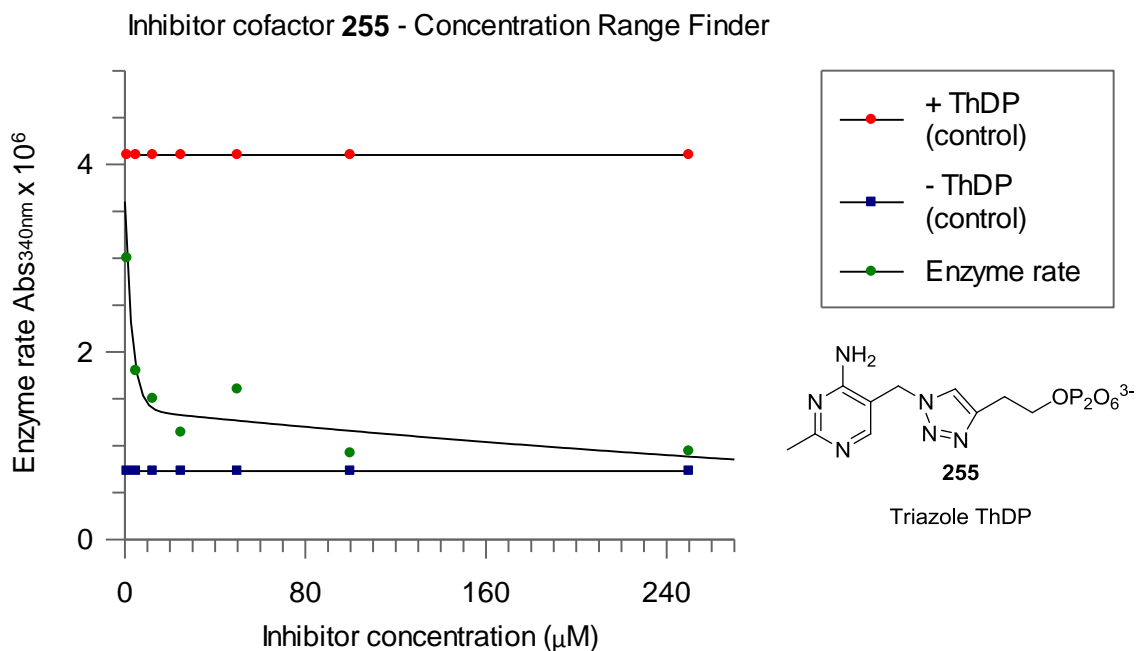
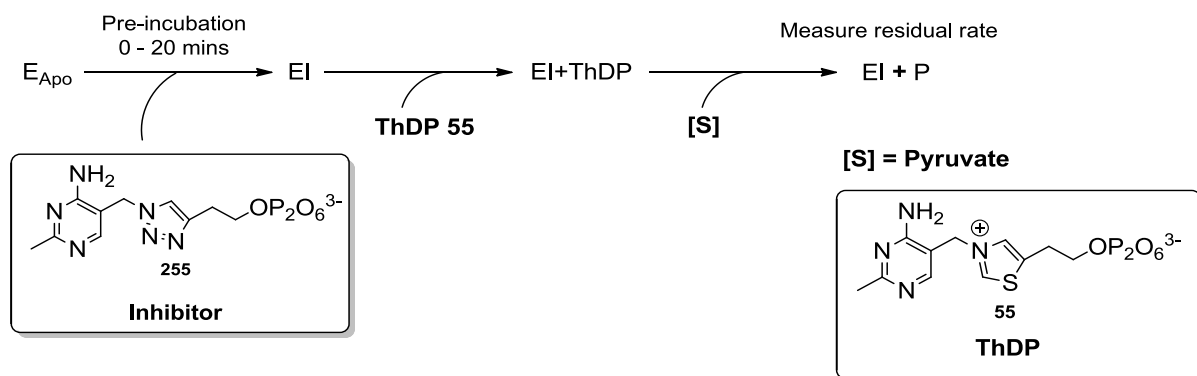


Figure 80: Inhibitor 255 concentration range finder

5.12 Testing of Methyl – Butyl ThDP analogues

This data was then applied to the subsequent pre-incubation experiments. Different concentrations of inhibitor **255** were then added to the apoenzyme [**E**] and left for set pre-incubation times (scheme **141**). To this assay solution containing the natural ThDP cofactor **55**, Mg²⁺ and buffer was then added the pre-incubation mixture of inhibitor **255** and PDC enzyme [**EI**]. This mixture was left for set time periods of (0, 30, 120, 300, 600 and 1200 seconds) and then pyruvate was added to initiate the reaction. Any free enzyme [**E**] not bound by inhibitor would then react with substrate and catalyse product formation as normal. Therefore, a longer period of pre-incubation should decrease the observed rate as additional free enzyme becomes inhibited.



Scheme 141: Pre incubation of different inhibitor concentrations (500μM) for differing periods of time (secs)

The activity of the enzyme was observed over five minutes and converted to a residual percentage activity of the uninhibited enzymatic reaction. This allowed simpler comparison between the test conditions on different days. As the coupled assay conditions were already established for the previous cofactor at 250 μM (figure 80, compound 255) we sought to test our methyl-butyl analogues 291-294 at this concentration, to observe which of the cofactors bind effectively. Testing began with the methyl ThDP analogue 291 and all others were then tested sequentially after this. Hence, any results from these experiments would allow direct comparison of Leepers cofactor 255 and the ones containing a modified methylene bridge (figure 81).

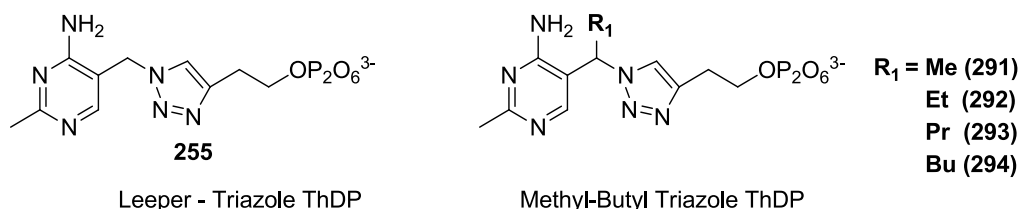


Figure 81: Structures of triazole ThDP and analogues

Initial testing of these compounds showed that addition of the inhibitor 255 (figure 82) at time zero would half the rate when compared to the un-inhibited enzyme. Time dependant assays then confirmed the loss of activity which in most cases lasted roughly 20 to 30 minutes as previously reported by Leeper *et al*⁽¹⁰⁵⁾. It was clear that the initial rate of the reaction for the methyl analogue 291 (figure 82 – green dot) is not too dissimilar to that of the un-modified cofactor 255 (figure 82 – purple dot) although the efficacy of both the methyl 291 and ethyl-ThDP 292 are not as strong.

Unfortunately, full deactivation was not achieved even after 20 minutes as described previously by Leeper *et al.* ^{(105), (6)}

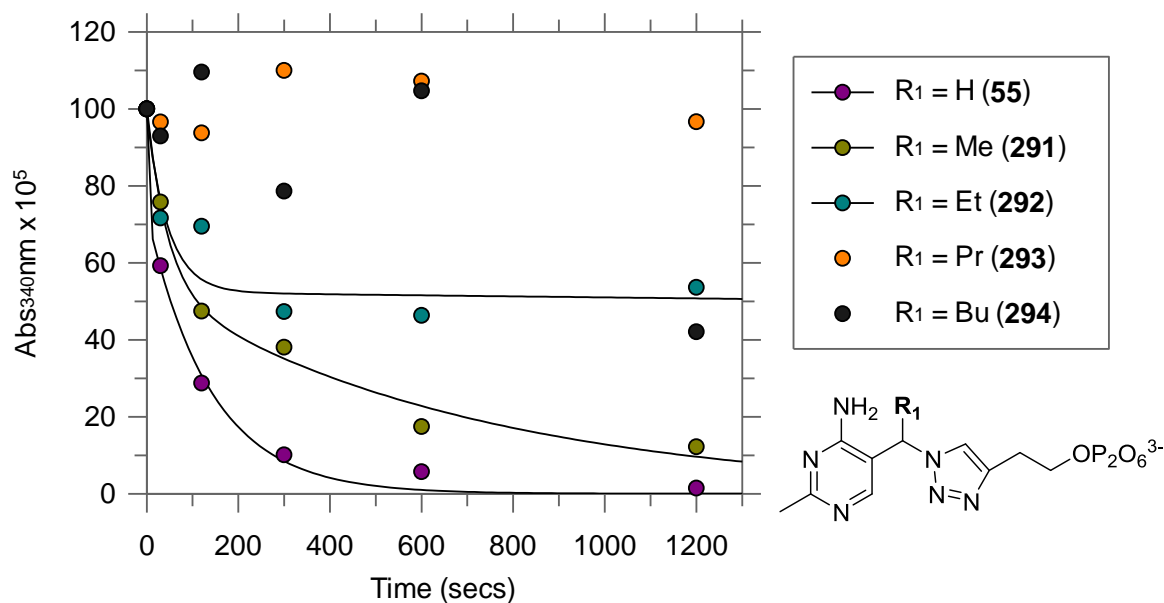


Figure 82: Comparison of % recovery for Leeper cofactor ($R_1 = H$) vs Methyl, Ethyl, Propyl, Butyl triazole ThDP at 500 μM concentrations

This pronounced change in binding efficacy is clearly a consequence of the increased steric bulk caused by lengthening of the alkyl chain into the region surrounding the active site. As such, the unnatural cofactor could assume more structural conformations that are not compatible with the three-dimensional binding regions of the active site amino acids (figure 83). As discussed within the introduction, ThDP adopts a perpendicular arrangement of its pyrimidine and thiazole rings when bound in PDC enzymes (S-LTDP, scheme 20, page 37). Henceforth extra modifications at this position may introduce changes to that binding pattern that the enzyme cannot accommodate and so prevents a suitable enzymatic fit.

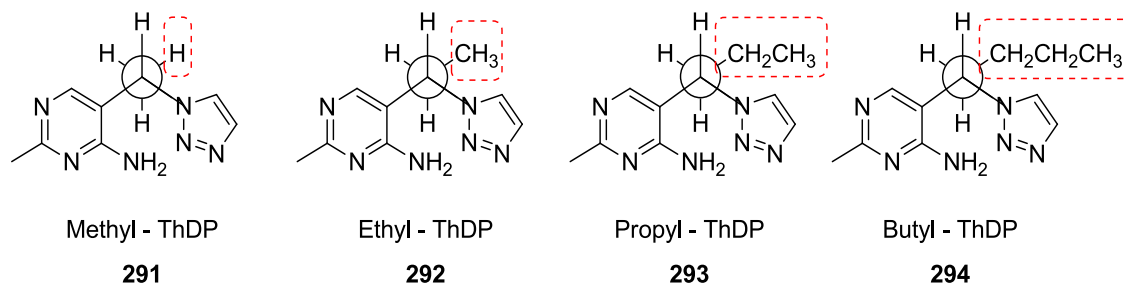
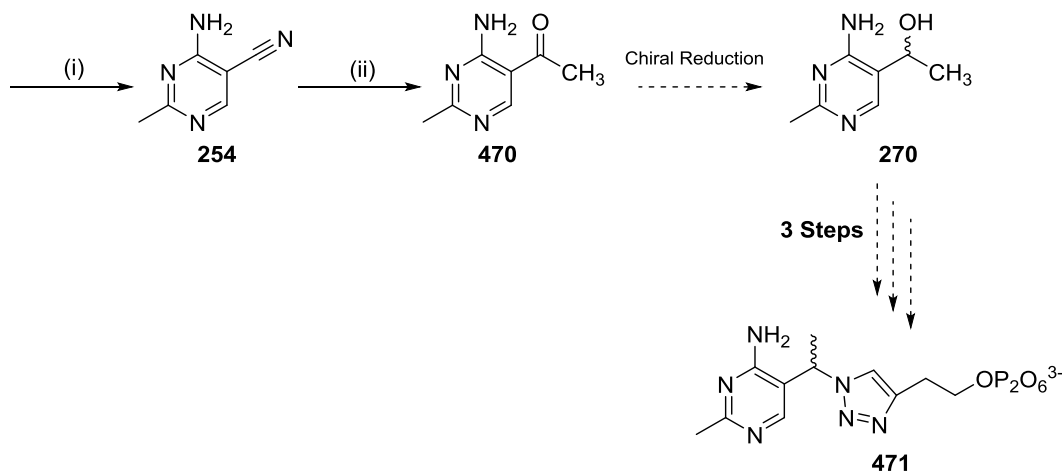


Figure 83: Anti conformation of butyl ThDP

Some of these issues were potentially highlighted upon testing of the propyl **293** and butyl **294** ThDP analogues (figure **82**, black & orange dots). Further lengthening of the alkyl chain seemed to have a detrimental effect upon the activity, whilst the smaller methyl **291** and ethyl **292** motifs were accommodated, albeit with lower efficacy. Results for the propyl **293** and butyl **294** experiments were consistent with the expected trend, with both showing little inhibition over a 10 minute period. Due to this, it was decided that a chain length of two or more carbons may not be able to locate itself sufficiently into the space found within the tight enzymatic cleft of the enzyme. These results prevented any further synthetic attempts to construct either the three or four carbon chains containing the tertiary amine motifs. Another potential problem could be the new chiral centre introduced by the alkyl chain, which decreases the efficacy when compared to the unmodified cofactor **255** (figure **81**). Due to this new chiral centre, half of the inhibitor could be resolved by the enzyme and therefore larger concentrations of inhibitor would be required to inhibit the enzyme (lower efficacy). Consequently, synthesis of an enantiopure cofactor was being undertaken to give a single enantiomer inhibitor (*R* or *S*), which could have undergone similar kinetic studies (scheme **142**). Unfortunately the synthesis of **471** is ongoing due to the limited time left during the end of this doctoral research and some issues encountered during the enantioselective synthesis of **270**.

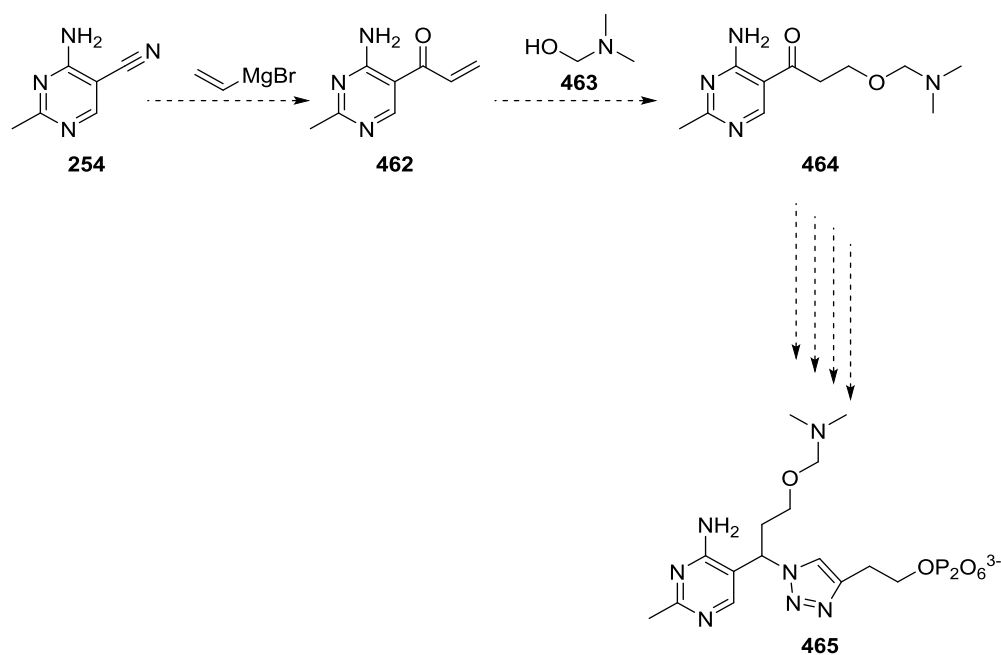


Reagents & Conditions: (i) NaOEt (2 M), EtOH, r.t, 2 hr, 78%, (ii) CH_3MgBr (3M), THF, 0°C -r.t, 50%.

Scheme 142: Synthesis of chiral ThDP

Work from this point then focused on synthesis of a cofactor which contained a heteroatom linker chain (scheme **143**). It was hoped that this linker may introduce extra flexibility within the unnatural cofactor, and remove some of the problems associated with the conformations found

when using a carbon chain. Currently the synthesis of compound has not been achieved using this proposed pathway as discussed in the previous chapter (see chapter 4).



Scheme 143: Proposed synthesis of O-linker 1,4-disubstituted [1,2,3] triazole

Further studies of the methyl **291** and ethyl **292** analogues were then tested to assess their inhibitory effects at a series of concentrations to calculate the K_i value (inhibitor constant). Calculation of K_i required that all the cofactor analogues are tested at different concentrations (figures **84**, **85** & **86**) by incubating the cofactor with the apoenzyme (6 different incubation times) to obtain their K_{obs} values (pseudo 1st order rate constant).

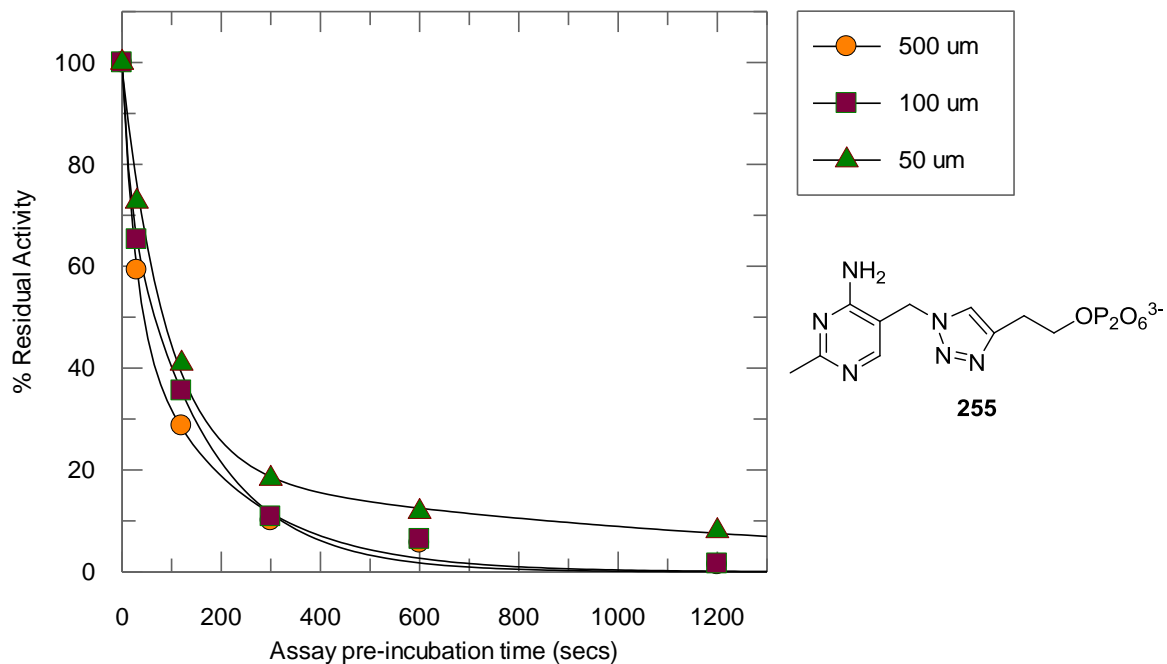


Figure 84: Varying concentrations of % recovery using the Leeper inhibitor (255) 100 μM -50 μM

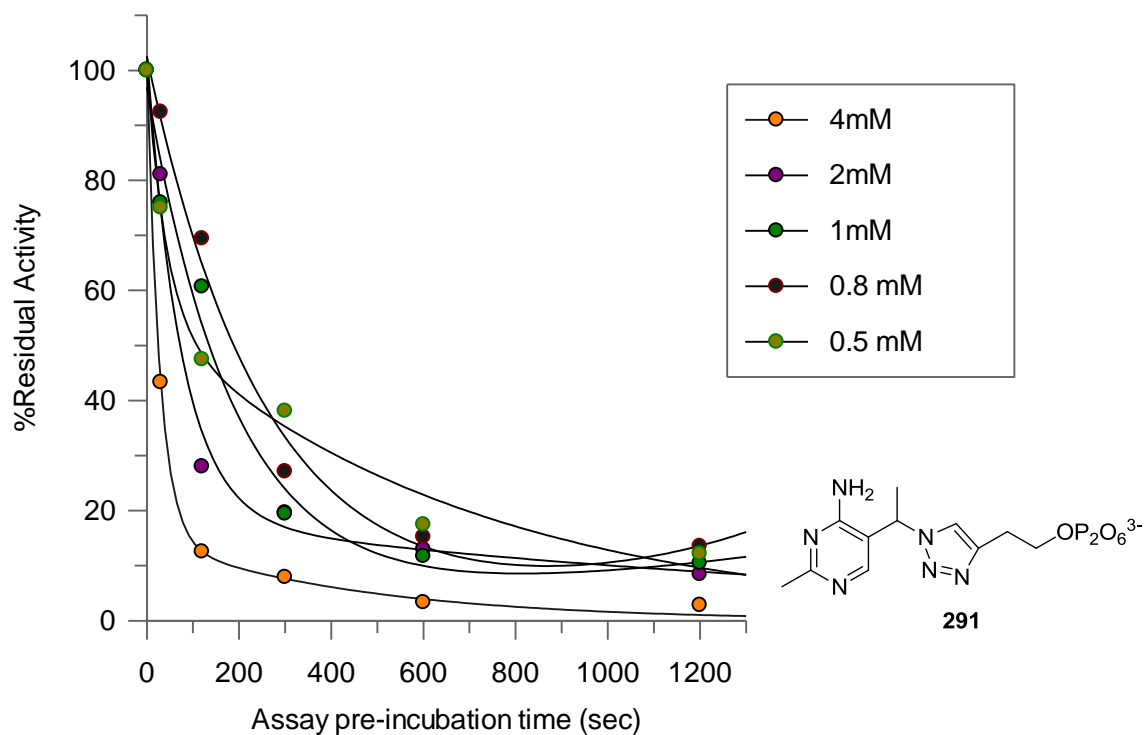


Figure 85: Varying concentrations of % recovery for Methyl ThDP triazole (291) 4.0-0.5 mM

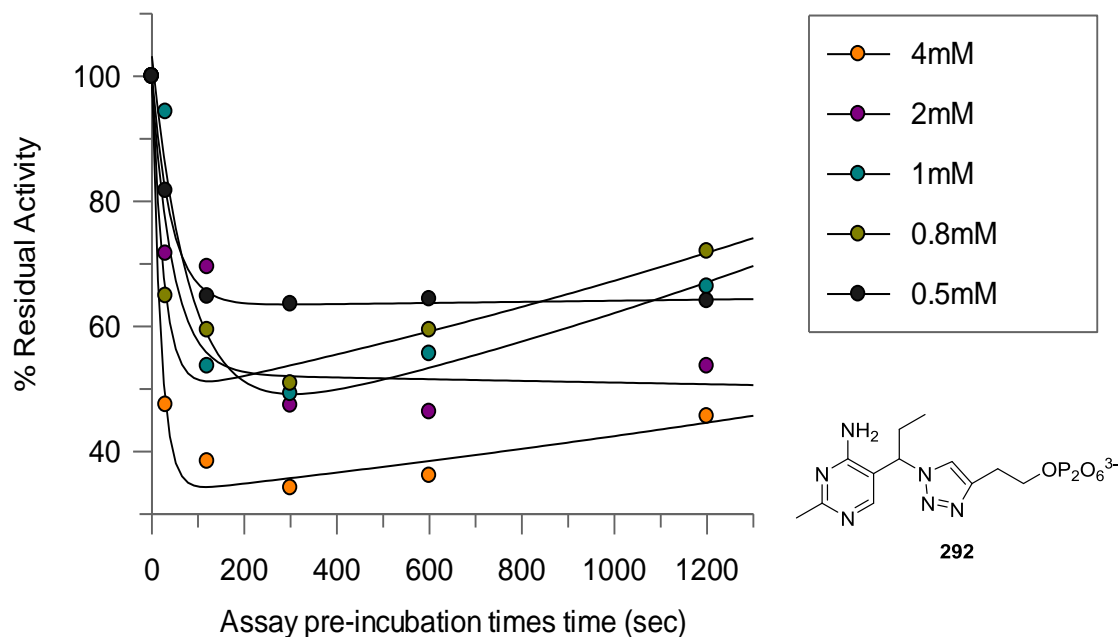


Figure 86: Varying concentrations of % recovery for ethyl ThDP triazole (292) 4.0-0.5 mM

Remarkably the trend between each cofactor was very noticeable in their ability to bind effectively. As expected, it is apparent that a fast initial rate is observed for the shorter pre-incubation times (less time for [EI] formation). The expected slower rate is observed when incubating the inhibitor for longer periods of time and follows the reported double exponential decay. This two stage binding has been identified before, and is thought to arise from either a slow conformational change of the enzyme or by communication between the active sites involving a proton wire^{(22), (14)}. Testing of the Leeper cofactor (compound **55**, figure **84**) showed the residual activity to be 2% after 20 minutes in comparison to the methyl-ThDP **291** (figure **85**) which declines to 12% and ethyl-ThDP **292** at 53% (figure **86**). This clearly indicated that the unmodified Leeper cofactor **55** (figure **84**) binds more effectively and can achieve near total inactivation after 20 minutes. In comparison, both methyl **291** and ethyl **292** analogues require elevated inhibitor concentrations, longer incubation times and cannot obtain similar responses in initial rate. Currently these preliminary results do show some interesting trends with regards to the lengthening of alkyl chains into the active site, but additional duplicate experiments are now required to ensure the reliability of these findings and to calculate their inhibitory effects. Due to time constraints/financial aspects of the PhD, repeat experiments will be needed to ensure

calculation of the K_i and K_{obs} are accurate, so these inhibitors can be compared to other PDC enzyme inhibitors.

5. 13 Conclusion to chapter

The testing of ThDP analogues bearing an alkyl substituent on the bridging carbon between the pyrimidine ring and [1,2,3] triazole has been achieved. An increasing chain length has resulted in a slower enzymatic rate and lower binding efficacy of PDC-*S. Cerevisiae* when compared to the analogue **55** (figure **84**) prepared previously by Leeper ^{(105), (6)}. This is thought to occur by increased steric interactions with the surrounding enzyme amino acids and the possibility of enzymatic resolution of one enantiomer. Further increases in chain length beyond three carbon units seems to effectively diminish any enzymatic response and so further studies and enzymatic manipulation maybe required to install the desired novel cofactor.

Chapter 6

Enantioselective Synthesis of Pyrimidine Secondary Alcohols as Chiral

Building Blocks

Chapter 6 – Enantioselective Synthesis of Secondary Alcohols

6.1 Enzyme Three Point Rule

An enantioselective synthesis of the cofactor analogues was then started to remove any possibilities of resolution by the enzyme. It was thought that a single enantiomer could improve the efficacy, and provide other structural motifs for probing the mechanistic studies of PDC enzymes. The three point attachment principle was proposed by Ogston⁽⁶⁴⁾ in 1948 and reviewed by Mesecar and Bentley in 1978^{(65), (66)} (figure 87). It designates that a chemical motif on a substrate molecule must coordinate with that of the surrounding architecture for catalysis to be successful.

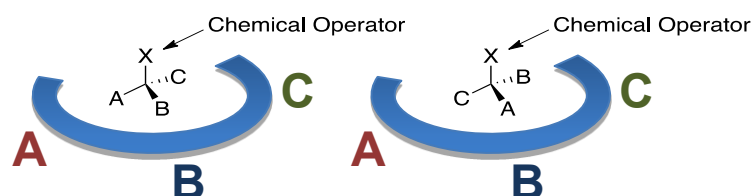


Figure 87: Ogston three point attachment rule

Synthesis of cofactors that obey these criteria can align their functional groups easier with the amino acids, and promote their chemical operators position between the dimer-dimer interfaces (figure 88). Furthermore, to our knowledge there are only a handful of chiral cofactors like that of B₁₂ which are able to catalyse isomerisation's and reductions enantioselectively⁽⁶⁷⁾. Thus, a chiral version of vitamin B₁ may provide interesting results which could add to the existing chiral pool transformations.

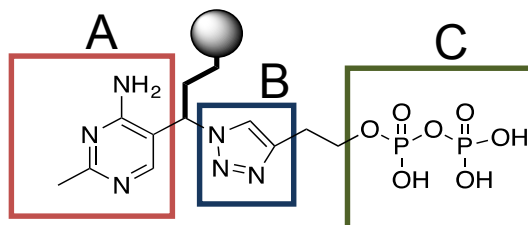


Figure 88: Three point attachment of cofactor to active site

6.2 Synthesis of Chiral Secondary Alcohols

There have been numerous approaches to the enantioselective synthesis of secondary alcohols as they are useful intermediates in drug discovery and are versatile synthons for the chiral pool. One good example is the stimulant drug ephedrine for treatment of hypertension (figure 89, compound 472).⁽⁶⁷⁾

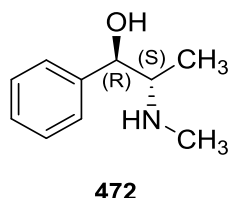
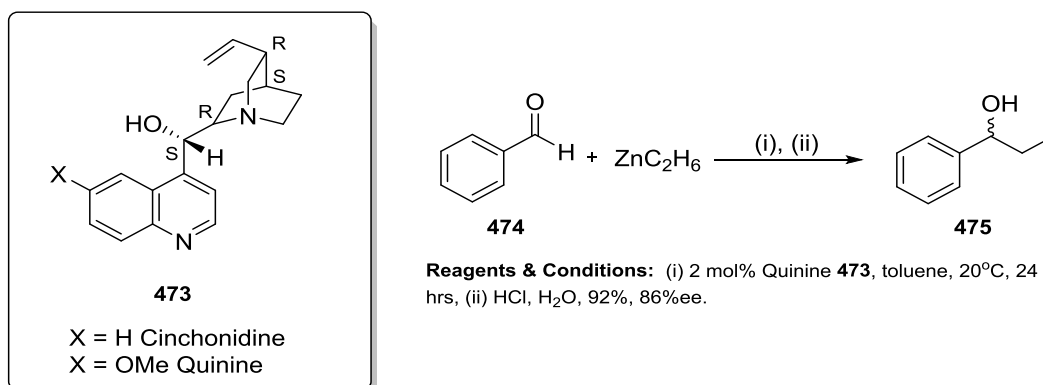


Figure 89: Ephedrine secondary alcohol as chiral auxiliary

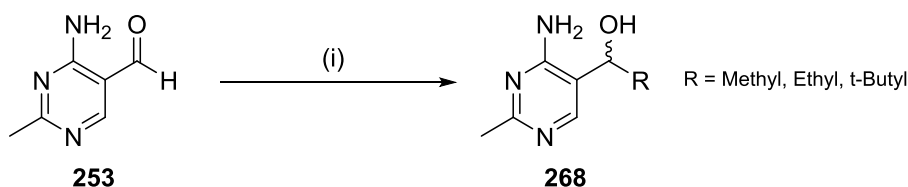
Some of these methods include dynamic kinetic resolution, asymmetric hydrogenation, and the enantioselective reduction of prochiral ketones⁽⁶⁸⁾. As the chemistry to make the racemic secondary alcohols had already been established, it seemed appropriate to utilise this chemistry first. A primary way to achieve enantioselective synthesis of secondary alcohols from prochiral aldehydes is from the addition of expensive organozinc reagents in the presence of an alkaloid chiral auxiliary (scheme 144, compound 473)^{(69), (70)}.



Scheme 144: Structures of Cinchonidine and Quinine chiral auxiliaries

6.3 Synthesis of 2-methyl-4-amino-5-ethanol pyrimidine

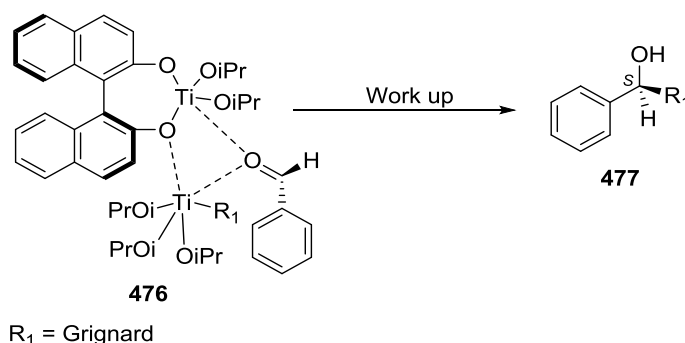
Based on this chemistry and because Grignard reagents had featured heavily throughout the synthesis, it seemed logical to search for reported procedures of asymmetric approaches. One such example used Grignard reagents in the presence of a BINOL mediated chiral auxiliary ⁽⁷⁰⁾, ⁽⁷¹⁾ (scheme 145).



Reagents & Conditions: (i) bis(dimethylaminoethyl ether), Ti(OiPr)₄, (S)-BINOL, CH₃MgBr (3.5 eq), TBME, THF, 24hr, 0°-r.t.

Scheme 145: Enantioselective addition of Grignards to aldehydes

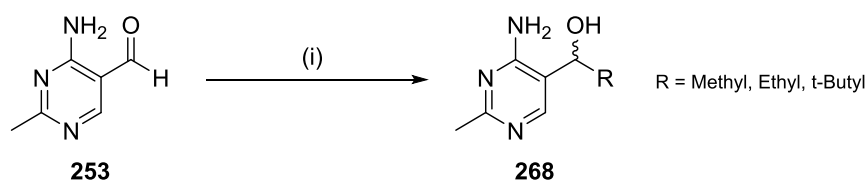
This approach required the *in situ* formation of the titanium-BINOL complex **476** (scheme 146) by treatment of *S*-BINOL with Ti(OiPr)₄ and the desired Grignard reagent. ⁽⁷⁰⁾ The Grignard reagent then favours nucleophilic attack at the least hindered *Si* face and generally results in formation of the corresponding *S*-alcohol.



Scheme 146: Intermediate *S*-BINOL-titanium chiral catalyst

Benzaldehyde was then tested with similar stoichiometric quantities to acquire the necessary skills and conditions for these transformations. Formation of the phenylethanol was observed by the characteristic splitting pattern of the methyl and C-H as the doublet (*d*) and quartet (*q*) in the crude ¹H NMR. The product however, could not be separated from the chiral catalysts even after column chromatography and required very harsh distillation conditions to isolate it. Testing of compound **253** (scheme 147) then began with the same 3.5 equivalents of Grignard reagent to ensure the standard Grignard addition took place (table 22, entry 2). This did not permit the anticipated

outcome and was believed to be due to the deactivation caused by the *bis*(dimethylaminoethyl ether) (BDMAEE). Because of this, the equivalence of Grignard reagent was gradually increased (table 22, entries 4 & 5). A control was then tried to prove/disprove if this was actually the case (table 22, entry 3) but this also gave no result. After reaching a large excess of reagent, it was decided to try one large addition but with longer reaction times. After three days the desired secondary alcohol was recovered in good yield, but with relatively low enantiomeric excess (ee%) of 31% (table 22, entry 6). Further examples (scheme 147, table 22) were then attempted to increase the ee% by lengthening the alkyl groups and/or increasing the steric bulk surrounding the carbonyl functionality. This initially included the larger ethyl group which was isolated in low yield and with no ee% (entry 7). The larger *t*-butyl analogue was then attempted, but this also gave no isolatable product and possibly confirmed that the increased bulkiness of the R group results in lower yields and no enantiomeric excess (entry 8).



Reagents & Conditions: (i) *bis*(dimethylaminoethyl ether), Ti(O*i*Pr₄), (*S*)-BINOL, CH₃MgBr (3,5 eq), TBME, THF, 24hr, 0°-r.t.

Scheme 147: Enantioselective Grignard addition

Entry	BDMAEE (Eqv)	Ti(O <i>i</i> Pr ₄) (Eqv)	(<i>S</i>)- BINOL (mol %)	Grignard (Eqv)	Time (hr)	Temp (°C)	Yield (%)	ee (%)
1*	2.5	1.15	40 mol %	2.5	24	0°C - rt	-	-
2	3.5	0.89	40 mol %	3.5	24	0°C - rt	-	-
3	-	0.89	40 mol %	3.5	24	0°C - rt	-	-
4	5	0.89	40 mol %	5	24	0°C - rt	-	-
5	10	0.89	40 mol %	10	24	0°C - rt	-	-
6	10	0.89	40 mol %	10	72	0°C - rt	78%	31%
7**	10	0.89	40 mol %	10	72	0°C - rt	23%	0%
8***	10	0.89	40 mol %	10	72	0°C - rt	-	-

*Entry with benzaldehyde as test reaction ** ethyl, ****t*-butyl

Table 22: Ti(O*i*Pr)₄-(*S*)-BINOL assisted Grignard reduction of aldehydes

These trends were not reflected in the respective literature ⁽⁷⁰⁾ as they describe that an increasing steric bulk will give appreciable increases in yields and ee%. Maybe the increasing steric bulk of the Grignard reagents and the amine functionality found within our pyrimidines resulted in a decreased reaction when attacking the prochiral aldehyde (figure **90**). Due to the large excesses of reagent, low yields and poor ee% it was decided to modify the synthetic strategy to improve upon these results.

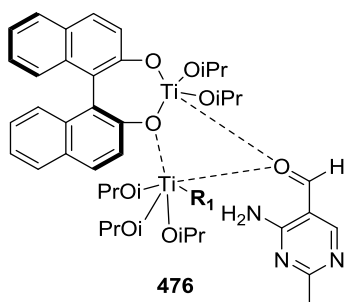
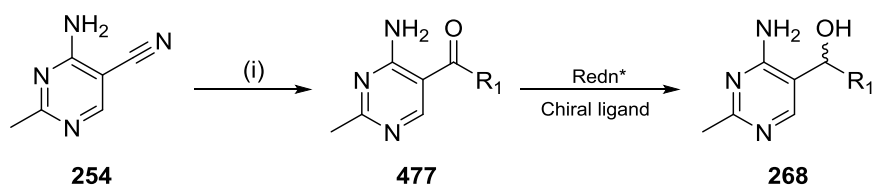


Figure 90: Proposed $\text{Ti}(i\text{OPr})_4$ -(S)-BINOL enantioselective reduction of 2-methyl-4-aminopyrimidine carbaldehyde

6.4 Synthesis of Prochiral Ketone

The Grignard additions to nitriles has always been a useful method for synthesising ketones, and in some instances can be shorter than other synthetic routes. Initially the conditions for this transformation (scheme **148**) had only been reported in a patent outlining the rudimentary conditions.



Reagents & Conditions: (i) $R_1\text{MgX}$ (3.5 eq.), THF, various temps

Scheme 148: Proposed synthetic route to 2-methyl-4-amino-ethanoate pyrimidine

Based on this information a series of reactions were undertaken at varying temperatures to find the best conditions. The Grignard reagent was then added to the nitrile **254** at increasing temperatures and then quenched the next morning with ammonium chloride. This was achieved by testing the same reaction at a range of temperatures between 60°C and -10°C, and then

calculating the ratio of integrals between the pyrimidine proton on the starting nitrile **254** and the ketone product **470**. The results show a decrease of nitrile as the temperature increases, therefore suggesting that more nitrile is converted into ketone product at the higher temperatures of 40°C and above (figure **91**).

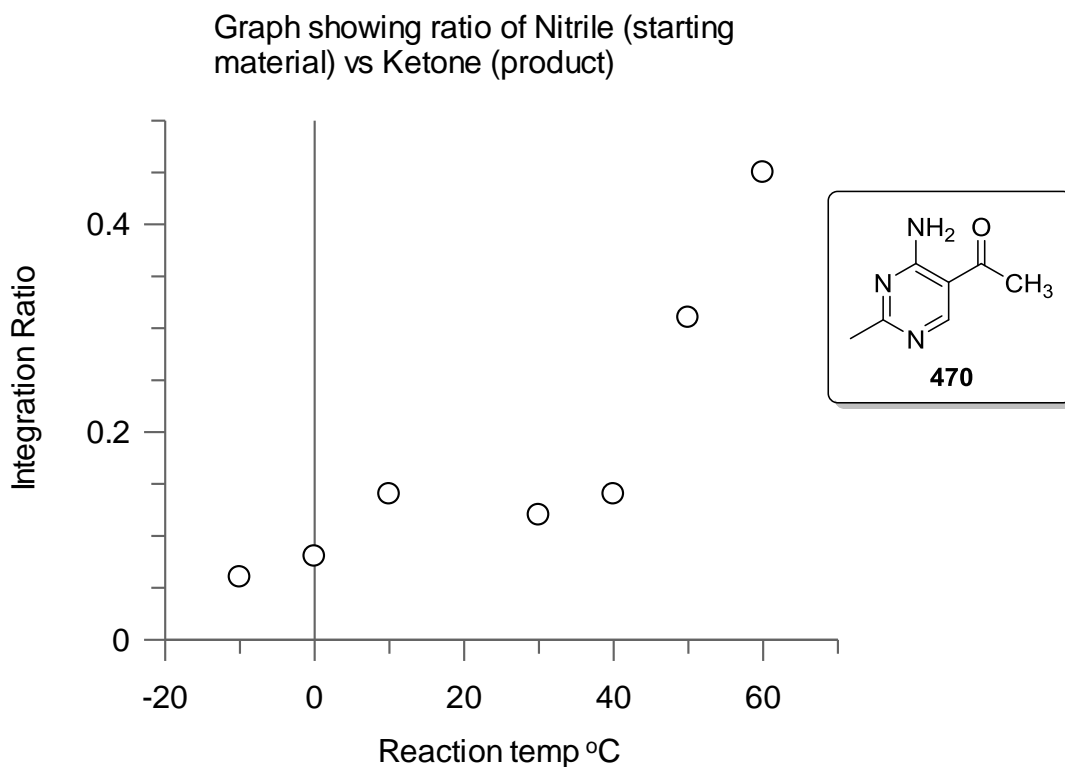


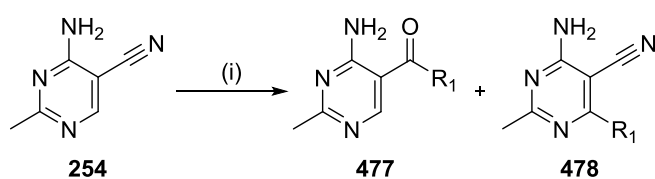
Figure 91: Graph showing ratio of nitrile (starting material) to product (ketone)

Synthesis of the ketones was relatively straightforward and gave the methyl, ethyl and propyl analogues after chromatography. On some occasions the longer alkyl chains either formed side products with total consumption of starting material or failed to work like the butyl analogue **478** (table **23**, scheme **149**).

Entry	R ₁	Grignard equivalence	Temp (°C)	Time (hr)	Yield (%)
1	Methyl	3.5	40	16	50%
2	Ethyl	3.5	40	16	68%
3	Propyl	3.5	40	16	16%
4	Butyl	3.5	40	16	-

Table 23: Conditions and yields of ketone analogues

Upon synthesising the methyl, ethyl and propyl ketones it was clear that the starting material had been completely consumed as indicated by TLC. An R_f for the ketone products was normally located around 0.3 in EtOAc: MeOH (95:5 v/v), but on some occasions a second spot was located around 0.7. After column chromatography the desired products were recovered and are depicted in scheme 149 (table 24). The methyl and ethyl derivatives have been synthesised before, but are typically formed by the classic condensation reactions of these structures ⁽⁷²⁾. Synthesis of the propyl was without difficulties, yet attempts to synthesise the butyl ketone was unsuccessful and only produced the side product.



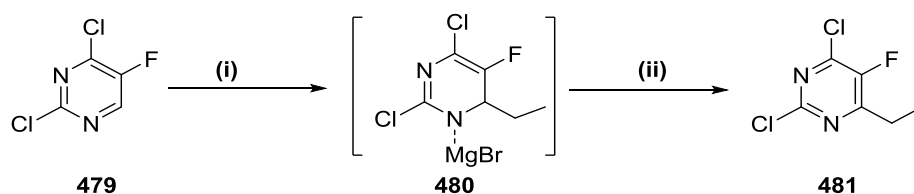
Reagents & Conditions: (i) R_1MgX (3.5 eq.), 40°C, 16 hrs

Scheme 149: Synthesis of ketone and schlenk product

R_1	Compound 477 (ketone)	Compound 478 (schlenk addition)	Ratio
	Yield	Yield	
Methyl	50%	-	-
Ethyl	68%	27%	2.5:1
Propyl	16%	20%	1:1.25
Butyl	-	18%	-

Table 24: Ratio of ketone: schlenk product formation

One possible reason for this outcome has been mentioned before by Butters *et al.* in the synthesis of Voriconazole, whereby an intermediate was formed that resembled our structure and contained a EWG in the 5-position (scheme 150) ^{(73), (74)}.



Reagents & Conditions: (i) EtMgMg, THF, 0-15°C, 1hr, (ii) Et₃N, I₂, THF, 15°C, 75%.

Scheme 150: Intermediate formed during Voriconazole synthesis

6.5 The Schlenk Equilibrium and Conjugate Addition Product

It is thought that once formed, the Grignard establishes the Schlenk equilibrium as shown in scheme 151. During this process the formation of MgX₂ can act as a Lewis acid and promote addition of a nucleophile to an otherwise unreactive position.



Scheme 151: Formation of the Schlenk Equilibrium

The MgX₂ salts described above may bind to the N'1 of the pyrimidine ring and assist in removing electron density (figure 92). One way to counteract this could be to remove the MgX₂ salts by precipitation in dioxane, and therefore lower the possibility of this effect.

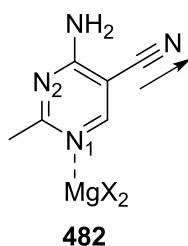


Figure 92: Potential Lewis acid and inductive effects upon pyrimidine

Another contributing factor to this problem is the electron deficient nature of the pyrimidine ring by virtue of its ring nitrogens. In this example the adjacent nitrile will be contributing to a heightened decrease in electron density from the aromatic ring ⁽²⁴⁾, thus helping to explain the possible addition by the Grignard onto the electrophilic 6' position.

6.6 Synthesis of Dihydropyrimidine

Sometimes addition of the Grignard reagent exclusively gave one spot which was not the ketone **477**, or side product **478** (scheme **149**, page **183**). This occurred more frequently than formation of the other products and gave the methyl **483** and ethyl **484** analogues in decent yields of 85% and 80% (figure **93**). Both analogues **483** and **484** were easily recovered by recrystallisation in DCM: pet ether as sharp crystals. Analysis of the ^1H NMR for these compounds was at deceiving, because the product looked like the chiral secondary alcohol **268** (figure **93**). However, the infra-red spectrum showed the sharp and distinctive nitrile stretch at 2152cm^{-1} and lacked a broad OH stretch. Furthermore, the ^1H NMR did not show the pyrimidine proton as a singlet at $\sim 8.00\text{ppm}$ and therefore suggested that the Grignard addition had took place at this position.

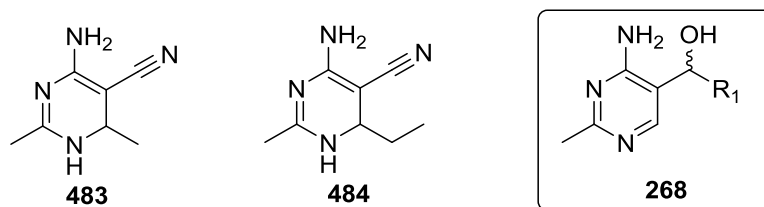


Figure 93: Dihydropyrimidine products

6.7 XRD structure and Analysis

The XRD data then confirmed the actual structure as shown in figure **94**. This strongly resembles the motif described during the Voriconazole synthesis and suggests that the pyrimidine ring is essentially planar, except for the loss of aromaticity around the C_6 position. This atom adopts the classic tetrahedral geometry with a bond angle for the atom group $\text{N}_5\text{-C}_6\text{-H}_6$ at 109° and the bond length for $\text{C}_1\text{-C}_6$ at 1.51 \AA , whereas and the shorter sp^2 bonds of $\text{C}_1\text{-C}_2$ and $\text{C}_4\text{-N}_3$ are found at 1.38 \AA and 1.32 \AA respectively. Once again the hydrogen bonded dimer pair exists around a C_2 symmetry axis, but the aromatic rings are no longer stacked in parallel sheets, presumably because of the disturbances to the planar ring arrangements discussed earlier.

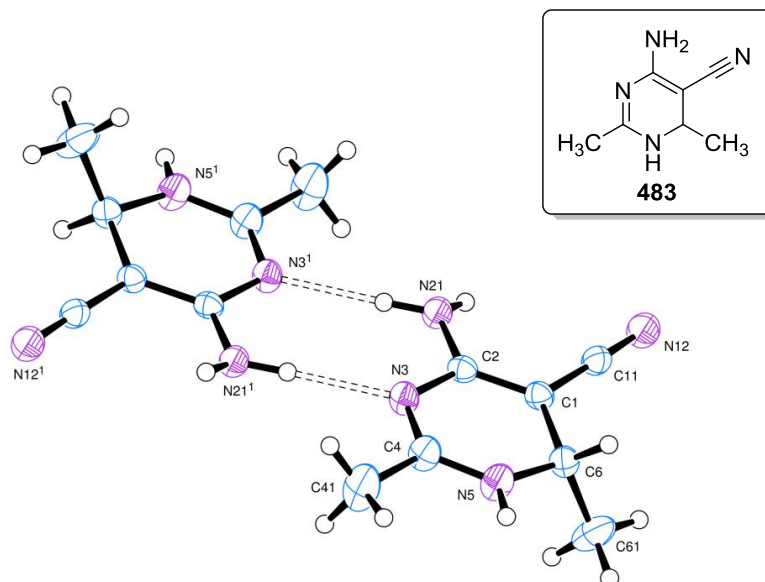


Figure 94: Crystal structure of compound 483

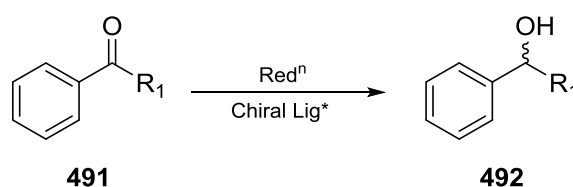
The stability of these structures was rather surprising, as they could be kept over a period of months at room temperature. The synthesis of these novel compounds was then continued for three reasons: 1.) to prepare the desired prochiral ketones for the enantioselective reductions, 2.) to observe if a general pattern emerged by introducing new R groups and, 3.) because these motifs may have potential pharmacological properties or synthetic value. From table **25** it is apparent that similar reaction conditions produced a variety of products which will require further tests to assess which conditions favour formation of each product. This will be explored further in later synthetic studies, and attempts to synthesise the ketone will require a different synthetic route.

Entry	Structure	Compound	Time (hrs)	Yield %	
1		485	40	72	68%
2		486	40	72	16%
3		487	40	72	27%
4		488	40	72	20%
5		489	40	72	18%
6		490	40	72	76%

Table 25: Structures synthesised by addition of Grignard reagents to nitrile 254

6.8 Asymmetric Reactions

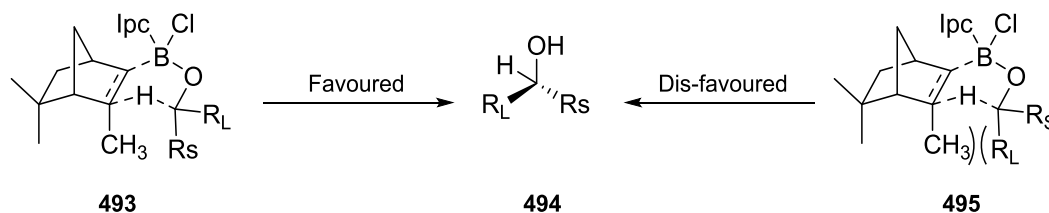
In light of the low enantioselective excess (ee%) observed with the chiral Grignard approach, and with reproducibility being a tricky point, it was time to investigate other enantioselective reagents that could react with our ketones. Testing began on the methyl and ethyl ketones as these were the only ones in large enough quantities. There are quite a few methods throughout the literature to effect this transformation including the Noyori BINAL-H reagent⁽⁶⁸⁾, and the boron-camphenyl derived reagents which have seen wide spread application as reported by Midland.⁽⁷⁵⁾



Scheme 152: Asymmetric reduction of a prochiral ketone

Other group members had previously attempted the *in situ* formation of Noyori's asymmetric BINAL-H reducing agent due to its low cost and availability, but problems associated with

precipitation meant that this method was discarded. Attention then turned toward the use of the boron-camphenyl reagents such as Alpine borane and DIP-Cl which have been used on acetophenone analogues before. Alpine borane is reported to react slowly with acetophenone and can take up to one week^{(68), (76), (75)}. Consequently, DIP-Cl was used because of its much higher affinity for the carbonyl oxygen, which is caused by boron's bonding to the electronegative chlorine atom⁽⁷⁶⁾ (scheme 153).



Scheme 153: Enantiofacial control with (+) DIP-Cl

The largest group on the incoming electrophile is usually directed away from the methyl on (+)-**493** to minimise any 1,3-diaxial strain. This allows the β -proton to accomplish the reduction step in a stable 6-membered transition state which results in *syn* elimination of the product. Another factor which may promote this process on our analogues is shown by compound **470** in figure **95**. Interpretation of the ^1H NMR shows splitting of the NH_2 protons and is thought to occur through H-bonding which gives Lewis acid assistance to the carbonyl oxygen. This effect could explain why the amine protons are observed at slightly different chemical shifts and explain the lack of a strong $\text{C}=\text{O}$ sp^2 stretch in the infra-red spectrum at 1700 cm^{-1} . This H-bonding could thus increase the electrophilicity of the carbonyl bond and promote reaction rates.

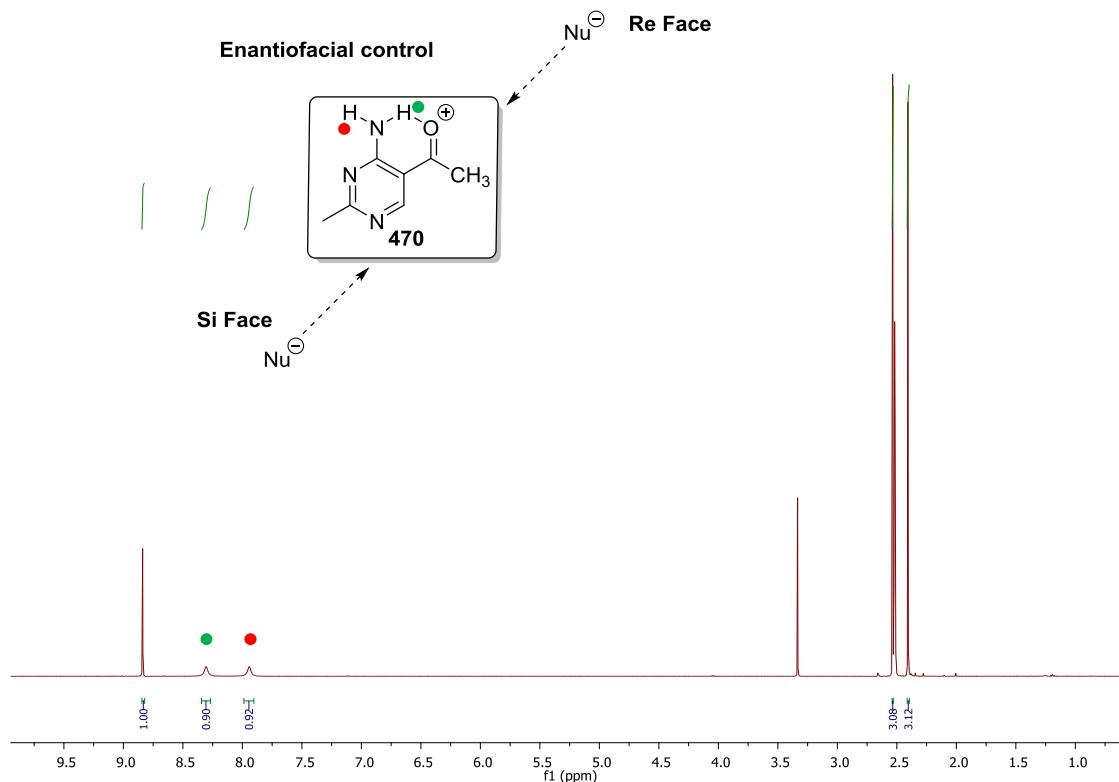


Figure 95: Possible H-bonding to keto compound

After 48 hours at -25°C the desired methyl alcohol product **270** (figure **96**) was observed at an R_f of 0.7 in a mobile phase of EtOAc: MeOH (95:5 v/v). A chiral cellulose lux HPLC column and a mobile phase of IPA: Hex (50:50 v/v) gave an enantiomeric excess of 97% of the *S*-enantiomer based upon the predicted reduction mechanism of DIP-Cl (table **26**, entry **1**), which was compared to the racemic HPLC trace as a control.

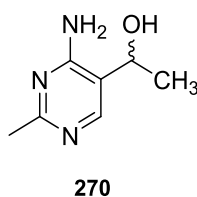


Figure 96: Secondary alcohol structure

To assess reproducibility of this step, a repeat reaction was performed but on the second and third attempts no reaction could be achieved. Addition of (+) DIP-Cl to the ethyl ketone was also tried but gave no results.

Entry	R ₁	[α] ²² _D	Yield%	%ee
1	Methyl	-84°	29.7	94%
2	Ethyl	-	-	-

Table 26: Results for enantioselective reduction of prochiral ketone with (+) DIP- Cl

6.9 Conclusion to chapter

The novel conditions to achieve enantioselective reduction of these prochiral 2-methyl-4-aminopyrimidines ketones using (+)-DIP-Cl have worked briefly but will now require further optimization of conditions to repeat the desired transformation effectively. The future potential for chiral variants for this motif are extremely advantageous to permit additional studies relating to that of thiamine dependant enzymes, and the mechanisms of other biological studies that include the pyrimidine ring ⁽⁷⁷⁾. This could include the enantioselective synthesis of analogues resembling the antibiotics bacimethrin **56** ⁽⁷⁸⁾ and/or GSK's bacteriostatic trimethoprim ⁽⁷⁹⁾ **496** (figure **97**). Any further enhancement of these structures may lead to novel sets of antibiotics which are of current global interest.

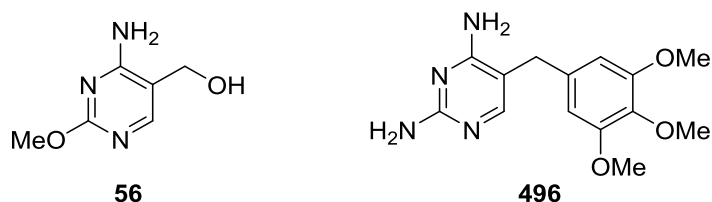


Figure 97: Structures of Bacimethrin and Trimethoprim

Chapter 7

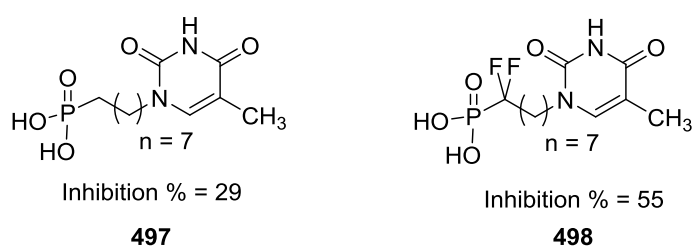
Synthesis of Difluorinated Monophosphates for Probing Thiamine

Dependant Enzymes

Chapter 7-Synthesis of Diisopropyldifluoromonophosphate alkyne's

7.0 Aim & Previous Difluoromonophosphates

In collaboration with LCMT Caen, a project involving the synthesis of diisopropyldifluoromonophosphates was envisaged that could potentially provide interesting studies towards the enzymatic pathways of thiamine dependant enzymes. Isosteres and bioisosteres are interesting ways to mimic the standard chemical group, by introducing new atoms such as fluorine into the structure to improve efficacy as depicted by the thymidine phosphorylase inhibitors (figure 98, compounds 497 & 498).

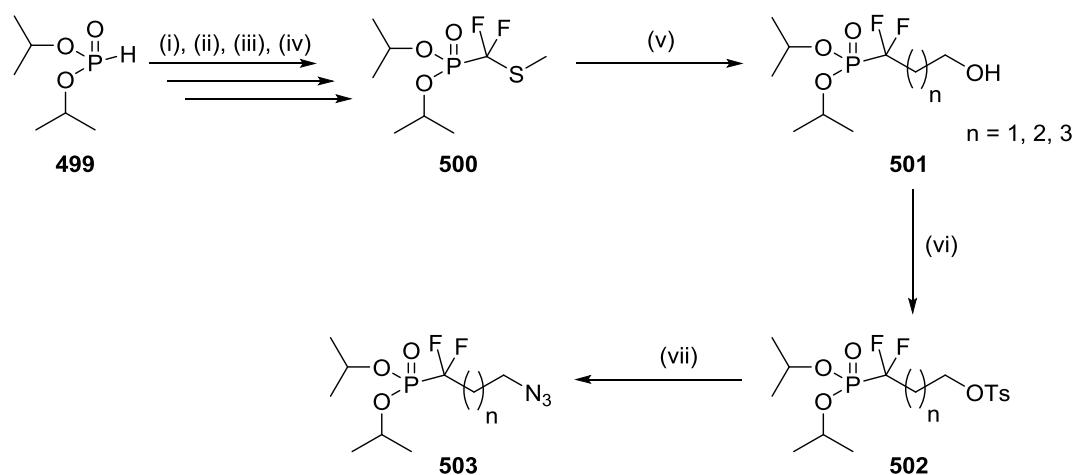


Figures 98: Thymidine phosphorylase inhibitors with/without fluorine and depicting increased % inhibition

Although Leeper published ⁽¹⁰⁵⁾ a study on phosphate isosteres, investigations towards fluorinated phosphates structures were few and focused only on alternative structural scaffolds. As difluoromethylphosphonates are reported ⁽⁸⁰⁾ to be one of the best motifs for mimicking such features, our group sought to incorporate the difluorophosphate to confer metabolic stability, increased receptor affinity and hydrogen bonding. In addition to this, the diphosphate group is a poor candidate for drug development due to its low bioavailability and cellular uptake ⁽¹⁰⁵⁾, therefore suggesting that our novel difluoro-triazole ThDP could be a more suitable ligand for inhibiting standard ThDP biological pathways. It may also provide some monophosphate structures that are easier to assemble and click, instead of the usual tosylate formation, S_N2 displacement, and tedious purification methods that follow. ⁽¹⁰⁵⁾.

7.1 Previous Synthesis of Difluorophosphonylated chains

Previous synthetic routes of these compounds follows that depicted in scheme 154, where diisopropylphosphite **499** is converted in four steps to the difluoro intermediate **500** as reported by Lequeux *et al.* ^{(80), (81)}. Treatment with *t*-BuLi, BF₃.OEt₂ and the desired oxirane then gives the specific chain length and hydroxyl functionality **501**, which is available to be converted into a good leaving group **502**. This procedure can then permit displacement by a host of nucleophiles such as sodium azide to give compound **503**.

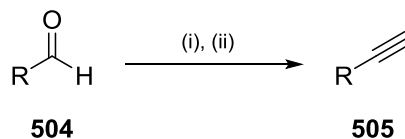


Reagents & conditions: (i) NaH, CS₂, MeI, 75% (ii) NaBH₄, MeOH, MeI, 71% (iii) SO₂Cl₂, (iv) HF₃.EtN₃, 62% (v) *t*-BuLi, BF₃.OEt₂, ethylene glycol, trimethylene oxide, THF, n = 2 (22%), n = 3 (63%), n = 4 (60%). (vi) TsCl, Et₃N, CH₂Cl₂ rt, n = 2 (83%), n = 3 (78%), n = 4 (85%). (vii) NaN₃, r.t., 16hr, n = 2 (80%), n = 3 (83%), n = 4 (90%).

Scheme 154: Previous synthetic strategy by Lequeux *et al*

7.2 Synthesis of Alkyne Synthon

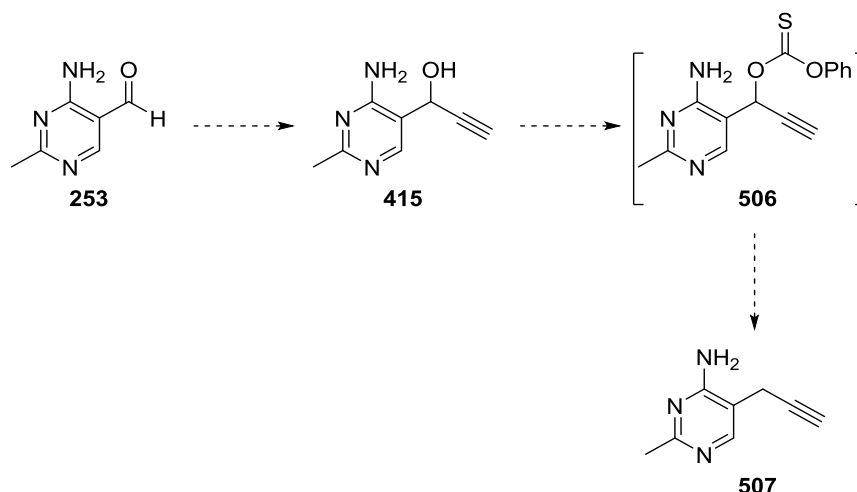
One difficulty surrounding the synthesis of any analogue using click chemistries is the respective synthons of the starting materials. It is common for many research groups to construct the azide group by a simple S_N2 displacement of a satisfactory leaving group, whereas synthesis of any alkyne tether normally requires multiple synthetic steps. These can include some protection/deprotection steps of the acidic alkyne proton, and in some cases the pre installation of an aldehyde functionality for the Corey-Fuchs ⁽⁸²⁾ (scheme 155) and Seyferth-Gilbert homologations ^{(83) (96)}.



Reagents & Conditions: (i) PPh_3 , CBr_4 , (ii) $n\text{-BuLi}$, H_3O^+

Scheme 155: The Corey-Fuchs reaction

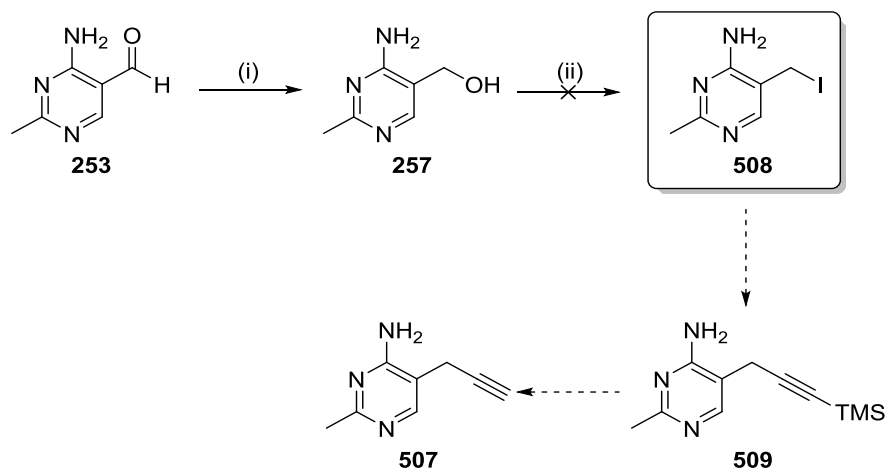
The reported procedure for the diisopropyldifluoromonophosphates azide tethers had already been established⁽⁸¹⁾ as seen above (scheme 155, compound 505), so it seemed sensible to try to reverse the synthons for our compound to assess if the click reaction of these two compounds was feasible (scheme 156, compound 507). As there was no precedent for this synthon, it was presumed that a Barton-McCombie deoxygenation⁽⁹⁷⁾ of 415 may reveal the required alkyne motif 507, but unfortunately formation of the *o*-thiocarbamate 506 was not achieved.



Scheme 156: Synthesis of alkyne via Barton-McCombie deoxygenation

7.3 Synthesis of 2-methyl-4-amino-5-methyl iodide pyrimidine

Attention was now placed on synthesising a compound that consisted of the typical 2-methyl-4-amino pyrimidine ring, but with a methanol handle that could be converted into a good leaving group, and be subsequently displaced by an $\text{S}_{\text{N}}2$ pathway (scheme 157). TMS-acetylene with a strong base could then generate the free anion of the alkyne which could undergo $\text{S}_{\text{N}}2$ displacement of the iodide leaving group to give 509. A TBAF deprotection of the alkyne would then remove the TMS group and reveal the free alkyne 507 to facilitate the 1,4-CuAAC reactions.



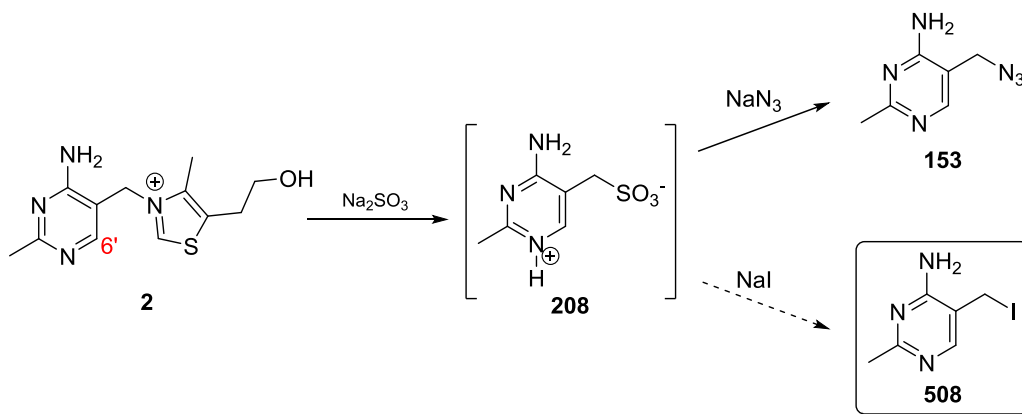
Reagents & Conditions: (i) NaBH_4 , MeOH, rt, 56%, (ii) I_2 , PPh_3 , Imidazole

Scheme 157: Proposed synthesis of alkyne synthon via iodide intermediate

Following a reported procedure by Baxter *et al.* ⁽²⁶⁾ compound **253** was easily reduced by NaBH_4 . Conversion to the iodo-derivative then took place via treatment of the **257** with imidazole, triphenylphosphine and iodine to give a crude mixture that was difficult to purify. After column chromatography all spots were recovered, but the ^1H NMR was extremely messy for all fractions and did not resemble either starting material or side products.

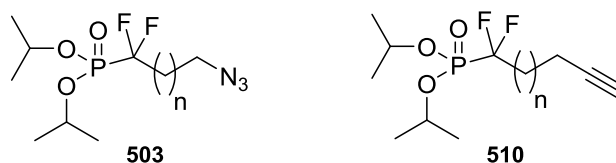
7.4 Synthesis of 2-methyl-4-amino-5-methyl iodide pyrimidine via $\text{S}_{\text{N}}\text{Ar}$ with NaI

One last attempt to introduce the iodine onto the structure was using the $\text{S}_{\text{N}}\text{Ar}$ mechanism that was described at the beginning of the R & D section (scheme **45**, page **68**). Sodium azide was now replaced by sodium iodide in hope that the iodine may insert itself into the required position for nucleophilic displacement (scheme **158**).



Scheme 158: $\text{S}_{\text{N}}\text{Ar}$ sodium iodide displacement

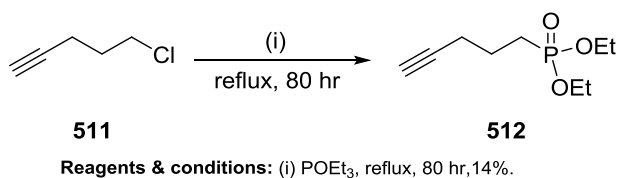
Even though the reaction conditions were the exact same as those used for the previous synthesis, no desired product was formed and only starting material was recovered in near quantitative yield. As difficulties had arisen in attempting these routes it was decided to revert back to making the original azide compound **503** (scheme **159**), but with the alkyne synthon instead so that the 1,4-CuAAC could take place with the correct regiochemistry.



Scheme 159: Changing of synthetic synthons for ThDP synthesis

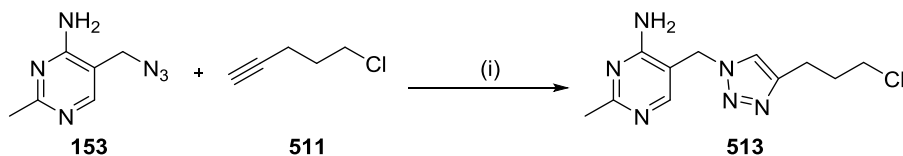
7.5 Synthesis of Alkyne Diisopropyldifluoromonophosphate

As the synthesis of compound **510** would be a lengthy synthetic route, it was decided that a smaller test reaction could be carried out, so that conditions for the click product could be established without using up valuable starting material. After a quick search through the literature it was found that cheap triethylphosphite and 5-chloropentyne **511** were readily accessible from commercial sources. Arbuzov reaction of **511** would then result in the release of chloroethane which has a boiling point of 12°C and so is easily removed *in vacuo* (scheme **160**).



Scheme 160: Arbuzov reaction for test monophosphate

Although synthesis of compound **512** was successful, its purification was very difficult and always contained a small 10% impurity after several attempts of Kügerohr distillation. The click reaction was then attempted to see if the reaction would work with the impurity present, but after several attempts the 1,4-CuAAC was not successful and so the synthetic route was adjusted slightly. This new path involved first clicking the azide compound **153** with **511** (scheme **161**), and then conducting the same Arbuzov reaction as depicted earlier in scheme **160**. The 1,4-CuAAC successfully gave the triazole **513** in a good yield of 77%, but the subsequent Arbuzov reaction did not proceed and so synthesis began on the normal difluorophosphonylated chains.

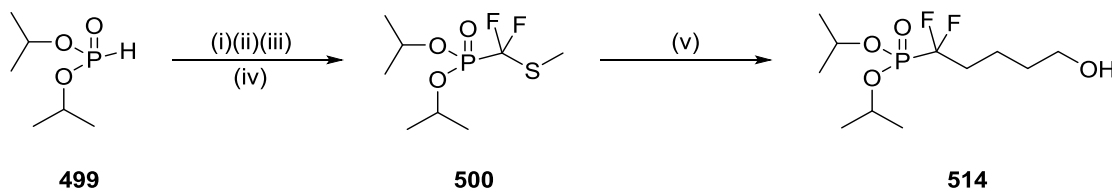


Reagents & Conditions: (i) 5-chloropentyne, *t*-BuOH/H₂O (2:1 v/v), sodium ascorbate (0.1 eq.), CuSO₄·5H₂O (0.01 eq.), r.t., 77%.

Scheme 161: Test CuAAC reaction

7.6 Synthesis of Diisopropyldifluoro derivatives

Due to our collaboration and to save some time, compound **500** (scheme **162**) was pre-supplied by the collaborating group in Caen to test the sequential steps whilst work began on the synthesis in parallel from the start (scheme **162**)^{(80), (84), (85)}. Compound **500** can be synthesised in four steps from the commercially available diisopropyl phosphate **499** using the literature procedures of Grisley⁽⁸⁴⁾ and Lequeux *et al.*^{(85), (80)}. Deprotonation with NaH and quenching with carbon disulfide generates the thiolate anion which can be trapped by methyl iodide. Reduction with NaBH₄ in MeOH then gives the thiol which again requires methylation by MeI. Chlorination using sulfuryl chloride and fluoride displacement with HF₃·Et₃N then exchanges the two heteroatoms to give compound **514**.

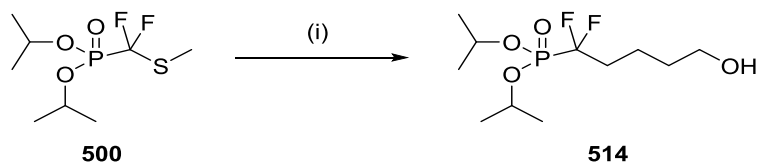


Reagents & conditions: (i) NaH, CS₂, MeI, 75% (ii) NaBH₄, MeOH, MeI, 71% (iii) SO₂Cl₂, (iv) HF₃·Et₃N, 62% (v) *t*-BuLi, BF₃·OEt₂, THF, 60%.

Scheme 162 Synthetic overview of diisopropyldifluorobutanol synthesis

7.7 Synthesis of diisopropyldifluorobutanol phosphate

Synthesis of compound **514** (scheme **163**) is by the literature procedure of Catel *et al.*^{(85), (81)} and involves a radical *t*-BuLi reaction upon the β-carbon-sulfur bond which are reported to undergo rapid scission^{(86), (87)}. A Lewis acid mediated ring opening of THF is then accomplished by BF₃·OEt₂ to produce the four carbon chain compound **514**. Alternative chain lengths of 2, 3 and 4 carbons can then be synthesised by changing the electrophilic species from oxirane to trimethylene oxide or THF respectively. On this occasion, the four carbon chain was formed in good yield and with no extra purification needed.



Reagents & Conditions: (i) *t*-BuLi, BF₃·OEt₂, -78°C, THF, 60%.

Scheme 163: Synthesis of Diisopropyldifluorobutanol phosphate

The reason for selecting the four carbon chain was because any future oxidation step and subsequent alkyne insertion would still produce the chain **516** (figure **99**), which is of similar length to the native ThDP structure **515**. Thereby allowing the chain to accommodate itself more easily in the tight hydrophobic tunnel of the gamma domain.⁽⁸⁸⁾

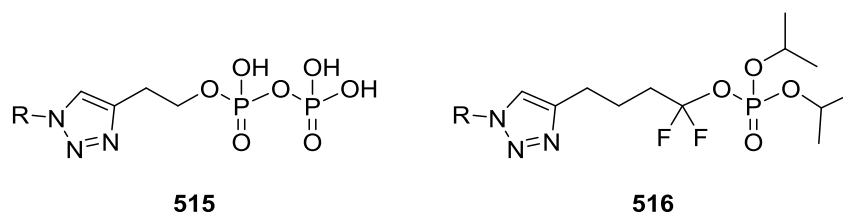
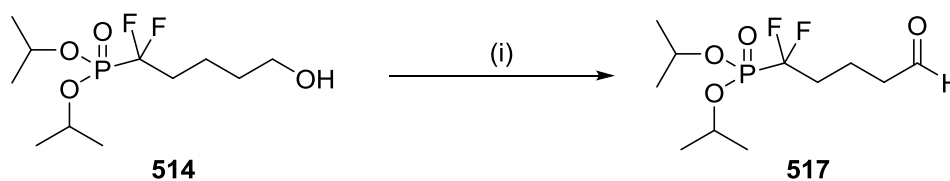


Figure 99: Standard ThDP diphosphate **515** and difluoromonophosphate ThDP **516**

7.8 Synthesis of Diisopropyldifluorobutanol phosphate

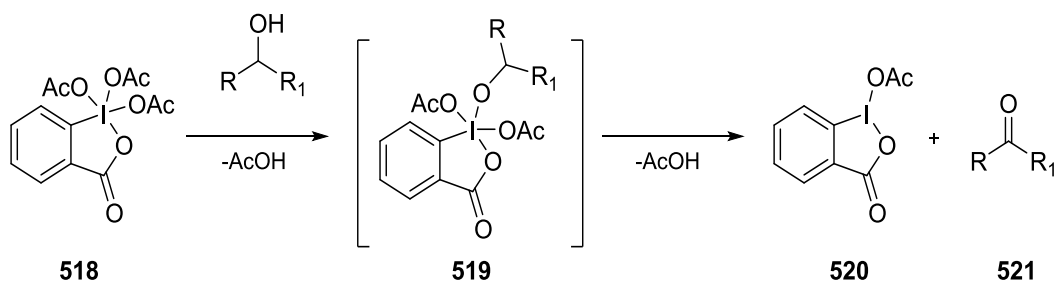
The 1,4-CuAAC click now required the formation on an alkyne. This could be facilitated in various ways, but initially it was decided to attempt the synthesis of aldehyde **517** from the primary alcohol **514** via a PCC oxidation (scheme **164**).



Reagents & Conditions: PCC, DCM, r.t., 85%

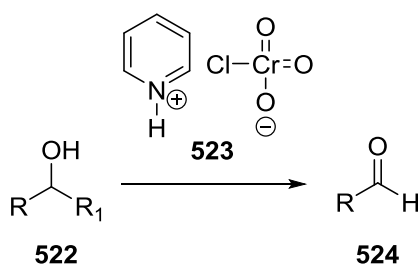
Scheme 164: PCC oxidation of primary alcohol to aldehyde

There are numerous methods for the conversion of primary alcohols into aldehydes in the literature including the Dess-Martin periodane oxidation⁽⁸⁹⁾ (scheme **165**) and the chromium (VI) oxidations using PCC or PDC⁽⁹⁰⁾.



Scheme 165: The Dess-Martin oxidation

Owing to the availability of PCC in the lab, and with the method being relatively straightforward, it was decided that the PCC oxidation would be attempted first using the published procedure of Corey⁽⁹⁰⁾ (scheme 166).



Scheme 166: Standard PCC oxidation

As expected with most PCC oxidations, formation of a black tar was evident on completion of the reaction, and subsequent filtration over a pad of celite/silica removed the Cr(IV) and any remaining PCC from the crude material to give the pure product **517** in 85% yield. Confirmation of the product was given by the additional aldehyde peak at δ 9.71 ppm in the ¹H NMR (figure 100). This was corroborated by the mass spectrum and the distinct sharp band in the infra-red at 1726 cm⁻¹ for the sp² C=O stretch.

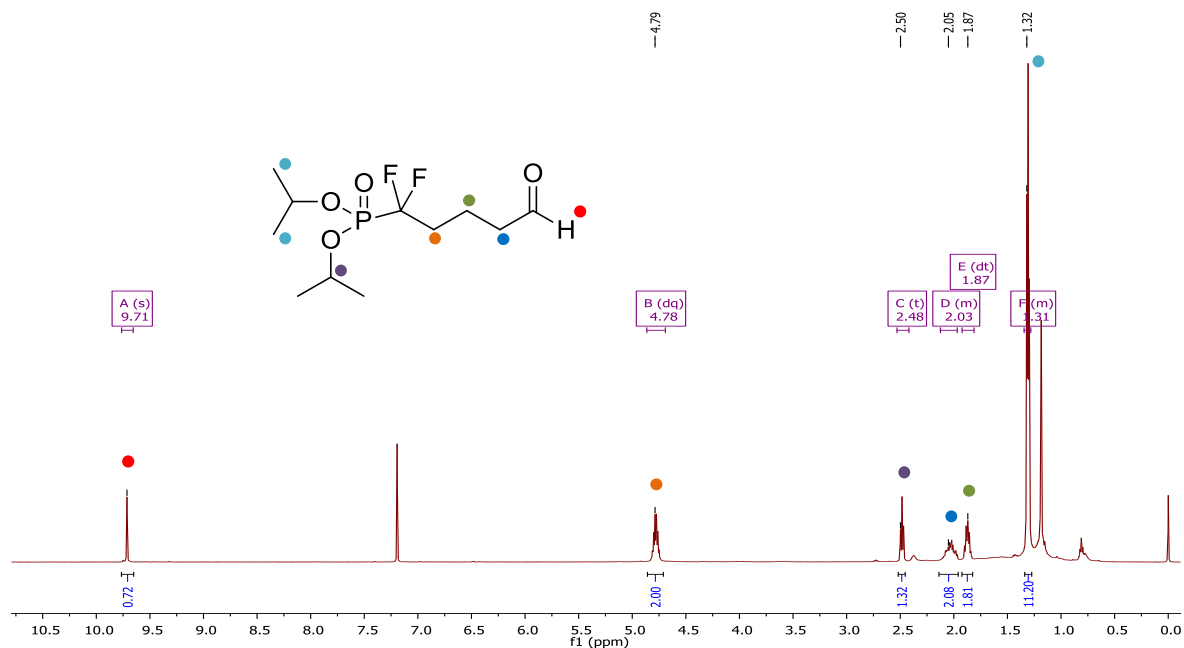
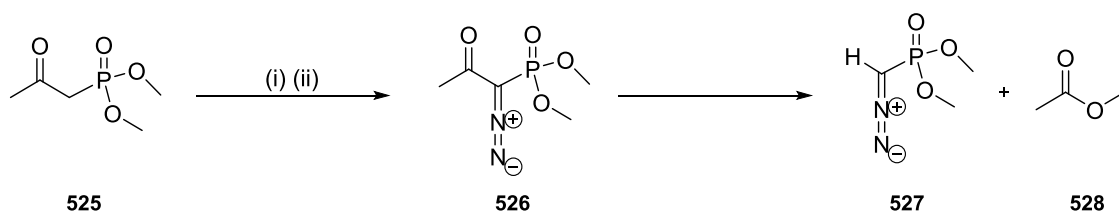


Figure 100: ^1H NMR depicting aldehyde **517** formation

7.9 Synthesis of diisopropyldifluoropentyne phosphate

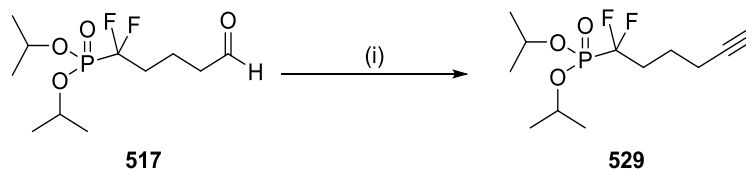
Once the aldehyde had been successfully made, it was now feasible to use either the Corey-Fuchs⁽⁸²⁾ or Bestmann-Ohira reagent **526** (scheme **167**) to form the alkyne tether as described earlier. The Seyferth-Gilbert homologation was used for its mild approach, avoidance of strong bases and its suitability at room temperature^{(83), (91), (92)}. One drawback however is the reagent cost, so it was prepared from dimethyl-2-oxopropylphosphonate **525** by a diazo transfer reaction with the tosyl azide prepared *in situ* (scheme **167**)⁽⁹³⁾.



Reagents & Conditions: (i) NaH (57%), (1.1 eq), tosyl azide (1.0 eq). THF, 0°C, 3 hr, (ii) TsN₃ (1.1 eq), THF, r.t, 60%.

Scheme 167: Preparation of Bestmann-Ohira reagent

Using the reported procedure of Bestmann *et al.*⁽⁸³⁾, the Ohira-Bestmann reagent⁽⁹⁸⁾ **526** was prepared and added *in situ* to the aldehyde **517**. Overall the reaction went smoothly and required little workup with compound **529** (scheme **168**) being isolated as a clear oil in 36% yield after filtering over a pad of silica.



Reagents & Conditions: (i) Ohira bestman reagent **526** (1.1 eq), aldehyde **517** (1.4 eq), MeOH, K₂CO₃ (1.9 eq), 24hr, 60%.

Scheme 168: Aldehyde to alkyne via Bestmann reagent

Confirmation of the product was obtained by the disappearance of the aldehyde proton observed at δ 9.71 in the ¹HNMR and the appearance of the characteristic alkyne proton found at 2.91 ppm as a triplet (*t*), which was corroborated by the coupling in the COSY to the adjacent CH₂ protons as a (*td*). Further evidence was given by the mass spectra and the lack of an aldehyde peak at 1726 cm⁻¹ in the infra-red spectra (figure **101**).

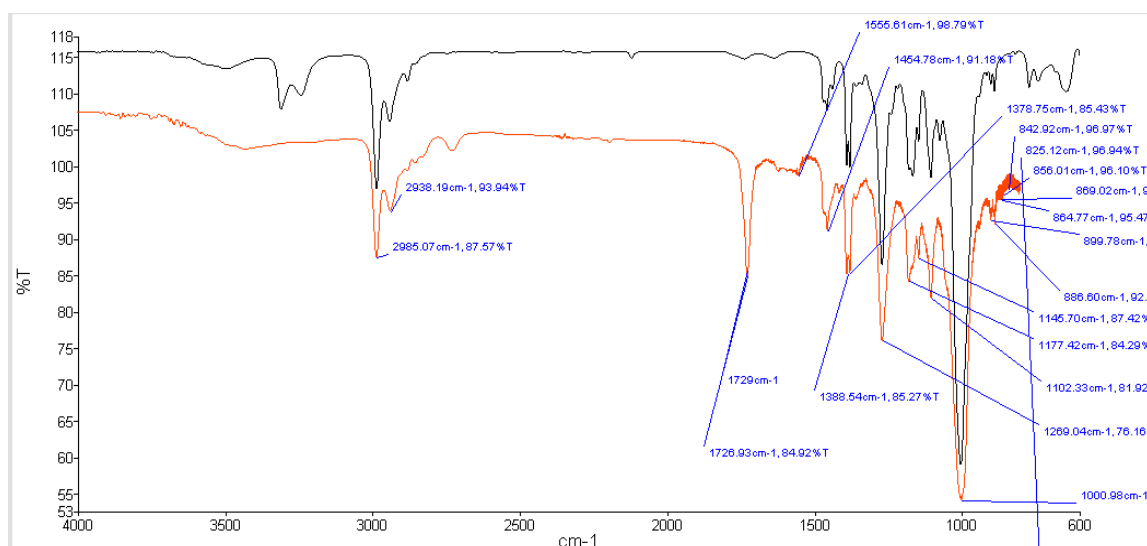
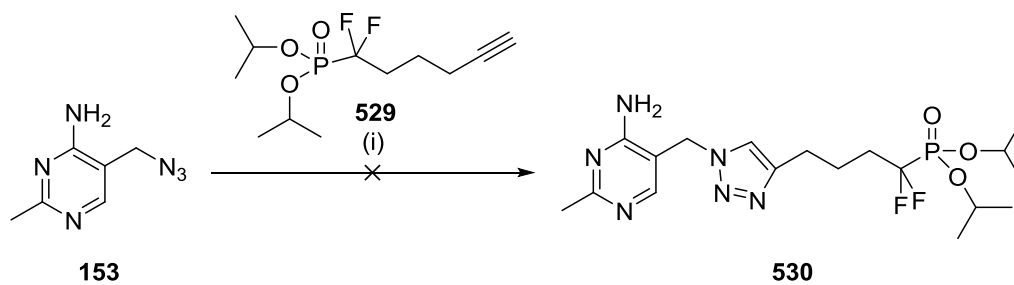


Figure 101: Infrared spectrum comparing (alkyne-black) vs (aldehyde- orange)

7.10 The 1, 4-CuAAC Synthesis of Diisopropyldifluorophosphenylnpentyne

Completion of the synthesis then required another 1,4-CuAAC reaction which has been used extensively throughout this research topic (scheme **169**). Using the previous conditions and reagents, compound **153** was reacted with compound **529** to give a new spot after three days at an R_f of 0.6 in EtOAc: MeOH (95:5 v/v).



Reagents & Conditions: (i) *t*-BuOH/H₂O (2:1 v/v), sodium ascorbate (0.1 eq.), CuSO₄·5H₂O (0.01 eq.), r.t. 16 hrs

Scheme 169: 1,4-CuAAC of 2-methyl-4-amino-5-azidopyrimidine with diisopropyl difluoro-4-pentyne

The ¹H NMR (figure 102) of the crude reaction mixture suggested the formation of the novel click compound **530**. It was apparent from the spectrum that both the CH₃ peak relating to the methyl group on the pyrimidine ring, and the primary amine (NH₂) were both duplicated suggesting the presence of two similar structures. To remove what was thought to be starting material **153**, the crude mixture was purified by column chromatography which unfortunately had a destructive effect upon the product, and the ¹H NMR obtained of the recovered material was not that of the original crude material. Having used up all the remaining material given to us by the Caen group and taking the time to start the synthesis from scratch, it was not possible to complete the synthesis of this click compound **530**. Future attempts of course, will focus on other purification methods.

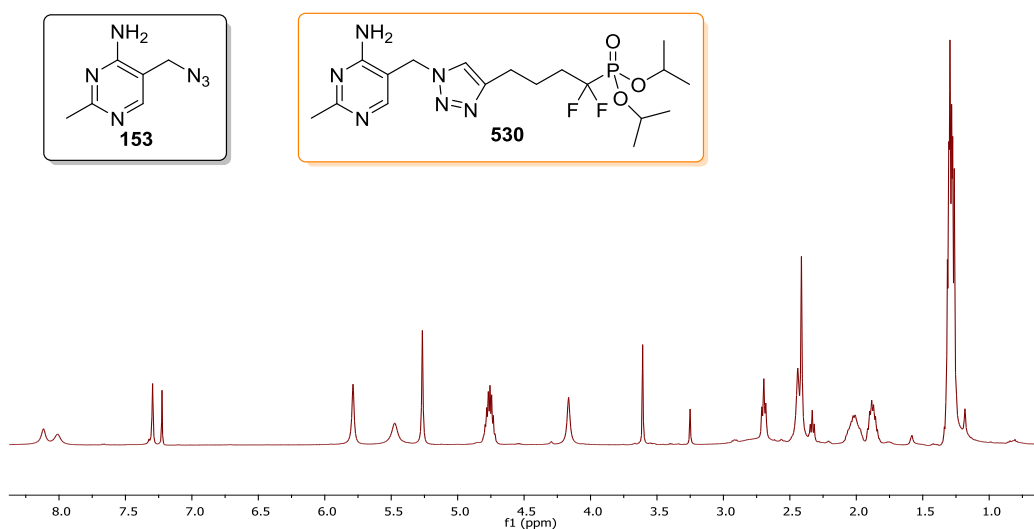


Figure 102: ¹H NMR of crude click product potentially containing diisopropyl difluoroalkyne (orange) and starting material (black)

7.11 Conclusion to Chapter

A novel synthesis has been achieved for both the aldehyde **517** and its alkyne derivative **529**. This can now allow further synthetic targets to be assembled with the reverse “synthons” instead of the typical compounds prepared previously by Lequeux *et al.* ^{(80), (81)}. Furthermore the synthesis and conditions required for assembly of the novel alkyne motif will hopefully allow future attempts to establish the thiamine monophosphate structure **530**, so it can be tested for biological activity in PDC enzymes.

Conclusion to Thesis

The decision to synthesise an unnatural cofactor is a bold and adventurous journey as the difficult chemistries involved within synthetic manipulation are combined with the need to understand the biological background for effectively designing target molecules. During this research multiple areas of chemistry have been encountered including *in silico* design, assembly of test compounds and biological assays. The journey to creating these structures has generated potential for many other investigations including to our knowledge, the first rearrangement of 1,4-disubstituted[1,2,3] triazoles to form cyclised ionic liquid type motifs, a potentially novel method for generating epoxy benzazepines which have previously been reported by other synthetic routes⁽⁹⁴⁾ and the first enantioselective reduction of 2-methyl-4-amino-pyrimidine using DIP-Cl reagents. Additionally, the formation of a unique set of products has been achieved by the Lewis assisted MgX_2 coordination to the pyrimidine ring. These entities may reveal further investigations, which will hopefully provide a series of compounds that are both useful to the synthetic chemist as tools to investigate ThDP roles within biological areas, and in the development of additional antibiotics like Trimethoprim and Bacimethrin.

In collaboration with the LCMT of Caen, we have also developed a new synthon for the diisopropyldifluoro monophosphates that have seen widespread biological applications that can act as extremely good bioisosteres. Based on an existing azide equivalent, the alkyne variant of this can now successfully be obtained in a few steps with little or no purification from a similar intermediate therefore requiring no changes to the initial synthesis. This will now permit further studies within our research towards their interaction in PDC enzymes, and for those interested in click chemistry motifs.

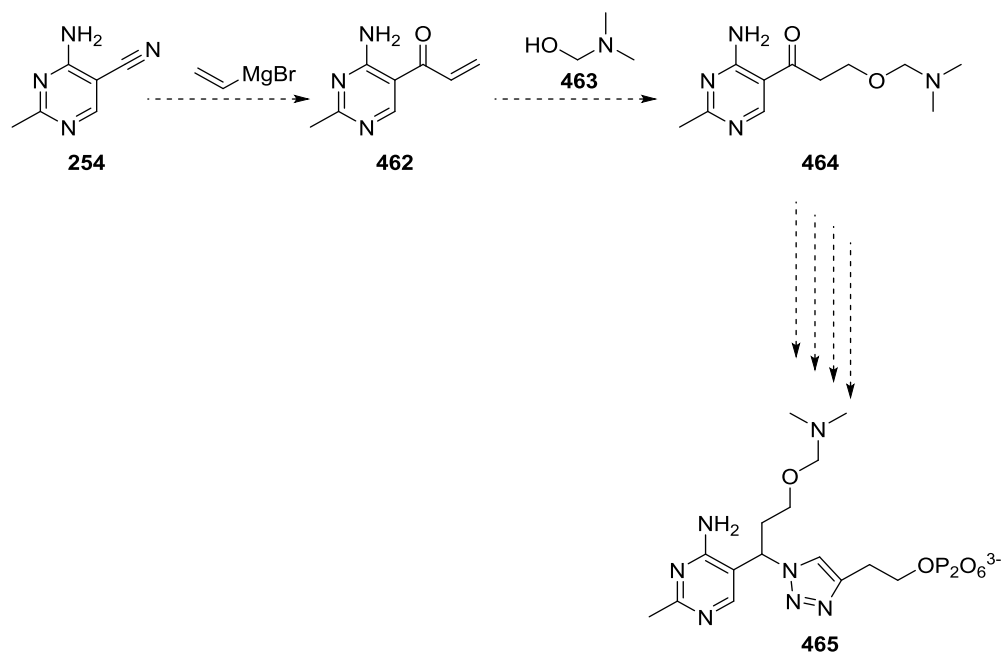
Finally we have synthesised a series of test substrates containing various alkyl lengths of methyl to butyl, as model probes for testing the ability of PDC to incorporate our novel cofactor systems. Preliminary biological testing has indicated that a lengthening of alkyl chain into the active site gives a detrimental effect upon binding affinity. Preliminary kinetic experiments with the methyl and ethyl analogues showed that a mMolar concentration is needed to give a similar inhibition of the PDC enzyme. Whereas the original cofactor prepared by Leeper only requires μM quantities

to achieve total inhibition. Additionally the carbon chains containing three/four carbon units are not easily accommodated within the active site pocket. This is probably due to the increased steric interaction within the active site and/or the many possible conformations adopted by these cofactors. In combination with this, a new chiral centre has been generated which may undergo some resolution by the enzyme and therefore reduce its binding efficacy. This chiral centre has now generated a tetrahedral carbon which changes the three-dimensional structure. From the introduction of this doctoral thesis, it was noted that ThDP cofactors and their three dimensional orientation become changed to permit different transition states i.e LTDP, HEDTP. Although these results are based loosely on a series of small findings, additional experiments will now be required to address and confirm these. Furthermore, these early results may highlight some of the changes needed in cofactor design for future synthetic targets in this research. As a whole, this research has generated the possibility for future projects on multiple synthetic routes whilst still lending potential motifs for investigation of ThDP enzymatic reactions.

Future Work

The biological assays have shown how the alkyl chains of three and four carbon units are too long to bind efficiently. However site directed mutagenesis could be used in combination with *in silico* studies to modify some of the existing amino acids in the surrounding active site. Altering amino acids that are not involved during catalysis could increase the space found within the active site and hopefully promote new reactions? Alternatively *in silico* studies could be undertaken on other enzyme classes that use ThDP, such as in the terpene synthetic pathways which possess larger active sites due to the greater sizes of terpenoid motifs. If this was successful, attempts to synthesise the alkyl tertiary amine chain could continue, but using a new synthetic routes to acquire the desired product.

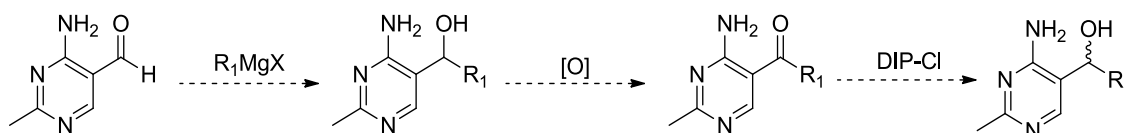
Towards the end of this research topic, synthesis had begun on the vinyl ketone **462** which after conjugate addition by **463** has the potential to produce intermediate **464** (scheme **170**). A chain containing an oxygen linker in place of a carbon unit was proposed to facilitate more rotation about the problematic three position and remove some of the tetrahedral rigidity found in the previous structures. Unfortunately synthesis of this is ongoing due to another side product formed during the Grignard step as mentioned in chapter 6.



Scheme 170: Future synthesis of oxygen-linker tertiary amine scaffold

Synthesis had already re-started on the diisopropyldifluoromonophosphate alkyne so that it could undergo the CuAAC process, but next time under different purification approaches such as recrystallisation. Then if successful, the compound would undergo biological evaluation like that discussed earlier and could be manipulated for testing with other biological compounds of interest. The combination of MBH-promoting side chain functionality with the more chemically-resistant isostere is the ultimate destination of this research to provide truly practical unnatural cofactors for promotion of unnatural reactions in an enzyme active site.

Although the enantioselective reduction of 2-methyl-4-aminopyrimidine ethanone had been achieved with (+) DIP-Cl, conditions to replicate the reduction have not been formed. Future attempts on this research would focus upon varying conditions to establish the method or by changing the synthetic route (scheme 171) to facilitate future testing upon a series of ketone analogues.



Scheme 171: Future synthetic route to prochiral ketone

These would include increasing the length, bulkiness and chemical nature of the R group to assess what affect if any is observed. In addition, the intermediate compounds formed during the ketone synthesis would also be investigated further. This would include varying the conditions within the reaction to monitor what products are preferred and examining if the removal of MgX_2 salts by precipitation in dioxane causes a change in yields or observed products.

References - Results & Discussion

1. M. T. Reetz, R. Mondiere, J. D. Carballeira, *Tetrahedron Lett.*, **2007**, *48*, 1679-1681.
2. B. Imperiali, R. Roy, *Protein Engineering*. **1997**, *10*, 691-698.
3. C. N. Jensen, J. Cartwright, J. Ward, S. Hart, J. P. Turkenburg, S. T. Ali, M. J. Allen, G. Grogan, *Chem. Bio. Chem.*, **2012**, *13*, 872-878.
4. K. M. Erixon, C. L. Dabalos, F. J. Leeper, *Org. Biomol. Chem.*, **2008**, 3561-3572.
5. R. Kluger, T. Smyth, *J. Am. Chem. Soc.*, **1981**, *103*, 884-888.
6. S. Mann, C. P. Perez, D. Hawksley, F. J. Leeper, *Org. Biomol. Chem.*, **2004**, *2*, 1732-1741.
7. J. A. Zoltewicz, G. M. Kauffman, *J. Am. Chem. Soc.*, **1997**, *58*, 5278-5281.
8. G. Uray, I. Kriessmann, J. A. Zoltewicz, *Bioorg. Chem.*, **1993**, *21*, 294-365.
9. J. A. Zoltewicz, G. Uray, G. M. Kauffmann, *J. Am. Chem. Soc.*, **1980**, *102*, 3653.
10. F. Himo, T. Lovell, R. Hilgraf, V. V. Rostovtsev, L. Noodleman, K. B. Sharpless, V. V. Fokin, *J. Am. Chem. Soc.*, **2005**, *127*, 210-216.
11. J. C. Tripp, J. E. Hein, L. B. Krasnova, K. B. Sharpless, V. V. Fokin, *Angew. Chem. Int Ed. Engl.*, **2009**, *48*, 8018-8021.
12. F. Fang, M. Fogel, J. V. Hines, S. C. Bergmeier, *Org. Biomol. Chem.*, **2012**, *10*, 3080-3091.
13. D. Dobritzsch, S. Konig, G. Lu, *J. Biol. Chem.*, **1998**, *273*, 20196-20204
14. G. Schenk, F. J. Leeper, P. F. Nixon, R. G. Duggleby, *Eur. J. Biochem.*, **1997**, *248*, 63-71.
15. R. Kluger, K. Tittmann, *Chem. Rev.*, **2008**, *108*, 1797-1833.
16. I. Barburina, Y. Gao, F. Jordan, S. Hohmann, W. Furey, *Biochemistry*, **1994**, *33*, 5630-5635.
17. W. Verses, S. Sparpen, M. D. H. Wood, F. J. Leeper, J. Vanderleyden, J. Steyaert, *J. Biol. Chem.*, **2007**, *282*, 35269-35278.
18. D. Seebach, E. J. Corey, *J. Org. Chem.*, **1975**, *40*, 231-237.
19. H. Stetter, *Angew. Chem.*, **1976**, *15*, 639-647.
20. R. R. Williams, J. K. Cline, *J. Am. Chem. Soc.*, **1936**, *58*, 1504-1505.
21. H. C. Koppel, R. H. Springer, R. K. Robins, C. C. Cheng, *J. Org. Chem.*, **1962**, *27*, 3614-3617.

22. A. Iqbal, E-H. Sahraoui, F. J. Leeper, *J. Org. Chem*, **2014**, *10*, 2580-2585.
23. L. R. Bennett, C. J. Blankley, R. W. Fleming, *J. Med. Chem.*, **1981**, *24*, 382-389.
24. T. L. V. Ulbricht, *Purines, Pyrimidines and Nucleotides: and the chemistry of nucleic acids*. **2013**, Oxford press, Elsevier.
25. R. Nicewonger, A. Rammelsberg, C. A. Costello, T. P. Begley. *Bioorg. Chem.*, **1995**, *23*, 512-518.
26. R. L. Baxter, A. B. Hanley, H. W. S. Chan, *J. Chem. Soc. Perkin Trans. 1*, **1990**, 2963-2966.
27. D. Price, E. L. May, F. D. Pickel, *J. Am. Chem. Soc.*, **1940**, *62*, 2818-2820.
28. J. Clayden, N. Greeves, S. Warren. *Organic Chemistry*. Manchester: Oxford University Press, **2012**.
29. S. E. Drewes, G. H. P. Roos, *Tetrahedron*, **1987**, *44*, 4463-4481.
30. K. E. Price, S. J. Broadwater, B. J. Walker, D. T. McQuade, *J. Org. Chem.*, **2005**, *70*, 3980-3987.
31. P. J. Dunn, M. L. Hughes, P. M. Searle, A. S. Wood, *J. Org. Proc. Res. Dev.*, **2003**, *7*, 244-253.
32. R. S. Porto, M. L. A. A. Vasconcellos, E. Ventura, F. Coelho, *Synthesis*, **2005**, *14*, 2297-2306.
33. B. R. Riebel, P. R. Gibbs, W. B. Wellborn, A. S. Bommarium, *Adv. Synth. Catal.*, **2003**, *345*, 707-712.
34. H. Pellissier, *Tetrahedron*. **2003**, *59*, 8291-8327.
35. J. Hine, Y-Jung. Chen, *J. Org. Chem.*, **1987**, *52*, 2091-2092.
36. J. Auge, N, Lubin, A. Lubineau, *Tetrahedron Lett.*, **1994**, *35*, 7947-7948.
37. J. Cai, Z. Zhou, G. Zhao, C. Tang, *Org. Lett.*, **2002**, *4*, 4723-4725.
38. M. Buswell, I. Fleming, *Org. Biomol. Chem.*, **2004**, *2*, 3006-3017.
39. J. A. Joule, K. Mills. *Heterocyclic Chemistry*. **2010**. Chichester: Blakwell Publishing
40. S. H. Pine, G. S. Shen, H. Hoang, *Synthesis*, **1991**, 165-166.
41. R. L. Sowerby, R. M. Coates, *J. Am. Chem. Soc.*, **1972**, *94*, 4758-4759.
42. R. G. Hartley, J. L. Calver, G. J. Mckiemman, *Tetrahedron*, **2007**, *63*, 4825-4864.

43. E. J. Corey, M. Chaykovsky, *J. Am. Chem. Soc.* **1962**, *84*, 866-867.
44. M. Cleij, A. Archelas, R. Furstoss, *J. Org. Chem.*, **1999**, *64*, 5029-5035.
45. J. B. Friesen, R. Schretzman, *J. Chem. Educ.*, **2011**, *88*, 1141-1147.
46. M. Scholl, T. M. Trnka, J. P. Morgan, R. H. Grubbs, *Tetrahedron Lett.*, **1999**, *40*, 2247-2250.
47. A. K. Chatterjee, T.-L. Choi, D. P. Sanders, R. H. Grubbs, *J. Am. Chem. Soc.*, **2003**, *125*, 11360-11370.
48. R. Huisgen, *Proc. Chem. Soc.*, **1961**, 357-396.
49. E. R. Alexander, R. B. Wildman, *J. Am. Chem. Soc.*, **1948**, *70*, 1187-1189.
50. J. Sun, Y. Dong, L. Cao, X. Wang, S. Wang, Y. Hu, *J. Org. Chem.*, **2004**, *69*, 8932-8934.
51. B. V. Rkade, K. R. Prabhu. *J. Org. Chem.*, **2012**, *77*, 5394-5370.
52. E. Lieber, C. N. R. Rao, T. S. Chao, C. W. W. Hoffman, *Anal. Chem.*, **1957**, *29*, 916-918.
53. K. Banert, *Chem. Ber.*, **1989**, *122*, 911-918,
54. N. Miyaura, A. Suzuki. *Chem. Rev.*, **1995**, *95*, 2457-2483.
55. K. Sonogashira, Y. Tohda, N. Hagihara, *Tetrahedron Lett.*, **1975**, *50*, 4467-4470.
56. P. Bovonsombat, E. McNelis, *Tetrahedron Lett.*, **1992**, *33*, 7705-7708.
57. E. J. Corey, D. Seebach, *J. Org. Chem.*, **1966**, *31*, 4097-4099.
58. M. J. White, F. J. Leeper. *J. Org. Chem.*, **2001**, *66*, 5124-5131.
59. H. Firouzabadi, N. Iranpoor, B. Karimi, *Synthesis*. **1999**, *1*, 58-60.
60. J. H. Gong, Y. J. Lm, K. Y. Lee, J. N. Kim, *Tetrahedron*, **2002**, *43*, 1247-1251.
61. S. M. Hannick, Y. Kishi, *J. Org. Chem.*, **1983**, *48*, 3833-3835.
62. H. S. P. Rao, S. Rafi, K. Padmavathy, *Tetrahedron*, **2008**, *64*, 8037-8043.
63. K. Mineno, Y. Sawai, K. Kanno, N. Sawada, H. Mizufune, *J. Org. Chem.*, **2013**, *78*, 5843-5850.
64. A. G. Ogston, *Nature*, **1948**, *162*, 963-964.
65. A. Meseca, D.E. Koshland, *Nature*. **2000**, *403*, 614-615.
66. R. Bentley, *Nature*, **1978**, *276*, 673-676.

67. H.-V. Blaser, *Chem. Rev.*, **1992**, 92, 935-952.
68. P. Daverio, M. Zanda, *Tetrahedron*, **2001**, 12, 2225-2259.
69. A. A. Smaardijk, H. Wynberg, *J. Org. Chem.*, **1987**, 52, 135-137.
70. Y. Liu, C. Shan-Da, S.-L. Yu, X. G. Yin, J. R. Wang, X. Fan, W. P. Li, R. Wang, *J. Org. Chem.*, **2010**, 75, 6869-6878.
71. E. Fernandez-Mateos, B. Macia, D. J. Ramon, M. Yus, *Eur. J. Org. Chem.*, **2011**, 6851-6855.
72. B. Sundoro, C-Y. Chang, R. Aslanian, F. Jordan, *Synthesis*, **1983**, 7, 555-556.
73. M. Butters, J. Ebbs, S. P. Green, J. MacRae, M. C. Morland, C. W. Murtiashaw, A. J. Pettman, *Org. Process Research and Development*, **2001**, 5, 28-36.
74. E. Epifani, S. Florio, G. Ingrosso, *Tetrahedron Lett.*, **1987**, 28, 6385-6388.
75. M. M. Midland, *Chem. Rev.*, **1989**, 89, 1553-1561.
76. H. C. Brown, J. Chandrasekharan, P. V. Ramachandran, *J. Am. Chem. Soc.*, **1988**, 110, 1539-1546.
77. R. Krishnamurthy, *J. Mex. Chem. Soc.*, **2009**, 53, 23-33.
78. J. J. Reddick, S. Saha, J.-M. Lee, J. S. Melnick, J. Perkins, T. P. Begley, *Biorg. Med. Chem. Lett.*, **2001**, 11, 2245-2248.
79. E. L. Stogryn, *J. Med. Chem.*, **1972**, 15, 200-202.
80. S. A. Diab, C. D. Schutter, M. Muzard, R. P. Royon, E. Pfund, T. Lequeux *J. Med. Chem.*, **2012**, 55, 2758-2768.
81. S. A. Diab, A. Sene, E. Pfund, T. Lequeux, *Org. Lett.*, **2008**, 10, 3895-3898.
82. E. J. Corey, P. L. Fuchs, *Tetrahedron Lett.*, **1972**, 36, 3769-3772.
83. S. Muller, B. Liepold, G. J. Roth, H. J. Bestmann, *Synlett*, **1996**, 521-522.
84. D. W. Grisley, *J. Org. Chem.*, **1961**, 26, 2544-2546.
85. Y. Catel, V. Besse, A. Zulauf, D. Marchat, E. Pfund, T. N. Pham, D. Bernache-Assolant, M. Degrange, T. L. Lecueux, P-J. Madec, L. Le Pluart. *European Polymer J.* **2012**, 48, 318-330.
86. S. N. Lewis, J. J. Miller, S. Winstein, *J. Org. Chem.*, **1972**, 37, 1478-1486.

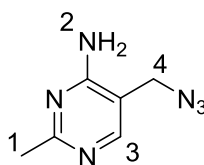
87. B. Giese, *Radicals in organic synthesis: formation of carbon-carbon bonds*. **1986**, Oxford: Pergamon Press.
88. Y. A. Muller, Y. Lindqvist, W. Furey, G. E. Schultz, F. Jordan, G. Schneider, *Structure*, **1993**, *1*, (2), 95-103.
89. D. B. Dess, J. C. Martin, *J. Org. Chem.*, **1983**, *48*, 4155-4156.
90. E. J. Corey, W. J. Suggs, *Tetrahedron Lett.*, **1975**, *31*, 2647-2650.
91. T. H. Jepsen, J. L. Kristensen, *J. Org. Chem.*, **2014**, *79*, 9423-9426.
92. G. J. Roth, B. Liepold, S. G. Muller, H. J. Bestmann, *Synthesis*. **2004**, 59-62.
93. M. Pisset, D. Maihol, Y. Coquerel, J. Rodriguez, *Synthesis*, **2011**, *16*, 2549-2552.
94. M. G. Lauer, M. K. Thompson, K. H. Shaughnessy, *J. Org. Chem.*, **2014**, *79*, 10837-10848.
95. P. Stenbuck, R. Baltzly, H. M. Hood, *J. Org. Chem.*, **1963**, *28*, 1983-1988.
96. J. C. Gilbert, U. Weerasooriya, *J. Org. Chem.*, **1982**, *47*, 1837-1845.
97. Barton, D. H. R.; McCombie, S. W. *J. Chem. Soc., Perkin Trans. 1*, **1975**, 1574-1575.
98. Ohira, S. *Synthetic Commun.* **1989**, *19*, 561-564.
99. Coelho, F.; Rossi, R.C. *Tetrahedron Lett.*, **2002**, *43*, 2797-2800.

Experimental

General Conditions and Reagents

All reactions were carried out in dry solvents unless otherwise stated. Anhydrous solvents were prepared using literature procedures, with THF, diethyl ether and toluene being distilled over sodium following literature methods. All solvents and chemicals were purchased from appropriate suppliers including Sigma Aldrich, Acros, TCI, Fluorochem, Alfa Aesar and Fisher scientific. Infrared spectra were obtained on a Perkin Elmer FT-IR spectrometer, with most compounds dissolved in dichloromethane on a NaCl disc. Where compounds were not soluble in this solvent, the Infra-red spectrum was obtained using an ATR spectrometer. All HPLC samples were run on a Shimadzu LC-20AB liquid chromatography unit, equipped with a SIL-20A – autosampler and SPD-M20A Diode array detector using HPLC grade solvents. Most samples were run on an isocratic mobile phase of IPA/hexane to acquire the desired chromatographic separation. These were undertaken on a cellulose 1 column: Lux3u (250 x 4.6 mm) chiral column. Optical rotations were recorded on an ADP 440 BS polarimeter using a concentration as stated for each sample and at room temperature unless otherwise stated. Coupled bio-assays were undertaken on a Perkin Elmer Lambda 25 with the wavelength set at 340 nm to monitor the absorption of NADH. These were recorded in a water bath set at 31°C and using a polystat 101 pump. ¹H, ¹³C, ³¹P and any other NMR nuclei spectra were obtained using a Bruker (Ascend) 500 MHz spectrometer and a sample express autosampler. Mass spectra were acquired in collaboration with EPSRC UK National Mass Spectrometry Facility, Swansea. Melting points were recorded on a Buchi melting point apparatus B545. All XRD data was acquired at the UEA by Dr D. Hughes on an Oxford Diffraction Xcalibur-3/Sapphire3 CCD diffractometer. Data was then analysed by CrysAlisPro-CCD and RED (1) programs.

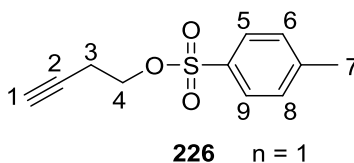
Synthesis of 5-azidomethyl-2-methylpyrimidin-4-ylamine ^{(1), (6), (7)}



153

To a dried round-bottomed flask was added thiamine hydrochloride (10.3 g, 31.5 mmol) in water (100 mL). To this was added sodium azide (4.90 g, 75.4 mmol) and sodium sulfite (0.38 g, 3.0 mmol). The reaction mixture was stirred at 65 °C for approximately five hours. Citric acid (192 g, 100 mmol) was added until pH 4 was obtained. The aqueous layer was then washed with dichloromethane (3 x 30 mL) and basified with potassium carbonate to pH 8. Some precipitation of the product was observed at this point, and this was collected by filtration and kept aside. The remaining organic layer was dried over magnesium sulfate, filtered and evaporated to dryness to yield a white crude product. Recrystallisation of the recovered products from ethyl acetate/hexane gave the product as sharp white crystals (3.24 g, 65%). m.p: 153-154°C. [Lit. ⁽⁷⁾ m.p: 150-153 °C]. **¹H NMR** (400 MHz, DMSO-*d*₆) δ 7.95 (1H, s, C-H, H-3), 6.86 (2H, broad s, NH₂, H's-2), 4.27 (2H, s, CH₂, H-4), 2.26 (3H, s, CH₃, H-1). **¹³C NMR** (101 MHz, DMSO-*d*₆) δ 166.9, 161.8, 155.8, 107.6, 47.4, 25.2. **IR** ν_{\max} / cm^{-1} : 3274, 3088 (NH₂), 2105 and 2085 (N₃), 1667, 1586 and 1560 (C-H, sp² stretch).

Synthesis of but-3-ynyl toluene-4-sulfonate ^{(2), (3), (6)}



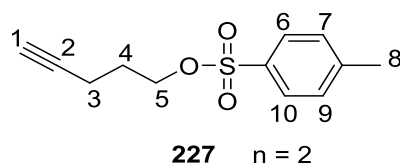
226 n = 1

Method A

To a flame dried round-bottomed flask was added 3-butyn-1-ol (1.02 mL, 14.6 mmol) in anhydrous pyridine (150 mL). To this was slowly added *p*-toluenesulphonyl chloride (6.97g, 36.5 mmol) at 10 °C. The reaction mixture was allowed to stir at r.t for approximately 3 hours. The reaction was then quenched with HCl_{aq} (1M), producing an exothermic reaction. After extraction with ethyl acetate (3 x 30 mL), the combined organic phases were washed with potassium carbonate (sat.), CuSO₄ (aq), and brine. The organic layer was dried over magnesium sulfate,

filtered and evaporated under reduced pressure to yield viscous brown oil. This was purified by flash column chromatography on silica with a mobile phase of ethyl acetate: hexane (2:1 v/v) to give the product as a clear viscous oil (1.8 g, 57%). **¹H NMR** (500 MHz, CDCl₃) δ 7.84 (d, ³J = 8.3 Hz, 2H, H-5,9), 7.39 (d, ³J = 8.3 Hz, 2H, H-6,8), 4.14 (t, ³J = 7.1 Hz, 2H, H-4), 2.59 (td, ³J = 7.1, 2.7 Hz, 2H, H-3), 2.49 (s, 3H, H-7), 2.00 (t, ³J = 2.7 Hz, 1H, H-1). **¹³C NMR** (126 MHz, CDCl₃) δ 145.0, 132.8, 129.9, 128.0, 78.3, 70.7, 67.4, 21.6, 19.4. **IR** ν_{max}/cm⁻¹: 3289, (C-H, sp stretch), 1597, 1492, 1463, 1356 (sp² C=C ar stretch), 1172 (SO₂, sp², stretch).

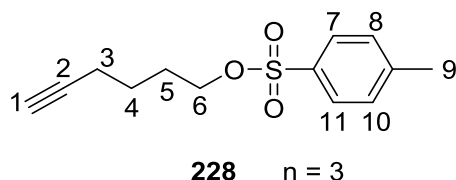
Synthesis of 4-butyn-1-tosylate ^{(2), (3)}



Following Method A for but-3-ynyl toluene-4-sulfonate:

Pent-4-ynyl-1-ol (2.78 g, 33.1 mmol) was added to *p*-toluenesulphonate (15.8 g, 82.8 mmol) at -10 °C and stirred for 3 hours at r.t. Following the usual work up a crude oil was obtained (5.56 g, 71%). Purification on silica with a mobile phase of ethyl acetate: hexane (2:1 v/v) produced a clear oily residue (3.62 g, 46%). **¹H NMR** (400 MHz, DMSO-*d*₆) δ 7.80 (d, ³J = 8.3 Hz, 2H, H-6, 10), 7.48 (d, ³J = 8.3 Hz, 2H, H-7, 9), 4.09 (t, ³J = 7.0 Hz, 2H, H-5), 2.75 (t, ³J = 2.7 Hz, 1H, H-1), 2.42 (s, 3H, H-8), 2.18 (td, ³J = 7.0, 2.7 Hz, 2H, H-3), 1.75 (quin, J = 7.0 Hz, 2H, H-4). **¹³C NMR** (101 MHz, DMSO-*d*₆) δ 144.9, 132.3, 130.1, 127.5, 82.5, 71.8, 69.3, 27.2, 21.0, 13.9. **IR** ν_{max}/cm⁻¹: 3472 (C-H, sp stretch), 1356, 1172 (SO₂, sp², stretch).

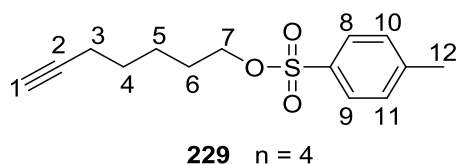
Synthesis of 5-hexyn-1-tosylate ^{(2), (3)}



To a stirred solution of 5-hexyn-1-ol (5.00 g, 51.0 mmol) in pyridine (100 mL) at 0 °C was added *p*-toluenesulfonyl chloride (10.7 g, 56.0 mmol). The solution was stirred at 0 °C for approx. 16 hours and then saturated with sodium hydrogen carbonate (200 mL). After stirring for a further 10 minutes the solution was poured into sat. sodium hydrogen carbonate (200 mL), and extracted

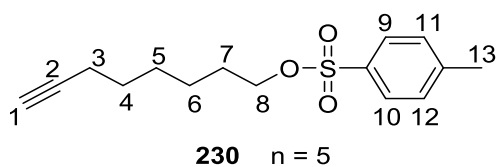
with diethyl ether (3 x 200 mL). The organic phase was then washed with dilute hydrochloric acid aq (2M) (3 x 200 mL) and water (200 mL). The combined organic phases were then dried over magnesium sulphate, filtered and evaporated to remove excess solvent. The resultant oil was purified by column chromatography on silica using a mobile phase of hexane: ethyl acetate (4:1 v/v) to produce a clear viscous oil (4.48 g, 37%). **¹H NMR** (500 MHz, CDCl₃) δ 7.72 (d, ³J = 8.3 Hz, 2H, H-7, 11), 7.28 (d, ³J = 8.3 Hz, 2H, H-8, 10), 3.98 (t, ³J = 6.3 Hz, 2H, H-6), 2.38 (s, 3H, H-9), 2.09 (td, ³J = 7.0, 2.6 Hz, 2H, H-3), 1.85 (t, ³J = 2.6 Hz, 1H, H-1), 1.73-1.677 (m, 2H, H-5), 1.51-1.455 (m, 2H, H-4). **¹³C NMR** (126 MHz, CDCl₃) δ 144.79, 133.10, 129.87, 127.89, 83.41, 69.93, 68.98, 27.77, 24.23, 21.65, 17.73. **IR** ν_{\max} /cm⁻¹: 3289 (C-H, sp stretch), 2955 (C-H, sp³ stretch), 1598, 1495, 1454 (sp² aromatic stretch) 1172 (SO₂ stretch).

Synthesis of 5-heptyn-1-tosylate ^{(2), (3)}



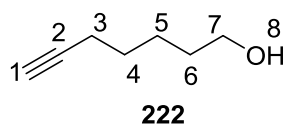
6-Heptyn-1-ol (752 mg, 6.16 mmol) in dry dichloromethane (20 mL) was cooled to 0°C and then treated with *p*-toluenesulphonyl chloride (1.41 g, 7.4 mmol), DMAP (75.0 mg, 0.61 mmol) and triethylamine (2.0 mL). The mixture was stirred overnight and then quenched with aqueous ammonium chloride solution, extracted with ethyl acetate (3 x 10 mL), dried over magnesium sulphate, filtered and concentrated to give a yellow crude product. Column chromatography on silica with a mobile phase of hexane: ethyl acetate (10:1 v/v) gave a clear viscous oil (0.82 g, 58%). **¹H NMR** (500 MHz, CDCl₃) δ 7.82 (d, ³J = 8.3 Hz, 2H, H-8, 9), 7.38 (d, ³J = 8.3 Hz, 2H, H-10, 11), 4.06 (t, ³J = 6.5 Hz, 2H, H-7), 2.48 (s, 3H, H-12), 2.18 (td, ³J = 6.8, 2.6 Hz, 2H, H-3), 1.96 (t, ³J = 2.6 Hz, 1H, H-1), 1.70-1.65 (m, 2H, H-4), 1.55 – 1.43 (m, 4H, H-5, 6). **¹³C NMR** (126 MHz, CDCl₃) δ 144.7, 133.2, 129.8, 127.9, 84.0, 70.3, 68.5, 28.3, 27.7, 24.5, 21.6, 18.2. **IR** ν_{\max} /cm⁻¹: 3290 (C-H, sp stretch), 2941 (C-H, sp³ stretch), 1598, 1495, 1460 (sp² aromatic stretch) 1173 (SO₂ stretch).

Synthesis of 6-octyn-1-tosylate ^{(2), (3)}



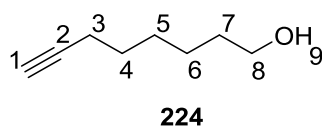
7-Octyn-1-ol (1.47 g, 11.6 mmol) in dry dichloromethane (20 mL) was cooled to 0 °C and then treated with *p*-toluenesulphonyl chloride (2.44 g, 12.8 mmol), DMAP (143 mg, 1.17 mmol) and triethylamine (2.33 g, 23 mmol, 2.0 mL). The mixture was then stirred overnight and quenched with aqueous ammonium chloride solution and extracted with ethyl acetate (3 x 20 mL). The combined organic extracts were dried over magnesium sulphate, filtered and concentrated to give a yellow crude product. Column chromatography on silica with a mobile phase of hexane: ethyl acetate (10:1 – 1:1) gave the product as a clear viscous oil (1.32 g, 41%). **¹H NMR** (500 MHz, CDCl₃) δ 7.82 (d, ³*J* = 8.3 Hz, 2H, H-8, 9), 7.42 (d, ³*J* = 8.3 Hz, 2H, H-10, 11), 4.03 (t, ³*J* = 6.5 Hz, 2H, H-7), 2.49 (s, 3H, H-12), 2.18 (td, ³*J* = 7.0, 2.6 Hz, 2H, H-2), 1.96 (t, ³*J* = 2.6, 1H, H-1), 1.71-1.64 (m, 2H, H-6), 1.56 – 1.45 (m, 2H, H-3), 1.39 – 1.35 (m, 4H, H-4, 5). **¹³C NMR** (126 MHz, CDCl₃) δ 144.7, 133.2, 129.8, 127.9, 77.2, 70.5, 68.3, 28.7, 28.1, 28.0, 24.9, 21.6, 18.2. **IR** ν_{\max} /cm⁻¹: 2939, 2862 (sp³ C-H stretch), 1598, 1463, 1455 (sp² C-H aromatic stretch).

Synthesis of hept-6-yn-1-ol ⁽⁴⁾



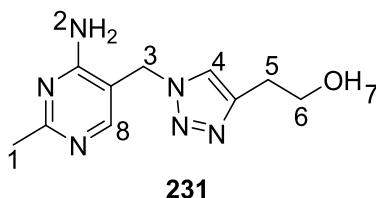
In a dry round-bottomed flask in anhydrous THF (50 mL) at 0 °C was suspended lithium aluminium hydride (540 mg, 14.3 mmol). 6-Heptynoic acid (900 mg, 7.13 mmol) in THF (10 mL) was then added dropwise and stirred overnight at r.t. The reaction was quenched with dilute aqueous HCl (1M, 20 mL) at 0 °C and the aqueous layer was separated and extracted with diethyl ether (3 x 10 mL). Drying over magnesium sulfate, filtration and evaporation gave a clear oil (350 mg, 73%). **¹H NMR** (500 MHz, DMSO-*d*₆) δ 4.36 (t, ³*J* = 5.2 Hz, 1H, H-8), 3.39 (td, ³*J* = 5.2, 6.2 Hz, 2H, H-7), 2.73 (t, ³*J* = 2.7 Hz, 1H, H-1), 2.15 (td, ³*J* = 6.9, 2.7 Hz, 2H, H-3), 1.45 – 1.39 (m, 6H, H-4, 5, 6). **¹³C NMR** (126 MHz, DMSO-*d*₆) δ 85.0, 71.5, 61.0, 32.4, 28.3, 25.2, 18.2. **IR** ν_{\max} /cm⁻¹: 3297, 2933 and 2859 (sp³ C-H stretch), 1463 and 1431 (C-H, sp² stretch).

Synthesis of oct-7-yn-1-ol ⁽⁵⁾



Potassium hydride (30%) in mineral oil (3.6 g, 23.7 mmol, 3.0 eq) under an argon atmosphere was washed with dry pet ether and treated dropwise with 1,3-diaminopropane (2.1 mL, 3.1 eq) to give an exothermic reaction. This was stirred until homogeneous and then cooled to 0 °C. 3-Octyn-1-ol (1.14 g, 9.00 mmol, 1.0 eq) was added dropwise to produce a dark black solution and left to stir overnight at r.t. The reaction was quenched with water (20 mL) and extracted with diethyl ether (3 x 30 mL). The organic layer was washed with 10% aqueous HCl (10 mL), brine (10 mL), dried over magnesium sulphate and filtered. Evaporation gave a clear viscous oil which required no further purification (851 mg, 85%). ¹H NMR (500 MHz, CDCl₃) δ 3.65 (t, ³J = 6.6 Hz, 2H, H-8), 2.21 (td, ³J = 7.1, 2.6 Hz, 2H, H-3), 1.96 (t, ³J = 2.6 Hz, 1H, H-1), 1.61-1.52 (m, 4H, H-4, 7), 1.49 – 1.35 (m, 4H, H-5, 6). ¹³C NMR (126 MHz, CDCl₃) δ 84.6, 68.2, 62.7, 32.5, 28.4, 28.3, 25.2, 18.3. IR ν_{\max} /cm⁻¹: 3304, 2936, 2860, 1463, 1433.

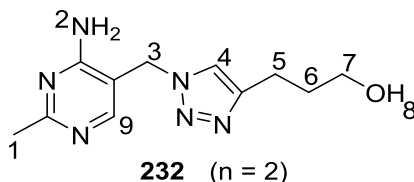
Synthesis of 2-[1-(4-amino-2-methylpyrimidin-5-ylmethyl)-1H-[1,2,3]triazol-4-yl]-ethanol ^{(6), (7), (8)}



To compound **153** (1.97 g, 12.0 mmol) in a solvent mixture of *t*-butanol/ water (12 mL, 2:1 v/v), was added 3-butyn-1-ol (907 μ L, 12.0 mmol), sodium ascorbate (238 mg, 1.20 mmol) and CuSO₄·5H₂O (30 mg, 0.12 mmol). The clear blue solution was stirred for 16 hours at r.t. The mixture was evaporated to dryness and re-dissolved in 1-butanol (20 mL). The organic layer was then washed with minimal aqueous potassium carbonate (0.1 M), brine and filtered over magnesium sulfate. Evaporation to dryness gave a white crude product, which was recrystallised from ethyl acetate: hexane to give fine white crystals (0.39 g, 62%). M.p: 165°C. [Lit. ⁽⁷⁾ m.p: 164 -166 °C]. ¹H NMR (400 MHz, DMSO-*d*₆) δ 7.96 (s, 1H, H-8), 7.86 (s, 1H, H-4), 6.88 (broad s, 2H, H-2), 5.38 (s, 2H, H-3), 4.68 (t, ³J = 5.2 Hz, 1H, H-7), 3.61 (td, ³J = 6.8, 5.2 Hz, 2H, H-6),

2.75 (t, $^3J = 6.8$ Hz, 2H, H-5), 2.31 (s, 3H, H-1). ^{13}C NMR (101 MHz, DMSO- d_6) δ 166.8, 161.4, 156.0, 144.5, 122.4, 108.4, 60.2, 46.4, 29.0, 25.2. IR ν_{max} cm^{-1} : 3400 (Broad OH) 3138, 1644, 1594, 1566 (C-H sp^2 stretch).

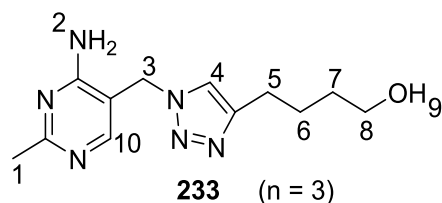
Synthesis of 2-[1-(4-amino-2-methylpyrimidin-5-ylmethyl)-1H-[1,2,3]triazol-4-yl]propanol



Following method A for 2-[1-(4-amino-2-methylpyrimidin-5-ylmethyl)-1H-[1,2,3]triazol-4-yl]ethanol:

To compound **153** (425 mg, 2.60 mmol) in *t*-butanol/ water (12 mL, 2: 1 v/v) was added 4-pentyn-1-ol (218 mg, 2.60 mmol), sodium ascorbate (52.0 mg, 0.26 mmol) and $\text{CuSO}_4 \cdot 5\text{H}_2\text{O}$ (6.50 mg, 0.03 mmol). The work up followed that from the previous method to give a light orange crude product (354 mg, 55%). This was recrystallised from ethanol to yield fluffy white crystals (209 mg, 33%). m.p: 200 – 202 °C. ^1H NMR (400 MHz, DMSO- d_6) δ 7.94 (s, 1H, H-9), 7.84 (s, 1H, H-4), 6.87 (brd s, 2H, H-2), 5.38 (s, 2H, H-3), 4.47 (t, $^3J = 4.8$ Hz, 1H, H-8), 3.42 (td, $^3J = 6.4, 4.8$ Hz, 2H, H-7), 2.63 (t, $^3J = 7.6$ Hz, 2H, H-5), 2.31 (s, 3H, H-1), 1.77 (quin, $^3J = 7.6$ Hz, 2H, H-6). ^{13}C NMR (101 MHz, DMSO- d_6) δ 166.8, 161.3, 155.9, 146.8, 121.8, 108.4, 59.9, 46.4, 32.2, 25.1, 21.5. IR ν_{max} cm^{-1} : 3414 (OH), 2950 (C-H, sp^3) 1667, 1597 and 1566 (C-H, sp^2 stretch). MS ESI (MeOH: NH_4OAc) [Found M + H] m/z 249.1460, $\text{C}_{11}\text{H}_{16}\text{N}_6\text{O}$, requires [M + H], m/z 249.1458].

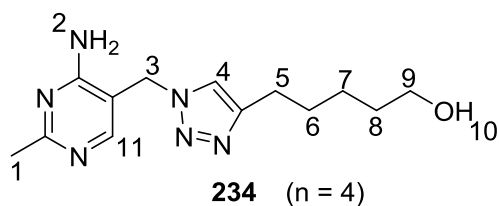
Synthesis of 2-[1-(4-amino-2-methylpyrimidin-5-ylmethyl)-1H-[1,2,3]triazol-4-yl]-butanol



Following method A of 2-[1-(4-amino-2-methylpyrimidin-5-ylmethyl)-1H-[1,2,3]triazol-4-yl]ethanol:

To compound **153** (362 mg, 2.21 mmol) in a solvent mixture of *t*-butanol/ water (12 mL, 2:1 v/v) was added 5-hexyn-1-ol (217 mg, 2.21 mmol), sodium ascorbate (44.0 mg, 0.22 mmol) and CuSO₄·5H₂O (5.00 mg, 0.02 mmol). The solvent was then removed under *vacuo* to give a viscous brown oil. The work up followed that of the previous method to give a soft white powder (0.50 g, 66%). m.p: 142 – 143 °C. ¹H NMR (500 MHz, DMSO-*d*₆) δ 7.95 (s, 1H, H-10), 7.86 (s, 1H, H-4), 6.89 (s, 2H, H-2), 5.39 (s, 2H, H-3), 4.39 (t, ³J = 5.2 Hz, 1H, H-9), 3.42 - 3.77 (m, 2H, H-8), 2.60 (t, ³J = 7.6 Hz, 2H, H-5), 2.31 (s, 3H, H-1), 1.64-1.55 (m, 2H, H-6), 1.48 – 1.42 (m, 2H, H-7). ¹³C NMR (126 MHz, DMSO-*d*₆) δ 167.3, 161.9, 156.4, 147.5, 122.3, 109.0, 60.6, 47.3, 32.4, 26.0, 25.6, 25.2. IR ν_{max}/cm⁻¹: 3405 (OH), 2935 (sp³ C-H stretch), 1675, 1645, 1600, 1556 (C-H sp² stretch). MS ESI+ (MeOH+NH₄OAc) [Found M + H⁺], *m/z* 263.1609, C₁₂H₁₈N₆O, requires [M + H], *m/z* 263.1615.

Synthesis of 2-[1-(4-amino-2-methylpyrimidin-5-ylmethyl)-1H-[1,2,3]triazol-4-yl]-pentanol

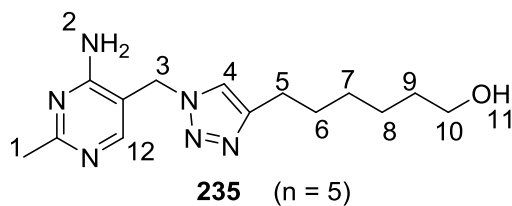


Following method A for 2-[1-(4-amino-2-methylpyrimidin-5-ylmethyl)-1H-[1,2,3]triazol-4-yl]ethanol:

To compound **153** (287 mg, 1.75 mmol) in a solvent mixture of *t*-butanol/ water (12 mL, 2:1 v/v) was added to 6-heptyne-1-ol (196 mg, 1.75 mmol), sodium ascorbate (35.7 mg, 0.18 mmol) and CuSO₄·5H₂O (5.00 mg, 0.017 mmol). The solvent was removed under *vacuo* to give brown oil

which after washing with minimal aqueous potassium carbonate (0.1 M) and brine gave after evaporation a yellow clay-like material. This was washed with dichloromethane to remove remaining unreacted starting material (393 mg, 51%). M.p: 139 – 141 °C. **¹H NMR** (500 MHz, DMSO-*d*₆) δ 7.95 (s, 1H, H-11), 7.85 (s, 1H, H-4), 6.88 (s, 2H, H-2), 5.38 (s, 2H, H-3), 4.34 (t, ³*J* = 5.5 Hz, 1H, H-10), 3.38 (td, ³*J* = 10.5, 5.5 Hz, 2H, H-9), 2.60 (t, ³*J* = 7.6 Hz, 2H, H-5), 2.32 (s, 3H, H-1), 1.62 – 1.53 (m, 2H, H-8), 1.49 – 1.40 (m, 2H, H-6), 1.36 – 1.28 (m, 2H, H-7). **¹³C NMR** (126 MHz, DMSO-*d*₆) δ 167.3, 161.9, 156.4, 147.5, 122.3, 108.9, 61.0, 46.9, 32.7, 29.3, 25.7, 25.6, 25.5. **IR** ν_{\max} / cm^{-1} : 3333 (OH), 3176, 2928 2857 (sp³ C-H stretch), 1651, 1598, 1563 (sp² C-H stretch aromatic). **MS** ESI+ (MeOH+NH₄OAc) [Found M + H⁺] *m/z* 277.1770, C₁₃H₂₀N₆O, requires [M + H], *m/z* 277.1771.

Synthesis of 2-[1-(4-amino-2-methylpyrimidin-5-ylmethyl)-1*H*-[1,2,3]triazol-4-yl]-hexanol



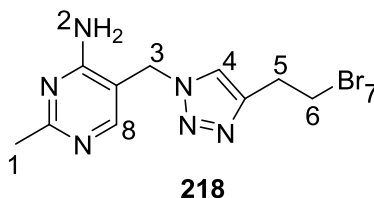
Following method A for 2-[1-(4-amino-2-methylpyrimidin-5-ylmethyl)-1*H*-[1,2,3]triazol-4-yl]ethanol:

To compound **153** (397 mg, 2.42 mmol) in a solvent mixture of t-butanol/ water (12 mL, 2:1 v/v) was added 7-octyne-1-ol (305 mg, 2.42 mmol), sodium ascorbate (48.0 mg, 0.240 mmol) and CuSO₄·5H₂O (6.00 mg, 0.024 mmol). The solvent was removed under *vacuum* to give a red/brown oil which was dissolved in dichloromethane/methanol, mixed with activated charcoal and filtered over celite. After further washes with MeOH and evaporation to dryness, a crude white clay material was obtained. Recrystallisation in isopropanol/hexane gave a fluffy white powder (271 mg, 40%). m.p: 126 – 128 °C. **¹H NMR** (500 MHz, DMSO-*d*₆) δ 7.95 (s, 1H, H-12), 7.85 (s, 1H, H-4), 6.88 (s, 2H, H-2), 5.38 (s, 2H, H-3), 4.33 (t, ³*J* = 5.0 Hz, 1H, H-11), 3.38 (td, ³*J* = 6.5, 5.0 Hz, 2H, H-10), 2.59 (t, ³*J* = 7.6 Hz, 2H, H-5), 2.31 (s, 3H, H-1), 1.60 – 1.54 (m, 2H, H-6), 1.43-1.48 (m, 2H, H-9), 1.32-1.27 (m, 4H, H-7, 8). **¹³C NMR** (126 MHz, DMSO-*d*₆) δ 167.3, 161.9, 156.3, 147.5, 122.3, 108.9, 61.1, 46.9, 32.9, 29.4, 28.9, 25.9, 25.7, 25.4. **IR** ν_{\max}

$\nu_{\text{cm}^{-1}}$: 3334 (OH), 2927, 2864 (sp^3 C-H stretch), 1655, 1651, 1599 (sp^2 C-H aromatic stretch).

MS ESI+ (MeOH+NH₄OAc); [Found: [M+H] m/z 291.1928, C₁₄H₂₂N₆O, requires [M+H] m/z 291.1928.

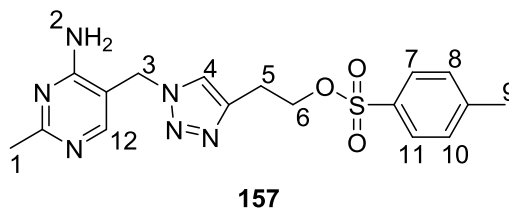
Synthesis of 2-bromo[1-(4-amino-2-methylpyrimidin-5-ylmethyl)-1H-[1,2,3] triazol-4-yl]ethane



Following method A for 2-[1-(4-amino-2-methylpyrimidin-5-ylmethyl)-1H-[1, 2, 3 triazol-4-yl]ethanol:

To a flame dried round-bottomed-flask was added compound **153** (643 mg, 3.92 mmol) in a solvent mixture of *t*-butanol/ water (12 mL, 2: 1 v/v). To this were added 3-bromo-1-butyne (521 mg, 3.92 mmol), CuSO₄·5H₂O (9.70 mg, 0.039 mmol) and sodium ascorbate (77.3 mg, 0.39 mmol). The clear blue solution was stirred for 16 hours at r.t. The mixture was evaporated to dryness and re-dissolved in 1-butanol (10 mL). The organic layer was washed with minimal aqueous potassium carbonate (0.1 M), brine and dried over magnesium sulphate and filtered. The organic layer was evaporated to dryness to give a brown-yellow crude product. This was hot filtered with ethanol to give a fine pale brown powder (876 mg, 76%). M.p: 143 - 146 °C. **¹H NMR** (400 MHz, DMSO-*d*₆) δ 7.98 (s, 1H, H-8), 7.95 (s, 1H, H-4), 6.90 (s, 2H, H-2), 5.42 (s, 2H, H-3), 3.73 (t, ³*J* = 6.9 Hz, 2H, H-6), 3.19 (t, ³*J* = 6.9 Hz, 2H, H-5), 2.32 (s, 3H, H-1). **¹³C NMR** (101 MHz, DMSO-*d*₆) δ 166.7, 161.4, 155.5, 144.1, 122.7, 108.5, 82.7, 55.9, 46.5, 25.0. **IR** ν_{max} $\nu_{\text{cm}^{-1}}$: 3108, 3064 (C-H, sp^3) 1654, 1594 and 1554 (C-H, sp^2 stretch). **MS** ESI+ (MeOH+NH₄OAc); [Found: [M+H] m/z 297.0453, C₁₀H₁₃N₆Br, requires [M+H] m/z 297.0458. [Found: [M+2] m/z 299.0437, C₁₀H₁₃N₆Br, requires [M+H] m/z 299.0437 (1:1 ratio).

Synthesis of 2-[1-(4-amino-2-methylpyrimidin-5-ylmethyl)-1H-[1,2,3]triazol-4-yl] ethyl toluene-4-sulfonate ^{(6), (7), (8)}



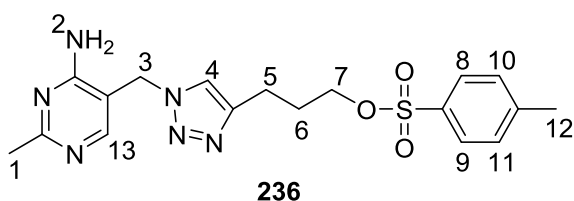
Following method A for 2-[1-(4-amino-2-methylpyrimidin-5-ylmethyl)-1H-[1,2,3 triazol-4-yl]ethanol:

To a flame dried round-bottomed flask was added compound **153** (217 mg, 1.32 mmol) in a solvent mixture of *t*-butanol/ water (6.0 mL, 2:1 v/v). To this but-3-ynyl toluene-4-sulfonate (297 mg, 1.32 mmol), CuSO₄·5H₂O (30 mg, 0.12 mmol) and sodium ascorbate (238 mg, 1.20 mmol) were added. The clear yellow solution was stirred for 16 hours at r.t. The mixture was evaporated to dryness and re-dissolved in 1-butanol (10 mL). The organic layer was washed with minimal aqueous potassium carbonate (0.1 M) and brine. The organic layer dried over magnesium sulphate, filtered and concentrated to give a white crude product. Recrystallisation with ethyl acetate: hexane gave clumpy yellow crystals (0.91 g, 60%). m.p: 88-90 °C, [Lit. ⁽⁷⁾ m.p: 86-88 °C].

¹H NMR (400 MHz, DMSO-*d*₆) δ 7.97 (s, 1H, H-12), 7.88 (s, 1H, H-4), 7.71 (d, ³*J* = 8.0 Hz, 2H, H-7, 11), 7.44 (d, ³*J* = 8.0 Hz, 2H, H-8, 10), 6.99 (s, 2H, H-2), 5.40 (s, 2H, H-3), 4.22 (t, ³*J* = 6.4 Hz, 2H, H-6), 2.96 (t, ³*J* = 6.4 Hz, 2H, H-5), 2.42 (s, 3H, H-1), 2.32 (s, 3H, H-9). **¹³C NMR** (101 MHz, DMSO-*d*₆) δ 166.6, 161.4, 155.6, 144.9, 142.1, 132.1, 130.1, 127.5, 122.9, 108.3, 69.4, 46.4, 25.4, 25.0, 21.0. **IR** ν_{max} /cm⁻¹: 3108 and 3065 (NH₂), 1644, 1594, 1566 (C-H sp² stretch).

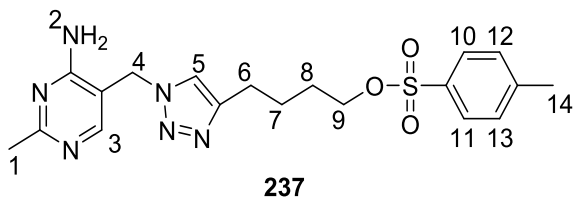
MS ESI+ (MeOH+NH₄OAc); [Found: [M+H] *m/z* 389.1392, C₁₇H₂₀N₆O₃, expected [M+H] *m/z* 389.1392.

Synthesis of 3-(1-(4-amino-2-methylpyrimidin-5-yl)methyl)-1H-[1,2,3]-triazol-4-yl)propyl 4-methylbenzenesulfonate



To a flame dried round-bottomed flask was added compound **153** (550 mg, 3.35 mmol) in a solvent mixture of *t*-butanol/ water (12 mL, 2:1 v/v). 5-hexyn-1-tosylate (844 mg, 3.35 mmol), CuSO₄·5H₂O (8.5 mg, 0.033 mmol) and sodium ascorbate (66 mg, 0.34 mmol) were then added. The orange/brown solution was stirred at 30 °C for 16 hours and then evaporated to dryness. Filtration over activated charcoal and trituration with ethyl acetate removed any remaining small impurities to yield a viscous yellow oil (619 mg, 46%). ¹H NMR (500 MHz, CDCl₃) δ 8.95 (s, 1H, H-3), 8.24 (s, 1H, H-5), 7.73 (d, ³J = 7.0 Hz, 2H, H-8, 9), 7.18 (d, ³J = 7.0 Hz, 2H, H-10, 11), 6.50 (br s, 2H, H-2), 5.88 (s, 2H, H-3), 4.62 (t, ³J = 7.5 Hz, 2H, H-7), 3.26 (t, ³J = 7.5 Hz, 2H, H-5), 2.94 – 2.85 (m, 2H, H-6), 2.52 (s, 3H, H-1), 2.37 (s, 3H, H-12). ¹³C NMR (126 MHz, CDCl₃) δ 169.3, 162.1, 158.1, 146.7, 142.8, 139.8, 128.8, 125.9, 125.7, 104.7, 52.2, 50.4, 26.3, 25.6, 22.5, 21.3. IR ν_{max} /cm⁻¹: 3336 and 3189 (sp³ C-H stretch), 1653, 1597, 1560 (C-H sp² stretch), 1030 (SO₂). MS NSI+ (MeOH+NH₄OAc); [Found: [M-OTs]⁺ m/z 231.1351, C₁₁H₁₅N₆ required C₁₁H₁₅N₆ [M-OTs]⁺ m/z 231.1353.

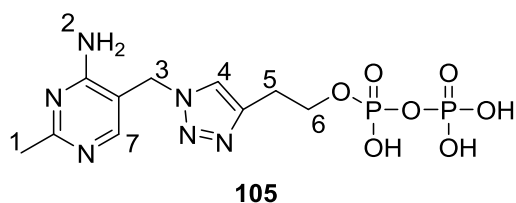
Synthesis of 3-(1-(4-amino-2-methylpyrimidin-5-ylmethyl)-1H-[1,2,3]-triazol-4-yl)-butyl 4-methylbenzenesulfonate



To a flame dried round-bottomed flask was added compound **153** (500 mg, 3.00 mmol) in a solvent mixture of *t*-butanol/ water (12 mL, 2:1 v/v). To this were added 5-hexyn-1-tosylate (7.56 mg, 3.00 mmol), CuSO₄·5H₂O (7.47 mg, 0.030 mmol) and sodium ascorbate (60.0 mg, 0.30 mmol). The orange/brown solution was stirred at 30 °C for 16 hours and was then evaporated

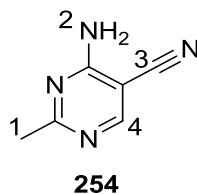
to dryness give a brown crude product. Filtration over activated charcoal and trituration with ethyl acetate removed any remaining small impurities to yield a pale yellow oil (1.35 g, 96%). **¹H NMR** (500 MHz, CDCl₃) δ 8.91 (s, 1H, H-3), 8.21 (s, 1H, H-5), 7.68 (d, ³J = 8.0 Hz, 2H, H-10, 11), 7.13 (d, ³J = 8.0 Hz, 2H, H-12, 13), 6.63 (s, 2H, H-2), 5.82 (s, 2H, H-3), 4.40 (t, ³J = 6.3 Hz, 2H, H-9), 2.94 (t, ³J = 6.3 Hz, 2H, H-6), 2.44 (s, 3H, H-1), 2.32 (s, 3H, H-14), 2.17 – 2.10 (m, 2H, H-8), 1.98 – 1.90 (m, 2H, H-7). **¹³C NMR** (126 MHz, CDCl₃) δ 162.2, 157.8, 142.9, 139.9, 139.7, 129.8, 128.7, 128.5, 125.7, 104.0, 51.5, 48.9, 25.5, 21.4, 21.3, 20.2, 18.0. **IR** ν_{max} /cm⁻¹: 3351, 3220 (NH₂), 1658, 1597, 1560 (C-H sp² stretch). **MS** ESI+ (MeOH+NH₄OAc); [Found: M+H] *m/z* 417.1694, required C₁₉H₂₄N₆O₃S [M+H] *m/z* 417.1703.

Synthesis of 2-(1-(4-amino-2-methylpyrimidin-5-yl)methyl)-1H-[1,2,3]-triazol-4-yl)ethyl diphosphate ^{(6), (7)}



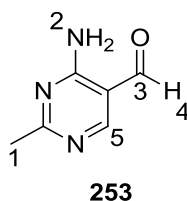
To a stirred solution of the corresponding tosylate **155** (20 mg, 0.05 mmol) in anhydrous acetonitrile (150 μL) at -10 °C was added *tris*(tetrabutylammonium) hydrogen pyrophosphate (93 mg, 0.10 mmol). The reaction was allowed to stir at room temperature under argon for 24 hours and then diluted with water (5 mL). This was purified; firstly by DEAE anion exchange with an increasing ammonium bicarbonate concentration (0 – 0.25 M), and then with DOWEX 50 H⁺. After elution with aqueous ammonia (1M) and lyophilisation, a white ammonium salt was recovered (45 mg, 23%). m.p: 200 – 203. [Lit. ⁽⁷⁾ m.p: 209-211 °C]. **¹H NMR** (400 MHz, D₂O) δ 8.02 (s, 1H, H-7), 7.93 (s, 1H, H-4), 5.40 (s, 2H, H-3), 4.07 (q, ³J = 6.6 Hz, 2H, H-6), 2.97 (t, ³J = 6.4 Hz, 2H, H-5), 2.34 (s, 3H, H-1). **¹³C NMR** (126 MHz, D₂O) δ 167.8, 161.8, 155.6, 145.4, 124.3, 108.4, 64.3, 47.6, 26.4, 23.8. **³¹P** (400 MHz, D₂O) – 6.59 and – 10.80 (each 1P, s, OPOPO). **IR** ν_{max} /cm⁻¹: 1674, 1602 and 1078 (C-H, sp² stretch), 807. **MS** ESI- (MeOH); [Found M - H⁺] *m/z* 393.0478, required C₁₀H₁₃N₆O₇P₂ [M - H] *m/z* 393.0483.

Synthesis of 2-methyl-4-aminopyrimidine carbonitrile ⁽⁹⁾



To a flame dried round-bottomed was added acetamide hydrochloride (0.80 g, 8.50 mmol) and NaOEt (2M) (4.0 mL), previously formed by adding sodium (0.18 g) to ethanol (4.0 mL). The solution was filtered over celite to give a clear solution, which upon addition of ethoxymethylene malonitrile (0.50 g, 4.10 mmol) produced a yellow precipitate. Recovery and subsequent recrystilisation from ethanol gave fluffy yellow needles (1.10 g, 70%). M.p 245-247 °C [Lit. ⁽⁹⁾ m.p: 246-248 °C]. ¹H NMR (500 MHz, DMSO-*d*₆) δ 8.52 (s, 1H, H-4), 7.77 (s, 2H, H-2), 2.40 (s, 3H, H-1). ¹³C NMR (126 MHz, DMSO-*d*₆). δ 170.5, 162.8, 161.5, 116.1, 87.1, 26.4. IR ν_{\max} /cm⁻¹: 3378, 3334 (NH₂), 2223 (CN), 1672, 1584, 1542 (C-H, sp² stretch).

Synthesis of 2-methyl-4-aminopyrimidine carbaldehyde



Method A – Raney Nickel ⁽¹⁰⁾

To nitrile **254** (500 mg, 3.73 mmol) was added activated Raney nickel in formic acid (98%, 50 mL). This was allowed to stir at 80 - 100 °C for 3 hours. After filtration through celite which was then washed with 3:2 v/v ethanol: water (3 x 30 mL), the combined filtrate was concentrated under vacuum to remove residual ethanol. The aqueous residue was neutralised with aqueous sodium hydrogen carbonate, extracted with ethyl acetate (3 x 10 mL) and dried over magnesium sulfate. Filtration and evaporation to dryness produced an off-white powder. Further purification by chromatography on silica with a mobile phase of ethyl acetate: hexane 1:2 v/v, gave the aldehyde as a white powder (51 mg, 10 %).

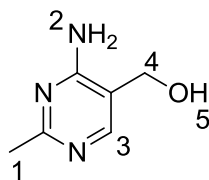
Method B – Lithium aluminium hydride reduction⁽¹¹⁾

To nitrile **254** (500 mg, 3.64 mmol) in THF (50 mL) was added lithium aluminium hydride (147 mg, 3.73 mmol) at -10 °C in small portions. The mixture was stirred at this temperature for approx. 90 minutes and slowly quenched with methanol (25 mL). Solvent was then removed in *vacuo* and the remaining mixture was purified by column chromatography on silica using a mobile phase of ethyl acetate/MeOH (95: 5 v/v) to afford a white powder (149 mg, 30%).

Method C – Hydrogenation⁽¹²⁾

To nitrile **254** (500 mg, 3.64 mmol) and activated charcoal (10% Pd/C) (40.8 mg, 0.38 mmol) was added a solution of water (4.0 mL) and concentrated sulfuric acid (800 uL). This was hydrogenated at 45-50 psi overnight at room temperature. The black solution was then filtered through celite, which was then washed with water (2 x 10 mL). To the combined filtrate was added ammonium hydroxide (35%) solution, producing a white precipitate almost immediately. This was collected by vacuum filtration and washed thoroughly with water. Flash column chromatography on silica using a mobile phase of ethyl acetate: MeOH (95:5 v/v) gave the aldehyde as a white solid (269 mg, 54%). M.p: 190 - 192 °C [Lit.⁽¹²⁾ m.p: 192 - 194 °C]. **¹H NMR** (400 MHz, DMSO-*d*₆) δ 9.83 (1H, s, H-4), 8.65 (1H, s, H-5), 8.16 (1H, br s, H-2), 7.91 (1H, br s, H-2) 2.42 (3H, s, H-1). **¹³C NMR** (101 MHz, DMSO) δ 192.4, 171.2, 164.1, 160.6, 109.8, 26.0. **IR** ν_{\max} /**cm**⁻¹: 3370, 3288 (NH₂), 3135 (C-H sp³), 1676, 1641 and 1537 (C-H, aromatic sp² stretch). **MS** [Found: [M+H⁺] *m/z* 138.0661, C₆H₇N₃OH requires [M+H⁺] *m/z* 138.0662.

Synthesis of 2-methyl-4-aminopyrididin-5-yl methanol⁽¹¹⁾

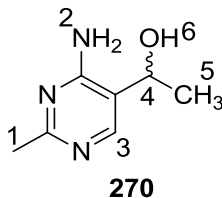


257

To a solution of **253** (200 mg, 1.46 mmol) in MeOH (20 mL) was added sodium borohydride (77.3 mg, 2.05 mmol) at r.t. and left to stir overnight. The reaction was then quenched with ice and evaporated to dryness. The solid was recrystallized from ethanol to give a white powder (113 mg, 56%). M.p: 190 - 192 °C. [Lit.⁽¹¹⁾ m.p: 198-199 °C]. **¹H NMR** (500 MHz, DMSO-*d*₆) δ 7.94

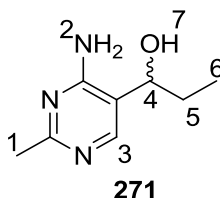
(s, 1H, H-3), 6.50 (s, 2H, H-2), 5.07 (s, 1H, H-5), 4.32 (s, 2H, H-4), 2.31 (s, 3H, H-1). ^{13}C NMR (126 MHz, DMSO- d_6) δ 165.8, 161.9, 153.3, 114.1, 58.2, 25.6. IR $\nu_{\text{max}}/\text{cm}^{-1}$: 3365 (OH), 3130 (sp^3 C-H stretch), 1650, 1602, 1567 (sp^2 C-H stretch).

Synthesis of (+/-)-1-(4-amino-2-methylpyrimidin-5-yl)ethanol ⁽¹³⁾



To aldehyde **253** (10 mg, 0.073 mmol) in dry THF (5.0 mL), under an inert atmosphere of nitrogen was added methylmagnesium bromide (85 μL , 3M, 3.5 eq.) at 0 $^{\circ}\text{C}$. The reaction mixture was allowed to warm to r.t and then stirred overnight. The reaction was quenched with ice water (10 mL), extracted with ethyl acetate (3 x 10 mL), 1-butanol (10 mL) and brine (10 mL). Drying over magnesium sulphate, filtration and concentration under vacuum furnished a yellow oil. Column chromatography on silica with a mobile phase of ethyl acetate: MeOH (95:5 v/v) gave a white solid (6.8 mg, 61 %). M.p: 145 - 147 $^{\circ}\text{C}$. ^1H NMR (500 MHz, DMSO- d_6) δ 7.97 (s, 1H, H-3), 6.49 (s, 2H, H-2), 5.26 (d, $^3J = 4.2$ Hz, 1H, H-6), 4.71 (quin, $^3J = 6.5$ Hz, 1H, H-4), 2.29 (s, 3H, H-1), 1.30 (d, $^3J = 6.5$ Hz, 3H, H-5). ^{13}C NMR (126 MHz, DMSO- d_6) δ 165.49, 161.13, 151.14, 118.67, 63.72, 26.13, 22.82. IR $\nu_{\text{max}}/\text{cm}^{-1}$: 3312 (OH brd), 1671, 1605 and 1536 (C-H, sp^2 stretch). MS ESI (MeOH: NH_4OAc); [Found: $\text{M}+\text{H}^+$] m/z 154.0972, $\text{C}_7\text{H}_{11}\text{N}_3\text{OH}$ requires $[\text{M}+\text{H}^+]$ m/z 154.0975.

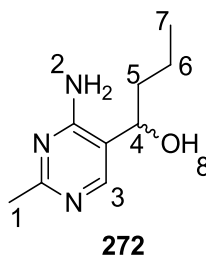
Synthesis of (+/-)-1-(4-amino-2-methylpyrimidin-5-yl)propanol



Following the procedure for (+/-)-1-(4-amino-2-methylpyrimidin-5-yl)ethanol:

To the aldehyde **253** (50 mg, 0.36 mmol) in dry THF (25 mL), under an inert atmosphere of nitrogen at 0 °C was added ethylmagnesium bromide (420 μ L, 3M, 3.5 eq.). This was worked up as described previously to give a pale yellow solid. Chromatography with ethyl acetate: methanol (90:10 v/v) gave a white powder (59 mg, 44%). M.p: 185 - 187 °C. **¹H NMR:** (500 MHz, DMSO-*d*₆) δ 7.93 (s, 1H, H-3), 6.47 (s, 2H, H-2), 5.26 (d, ³*J* = 4.3 Hz, 1H, H-7), 4.45 (q, ³*J* = 6.5 Hz, 1H, H-4), 2.29 (s, 3H, H-1), 1.66 – 1.55 (m, 2H, H-5), 0.84 (t, ³*J* = 7.4 Hz, 3H, H-6). **¹³C NMR:** (126 MHz, DMSO-*d*₆) δ 165.2, 161.2, 152.6, 117.0, 69.2, 29.0, 25.5, 10.4. **IR** ν_{max} / cm^{-1} : 3321, 3173 (NH₂), 2926, 2964 (sp³ C-H stretch), 1644, 1594, 1446 (sp² C-H stretch). **MS:** ESI+ (MeOH+NH₄OAc); [Found: [M+H] *m/z* 168.1128, C₈H₁₂N₃O, required [M+H] *m/z* 168.1131.

Synthesis of (+/-)-1-(2-methyl-4-aminopyrimidin-5-yl)butanol

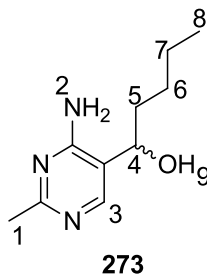


Following the procedure for (+/-)-1-(4-amino-2-methylpyrimidin-5-yl)ethanol:

To aldehyde **253** (200 mg, 1.5 mmol) in dry THF (25 mL), under an inert atmosphere of nitrogen was added propylmagnesium bromide (2.3 mL, 2M, 3.5 eq.) at 0 °C. This was worked up as described previously to give a pale yellow solid. Purification by column chromatography, eluting with ethyl acetate: methanol (90:10 v/v) gave a white powder (143 mg, 68%). M.p: 203 - 205 °C. **¹H NMR** (500 MHz, DMSO-*d*₆) δ 7.93 (s, 1H, H-3), 6.47 (s, 2H, H-2), 5.26 (d, ³*J* = 4.3 Hz, 1H, H-8), 4.53 (q, ³*J* = 6.5 Hz, 1H, H-4), 2.30 (s, 3H, H-1), 1.61 – 1.54 (m, 2H, H-5), 1.40 – 1.32 (m,

1H, H-6), 1.30 – 1.21 (m, 1H, H-6), 0.88 (t, $^3J = 7.4$ Hz, 3H, H-7). $^{13}\text{C NMR}$ (126 MHz, DMSO- d_6) δ 165.2, 161.2, 152.6, 117.2, 68.0, 38.3, 25.5, 18.9, 14.4. **IR** $\nu_{\text{max}}/\text{cm}^{-1}$: 3359 (OH), 3181 (sp^3 C-H stretch), 2954, 2933, 1656, 1557, 1597 (sp^2 C-H stretch). **MS** ESI+ (MeOH+NH₄OAc); [Found: [M+H] m/z 182.1285, C₉H₁₅N₃O, requires [M+H] m/z 182.1288.

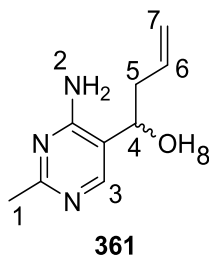
Synthesis of (+/-)-1-(2-methyl-4-aminopyrimidin-5-yl)pentanol



Following the procedure for (+/-)-1-(4-amino-2-methylpyrimidin-5-yl)ethanol:

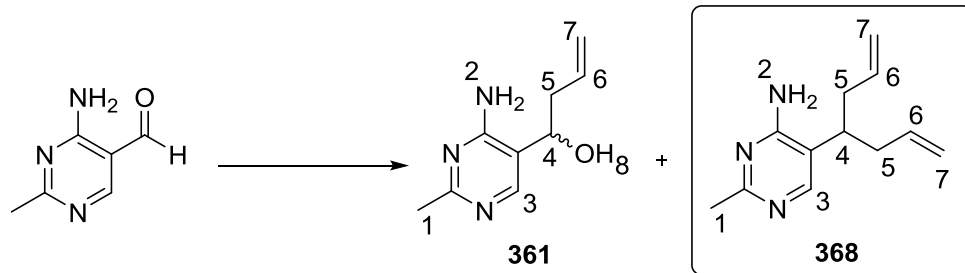
To aldehyde **253** (1.0 g, 7.30 mmol, 1.0 eq) in THF (50 mL) at 0°C was added butylmagnesium bromide (12.7 mL, 2M, 3.5 eq). This was then allowed to warm to r.t. and stirred for approx. 24 hours. This was worked up as described previously to give a pale white solid. Chromatography with ethyl acetate: methanol (90:10 v/v) gave a white powder (777 mg, 55%). M.p: 166-168 °C. $^1\text{H NMR}$ (500 MHz, DMSO- d_6) δ 7.93 (s, 1H, H-3), 6.47 (s, 2H, H-2), 5.27 (d, $^3J = 4.3$ Hz, 1H, H-9), 4.52 (td, $^3J = 6.5$ Hz, 4.3 Hz, 1H, H-4), 2.30 (s, 3H, H-1), 1.60-1.56 (m, 2H, H-5), 1.36 – 1.25 (m, 2H, H-6), 1.23 – 1.17 (m, 2H, H-7), 0.86 (t, $^3J = 7.1$ Hz, 3H, H-8). $^{13}\text{C NMR}$ (126 MHz, DMSO- d_6) δ 165.2, 161.2, 152.6, 117.3, 68.2, 35.9, 27.9, 25.5, 22.6, 14.4. **IR** $\nu_{\text{max}}/\text{cm}^{-1}$: 3386, (OH), 3173 (sp^3 C-H stretch), 1645, 1590, 1555 (sp^2 C-H stretch). **MS** ESI+ (MeOH+NH₄OAc); Found: [M+H] m/z 196.1442, C₁₀H₁₇N₃O, expected [M+H] m/z 196.1444.

Synthesis of (+/-)-1-(2-methyl-4-aminopyrimidine-3-en-5-yl)butanol



To aldehyde **253** (209 mg, 1.52 mmol, 1.0 eq) was added allylmagnesium bromide (1M) (772 mg, 5.34 mmol, 3.5 eq.) in THF (5 mL) at 0 °C. This gave a creamy white solution which was then brought to r.t. and stirred overnight. The reaction was quenched with ice water, extracted with ethyl acetate (3 x 10 mL), 1-butanol (10 mL), and dried over magnesium sulfate. Filtration and evaporation gave a crude product which was purified by column chromatography on silica, using a mobile phase of neat ethyl acetate to give the product as a fine white powder (74 mg, 27%). M.p: 172-173°C. ¹H NMR (500 MHz, DMSO-*d*₆) δ 7.93 (s, 1H, H-3), 6.50 (s, 2H, H-2), 5.78 (ddt, ³J = 17.4, 10.4, 7.0 Hz, 1H, H-6), 5.37 (d, ³J = 4.3 Hz, 1H, H-8), 5.02-5.00 (m, 1H, H-7), 5.00 (m, 1H, H-7) 4.62 (td, *J* = 17.5, 4.5 Hz 1H, H-4), 2.42 – 2.37 (m, 2H, H-5), 2.30 (s, 3H, H-1). ¹³C NMR (126 MHz, DMSO-*d*₆) δ 165.3, 161.0, 152.6, 135.4, 117.6, 116.6, 67.7, 40.5, 25.7. IR ν_{max} /cm⁻¹: 3370 (OH), 3151, 1651, 1593, 1557, 1427 (sp² C-H stretch). MS (MeOH/NH₄OAc); [Found: [M+H⁺] *m/z* 180.1129, C₉H₁₄N₃O requires [M+H⁺] *m/z* 180.1131.

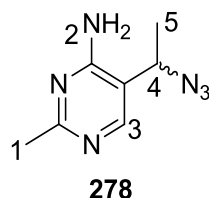
Synthesis of 2-methyl-4-amino-5-dipropene pyrimidine



Quantities and Conditions as following the Synthesis of (+/-) 2-methyl-4-aminopyrimidine-3-ene-butanol:

Yield (46 mg, 15%). **Mpt:** 78 – 80 °C. **¹H NMR** (500 MHz, CDCl₃) δ 7.93 (s, 1H, H-3), 5.66-5.55 (m, 2H, H-6), 5.10 (s, 2H, H-2), 5.00 (d, ³J = 10 Hz, 2H, H -7), 4.96 (d, ³J = 10 Hz, 2H, H-7), 2.45 (s, 3H, H-1), 2.38-2.35 (m, 2H, H-5), 2.30-2.27 (m, 2H, H-5). **¹³C NMR** (126 MHz, CDCl₃) δ 164.6, 161.5, 152.5, 135.1, 117.8, 116.2, 38.6, 37.1, 24.6. **IR** ν_{max} /cm⁻¹: 3324 (OH), 3182, 3076, 2925 C-H sp³ stretch), 1641, 1589, 1557 (sp² C-H stretch). **MS** [Found: [M+H⁺] m/z 204.1493 100%, C₁₂H₁₈N₃ requires [M+H⁺] m/z 204.1495.

Synthesis of (+/-)-1-(2-methyl-4-aminopyrimidin-5-ylethyl azide)⁽¹¹⁾

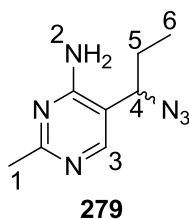


In a flame dried round-bottomed flask was added the corresponding compound **270** (44 mg, 0.28 mmol) in THF (10 mL) to form a grey solution. To this were added DBU (54 uL, 0.36 mmol, 1.3 eq) and DPPA (73 uL, 0.34 mmol, 1.2 eq). The reaction mixture was left to stir overnight at r.t. and then quenched with water (5 mL), extracted with ethyl acetate (3 x 5 mL) and 1-butanol (10 mL). The combined organic phases were washed with water (10 mL), brine (10 mL), dried over magnesium sulfate and filtered. Evaporation in *vacuo* gave a white solid which was purified by column chromatography on silica with a mobile phase of ethyl acetate: methanol (90:10 v/v), to produce a shiny white compound (28 mg, 49%). **M.p:** 118 - 120°C. **¹H NMR** (500 MHz, DMSO-*d*₆) δ 8.07 (s, 1H, H-3), 6.82 (s, 2H, H-2), 4.84 (q, ³J = 6.8 Hz, 1H, H-4), 2.32 (s, 3H, H-1), 1.48 (d, ³J = 6.8 Hz, 3H, H-5). **¹³C NMR** (126 MHz, DMSO-*d*₆) δ 166.7, 161.3, 153.2, 112.5, 54.1,

25.6, 18.6. **IR** ν_{\max} / cm^{-1} : 3316, 3141 (NH_2), 2095 (N_3) 1646, 1585 and 1553 (C-H, sp^2 stretch).

MS Found: $[\text{M}+\text{H}^+]$ m/z 179.1036 100%, $\text{C}_7\text{H}_{10}\text{N}_6$ requires $[\text{M}+\text{H}^+]$ m/z 179.1040.

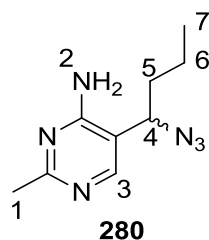
Synthesis of (+/-)-1-(2-methyl-4-aminopyrimidin-5-yl)propyl azide



Following procedure of (+/-)-1-(2-methyl-4-aminopyrimidin-5-yl)ethyl azide:

In a flame dried round-bottomed flask was added ethyl alcohol **271** (650 mg, 3.89 mmol, 1.0 eq) in THF (10 mL). To this was sequentially added DBU (755 μL , 5.06 mmol, 1.3 eq) and DPPA (1.0 mL, 4.67 mmol, 1.2 eq). The mixture was left to stir overnight at r.t and then quenched with water (5mL), extracted with ethyl acetate (3 x 5 mL) and 1-butanol (10 mL). The combined organic phases were washed with water (10 mL), brine (10 mL), dried over magnesium sulfate and filtered. Evaporation in *vacuo* gave a white solid which was purified by chromatography using a mobile phase of ethyl acetate: methanol (90:10 v/v). This produced a shiny white compound (194 mg, 49%). M.p: 106 – 108 °C. **^1H NMR** (500 MHz, CDCl_3) δ 8.05 (s, 1H, H-3), 5.44 (s, 2H, H-2), 4.28 (t, $^3J = 7.5$ Hz, 1H, H-4), 2.01 – 1.92 (m, 1H, H-5), 1.91 – 1.83 (m, 1H, H-5), 1.01 (t, $^3J = 7.5$ Hz, 3H, H-6). **^{13}C NMR** (126 MHz, CDCl_3) δ 167.3, 160.7, 153.8, 111.5, 64.5, 25.8, 25.3, 11.1. **IR** ν_{\max} / cm^{-1} : 3321, 3165 (NH_2), 2098 (N_3), 1643, 1590, 1557 (sp^2 C-H stretch). **MS** Found: $[\text{M}+\text{H}^+]$ m/z 193.1195 100%, $\text{C}_8\text{H}_{12}\text{N}_6$ requires $[\text{M}+\text{H}^+]$ m/z 193.1196.

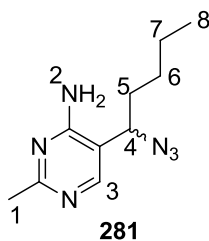
Synthesis of (+/-)-1-(2-methyl-4-aminopyrimidin-5-yl)butyl azide



Following procedure for (+/-)-1-(2-methyl-4-aminopyrimidine-5-yl ethyl azide:

In a flame dried round-bottomed flask was added propyl alcohol **272** (630 mg, 3.48 mmol) in anhydrous THF (10 mL). To this were sequentially added DBU (675 μ L, 4.52 mmol, 1.3 eq) and DPPA (900 μ L, 4.17 mmol, 1.2 eq) at r.t. The reaction was then worked up as previously described to give a white powder (321 mg, 45%). M.p: 218 – 220 °C. **¹H NMR** (500 MHz, DMSO-*d*₆) δ 8.05 (s, 1H, H-3), 6.82 (s, 2H, H-2), 4.75 (t, ³*J* = 7.7 Hz, 1H, H-4), 2.34 (s, 3H, H-1), 1.82 – 1.71 (m, 2H, H-5), 1.40 – 1.25 (m, 2H, H-6), 0.91 (t, ³*J* = 7.4 Hz, 3H, H-7). **¹³C NMR** (126 MHz, DMSO-*d*₆) δ 166.7, 161.6, 154.1, 111.7, 58.8, 35.0, 25.6, 19.5, 13.9. **IR** ν_{max} / cm^{-1} : 3332, 3134 (NH₂), 2091 (N₃) 1657, 1586, 1554 (sp² C-H stretch). **MS** [Found: [M+H⁺] *m/z* 207.1351 100%, C₉H₁₄N₆ requires [M+H⁺] *m/z* 207.1353.

Synthesis of (+/-)-1-(2-methyl-4-aminopyrimidin-5-yl)pentyl azide

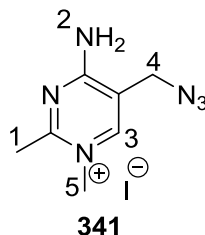


Following procedure for (+/-)-1-(2-methyl-4-aminopyrimidin-5-yl)ethyl azide:

In a flame dried round-bottomed flask was added the butyl alcohol **273** (777 mg, 3.98 mmol) in anhydrous THF (10 mL). To this were sequentially added DBU (773 μ L, 5.18 mmol, 1.3 eq) and DPPA (1.03 mL, 4.78 mmol, 1.2 eq) at r.t. The reaction was then worked up as previously described. The crude material was purified by column chromatography on silica with a mobile phase of ethyl acetate: methanol (95:5 v/v) to give the product as shiny white crystals (656 mg, 59%), Mpt: 86 - 90°C. **¹H NMR** (500 MHz, DMSO-*d*₆) δ 8.05 (s, 1H, H-3), 6.82 (s, 2H, H-2),

4.74 (t, $^3J = 7.2$ Hz, 1H, H-4), 2.33 (s, 3H, H-1), 1.83 – 1.75 (m, 2H, H-5), 1.36 – 1.22 (m, 4H, H- 6, 7), 0.88 (t, $^3J = 7.2$ Hz, 3H, H-8). $^{13}\text{C NMR}$ (126 MHz, DMSO- d_6) δ 166.7, 161.5, 153.7, 111.5, 58.9, 32.8, 28.5, 25.5, 22.0, 14.5. **IR** $\nu_{\text{max}}/\text{cm}^{-1}$: 3139, 2930 (NH₂), 2088 (N₃), 1650, 1587, 1551, 1471 (sp² C-H stretch). **MS** [Found: [M+H⁺] m/z 221.1508, 100%, C₁₀H₁₆N₆ requires [M+H⁺] m/z 221.1509.

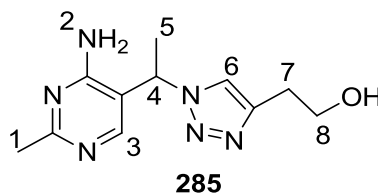
Synthesis of 1-*N*-(methyl)-2-methyl-4-amino pyrimidin-5-ylmethyl azide



To compound **153** (277 mg, 1.68mmol) in THF (10 mL) was added MeI (0.32 mL, 2.06 mmol) dropwise. The reaction was stirred overnight at r.t to give a creamy/white precipitate which was collected by vacuum filtration and washed with dichloromethane/MeOH 90:10 v/v. Air drying gave a white solid 24 mg, 5%. M.p: 200 – 202 °C. $^1\text{H NMR}$ (500 MHz, DMSO- d_6) δ 9.0 (s, brd 1H, H-2), 8.6 (s, brd 1H, H-2), 8.41 (s, 1H, H-3), 4.46 (s, 2H, H-4), 3.79 (s, 3H, H-5), 2.58 (s, 3H, H-1). $^{13}\text{C NMR}$ (126 MHz, DMSO- d_6) δ 163.0, 162.3, 148.3, 111.1, 46.7, 42.3, 22.1. **IR** $\nu_{\text{max}}/\text{cm}^{-1}$: 3277, 3132 (NH₂), 2099 (N₃), 1631, 1587, 1546, 1515 (sp² C-H stretch). **MS** [Found: [M- I⁻] m/z 179.1037, 100%, C₇H₁₁IN₆ requires [M+H⁺] m/z 179.1040.

Synthesis of 2-[1-(4-Amino-2-methylpyrimidin-5-ethyl)-1*H*-[1,2,3]triazol-4-yl]

ethanol ⁽⁸⁾

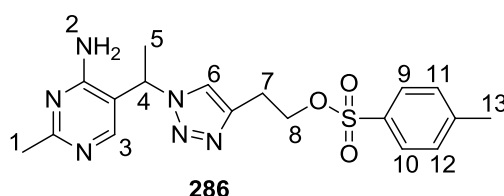


General synthesis of alcohol click:

To methyl azide **278** (148mg, 0.83 mmol, 1.0 eq) in a solvent mixture of *t*-butanol/ water (6 mL, 2:1 v/v) was added 3-butyn-1-ol **154** (58 mg, 0.83 mmol, 1.0 eq), sodium ascorbate (16.5 mg, 0.083 mmol, 0.1 eq) and CuSO₄·5H₂O (4.1 mg, 0.016 mmol, 0.01 eq). This was stirred overnight

at room temperature and then concentrated under vacuum to give viscous brown oil. The oil was diluted in ethanol, mixed with activated charcoal and filtered to give a clear oil (45 mg, 22%). **¹H NMR** (500 MHz, CDCl₃) δ 8.19 (s, 1H, H-3), 7.30 (s, 1H, H-6), 5.67 (q, ³J = 7.2 Hz, 1H, H-4), 5.49 (s, 2H, H-2), 3.86 (t, ³J = 5.9 Hz, 2H, H-8), 2.85 (t, ³J = 5.9 Hz, 2H, H-7), 2.41 (s, 3H, H-1), 1.92 (d, ³J = 7.2 Hz, 3H, H-5). **¹³C NMR** (126 MHz, CDCl₃) δ 168.1, 161.3, 152.9, 146.8, 119.9, 111.7, 61.3, 54.7, 28.7, 25.4, 18.2. **IR** ν_{max}/cm⁻¹: 3345 (OH), 3199 (sp³ C-H stretch), 1650, 1599, 1563, 1454 (sp² C-H stretch). **MS** [Found: [M+H⁺] m/z 249.1460, 100%, C₁₈H₂₂N₆O₃S requires [M+H⁺] m/z 249.1458.

Synthesis of 2-[1-(4-amino-2-methylpyrimidin-5-ethyl)-1H-[1,2,3]triazol-4-yl]ethoxy-tosylate ⁽⁸⁾

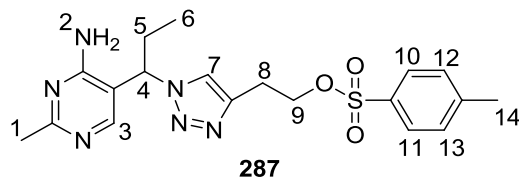


General synthesis of tosylate click:

Following the general procedure, to methyl azide **278** (100 mg, 0.56 mmol, 1.0 eq) in a solvent mixture of *t*-butanol/ water (6 mL, 2:1 v/v) was added 3-butynyl-1-tosylate **155** (126 mg, 0.56 mmol, 1.0 eq), sodium ascorbate (11.1 mg, 0.056 mmol, 0.1 eq) and CuSO₄·5H₂O (1.41 mg, 0.005 mmol, 0.01 eq). This was stirred overnight at r.t. and then concentrated under reduced pressure to give a viscous brown oil. The oil was diluted with ethanol, mixed with activated charcoal and filtered to give a white powder. Column chromatography (silica, ethyl acetate: MeOH 95:5 v/v) gave a white powder was recovered in (31 mg, 14%). Mpt: 164 – 166 °C. **¹H NMR** (500 MHz, CDCl₃) δ 8.25 (s, 1H, H-3), 7.71 (d, ³J = 8.3 Hz, 2H, H-9,10), 7.35 (s, 1H, H-6), 7.31 (d, ³J = 8.3 Hz, 2H, H-11, 12), 5.70 (q, ³J = 7.2 Hz, 1H, H-4), 5.50 (s, 2H, H-2), 4.25 (t, ³J = 6.6 Hz, 2H, H-8), 3.06 (t, ³J = 6.6 Hz, 2H, H-7), 2.49 (s, 3H, H-1), 2.44 (s, 3H, H-13), 1.98 (d, ³J = 7.2 Hz, 3H, H-5). **¹³C NMR** (126 MHz, CDCl₃) δ 168.3, 161.2, 153.2, 145.0, 143.8, 132.7, 129.9, 127.8, 120.4, 111.5, 68.6, 54.8, 25.9, 25.5, 21.6, 18.2. **IR** ν_{max}/cm⁻¹: 3332, 1643, 1594 and 1559 (C-H,

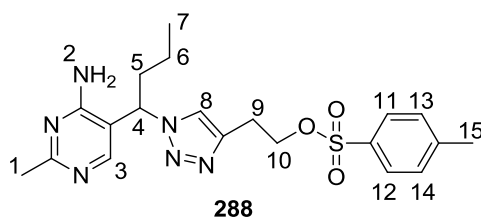
sp² stretch), 1175. **MS** [Found: [M+H⁺] *m/z* 403.1547, 100%, C₁₈H₂₂N₆O₃S requires [M+H⁺] *m/z* 403.1547.

Synthesis of 2-[1-(4-amino-2-methylpyrimidin-5-propyl)-1*H*-[1,2,3]triazol-4-yl]-ethoxy-tosylate



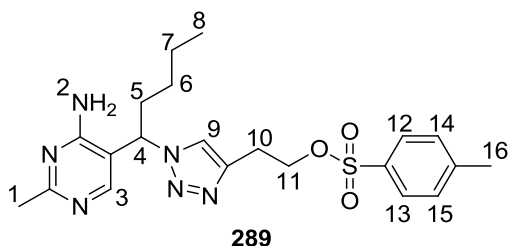
Following the general procedure, to ethyl azide **279** (137 mg, 0.71 mmol, 1.0 eq) in a solvent mixture of *t*-butanol/ water (6 mL, 2:1 v/v) was added 3-butynyl-1-tosylate **155** (160mg, 0.71 mmol, 1.0 eq), sodium ascorbate (14 mg, 0.07 mmol, 0.1 eq) and CuSO₄·5H₂O (1.7 mg, 0.075 mmol, 0.01 eq). The mixture was stirred overnight at r.t. and then concentrated under reduced pressure to leave a viscous brown oil. The oil was diluted in ethanol, mixed with activated charcoal and filtered to give a white powder. After purification via column chromatography (silica, ethyl acetate: MeOH, 95:5 v/v) a white powder was recovered (100 mg, 35%). Mpt: 168 – 170 °C. **¹H NMR** (500 MHz, CDCl₃) δ 8.23 (s, 1H, H-3), 7.71 (d, ³*J* = 8.3 Hz, 2H, H-10,11), 7.37 (s, 1H, H-7), 7.31 (d, ³*J* = 8.3 Hz, 2H, H-12,13), 5.65 (s, 2H, H-2), 5.34 (dd, ³*J* = 9.0, 6.7 Hz, 1H, H-4), 4.25 (t, ³*J* = 6.6 Hz, 2H, H-9), 3.07 (t, ³*J* = 6.6 Hz, 2H, H-8), 2.48 (s, 3H, H-1), 2.43 (s, 3H, H-14), 2.42 – 2.34 (m, 2H, H-5), 0.93 (t, ³*J* = 7.3 Hz, 3H, H-6). **¹³C NMR** (126 MHz, CDCl₃) δ 168.0, 161.5, 153.5, 145.0, 143.7, 132.7, 129.9, 127.8, 120.8, 110.9, 68.6, 61.5, 25.9, 25.4, 24.9, 21.6, 10.9. **IR** ν_{max} /cm⁻¹: 3356, 3148 (NH₂), 1638, 1592, 1555 (sp² C-H stretch). **MS** [Found: [M+H⁺] *m/z* 417.1702 100%, C₁₉H₂₄N₆O₃S requires [M+H⁺] *m/z* 417.1703.

Synthesis of 2-[1-(4-amino-2-methylpyrimidin-5-butyl)-1H-[1,2,3]triazol-4-yl]ethoxy-tosylate



Following the general procedure, to the propyl azide **280** (132 mg, 0.64 mmol) was added 3-butynyl-*p*-toluenesulfonate **155** (143 mg, 0.64 mmol), sodium ascorbate (12.7 mg, 0.064 mmol) and CuSO₄·5H₂O (1.6 mg, 0.006 mmol) at r.t. This gave a solid brown crude which after column chromatography eluting with ethyl acetate: methanol (silica, 95:5 v/v) gave a brown oil (118 mg, 43%). ¹H NMR (500 MHz, CDCl₃) δ 8.18 (s, 1H, H-3), 7.65 (d, ³J = 8.3 Hz, 2H, H-11,12), 7.33 (s, 1H, H-8), 7.24 (d, ³J = 8.3 Hz, 2H, H-13,14), 5.75 (s, 2H, H-2), 5.40 (dd, ³J = 9.1, 6.5 Hz, 1H, H-4), 4.19 (t, ³J = 6.6 Hz, 2H, H-10), 2.99 (t, ³J = 6.6 Hz, 2H, H-9), 2.41 (s, 3H, H-1), 2.37 (s, 3H, H-15), 2.33 – 2.29 (m, 2H, H-5), 2.26 – 2.18 (m, 1H, H-6), 1.27 – 1.13 (m, 1H, H-6), 0.90 (t, ³J = 7.4 Hz, 3H, H-7). ¹³C NMR (126 MHz, CDCl₃) δ 167.9, 161.7, 153.4, 145.1, 143.7, 132.8, 130.0, 129.0, 127.9, 125.9, 121.0, 111.3, 68.7, 59.6, 33.6, 26.0, 25.3, 21.7, 21.4, 19.6. IR ν_{max}/cm⁻¹: 3334, 3143 (sp³ C-H stretch), 2963, 1651, 1594, 1557 (sp² C-H stretch). MS [Found: [M+H⁺] m/z 431.1853, 100%, C₂₀H₂₆N₆O₃S requires [M+H⁺] m/z 431.1860.

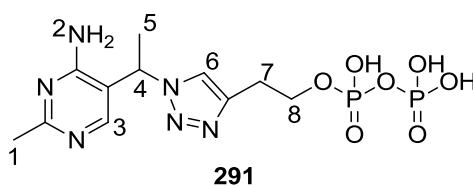
Synthesis of 2-[1-(4-amino-2-methylpyrimidin-5-propyl)-1H-[1,2,3]triazol-4-yl]ethoxy-tosylate



Following the general procedure, to the butyl azide **281** (120 mg, 0.54 mmol) was added 3-butynyl-*p*-toluenesulfonate **155** (122 mg, 0.54 mmol), sodium ascorbate (10.7 mg, 0.054 mmol) and CuSO₄·5H₂O (1.3 mg, 0.005 mmol) at r.t. This gave a solid brown crude after column chromatography eluting in ethyl acetate: methanol (silica, 95:5 v/v) to give a brown oil (27 mg, 23%). ¹H NMR (500 MHz, CDCl₃) δ 8.23 (s, 1H, H-3), 7.70 (d, ³J = 8.3 Hz, 2H, H-12,13), 7.39

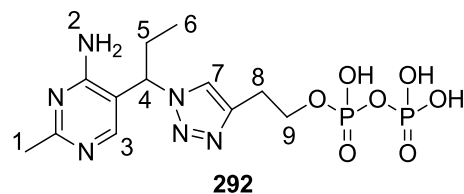
(s, 1H, H-9), 7.29 (d, $^3J = 8.3$ Hz, 2H, H-14,15), 5.78 (s, 2H, H-2), 5.43 (dd, $^3J = 8.8, 6.9$ Hz, 1H, H-4), 4.24 (t, $^3J = 6.6$ Hz, 2H, H-11), 3.05 (t, $^3J = 6.6$ Hz, 2H, H-10), 2.47 (s, 3H, H-1), 2.42 (s, 3H, H-16), 2.38 – 2.34 (m, 2H, H-5), 1.41 – 1.31 (m, 2H, H-7), 1.28 – 1.21 (m, 1H, H-6), 1.19 – 1.12 (m, 1H, H-6), H-7, 0.87 (t, $^3J = 7.3$ Hz, 3H, H-8). ^{13}C NMR (126 MHz, CDCl_3) δ 167.9, 161.5, 153.5, 145.0, 143.6, 132.7, 129.9, 128.9, 127.9, 125.8, 121.0, 111.2, 68.6, 59.8, 31.3, 28.3, 25.9, 25.3, 22.0, 21.6, 13.7. IR $\nu_{\text{max}}/\text{cm}^{-1}$: 3333, 3142, 2959, 2932, 1651, 1593, 1557 (sp^2 C-H stretch). MS [Found: $[\text{M}+\text{H}^+]$ m/z 445.2010, 100%, $\text{C}_{21}\text{H}_{28}\text{N}_6\text{O}_3\text{S}$ requires $[\text{M}+\text{H}^+]$ m/z 445.2016.

Synthesis of 2-(1-(4-amino-2-methylpyrimidin-5-ethyl)-1H-1,2,3-triazol-4-yl)ethyl trihydrogen diphosphate



To the methyl tosylate **286** (20 mg, 0.05 mmol, 1 eq) in anhydrous acetonitrile (5 mL) was added tris(tetrabutylammonium) pyrophosphate (90 mg, 0.1 mmol, 2, eq) at -10 °C. The reaction mixture was then warmed to r.t. overnight and quenched after 16 h. with water (10 mL). After purification using anion exchange resin (DEAE) on a glass column of 30cm x 10cm (length x diameter), increasing ammonium bicarbonate concentration and subsequent acidification by filtration through DOWEX 50H+, the product was isolated as a pale white powder (12 mg, 63%). ^1H NMR (500 MHz, D_2O) δ 7.98 (s, 1H, H-3), 7.89 (s, 1H, H-6), 5.82 (q, $^3J = 7.0$ Hz, 1H, H-4), 4.06 (q, $^3J = 6.0$ Hz, 2H, H-8), 2.97 (t, $^3J = 6.0$ Hz, 2H, H-7), 2.39 (s, 3H, H-1), 1.84 (d, $^3J = 7.0$ Hz, 3H, H-5). ^{13}C NMR (126 MHz, D_2O) δ 167.0, 161.1, 152.7, 145.1, 123.6, 112.6, 64.3, 53.2, 26.3, 23.8, 18.2. ^{31}P NMR (400 MHz, D_2O) δ -8.19 and -10.01 (each 1P, s, OPOPO). IR $\nu_{\text{max}}/\text{cm}^{-1}$: 2958, 1649, 1551, 1438. (C-H, sp^2 stretch). MS [Found: $[\text{M}-\text{H}]$ m/z 407.0628, 100%, $\text{C}_{11}\text{H}_{17}\text{N}_6\text{O}_7\text{P}_2$ requires $[\text{M}-\text{H}]$ m/z 407.0639.

Synthesis of 2-(1-(4-amino-2-methylpyrimidin-5-proyl)-1H-1,2,3-triazol-4-yl)ethyl trihydrogen diphosphate

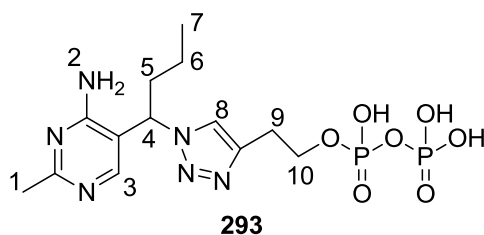


To the ethyl tosylate **287** (50 mg, 0.12 mmol, 1 eq) in anhydrous acetonitrile (5 mL) was added tris(tetrabutylammonium) pyrophosphate (216 mg, 0.24 mmol, 2, eq) at -10 °C. The reaction mixture was then warmed to r.t. overnight and quenched after 16 h. with water (10 mL). After purification using anion exchange resin (DEAE) on a glass column of 30cm x 10cm (length x diameter), increasing ammonium bicarbonate concentration and subsequent acidification by filtration through DOWEX 50H+, the product was isolated as a pale white material (27 mg, 53%).

¹H NMR (500 MHz, D₂O) δ 8.09 (s, 1H, H-3), 8.00 (s, 1H, H-7), 5.57 (dd, ³J = 15.1, 8.5 Hz, 1H, H-4), 4.08 (q, ³J = 6.0 Hz, 2H, H-9), 3.00 (t, ³J = 6.0 Hz, 2H, H-8), 2.38 (s, 3H, H-1), 2.36 – 2.30 (m, 1H, H-5), 2.30 – 2.20 (m, 1H, H-5), 0.84 (t, ³J = 7.2 Hz, 3H, H-6). **¹³C NMR** (126 MHz, D₂O) δ 165.7, 161.7, 150.2, 145.4, 123.5, 112.2, 64.3, 59.5, 26.4, 25.5, 22.91, 9.8. **³¹P** (400 MHz, D₂O) δ -6.59 and -10.80 (each 1P, s, OPOPO). **IR** ν_{max} /cm⁻¹: 3041, 1655, 1554, 1433 (sp² C-H stretch).

MS [Found: [M-H] *m/z* 421.0794, 100%, C₁₂H₁₉N₆O₇P₂ requires [M-H] *m/z* 421.0796.

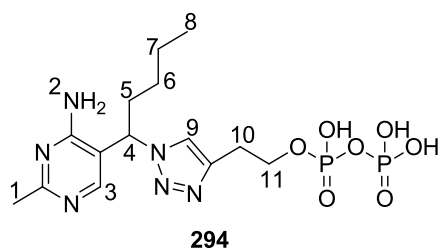
Synthesis of 2-(1-(4-amino-2-methylpyrimidin-5-butyl)-1H-1,2,3-triazol-4-yl)ethyl trihydrogen diphosphate



To the propyl tosylate **288** (78 mg, 0.18 mmol) in anhydrous acetonitrile (5 mL) was added tris(tetrabutylammonium) pyrophosphate (334 mg, 0.36 mmol) at -10 °C. The reaction mixture was then warmed to r.t. overnight and quenched after 16 h. with water (10 mL). After purification using anion exchange resin (DEAE) on a glass column of 30cm x 10cm (length x diameter), increasing ammonium bicarbonate concentration and subsequent acidification by filtration through

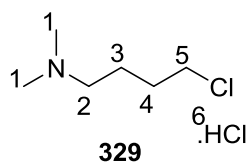
DOWEX 50H+, the product was isolated as a pale white material (37 mg, 47%). Mpt: 120 - 122 °C. **¹H NMR** (500 MHz, D₂O) δ 8.09 (s, 1H, H-3), 8.00 (s, 1H, H-8), 5.69 (dd, ³J = 9.1, 6.2 Hz, 1H, H-4), 4.08 (q, ³J = 6.2 Hz, 2H, H-10), 3.00 (t, ³J = 6.2 Hz, 2H, H-9), 2.42 (s, 3H, H-1), 2.30 (m, 1H, H-5), 2.22 – 2.13 (m, 1H, H-5), 1.29 – 1.21 (m, 1H, H-6), 1.19 – 1.10 (m, 1H, H-6), 0.85 (t, ³J = 7.4 Hz, 3H, H-7). **¹³C NMR** (126 MHz, D₂O) δ 164.3, 162.2, 146.9, 145.4, 123.4, 112.6, 64.5, 57.6, 33.7, 26.3, 22.8, 18.8, 12.4. **³¹P NMR** (202 MHz, D₂O) δ -9.84, -11.01. **IR** ν_{\max} /cm⁻¹: 3050, 2962, 1648, 1534, 1438 (sp² C-H stretch). **MS** [Found: [M-H] *m/z* 435.0950, 100%, C₁₃H₂₁N₆O₇P₂ requires [M-H] *m/z* 435.0952.

Synthesis of 2-(1-(4-amino-2-methylpyrimidin-5-pentyl)-1H-1,2,3-triazol-4-yl)ethyl trihydrogen diphosphate



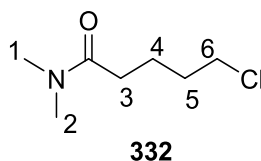
To the butyl tosylate **289** (53 mg, 0.12 mmol) in anhydrous acetonitrile (5 mL) was added tris(tetrabutylammonium) pyrophosphate (215 mg, 0.24 mmol) at -10 °C. The reaction mixture was then warmed to r.t. overnight and then quenched after 16 h. with water (10 mL). After purification using anion exchange resin (DEAE) on a glass column of 30cm x 10cm (length x diameter), increasing ammonium bicarbonate concentration and subsequent acidification by filtration through DOWEX 50H+, the product was isolated a pale white material (30 mg, 55%). Mpt: 178 – 180 °C. **¹H NMR** (500 MHz, D₂O) δ 8.11 (s, 1H, H-3), 8.01 (s, 1H, H-9), 5.66 (dd, ³J = 15.2, 9.0 Hz, 1H, H-4), 4.09 (q, ³J = 6.4 Hz, 2H, H-11), 3.00 (t, ³J = 6.4 Hz, 2H, H-10), 2.40 (s, 3H, H-1), 2.29 – 2.19 (m, 2H, H-5), 1.34 – 1.17 (m, 4H, H-6, 7), 0.78 (t, ³J = 9.1 Hz, 3H, H-8). **¹³C NMR** (126 MHz, D₂O) δ 165.5, 161.7, 149.0, 145.7, 123.4, 112.2, 64.4, 57.9, 31.4, 27.2, 26.3, 22.7, 21.3, 12.9. **³¹P NMR** (202 MHz, D₂O) δ -9.44, -11.04. **IR** ν_{\max} /cm⁻¹: 2691, 2934 (sp³ C-H stretch), 1653, 1540, 1467 (sp² C-H stretch). **MS** [Found: [M-H] *m/z*, 449.1108, 100%, C₁₄H₂₃N₆O₇P₂ requires [M-H] *m/z* 449.1109.

Synthesis of (*N,N*-dimethyl)-1-chlorobutan-1-ol hydrochloride ⁽¹⁴⁾



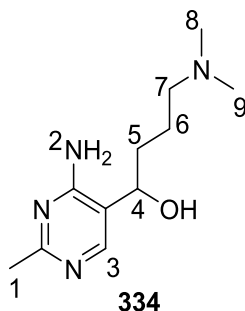
To thionyl chloride (463 μL , 6.37 mmol, 1.1 eq) at 0 $^{\circ}\text{C}$ was added *N,N*-dimethylaminobutan-1-ol (770 μL , 5.79 mmol, 1.0 eq.) over a 0.5 h. period. The reaction mixture was stirred at this temperature for 2 h. and then for a further 1h at r.t. Ethanol was then added and then subsequently removed under reduced pressure to leave a white ammonium salt. This was recrystallised from ethanol as sharp white crystals (701 mg, 70%). Mpt: 110-112 $^{\circ}\text{C}$. [Lit. ⁽¹⁴⁾ Mpt: 112-115 $^{\circ}\text{C}$]. **^1H NMR** (500 MHz, $\text{DMSO-}d_6$) δ 10.92 (brd s, 1H, H-6), 3.69 (t, $^3J = 6.1$ Hz, 2H, H-5), 3.06-3.04 (m, 2H, H-2), 2.72 (s, 3H, H-1), 2.71 (s, 3H, H-1), 2.53 – 2.51 (m, 4H, H-3,4). **^{13}C NMR** (126 MHz, $\text{DMSO-}d_6$) δ 55.9, 45.1, 42.3, 29.6, 21.7. **IR** $\nu_{\text{max}}/\text{cm}^{-1}$: 2961, 2678, 2514, 2477.

Synthesis of (*N,N*-dimethyl)-6-chlorohexanamide ⁽¹⁵⁾



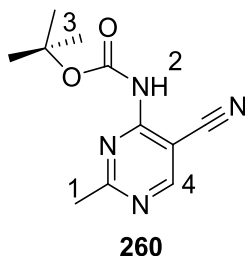
To chlorovaleroyl chloride (5.2 g, 32.2 mmol) in THF (25 mL) was added cold dimethylamine (2M, 114 mmol, 57 mL) in THF (25 mL) dropwise between 5-15 $^{\circ}\text{C}$. The reaction was stirred during the addition, and the reaction mixture was filtered after the final addition to remove any solid precipitates. The filtrate was concentrated under reduced pressure to yield a yellow oil (3.45g, 63%), which required no further purification. **^1H NMR** (500 MHz, CDCl_3) δ 3.49 (t, $^3J = 6.4$ Hz, 2H, H-6), 2.94 (s, 3H, H-1), 2.88 (s, 3H, H-2), 2.28 (t, $^3J = 7.1$ Hz, 2H, H-3), 1.81 – 1.69 (m, 6H, H-4, 5). **^{13}C NMR** (126 MHz, CDCl_3) δ 172.4, 44.8, 37.2, 35.4, 32.4, 32.2, 22.4. **IR** $\nu_{\text{max}}/\text{cm}^{-1}$: 2938, 2872 (C-H sp^3 stretch), 1645 (C=O amide, sp^2 stretch).

Synthesis of 4-(4-amino-2-methylpyrimidin-5-yl)-4-hydroxy-*N,N*-dimethylaminobutylamine



To compound **253** (200 mg, 1.45 mmol) in THF (10 mL) at 0 °C was added the tertiary amine Grignard reagent (3.0 M) (5.10 mmol, 1.7 ml 3.0 eq), prepared by washing *N,N*-dimethylamino propyl chloride HCl salt with NaOH, and then refluxing in THF with Mg turnings. The reaction mixture was allowed to warm to r.t and then stirred overnight. The reaction was quenched with ice water and left to stir for a further 1 h. and then extracted with ethyl acetate (3 x 20 mL) and 1-butanol (10 mL), dried over magnesium sulfate, filtered and evaporated under reduced pressure to yield a crude yellow oil which crystallised overnight. Further washes with cold diethyl ether gave a yellow solid (61 mg, 43%). Mpt: 137 - 139 °C. ¹H NMR (500 MHz, CDCl₃) δ 7.81 (s, 1H, H-3), 5.66 (s, 2H, H-2), 4.43 (dd, ³J = 9.7, 2.4 Hz, 1H, H-4), 2.34 (s, 3H, H-1), 2.22 (s, 6H, H-8,9), 1.86 – 1.60 (m, 6H, H-5,6,7). ¹³C NMR (126 MHz, CDCl₃) δ 166.0, 161.9, 152.4, 116.7, 71.4, 60.1, 44.9, 36.3, 25.5, 25.4. IR ν_{max} /cm⁻¹: 3334 (OH), 3211, 2948 (sp³ C-H stretch), 1621, 1615, 1594 (sp² C-H stretch). MS [Found: [M+H⁺] m/z 225.1711, 100%, C₁₁H₂₁N₄O requires [M+H⁺] m/z 225.1710.

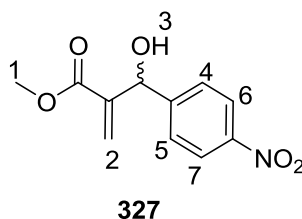
Synthesis of 2-methyl-4-(NH-BOC)pyrimidinecarbonitrile



To 2-methylaminopyrimidine carbonitrile **254** (100 mg, 0.75 mmol, 1.0 eq) dissolved in THF (5 mL) at r.t was added di-*tert*-butyl dicarbonate (164 mg, 0.75 mmol, 1.0 eq) dropwise. To this mixture were added triethylamine (125 uL, 91 mg, 0.90 mmol, 1.2 eq) and DMAP (92 mg, 0.75

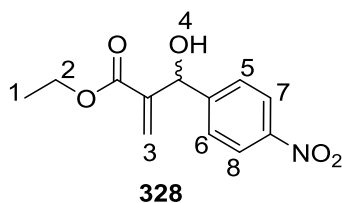
mmol, 1.0 eq). The resulting yellow solution was stirred overnight. Column chromatography eluting with ethyl acetate: methanol (silica, 95:5 v/v), gave a white powder (10.0 mg, 6%). Mpt: 168 - 170 °C. $^1\text{H NMR}$ (500 MHz, CDCl_3) δ 8.67 (s, 1H, H-4), 7.26 (s, 1H, H-2), 2.66 (s, 3H, H-5, H-1), 1.49 (s, 9H, H,-3). $^{13}\text{C NMR}$ (126 MHz, CDCl_3) δ 171.6, 161.4, 157.9, 149.2, 113.9, 94.8, 83.8, 28.0, 26.6. $\text{IR } \nu_{\text{max}} / \text{cm}^{-1}$: 2980, 2916, 2232 (CN), 1746 (C=O), 1586, 1551, 1504 (sp^2 C-H stretch). MS [Found: $[\text{M}+\text{H}^+]$ m/z 235.1190, 100%, $\text{C}_{11}\text{H}_{14}\text{N}_4\text{O}_2$ requires $[\text{M}+\text{H}^+]$ m/z 235.1190.

Synthesis of β -Hydroxy- α -methylene-4-nitrobenzenepropanoic acid methyl ester⁽¹⁶⁾



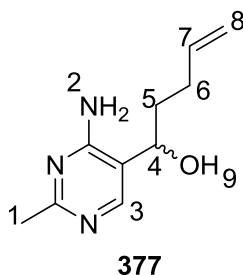
To a stirred solution of 4-nitrobenzaldehyde (0.30 g, 2.0 mmol) and *N,N*-dimethylbutylamine (253 mg, 2.50 mmol, 202 μL) in THF (3 mL) was added methyl acrylate (336 mg, 3.9 mmol, 353 μL). The transparent orange/yellow solution was stirred overnight at r.t for 16 h. Dichloromethane (2 mL) and water (2 mL) were then added to the reaction mixture which was stirred for a further 5 mins. The organic phase was separated and the aqueous phase was extracted with dichloromethane (2 x 10 mL). The combined organic layers were dried over magnesium sulfate, filtered and evaporated under reduced pressure to yield an orange crude oil. Column chromatography eluting with a mobile phase hexane: ethyl acetate (3:1 v/v) gave a white powder (75 mg, 16%). Mpt: 65-67 °C. [Lit.⁽¹⁶⁾mpt: 72-73 °C]. $^1\text{H NMR}$ (500 MHz, CDCl_3) δ 8.24 (d, $^3J = 8.8$ Hz, 2H, H-6,7), 7.61 (d, $^3J = 8.8$ Hz, 2H, H-4,5), 6.43 (s, 1H, H-3), 5.90 (s, 1H, H-2), 5.67 (s, 1H, H-2), 3.78 (s, 3H, H-1). $^{13}\text{C NMR}$ (126 MHz, CDCl_3) δ 166.4, 148.6, 147.5, 140.9, 127.3, 123.6, 72.7, 52.1, 31.0. $\text{IR } \nu_{\text{max}} / \text{cm}^{-1}$: 3493 (OH), 1715 (C=O sp^2 stretch), 1632, 1606, 1520 (sp^2 C-H stretch).

Synthesis of β -Hydroxy- α -methylene-4-nitrobenzenepropanoic acid ethyl ester ⁽¹⁶⁾



To a stirred solution of 4-nitrobenzaldehyde (0.30 g, 2.0 mmol) and *N,N*-dimethylbutylamine (253 mg, 2.5 mmol, 202 μ L) in THF (3 mL) was added ethyl acrylate (336 mg, 3.9 mmol, 353 μ L). The transparent orange/yellow solution was stirred at r.t. for seven days. Dichloromethane (2 mL) and water (2 mL) were then added to the reaction mixture which was left to stir for a further 5 min. The organic phase was then separated and the aqueous phase was extracted with dichloromethane (2 x 10 mL). The combined organic layers were dried over magnesium sulfate, filtered and evaporated under reduced pressure to yield an orange crude oil. Column chromatography eluting with hexane: ethyl acetate (silica, 3:1 v/v) gave a white powder (50 mg, 10%). Mpt: 74 – 76 °C [Lit. ⁽¹⁶⁾ Mpt 67-69 °C]. ¹H NMR (500 MHz, CDCl₃) δ 8.14 (d, ³J = 8.8 Hz, 2H, H-7, 8), 7.51 (d, ³J = 8.8 Hz, 2H, H-5, 6), 6.33 (s, 1H, H-4), 5.77 (s, 1H, H-3), 5.56 (s, 1H, H-3), 4.13 (q, ³J = 7.1 Hz, 2H, H-2), 1.20 (t, ³J = 7.1 Hz, 3H, H-1). ¹³C NMR (126 MHz, CDCl₃) δ 165.7, 148.6, 140.9, 127.3, 123.4, 72.8, 61.4, 31.8, 22.7, 13.9. IR ν_{max} /cm⁻¹: 3485 (OH), 2984, 1711 (C=O), 1629, 1607, 1521 (sp² C-H stretch).

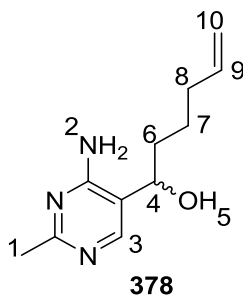
Synthesis of 5-(4-amino-2-methylpyrimidin-5-yl)-5-hydroxypent-1-ene



To compound **253** (3.0 g, 21.8 mmol, 1.0 eq) in THF (5mL) at 0 °C was added 4-but-enyl magnesium bromide solution (153 mL, 76.6 mmol), prepared *in situ* from 1-bromobut-4-ene, Mg and I₂). The solution was allowed to warm to r.t., stirred overnight, quenched with ice water and worked up as before to yield a white powder (2.90 g, 69%). Mpt: 175-177 °C. ¹H NMR (500 MHz, DMSO-*d*⁶) δ 7.94 (s, 1H, H-3), 6.51 (s, 2H, H-2), 5.84 (ddt, *J* = 17.0, 10.2, 6.5, 1H, H-7),

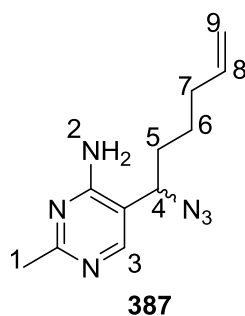
5.36 (d, $^3J = 4.5$ Hz, 1H, H-9), 5.01- 4.93 (m, 2H, H-8), 4.54 (dt, $^3J = 10.8, 4.5$ Hz, 1H, H-4), 2.30 (s, 3H, H-1), 2.15 – 2.06 (m, 1H, H-6), 2.06 – 1.98 (m, 1H, H-6), 1.69 - 1.63 (m, 2H, H-5). ^{13}C NMR (126 MHz, DMSO- d_6) δ 164.9, 161.0, 152.6, 139.0, 117.0, 115.0, 67.7, 35.3, 30.3, 25.6. IR $\nu_{\text{max}}/\text{cm}^{-1}$: 3382 (OH), 3189, 1655, 1594, 1563 (sp^2 C-H stretch). MS [Found: $[\text{M}+\text{H}^+]$ m/z 194.1286, 100%, $\text{C}_{10}\text{H}_{15}\text{N}_3\text{O}$ requires $[\text{M}+\text{H}^+]$ m/z 194.1288.

Synthesis of 6-(4-amino-2-methylpyrimidin-5-yl)-6-hydroxyhex-1-ene



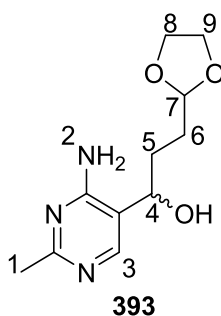
To the aldehyde **253** (705 mg, 5.14 mmol) in anhydrous THF (5 mL) was added 5-pent-1-enyl magnesium bromide solution (36 mL, 18.0 mmol), prepared *in situ* from 1-bromopent-5-ene, Mg and I_2 at 0 °C. The reaction was left to warm to r.t. overnight, and then quenched with ice water, extracted with ethyl acetate (3 x 20 mL), 1-butanol (10 mL) and dried over magnesium sulfate. Filtration and evaporation under reduced pressure gave a white product (560 mg, 53%). Mpt: 117 – 118 °C. ^1H NMR (500 MHz, CDCl_3) δ 7.54 (s, 1H, H-3), 5.95 (s, 2H, H-2), 5.69 (ddt, $^3J = 17.0, 10.2, 6.7$ Hz, 1H, H-9), 5.40 (s brd, 1H, H-5), 4.92 – 4.86 (m, 2H, H-10), 4.43 (t, $^3J = 7.1$ Hz, 1H, H-4), 2.28 (s, 3H, H-1), 2.04 – 1.96 (m, 2H, H-8), 1.83 – 1.75 (m, 1H, H-6), 1.68 – 1.61 (m, 1H, H-6), 1.49 – 1.39 (m, 1H, H-7), 1.30 – 1.21 (m, 1H, H-7). ^{13}C NMR (126 MHz, CDCl_3) δ 165.8, 161.6, 151.7, 138.1, 116.2, 114.9, 71.2, 34.2, 33.5, 25.62, 24.85. IR $\nu_{\text{max}}/\text{cm}^{-1}$: 3333 (OH), 3167, 2931, 2863 (NH_2), 1640, 1593, 1557 (sp^2 C-H stretch). MS [Found: $[\text{M}+\text{H}^+]$ m/z 208.1441, 100%, $\text{C}_{11}\text{H}_{17}\text{N}_3\text{O}$ requires $[\text{M}+\text{H}^+]$ m/z 208.1444.

Synthesis of 6-azido-6-(methyl-4-aminopyrimidin-5-yl)hex-1-ene



To compound **378** in anhydrous THF (5 mL) was added DBU (1.02 mL, 3.17 mmol, 1.3 eq.) and DPPA (720 μ L, 3.24 mmol, 1.2 eq.) at r.t. After stirring overnight the reaction was quenched with water (10 mL), extracted with ethyl acetate (3 x 10 mL). The combined extracts were washed with brine (10 mL), dried over magnesium sulfate, filtered and evaporated under reduced pressure to yield a white powder (656 mg, 50%). Mpt: 88 - 90 °C. $^1\text{H NMR}$ (500 MHz, CDCl_3) δ 7.95 (s, 1H, H-3), 5.76 (s, 2H, H-2), 5.68 (ddt, $^3J = 17.0, 10.2, 7.0$ Hz, 1H, H-8), 4.94 – 4.89 (m, 2H, H-9), 4.27 (t, $^3J = 7.5$ Hz, 1H, H-4), 2.42 (s, 3H, H-1), 2.02 (q, $^3J = 7.0$ Hz, 2H, H-7), 1.87 – 1.78 (m, 1H, H-5), 1.78 – 1.68 (m, 1H, H-5), 1.50 – 1.41 (m, 1H, H-6), 1.36 – 1.26 (m, 1H, H-6). $^{13}\text{C NMR}$ (126 MHz, CDCl_3) δ 166.4, 159.9, 153.2, 136.6, 114.3, 110.5, 61.7, 32.0, 30.8, 24.6, 24.4. $\text{IR } \nu_{\text{max}} / \text{cm}^{-1}$: 3317.6, 3158.7, 2937.8, 2099.5 (N_3), 1640.9, 1589.3 1557.7 (sp^2 C-H stretch). MS [Found: $[\text{M}+\text{H}^+]$ m/z 233.1509, 100%, $\text{C}_{11}\text{H}_{16}\text{N}_6\text{O}$ requires $[\text{M}+\text{H}^+]$ 233.1509 m/z .

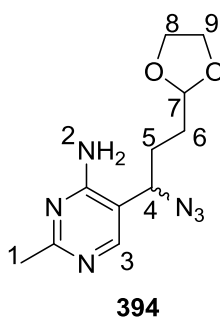
Synthesis of 3-(2-methyl-4-aminopyrimidin-5-yl-2-(1,3-dioxolanyl)propan-1-ol



To the aldehyde **253** (324 mg, 2.36 mmol, 1eq) in anhydrous THF (5 mL) was added 2-(1,3-dioxolanyl)ethylmagnesium bromide solution (8.2 mL, 7.80 mmol, 3.5 eq), prepared *in situ* from 2-(1-bromoethyl)1,3-dioxolane, Mg and I_2 at 0 °C. The mixture was left to warm to r.t. overnight and then quenched with ice water, extracted with ethyl acetate (3 x 20 mL), 1-butanol

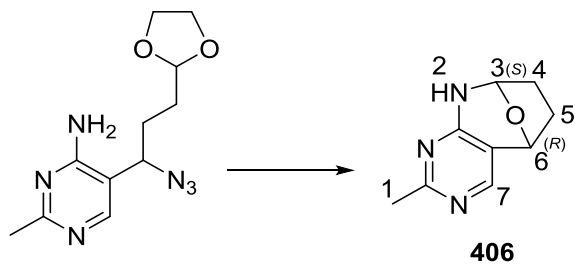
(10 mL) and dried over magnesium sulfate. After filtration and evaporation under reduced pressure, a white product was recovered (206 mg, 37%). Mpt: 96 – 98 °C. **¹H NMR** (500 MHz, CDCl₃) δ 7.66 (s, 1H, H-3), 5.89 (s, 2H, H-2), 4.84 (t, ³J = 4.5 Hz, 1H, H-7), 4.51 (t, ³J = 8.7 Hz, 1H, H-4), 3.89 (t, ³J = 8.7 Hz, 2H, H-8), 3.79 (t, ³J = 8.7 Hz, 2H, H-9), 2.30 (s, 3H, H-1), 1.95-1.88 (m, 1H, H-5), 1.81 – 1.72 (m, 2H, H-6), 1.72-1.66 (m, 1H, H-5). **¹³C NMR** (126 MHz, CDCl₃) δ 165.9, 161.5, 151.9, 116.3, 104.0, 70.7, 64.9, 30.1, 29.4, 25.1. **IR** ν_{\max} /cm⁻¹: 3334.9 (OH), 3182.2, 2965.5, 2883.8 (NH₂), 1621.5, 1597.5, 1557.6 (sp² C-H stretch). **MS** [Found: [M+H⁺] *m/z* 240.1344, 100%, C₁₁H₁₇N₃O₃ requires [M+H⁺] *m/z* 240.1343.

Synthesis of 1-azido-1-(2-methyl-4-aminopyrimidin-5-yl)-2-(1,3-dioxolanyl)propane



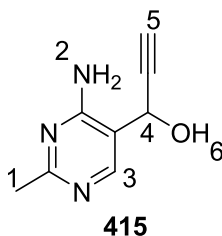
To the alcohol **393** (217 mg, 0.91 mmol, 1.0 eq.) in anhydrous THF (5 mL) was added DBU (176 μL, 1.18 mmol, 1.3 eq) and DPPA (235 μL, 1.09 mmol, 1.2 eq) at r.t. The reaction mixture was stirred overnight at r.t. and quenched after 24 h. with water (10 mL) and extracted with ethyl acetate (3 x 10 mL). The combined extracts were washed with brine (10 mL), dried over magnesium sulfate, filtered and evaporated under reduced pressure, to give the product as a white powder (101 mg, 42%) . Mpt: 92 – 94 °C. **¹H NMR** (500 MHz, CDCl₃) δ 8.00 (s, 1H, H-3), 5.68 (s, 2H, H-2), 4.84 (t, ³J = 4.3 Hz, 1H, H-7), 4.42 (t, ³J = 8.2 Hz, 1H, H-4), 3.91 (t, ³J = 8.7 Hz, 2H, H-8), 3.79 (t, ³J = 8.7 Hz, 2H, H-9), 2.43 (s, 3H, H-1), 1.95-1.90 (m, 1H, H-5), 1.84-1.80 (m, 1H, H-5) 1.69-1.65 (m, 2H, H-6). **¹³C NMR** (126 MHz, CDCl₃) δ 167.3, 160.8, 154.3, 111.6, 103.6, 64.9, 62.1, 29.8, 27.1, 25.43. **IR** ν_{\max} /cm⁻¹: 3325.3, 3172.33, 2099 (N₃), 1646.4, 1590.02, 1557.74 (sp² C-H stretch). **MS** [Found: [M+H⁺] *m/z* 265. 1410, 100%, C₁₁H₁₆N₆O₂ requires [M+H⁺] *m/z* 265.1408.

Synthesis of 2-methyl-4-aminobenzooxaazapine pyrimidine



To the protected compound **394** (30 mg, 0.11 mmol, 1.0 eq) was added 30% (aq) acetic acid (10 mL). This was refluxed for 16 h. until consumption of starting material was confirmed by TLC. The crude reaction was then dissolved in dichloromethane and filtered over silica and recrystallized from dichloromethane: petroleum ether to give the product as square brown crystals (15 mg, 77%). **¹H NMR** (500 MHz, CDCl₃) δ 7.81 (s, 1H, H-7), 6.54 (s, 1H, H-2), 5.38 (d, ³J = 4.2 Hz, 1H, H-3), 5.05 (d, ³J = 6.2 Hz, 1H, H-6), 3.03 (s, 3H, H-1), 2.39 – 2.21 (m, 2H, H-4), 2.04-1.97 (m, 2H, H-5). **¹³C NMR** (126 MHz, CDCl₃) δ 166.9, 156.8, 148.2, 116.3, 83.6, 75.1, 37.3, 35.9, 25.4. **IR** ν_{max}/cm⁻¹: 3217, 2954, 2873, 1614, 1567, 1531 (sp² C-H stretch). **MS** Found: [M+H⁺] *m/z* 178.0973, 100%, C₉H₁₂N₃O requires [M+H⁺] *m/z* 178.0975.

Synthesis of 3-(2-methyl-4-aminopyrimidin-5-yl)-3-hydroxyprop-1-yne

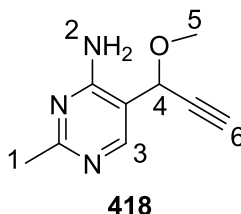


Using the procedure of 1-(4-amino-2-methylpyrimidin-5-yl)ethanol:

To compound **253** (225 mg, 1.64 mmol, 1.0 eq) in THF (5 mL) at 0 °C was added ethynylmagnesium bromide (0.5 M) (9.8 mL, 4.9 mmol, 3.0 eq) dropwise. The reaction was quenched with ice water, extracted with ethyl acetate (3 x 10 mL), 1-butanol (10 mL), dried over magnesium sulfate, filtered and evaporated under reduced pressure to give a crude product. Column chromatography eluting with ethyl acetate: methanol (95: 5 v/v) gave a light yellow powder (54 mg, 72%). Mpt: 174 – 176 °C. **¹H NMR** (500 MHz, DMSO-*d*⁶) δ 8.18 (s, 1H, H-3), 6.68 (s, 2H, H-2), 6.11 (d, ³J = 5.9 Hz, 1H, H-6), 5.40 (dd, ³J = 5.9, 2.3 Hz, 1H, H-4), 3.61 (d, ³J

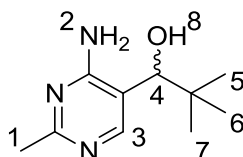
= 2.3 Hz, 1H, H-5), 2.37 (s, 3H, H-1). ^{13}C NMR (126 MHz, DMSO- d_6) δ 166.5, 161.1, 153.2, 113.8, 83.7, 76.6, 58.3, 25.6. IR $\nu_{\text{max}}/\text{cm}^{-1}$: 3388 (OH), 3335, 3032 (NH₂), 1677, 1586, 1544 (sp² C-H stretch). MS [Found: [M+H⁺] m/z 164.0816 100%, C₈H₉N₃O requires [M+H⁺] m/z 164.0818.

Synthesis of 3-(2-methyl-4-amino-pyrimidin-5-yl)-3-methoxyprop-1-yne



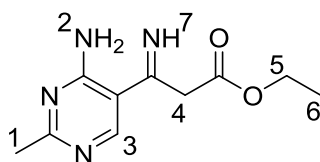
To compound **415** (660 mg, 4.04 mmol, 1.0 eq.) in anhydrous dichloromethane (20 mL) was added triethylamine (817 mg, 8.08 mmol, 1.12 mL). To this was added mesityl chloride (556 mg, 375 μL , 4.86 mmol, 1.2 eq) at r.t. After stirring for approximately one hour, the reaction was diluted with dichloromethane (10 mL). The organic layer was then washed with water (3 x 20 mL), brine (10 mL) and dried over magnesium sulfate and filtered. The yellow organic layer was evaporated under reduced pressure to give a dark brown oil, which was analysed by ^1H NMR, but showed no signals. Therefore the aqueous layer was evaporated to dryness and the residue was purified on silica eluting with ethyl acetate: MeOH (95: 5 v/v) to give the product as a fine yellow powder. Recrystallisation from dichloromethane/pet ether gave fluffy white crystals (30 mg, 0.5%). Mpt: 138-140 °C. ^1H NMR (500 MHz, CDCl₃) δ 8.26 (s, 1H, H-3), 5.71 (s, 2H, H-2), 5.11 (d, $^3J = 2.2$ Hz, 1H, H-4), 3.42 (s, 3H, H-5), 2.76 (d, $^3J = 2.2$ Hz, 1H, H-6), 2.54 (s, 3H, H-1). ^{13}C NMR (126 MHz, CDCl₃) δ 167.7, 161.2, 154.1, 109.9, 77.9, 77.3, 68.9, 55.1, 25.3. IR $\nu_{\text{max}}/\text{cm}^{-1}$: 3183, 2933, 2827 (sp³ C-H stretch), 1622, 1594, 1557 (sp² C-H stretch). MS: Found: [M+H⁺] m/z 178.0973, 100%, C₉H₁₂N₃O requires [M+H⁺] 178.0975 m/z .

Synthesis of 3-(2-methyl-4-aminopyrimidine-5-yl)-3-hydroxy-2,2-dimethylpropane



To compound **253** (200 mg, 1.45 mmol, 1.0 eq) was added *t*-butylmagnesium bromide in THF (1M) (5.1 mL, 5.10 mmol, 3.5 eq) at 0 °C to produce a yellow solution. This was allowed to warm to r.t. and stirred overnight. The reaction was quenched with ice and extracted with ethyl acetate (3 x 20 mL), 1-butanol (2 x 10 mL), dried over magnesium sulfate and filtered to give a clear yellow oil. Upon evaporation to dryness under reduced pressure, the product crystallised on standing as fine white crystals (70 mg, 25%). Mpt: 243 – 245 °C. **¹H NMR** (500 MHz, CDCl₃) δ 7.76 (s, 1H, H-3), 5.84 (s, 2H, H-2), 4.31 (s, 1H, H-4), 2.47 (s, 3H, H-1), 0.99 (s, 9H, H-5, 6, 7). **¹³C NMR** (126 MHz, CDCl₃) δ 166.1, 161.8, 154.7, 112.6, 80.7, 37.7, 26.2, 25.0. **IR** ν_{\max} /cm⁻¹: 2968, 2869, 1615, 1557, 1441 (sp² C-H stretch). **MS** [Found: [M+H⁺] *m/z* 196.1443, 100%, C₁₀H₁₇N₃O requires [M+H⁺] *m/z* 196.1444.

Synthesis of ethyl 3-(2-methyl-4-aminopyrimidin-5-yl)-3-imino-propanoate

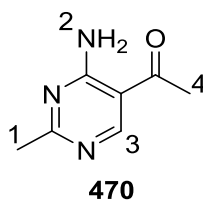


457

To the aldehyde **254** (335 mg, 2.44 mmol, 1.0 eq) was added the zinc bromo acetate **473** (2.81 g, 12.5 mmol, 5.0 eq) and freshly distilled TMEDA (5.67 mg, 4.88 mmol, 2.0 eq). This was then heated to 50 °C and stirred for 7 days. The reaction was quenched with water and extracted with ethyl acetate (10 mL). Column chromatography eluting with a mobile phase of ethyl acetate: hexane (silica, 1:1 v/v) gave the product as a red solid in (270 mg, 50%). Mpt: 69-71 °C. **¹H NMR** (500 MHz, CDCl₃) δ 8.10 (s, 1H, H-3), 5.76 (s, 2H, H-2), 4.74, (s, 1H, H-7), 4.09 (q, ³*J* = 7.1 Hz, 2H, H-5), 2.41 (s, 3H, H-1), 1.95 (s, 2H, H-4), 1.21 (t, ³*J* = 7.1 Hz, 3H, H-6). **¹³C NMR** (126 MHz, CDCl₃) δ 169.9, 168.4, 159.9, 155.1, 154.2, 112.1, 87.3, 59.2, 25.6, 14.1. **IR** ν_{\max} /cm⁻¹: 3316,

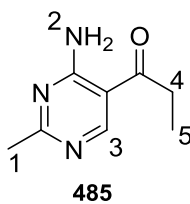
1715 (C=O), 1651, 1621, 1494, 144 (sp² C-H stretch). **MS** Found: [M+H⁺] 223.1190 *m/z* 100%, C₁₀ H₁₄ O₂ N₄ requires [M+H⁺] *m/z* 223. 1190.

Synthesis of 1-(2-methyl-4-aminopyrimidin-5-yl)ethanone



To 4-amino-2-methylpyrimidine-5-carbonitrile **254** (1.0 g, 7.45 mmol) in THF (5 mL) was added CH₃MgBr in THF (3M, 26.1 mmol, 8.70 mL, 3.5eq) dropwise at 0 °C to give a yellow solution which was warmed to 40 °C and then left to stir overnight. The reaction was quenched with ice water and left to stir for another 24 h. It was then extracted with ethyl acetate (3 x 10 mL), and 1-butanol (10 mL). After drying over magnesium sulfate, filtration and concentration *in vacuo*, a crude yellow product was obtained. Column chromatography eluting with ethyl acetate: hexane (1:3 v/v) gave the product as a white solid (470 mg, 50%). Mpt: 170 – 172 °C. **¹H NMR** (500 MHz, CDCl₃) δ 8.70 (s, 1H, H-3), 8.57 (s, 1H, H-2), 5.72 (s, 1H, H-2), 2.50 (s, 3H, H-4), 2.48 (s, 3H, H-1). **¹³C NMR** (126 MHz, CDCl₃) δ 198.2, 171.4, 161.8, 159.7, 109.7, 26.6, 26.1. **IR** ν_{max} /cm⁻¹: 3372, 3114, 1651 (sp² C=O), 1651, 1590, 1520 (sp² C-H aromatic stretch). **MS** Found: [M+H⁺] *m/z* 152, 0815 100%, C₇ H₉ O₁ N₃ requires [M+H⁺] *m/z* 152.0818.

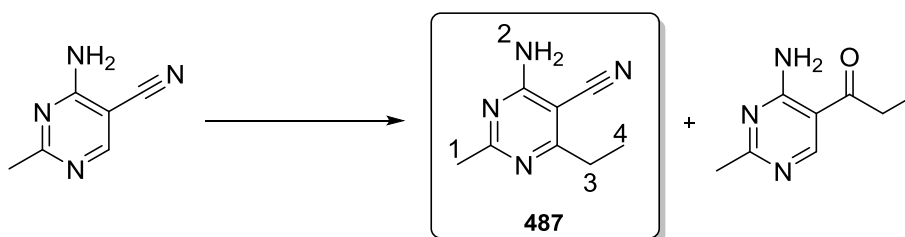
Synthesis of 1-(2-methyl-4-aminopyrimidin-5-yl)propanone



To 4-amino-2-methylpyrimidine-5-carbonitrile **254** (200 mg, 1.5 mmol) in THF (5 mL) was added ethylmagnesium bromide in THF (3M, 5.22 mmol, 1.74 mL, 3.5 eq) dropwise at 0 °C to give a yellow solution, which was warmed to 40 °C and left to stir overnight. The reaction was worked up as described previously and purified by flash column chromatography, eluting with ethyl acetate: hexane (1:3 v/v) to give the product as a white solid (169 mg, 68%). Mpt: 160 -162

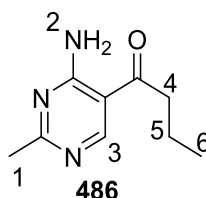
°C. **¹H NMR** (500 MHz, CDCl₃) δ 8.87 (s, 1H, H-3), 8.34 (s, 1H, H-2), 7.91 (s, 1H, H-2), 3.00 (q, ³J = 7.2 Hz, 2H, H-4), 2.40 (s, 3H, H-1), 1.07 (t, ³J = 7.2 Hz, 3H, H-5). **¹³C NMR** (126 MHz, CDCl₃) δ 201.8, 170.4, 161.8, 160.0, 108.8, 31.2, 26.1, 8.7. **IR** ν_{max}/cm⁻¹: 3385, 3263, 3109, 2980 (sp³ C-H stretch), 1657, 1625, 1528 (sp² C-H stretch). **MS** Found: [M+H⁺] 166.0972 *m/z* 100%, C₈ H₁₂ N₃O requires [M+H⁺] *m/z* 163.0975.

Synthesis of 1-(2-methyl-4-aminopyrimidin-5-yl)-cyano-6-ethyl



Following the procedure of 1-(2-methyl-4-aminopyrimidin-5-yl)propanone, and using the same quantities and purification procedure, the product was obtained as a white powder (66 mg, 27%). Mpt: 197-199 °C. [Lit. ⁽²⁶⁾ Mpt. 193-194 °C] **¹H NMR** (500 MHz, CDCl₃) δ 5.43 (s, 2H, H-2), 2.74 (q, ³J = 7.6 Hz, 2H, H-3), 2.38 (s, 3H, H-1), 1.16 (t, ³J = 7.6 Hz, 3H, H-4). **¹³C NMR** (126 MHz, CDCl₃) δ 175.5, 170.4, 163.3, 115.3, 86.3, 30.6, 26.4, 12.8. **IR** ν_{max}/cm⁻¹: 3377, 3340 (NH₂), 2223 (CN), 1682, 1553, 1577 (sp² C-H stretch). **MS** Found: [M+H⁺] 163.0974 *m/z* 100%, C₈ H₁₁ N₄ requires [M+H⁺] *m/z* 163.0978.

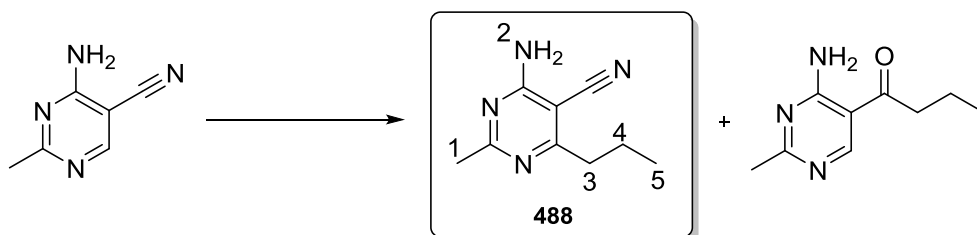
Synthesis of 1-(2-methyl-4-aminopyrimidine-5-yl)-butan-1-one



To compound **254** (200 mg, 1.5 mmol) in THF (5 mL) was added propylmagnesium bromide (3M, 5.22 mmol, 1.74 mL, 3.5 eq) dropwise at 0 °C to give a yellow solution which was warmed to 40 °C and left to stir overnight. The reaction was worked up as described previously and purified by flash column chromatography, using a mobile phase of ethyl acetate: hexane (1:3 v/v), to give the product as a white solid (43 mg, 16%). Mpt: 147-149 °C. **¹H NMR** (500 MHz, CDCl₃)

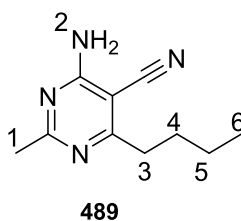
δ 8.73 (s, 1H, H-3), 2.81 (t, $J = 7.4$ Hz, 3H, H-4), 2.50 (s, 3H, H-1), 1.73 – 1.64 (m, 2H, H-5), 0.94 (t, $J = 7.4$ Hz, 3H, H-6). $^{13}\text{C NMR}$ (126 MHz, CDCl_3) δ 200.2, 170.4, 162.3, 158.2, 109.2, 40.4, 25.8, 17.5, 13.9. **IR** $\nu_{\text{max}}/\text{cm}^{-1}$: 3373, 3265 (NH_2) 1653, 1629, 1534 (sp^2 C-H stretch). **MS** Found: $[\text{M}+\text{H}^+]$ m/z 180.1129 100%, $\text{C}_9\text{H}_{13}\text{O}_1\text{N}_3$ requires $[\text{M}+\text{H}^+]$ m/z 180.1131.

Synthesis of 1-(2-methyl-4-aminopyrimidine-5-yl)-cyano-6-propyl



Following the procedure of 1-(2-methyl-4-aminopyrimidine-5-yl)-butan-1-one, and using the same quantities and purification procedure, the product was obtained as a yellow/white powder (53 mg, 20%). Mpt: 176 -177 °C. $^1\text{H NMR}$ (500 MHz, CDCl_3) δ 5.50 (s, 2H, H-2), 2.71 (t, $^3J = 10$ Hz, 2H, H-3), 2.47 (s, 3H, H-1), 1.75 – 1.66 (m, 2H, H-4), 0.94 (t, $^3J = 7.4$ Hz, 3H, H-5). $^{13}\text{C NMR}$ (126 MHz, CDCl_3) δ 173.01, 169.10, 162.1, 114.1, 85.6, 37.5, 25.1, 21.2, 12.4. **IR** $\nu_{\text{max}}/\text{cm}^{-1}$: 3368, 3338 (NH_2) 1653, 1629, 224 (CN), 1678, 1553, 1417 (sp^2 C-H stretch). **MS** Found: $[\text{M}+\text{H}^+]$ m/z 177.1133, 100%, $\text{C}_9\text{H}_{12}\text{N}_4$ requires $[\text{M}+\text{H}^+]$ m/z 177.1135.

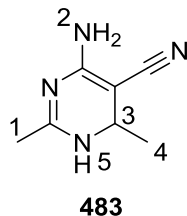
Synthesis of 1-(2-methyl-4-aminopyrimidine-5-yl)-5-cyano-6-butyl



To compound **254** (200 mg, 1.5 mmol) in THF (5 mL) was added propylmagnesium bromide in THF (3M, 5.22 mmol, 1.74 mL, 3.5 eq) dropwise at 0 °C to give a yellow solution which was warmed to 40 °C and left to stir overnight. The reaction was worked up as described previously and purified by flash column chromatography, eluting with ethyl acetate: hexane (1:3 v/v) to give the product as a white solid (50 mg, 18%). Mpt: 180 -182 °C. $^1\text{H NMR}$ (500 MHz, CDCl_3) δ 5.69 (s, 2H, H-2), 2.74 – 2.70 (t, $^3J = 10$ Hz, 2H, H-3), 2.46 (s, 3H, H-1), 1.68 – 1.60 (m, 2H, H-4),

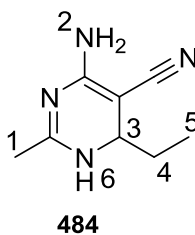
1.40 – 1.31 (m, 2H, H-5), 0.88 (t, $^3J = 7.4$ Hz, 3H, H-6). ^{13}C NMR (126 MHz, CDCl_3) δ 175.2, 170.4, 163.7, 115.9, 87.1, 37.0, 31.6, 26.8, 23.1, 14.2. IR $\nu_{\text{max}} / \text{cm}^{-1}$: 3339, 3379, 2227 (CN), 1687, 1559, 1461 (sp^2 C-H stretch). MS Found: $[\text{M}+\text{H}^+]$ m/z 191.1289, 100%, $\text{C}_{10}\text{H}_{15}\text{N}_4$ requires $[\text{M}+\text{H}^+]$ m/z 191.1291.

Synthesis 2-methyl-4-amino-5-cyano-6-methyl-dihydropyrimidine



To compound **254** (2.5 g, 19.0 mmol, 1.0 eq) was added methylmagnesium bromide in THF (3M, 65 mmol, 21.8 mL, 3.5 eq) at 40 °C and left to stir overnight. The reaction was then quenched with NH_4^+Cl (aq) (20 mL) at 0 °C and stirred for a further 48 h. The reaction mixture was then extracted with ethyl acetate (3 x 10 mL) and 1-butanol (10 mL) to give the product as a fine yellow powder (2.4 g, 85 %). Mpt: 221-222 °C. ^1H NMR (500 MHz, $\text{DMSO}-d_6$) δ 8.27 (s, 1H, H-5), 5.77 (s, 2H, H-2), 4.17 (q, $^3J = 6.0$ Hz, 1H, H-3), 1.84 (s, 3H, H-1), 1.18 (d, $^3J = 6.0$ Hz, 3H, H-4). ^{13}C NMR (126 MHz, $\text{DMSO}-d_6$) δ 160.9, 159.6, 122.4, 53.5, 45.4, 25.4, 22.1. IR $\nu_{\text{max}} / \text{cm}^{-1}$: 3399, 3304, 2152 (CN), 1658, 1608, 1563 (sp^2 C-H stretch). MS Found: m/z 151.0975 $[\text{M}+\text{H}^+]$ 100%, $\text{C}_7\text{H}_{11}\text{N}_4$ requires $[\text{M}+\text{H}^+]$ m/z 151.0978.

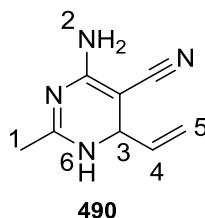
Synthesis 2-methyl-4-amino-5-cyano-6-ethyl-dihydropyrimidine



To compound **254** (2.5 g, 19.0 mmol, 1.0 eq) was added ethylmagnesium bromide in THF (3M, 65 mmol, 21.8 mL, 3.5 eq) at 40 °C and left to stir overnight. The reaction was then quenched with NH_4^+Cl (aq) (20 mL) at 0 °C and stirred for a further 48 h. The reaction mixture was then extracted with ethyl acetate (3 x 10 mL) and 1-butanol (10 mL) to give the product as a fine yellow powder (2.4 g, 80%). Mpt: 213-215 °C. ^1H NMR (500 MHz, $\text{DMSO}-d_6$) δ 8.19 (s, 1H, H-6), 5.75 (s, 2H, H-2), 4.09 (td, $^3J = 4.6, 2.3$ Hz, 1H, H-3), 1.86 (s, 3H, H-1), 1.50 – 1.38 (m, 2H, H-4),

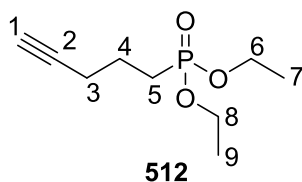
0.86 (t, $^3J = 7.4$ Hz, 3H, H-5). $^{13}\text{C NMR}$ (126 MHz, $\text{DMSO-}d^6$) δ 161.5, 160.2, 122.6, 50.9, 50.6, 31.2, 21.6, 8.0. **IR** $\nu_{\text{max}}/\text{cm}^{-1}$: 3372, 3326 (NH_2), 2180, 2149 (CN), 1659, 1600, 1565 ($\text{sp}^2\text{C-H}$ stretch). **MS** Found: $[\text{M}+\text{H}^+]$ m/z 165.1135 100%, $\text{C}_8\text{H}_{13}\text{N}_4$ requires $[\text{M}+\text{H}^+]$ m/z 165.1135.

Synthesis of 2-methyl-4-amino-5-cyano-6-vinyl dihydropyrimidine



To 4-amino-2-methylpyrimidine-5-carbonitrile compound **254** (2.5 g, 19.0 mmol, 1 eq) was added vinylmagnesium bromide in THF (3M, 65.0 mmol, 21.8 mL, 3.5 eq) at 40 °C and left to stir overnight. The reaction was then quenched with NH_4^+Cl^- (aq) (20 mL) at 0 °C and stirred for a further 48 h. The reaction mixture was then extracted with ethyl acetate (3 x 10 mL) and 1-butanol (10 mL) to give the product as a fine yellow powder (2.24 g, 73%). Mpt: 171-173 °C. $^1\text{H NMR}$ (500 MHz, $\text{DMSO-}d^6$) δ 8.47 (s, 1H, H-6), 5.88 (s, 2H, H-2), 5.76 (ddd, $^3J = 16.9, 9.9, 6.9$ Hz, 1H, H-4), 5.07-5.00 (m, 2H, H-5), 4.49 (d, $J = 6.9$ Hz, 1H, H-3), 1.88 (s, 3H, H-1). $^{13}\text{C NMR}$ (126 MHz, $\text{DMSO-}d^6$) 161.1, 159.9, 140.3, 122.3, 114.6, 52.7, 51.4, 22.1. **IR** $\nu_{\text{max}}/\text{cm}^{-1}$: 3316, 3302 (NH_2), 2171 (CN), 1734 (CO), 1683, 1638, 1601 ($\text{sp}^2\text{C-H}$ stretch). **MS** Found: $[\text{M}+\text{H}^+]$ m/z 163.0975 100%, $\text{C}_8\text{H}_{11}\text{N}_4$ requires $[\text{M}+\text{H}^+]$ m/z 163.0978.

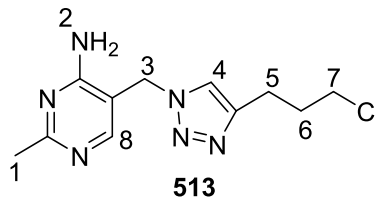
Synthesis of 5-diethylphosphonate-1-pentyne⁽¹⁸⁾



To diethylphosphite (25.9 g, 156 mmol, 1.6 eq) under a nitrogen atmosphere was added 5-chloropentyne dropwise (10.3 mL, 97.5 mmol, 1.0 eq). This was refluxed for a period of 4 days and then concentrated *in vacuo* to yield a yellow solution. This was then purified by Kügelrohr distillation at 150 °C/10 mbar to yield a clear oil (2.63 g, 14%). $^1\text{H NMR}$ (500 MHz, CDCl_3) δ 4.17 – 4.07 (m, 4H, H-6, 8), 2.32 (td, $^3J = 6.7, 2.6$ Hz, 2H, H-3), 2.00 (t, $^3J = 2.6$ Hz, 1H, H-1), 1.94 – 1.81 (m, 4H, H-4,5), 1.35 (t, $^3J = 7.0$ Hz, 6H, H-7,9). $^{13}\text{C NMR}$ (126 MHz, CDCl_3) δ 82.9,

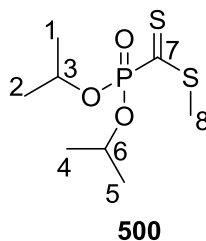
69.3, 61.5 (d), 24.0 (d), 21.6 (d), 19.2 (d), 16.4 (d). ^{31}P NMR (202 MHz, CDCl_3) δ 31.44 (d) (Lit ^{31}P . 32.30) ⁽¹⁸⁾. IR $\nu_{\text{max}}/\text{cm}^{-1}$: 3295, 3223 (sp C-H stretch), 2983, 2909.

Synthesis of 2-[1-(4-Amino-2-methylpyrimidin-5-ylmethyl)-1H-[1,2,3]triazol-4-yl]-1-chloropropane



To compound **153** (200 mg, 1.44 mmol, 1.0 eq.) in *t*-butanol/water (2:1 v/v 6 mL) was added 1-chloropentane (146 mg, 1.44 mmol, 1.0 eq.). To this was added sodium ascorbate (27 mg, 0.14 mmol, 0.1 eq.) and $\text{CuSO}_4 \cdot 5\text{H}_2\text{O}$ (3.5 mg, 0.014 mmol, 0.001 eq.). The mixture was stirred overnight at r.t and the resultant solution was evaporated to dryness to yield a pale white solid (293 mg, 77%). Mpt: 120 – 122 °C. ^1H NMR (500 MHz, CDCl_3) δ 8.16 (s, 1H, H-8), 7.33 (s, 1H, H-4), 5.99 (s, 2H, H-2), 5.31 (s, 2H, H-3), 3.48 (t, $^3J = 6.3$ Hz, 2H, H-7), 2.78 (t, $^3J = 6.3$ Hz, 2H, H-5), 2.41 (s, 3H, H-1), 2.13 – 2.00 (m, 2H, H-6). ^{13}C NMR (126 MHz, CDCl_3) δ 162.1, 147.7, 121.3, 48.7, 44.0, 31.6, 25.9, 22.5. IR $\nu_{\text{max}}/\text{cm}^{-1}$: 3144, 1651, 1597, 1563 (sp_2 stretch). MS [Found: $[\text{M}+\text{H}^+]$ m/z 267.1124 100%, $\text{C}_{11}\text{H}_{15}\text{ClN}_6$ requires $[\text{M}+\text{H}^+]$ m/z 267.1192.

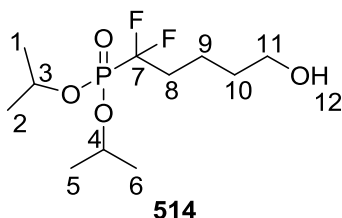
Synthesis of Diisopropylmercaptomethylphosphonate ⁽¹⁹⁾



To a slurry of NaH (57%, 8.4 g, 200 mmol, 1.0 eq) in THF (200 mL) was added dropwise diisopropylphosphite (33.2 g, 200 mmol, 1.0 eq) to maintain a slow evolution of $\text{H}_2(\text{g})$. After the total volume had been added, the reaction mixture was stirred at r.t for 3 h. The reaction was then cooled to 5 °C and carbon disulfide (25.1 g, 0.43 mol) was added slowly over a ten minute period to produce a dark brown solution. During five minutes, iodomethane (28.4 g, 200 mmol, 1.0 eq) was then added dropwise to give a dark red solution. This was then allowed to warm to r.t. and stirred overnight. The crude reaction mixture was evaporated under vacuum and distilled using a

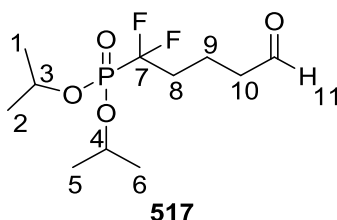
Vigreux column (140 °C/0.5 mTorr) 47%. ¹H NMR (500 MHz, CDCl₃) δ 4.92-4.83 (m, 2H, H-3, 6), 2.71 (s, 3H), 1.42 (d, *J* = 6.2 Hz, 6H), 1.37 (d, *J* = 6.2 Hz, 6H). ¹³C NMR (126 MHz, CDCl₃) δ 73.3, 24.0, 23.5, 19.0. ³¹P NMR (202 MHz, CDCl₃) δ -3.37 (Lit ³¹P. 6.5).

Synthesis of Diisopropyldifluorobutanol ^{(19), (20)}



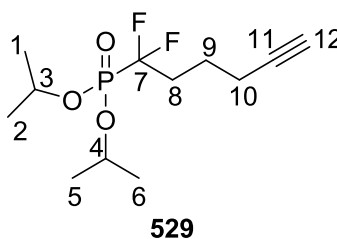
To dry THF (15 mL) was added *t*-butyllithium (1.9 M) in hexane (2.4 mL, 4.59 mmol, 1.2 eq) at -78 °C under an inert argon atmosphere. To this was added the diisopropyl methylsulfanyldifluoromethylphosphonate (1.0 g, 3.81 mmol, 1.0 eq) in dry THF (3 mL) dropwise over a period of 5 minutes. Boron trifluoride diethyl etherate (48% v/v), (3.04 g, 10.28 mmol, 2.7 mL, 2.7 eq) was then added dropwise and the resulting solution was left to stir for 45 min. The reaction was then quenched with a satd. aqueous ammonium chloride solution (2 mL) and extracted with dichloromethane: diethyl ether (50:50 v/v, 100 mL). The remaining organic layer was then washed with brine (2 x 10 mL), filtered and evaporated under reduced pressure to give a potent-smelling clear yellow oil (650 mg, 60%). ¹H NMR (500 MHz, CDCl₃) δ 4.84 (dq, *J* = 12.5, 6.2 Hz, 2H, H-8), 3.67 (t, ³*J* = 6.1 Hz, 2H, H-11), 2.17 (s, 1H, H-12), 2.13 – 1.99 (m, 2H, H-3, 4), 1.71 – 1.60 (m, 4H, H-9, 10), 1.37 (dd, ³*J* = 6.1, 4.7 Hz, 12H, H-1, 2, 5, 6). ¹³C NMR (126 MHz, CDCl₃) δ 73.6 (d), 62.3, 33.7, 32.1, 24.1 (d), 23.8 (d), 17.3. ³¹P NMR (202 MHz, CDCl₃) δ 5.54 (t, *J*_{P-F}, 108 Hz). ¹⁹F NMR (471 MHz, CDCl₃) δ -112.48, -112.71 (d, *J*_{P-F}, 108 Hz). IR ν_{max}/cm⁻¹: 3445 (OH), 2984, 2940, 1356, 1469 (C-F stretch), 1378, 1259.

Synthesis of Diisopropyldifluorobutaldehyde



To a stirred solution of pyridinium chlorochromate (49 mg, 0.23 mmol) in dry dichloromethane (2 mL) was added dropwise diisopropyldifluorobutan-1-ol **514** (44 mg, 0.16 mmol) in anhydrous dichloromethane (2.0 mL). This caused the reaction to change from orange to black within 30 seconds. The mixture was then stirred at r.t. for 16 h., diluted with diethyl ether (20 mL) and filtered through celite. The celite was washed with dichloromethane (2 x 10 mL) and the combined filtrates were evaporated under reduced pressure to yield a blue/green oil (37 mg, 85%). **¹H NMR** (500 MHz, CDCl₃) δ 9.78 (s, 1H, H-11), 4.85 (dq, ³J = 12.5, 6.2 Hz, 2H, H-3, 4), 2.55 (t, ³J = 7.1 Hz, 2H, H-10), 2.17 – 2.03 (m, 2H, H-8), 1.94 (pentet, 2H, H-9), 1.38 (t, J = 7.3 Hz, 12H, H-1,2,5,6). **¹³C NMR** (126 MHz, CDCl₃) δ 201.3, 73.6 (d), 42.8, 29.8, 24.1 (d), 23.7 (d), 13.8. **³¹P NMR** (202 MHz, CDCl₃) δ 5.20 (t, J_{P-F}, 107 Hz). **¹⁹F NMR** (471 MHz, CDCl₃) δ -112.85, -113.08 (d, J_{P-F}, 107 Hz). **IR** ν_{max}/cm⁻¹: 2985, 2940, 1726 (C=O), 1388, 1378, 1269 (sp² stretch). **MS** Found: [M+H⁺] m/z 273.1057 100%, C₁₀H₁₉F₂O₄PH requires [M+H⁺] m/z 273.1062.

Synthesis of Diisopropyldifluoro-4-pentyne

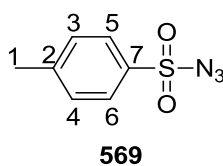


To the Ohira-Bestmann reagent **526**, (215 mg, 1.12 mmol) in MeOH (5 mL) and potassium carbonate (259 mg, 1.88 mmol) at r.t. was added a solution of compound **517** (37 mg, 0.14 mmol) in dry methanol (2 mL). The reaction mixture was left to stir overnight and then diluted with diethyl ether (10 mL) and filtered through celite. The celite was washed with dichloromethane (2 x 10 mL). The combined filtrates were evaporated under reduced pressure to leave a light brown/yellow solid. This was purified by silica gel chromatography eluting with ethyl acetate: methanol (95:5 v/v) to give a clear oil (96 mg, 36%). **¹H NMR** (500 MHz, CDCl₃) δ 4.84 – 4.74 (m, 2H, H-3,4), 2.21 (td, J = 7.0, 2.6 Hz, 2H, H-10), 2.18 – 2.05 (m, 2H, H-8), 1.91 (t, J = 2.6 Hz,

1H, H-12), 1.79 – 1.73 (m, 2H, H-9), 1.33 – 1.29 (m, 12H, H-1,2,5,6). $^{13}\text{C NMR}$ (126 MHz, CDCl_3) δ 83.2, 73.6 9 (d), 69.3, 32.8, 24.2 (d), 23.8 (d), 19.9 (d), 18.3. **IR** $\nu_{\text{max}}/\text{cm}^{-1}$: 3309, 3241, 2984, 2940, 1388, 1378, 1268. $^{31}\text{P NMR}$ (202 MHz, CDCl_3) δ 5.27 (t, $J_{\text{P-F}}$, 108 Hz). $^{19}\text{F NMR}$ (471 MHz, CDCl_3) δ -112.54, -112.77 (d, $J_{\text{P-F}}$, 108 Hz). **MS** [Found: $[\text{M}+\text{H}^+]$ m/z 283.1269, 100%, $\text{C}_{12}\text{H}_{21}\text{F}_2\text{O}_3\text{PH}$ requires $[\text{M}+\text{H}^+]$ m/z 283.1269.

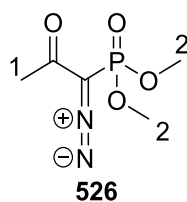
Synthesis of Ohira-Bestmann reagent ^{(21), (22)}

Preparation of Tosyl azide



To *p*-toluenesulfonyl chloride (5.72 g, 27 mmol, 1.0 eq) in acetone (85 mL) and water (85 mL) at 0 °C was added NaN_3 (1.5 g, 23 mmol, 1.17 eq). The reaction mixture was stirred at this temperature for 2 hours. The acetone was then removed under reduced pressure and the remaining aqueous layer was extracted with ethyl acetate (3 x 75 mL), dried over magnesium sulfate, filtered and evaporated under reduced pressure to furnish a clear oil (4.19g, 82%). $^1\text{H NMR}$ (500 MHz, CDCl_3) δ 7.88 (d, $^3J = 8.4$ Hz, 2H, H-5, 6), 7.46 (d, $^3J = 8.4$ Hz, 2H, H-3, 4), 2.53 (s, 3H, H-1). $^{13}\text{C NMR}$ (126 MHz, CDCl_3) δ 146.7, 134.9, 130.5, 127.5, 22.4. **IR** $\nu_{\text{max}}/\text{cm}^{-1}$: 2174 (N_3), 1595, 1397, 1371 (sp^2 C-H stretch).

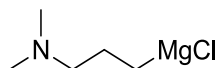
Preparation of Ohira-Bestmann reagent ^{(21), (22)}



To NaH (57%, 751 mg, 17.8 mmol, 1.1 eq) in THF (15 mL) at 0 °C was added acetoxydimethoxyphosphonate (3.2 g, 16.23 mmol 1.0 eq) dropwise. The reaction mixture was stirred for approximately 3 h. until the evolution of $\text{H}_2(\text{g})$ had ceased. The mixture was then added *p*-toluenesulfonyl azide (3.2 g, 16.2 mmol, 1.0 eq) dissolved in THF (5 mL) at r.t. This was left to stir overnight at then filtered through celite. The filtrate was evaporated under reduced pressure and the residue was used *in situ* without further purification (1.87 g, 60%). $^1\text{H NMR}$ (500 MHz,

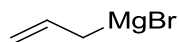
CDCl₃) δ 3.89 (s, 3H, H-2), 3.86 (s, 3H, H-2), 2.30 (s, 3H, H-1). ³¹P NMR (202 MHz CDCl₃) δ 14.9 (PO). IR ν_{max}/cm⁻¹: 2958 (C-H Sp³ stretch), 2124 (N₂), 1658 and 1505, 1365.

Preparation of 3-dimethylamino-1-propylmagnesium chloride



To 3-dimethylamino-1-propyl chloride hydrochloride (10.0 g, 63.3 mmol, 1 eq) in diethyl ether (50 mL) was added NaOH (1M, 50 mL). The organic layer was washed with water (2 x 20 mL) and then filtered through magnesium sulfate and concentrated under vacuum to approximately a volume of 10 mL. To an oven dried three neck round-bottomed flask fitted with condenser and dropping funnel was added magnesium turnings (3.0 g, 127 mmol, 2.0 eq), THF (53.0 mL), (1,2-dibromoethane) and a crystal of iodine if needed for activation. To this was added dropwise the free base 3-dimethylamino-1-propyl chloride (9.18 g, 63.3 mmol, 1 eq) at such a rate as to maintain constant reflux. After initiation had ceased the reaction mixture was refluxed for a further 3h. and then transferred to a separate vessel. A portion was then taken to allow for calculation of the concentration by titration against 1,10-phenanthroline with IPA.

Preparation of allylmagnesium bromide ⁽²³⁾



Magnesium turnings (1.06 g, 44 mmol) and were added to a round-bottom flask fitted with a constant pressure funnel, which had been previously flame dried and allowed to cool under a stream of nitrogen. Freshly distilled THF (44 mL) mixed with allyl bromide (3.4 mL, 40 mmol) in a constant pressure funnel was then slowly added to the flask. After several minutes, the reaction mixture turned from yellow to turbid grey. The flask was then cooled to 0 °C with an ice bath. After addition had finished, the reaction was stirred for 3 h. at r.t. Solvent transfers were made using standard cannulation techniques. The concentration of Grignard reagent was determined by titration, using IPA and 1,10-phenanthroline as an indicator.

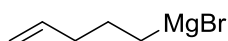
Preparation of 4-but-1-enylmagnesium bromide ⁽²³⁾



Following the procedure used for allylmagnesium bromide:

A solution of 4-bromobutene (1.0 mL, 9.8 mmol) in dry ether (ca. 2 mL) was added dropwise at room temperature under nitrogen to a stirred mixture of magnesium turnings (0.5 g, 20.8 mmol) (activated by the addition of a small amount of iodine) in *dry* ether (ca. 10 mL). Dropwise addition was regulated to maintain a gentle reflux. After the alkyl bromide addition was complete, the mixture was stirred an additional 30 min at r.t. and titrated as described previously.

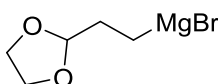
Preparation of 5-pent-1-enyl magnesium bromide ⁽²³⁾



Following the procedure used for synthesis of allylmagnesium bromide:

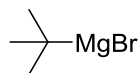
A solution of 5-bromo1-pentene (1.0 mL, 8.44 mmol, 1 eq) in *dry* ether (ca. 2 mL) was added dropwise at r.t. under nitrogen to a stirred mixture of magnesium turnings (405 mg, 16.8 mmol, 2 eq) (activated by the addition of a small amount of iodine) in *dry* THF (ca. 9.0 mL). The dropwise addition was regulated to maintain a gentle reflux. After the pentyl bromide addition was complete, the mixture was stirred an additional 30 min at r.t. Grignard titration was performed as described previously.

Preparation of 2-(1,3-dioxolanyl) ethyl magnesium bromide



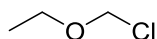
2-(2-Bromo)ethyl-1,3-dioxolane (1.0 mL, 8.52 mmol, 1 eq) was added dropwise at r.t. under nitrogen to a stirred mixture of magnesium turnings (408 mg, 17.0 mmol, 2 eq) (activated by the addition of a small amount of iodine) in *dry* THF (ca. 9.0 mL). The dropwise addition was regulated to maintain a gentle reflux. After the alkyl bromide addition was complete, the mixture was stirred an additional 30 min at room temperature. The Grignard reagent was titrated as described previously.

Preparation of *t*-butylmagnesium bromide



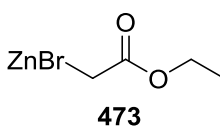
2-Methyl-2-bromopropane (1.0 mL, 8.9 mmol, 1 eq.) in dry THF (9.0 mL) was added dropwise to a pre dried round-bottomed flask containing magnesium turnings (427 mg, 17.8 mmol, 2.0 eq.) in anhydrous THF (20 mL) (activated with a small amount of iodine). Addition was maintained to keep a gentle reflux. The reaction was then stirred at r.t for 3 h. The Grignard reagent was titrated as described previously.

Preparation of MOM-chloride ⁽¹⁷⁾



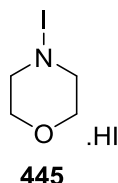
To a three neck round-bottomed-flask (500 mL), fitted with a dropping funnel and condenser under a N₂ atmosphere was added anhydrous toluene (133 mL), zinc acetate (9.2 mg, 0.01%) and dimethoxymethane (44.25 mL, 0.50 mol, 1 eq.). Acetyl chloride was then placed in the dropping funnel and slowly added to the reaction mixture over a 5 minute period. The reaction mixture was gently heated to 45 °C for 15 min. and then allowed to cool to ambient temperature during 3 h. An aliquot was then taken for ¹H NMR analysis to confirm the consumption of dimethoxymethane. Solutions of MOM-Cl prepared via this procedure have a density of 0.91 g/mL and are approximately 2.1 M. ¹H NMR (500 MHz, CDCl₃) δ 5.45 (s, 2H) (MOM-Cl), 3.66 (s, 3H) (MeOAc), 3.50 (s, 3H), (MOM-Cl), 2.04 (s, 3H) (MeOAc).

Preparation of Reformatsky reagent ⁽¹⁷⁾



To a 200 mL round-bottomed-flask flushed with N₂ was added zinc powder (11.5 g, 176 mmol, 2.0 eq.) To this was added anhydrous THF (44 mL) and TMSCl (0.96 g, 8.8 mmol, 0.1 eq). The solution was then warmed to 40 – 50 °C and ethyl bromo acetate (14.7 g, 88.2 mmol) in THF (110 mL) was added dropwise to the suspension to give a light orange solution. The orange supernatant was then transferred to a fresh round-bottomed-flask and stored under N₂ and used without further purification.

Synthesis of *N*-iodomorpholine ⁽²⁴⁾



To MeOH (400 mL) was added iodine (25.4 g, 0.10 mol) whilst stirring. To this was added dropwise *N*-morpholine (8.71 mL, 0.10 mol). The colour changed from dark purple to a dark orange/brown upon which fine orange crystals began to form. The reaction was left to stir for a further 45 minutes, and then the crystals were collected via vacuum filtration. The crystals were then dried further under vacuum until they became a fine powder. This method gave the *N*-iodomorpholine hydrogen iodide salt as an orange crystalline powder (9.8 g, 61%) which was used without any further purification.

HPLC Conditions

The mobile phase used was HPLC grade IPA 50% and HPLC grade hexane 50%. This was used as an isocratic mobile phase at a pressure of ~65 psi, with most run times being within 15 minutes unless otherwise stated. All racemic compounds were tested first to assess the optimum conditions for chiral separation and to measure their average retention times. The enantiopure compounds were then tested with the same isocratic mobile phase, and their peak areas were used to calculate the enantiomeric excess (ee %).

Biological Assay Procedures

Assay Conditions

Bath temp: 31 °C

Abs NADH-disodium salt (340_{nm})

Assay final volume 1.0 mL

Preparation of MES.KOH Buffer

To milli-Q water (500 mL) was added MES (9.76 g, 50 mM) and magnesium chloride pentahydrate (1.02 g, 5 mM). The pH was adjusted to 6.5 using KOH pellets. The volume was then made up to 1 L and stirred overnight.

Preparation of the apo enzyme

PDC (*pyruvate decarboxylase – S. cerevisiae*) stock solution was acquired from Sigma Aldrich™. Using a micropipette 200 µL of the holoenzyme was withdrawn and placed into a polypropylene tube and made up to 3 mL with MES.KOH buffer solution. This was then mixed and transferred into the dialysis membrane as described below.

Preparation and filling of a dialysis membrane

The membrane was initially pre equilibrated by placing the membrane into a beaker containing MES-KOH buffer (20 mL). To the pre equilibrated dialysis membrane at one corner was slowly added the solution containing the holoenzyme (3.0 mL). Injecting the sample into the membrane requires a syringe fitted with a hypodermic needle, and is slowly used to puncture the septum through one of the corners. The solution is then slowly injected, whilst making sure to remove any remaining air within the membrane. This ensured a good surface area in contact with the buffer solution (400 mL). The beaker containing the membrane and buffer solution (400 mL) was then placed in the refrigerator at 2 – 8 °C overnight. The process was repeated by changing the buffer solution on the second day for a second batch (400 mL).

Removing the apo enzyme from membrane

To remove the apo enzyme, a needle was inserted into the corner of the dialysis membrane that was originally used to inject the holoenzyme. The membrane was then inverted and the liquid was slowly removed from inside the membrane down towards the corner where the needle is located. This solution was then transferred to the centrifuge vial and diluted/concentrated to the desired final volume.

Centrifuge Vials

A centrifuge tube with a 10,000 MWCO (molecular weight cut-off) filter was used to acquire the final apo PDC volume. To the vial was added the solution from the membrane (3 mL) and the vials were spun at 5000 rcf at 5°C at 30 minute intervals. This process was repeated once more and then the remaining volume was removed into a separate vial. Dilutions were then made from this stock into the assay mixtures.

General Enzyme Assay ⁽²⁵⁾

To the assay solution containing ThDP (10 µL of a 10 mM solution), ADH (5 µL of a 2000 U/mL⁻¹ solution), NADH (10 µL of a 10 mM solution) and apo enzyme (20 µL), was added pyruvate (20 µL of a 100 mM solution) to initiated the assay. The residual activity of NADH absorption was monitored at 340 nm over a five minute period until a plateau was observed.

Timed pre-incubation assay

The apo enzyme (20 µL) was pre incubated at 31 °C with the desired inhibitor at concentrations of 500 µM, 250 µM, 100 µM, 50 µM, 25µM, or 5 µM, for a set time interval and then added to the assay mixture containing the native ThDP, ADH, NADH. The reaction was then initiated by addition of pyruvate (20 µL of a 100 mM solution) and the assay was run for 5 minutes to monitor the residual activity of the assay by loss of NADH activity.

Experimental references

1. J. A. Zoltewicz, G. M. Kauffman. *J. Am. Chem. Soc.*, **1977**, *99*, 3134-3135.
2. F. Fang, M. Vogel, J. V. Hines, S. C. Bergmeier. *Org. Biomol. Chem.*, **2012**, *10*, (15), 3080-3091.
3. E. C. Davidson, M. E. Fox, A. B. Holmes, S. D. Roughley, C. J. Smith, G. M. Williams, J. E. Davies, P. R. Raithby, J. P. Adams, I. T. Forbes, N. J. Press, M. J. Thompson. *J. Chem. Soc. Perkin Trans. I*, **2002**, 1494-1514.
4. A. P. Gagne, F. St-Jean, C. Morin, L. Gendron, E. Rousseau, Y. L. Dory, *Chem.Nat. Compd*, **2011**, *46*, 841-847.
5. R. A. Daines, P. A. Chambers, I. Pendrak, D. R. Jakas, H. M. Sarau, J. J. Foley, D. B. Schmidt, W. D. Kingsbury. *J. Med. Chem.*, **1993**, *36*, 3321-3332.
6. K. M. Erixon, C. L. Dabalos, F. J. Leeper, *Chem. Commun.*, **2007**, 960-962.
7. K. M. Erixon, C. L. Dabalos, F. J. Leeper, *Org. Biomol. Chem.*, **2008**, *6*, 3561-3572.
8. F. Himo, T. Lovell, R. Hilgraf, V. V. Rostovstev, L. Noodleman, K. B. Shapless, V. V. Fokin. *J. Am. Chem. Soc.*, **2005**, *127*, 210-216.
9. L. R. Bennett, C. J. Blankley, R. W. Fleming, R. D. Smith, D. K. Tessman. *J. Med. Chem.* **1981**, *24*, 382-389.
10. R. Nicewonger, A. Rammelsberg, C. A. Costello, T. P. Begley, *Bioorg. Chem*, **1995**, *23*, 512-518.
11. Robert L. Baxter, A. B. Hartley, H. W. S. Chan. *J. Chem, Soc, Perkin. Trans. I*, **1990**, 2963-2966.
12. K. Anderson, Y. Chen, Z. Chen, K. C. Luk, P. Rossman, S. Hongmao, P. M. Wovkulich. United States Patent, **2012**, US2012/184542 A1, p 58.
13. H. Tanaka, K. Ueda, S. Suzuki, H. Takenaka. (Shionogi & Co., Ltd., Osaka). **2002**, European Patent 1, 251, 129, A1, October 23.
14. F. F. Blicke, J. H. Biel. *J. Am. Chem. Soc.*, **1957**, *79*, 5508-5512.
15. M. Bushwell, I. Fleming, U. Ghosh, S. Mack, M. Russell, B. P. Clark, *Org. Biomol. Chem.*, **2004**, *2*, 3006-3017.
16. C. Juexiao, C. Z. Zhenghong, Z. Z. Guofeng, C. Tang, *Org. Lett.*, **2002**, *4*, 4723-4725.

17. M. Minero, Y. Sawai, K. Kanno, N. Sawada, H. Mizufune, *J. Org. Chem.*, **2013**, 78, (12), 5843-5850.
18. L. Delain-Bioton, D. Villemin, P. A. Jaffres, *Eur. J. Org. Chem.*, **2007**, 1274-1286.
19. D. W. Grisley, *J. Org. Chem.*, **1961**, 26, 2544-2546.
20. Y. Catel, V. Besse, A. Zulauf, D. Marchat, E. Pfund, T. N. Pham, D. Bernache-Assolant, M. Degrange, T. L. Lecueux, P. J. Madec, L. Le Pluart. *Eur. Polym. J.*, **2012**, 48, 318-330.
21. S. Muller, B. Liepold, G. J. Roth, H. J. Bestmann, *Synlett*, **1996**, 521-522.
22. M. Presset, D. Maihol, Y. Coquerel, J. Rodriguez, *Synthesis*, **2011**, 16, 2549-2552.
23. L. Fan, M. Zhang, S. Zhang, *Org. Biomol. Chem.*, **2012**, 10, 3182-3184.
24. M. Koyama, N. Ohtani, F. Kai, I. Moriguchi, S. Inouye, *J. Med. Chem.*, **1987**, 30, 552-562.
25. S. Mann, C. P. Melero, D. Hawksley, F. J. Leeper, *Org. Biomol.*, **2004**, 2, 1732-1741.
26. B. Sundoro, C-Yan. Chang, R. Aslanian, F. Jordan, *Synthesis*, **1983**, 7, 555-556.